Bioanalysis and metabolite identification of anticancer drugs in mass balance studies

ISBN: 978-94-6108-295-4

Cover design: Esther Ris – www.proefschriftomslag.nl

Printed by: Gildeprint drukkerijen – www.gildeprint.nl

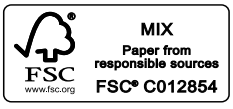

Bioanalysis and metabolite identification of anticancer drugs in mass balance studies

Bioanalyse en identificatie van metabolieten
van antikankermiddelen in massabalansstudies
(met een samenvatting in het Nederlands)

PROEFSCHRIFT

ter verkrijging van de graad van doctor aan de Universiteit Utrecht
op gezag van de rector magnificus, prof.dr. G.J. van der Zwaan, ingevolge
het besluit van het college voor promoties in het openbaar te verdedigen op
woensdag 23 mei 2012 des middags te 2.30 uur

door

Anne Charlotte Dubbelman
geboren op 15 december 1984 te Leiden

Promotoren:	Prof. dr. J.H.M. Schellens
	Prof. dr. J.H. Beijnen
Co-promotor:	Dr. H. Rosing

The research described in this thesis was performed at the Department of Medical Oncology of the Netherlands Cancer Institute, Amsterdam, the Netherlands, and the Department of Pharmacy & Pharmacology of the Netherlands Cancer Institute / Slotervaart Hospital, Amsterdam, the Netherlands.

Publication of this thesis was financially supported by:
GotoGemba, Noordwolde (Fr.), the Netherlands;
Eisai Ltd, Hatfield, United Kingdom;
J.E. Jurriaanse Stichting, Rotterdam, the Netherlands;
The Netherlands Laboratory for Anticancer Drug Formulation (NLADF), Amsterdam, the Netherlands;
Boehringer Ingelheim bv, Alkmaar, the Netherlands;
Roche Nederland bv; Woerden, the Nederlands;
Mundipharma Pharmaceuticals bv, Hoevelaken, the Netherlands.

"Rien ne se perd, rien ne se crée, tout se transforme"

Adapted from Antoine Lavoisier, *Traité élémentaire de chimie*, 1789

Voor opa en opapa

Contents

Preface

Preface

Cancer is known to have affected people's lives throughout the history. Some of the earliest written medical details consistent with modern descriptions of cancer were found in ancient Egyptian manuscripts and date back to around the 16th century B.C. The treatment in those days included excision with a knife, burning with red-hot irons and topical application of pastes, however, it was concluded that there was no effective therapy for this disease [1]. In the centuries thereafter, the attempts to cure cancer were mostly unsuccessful. Surgery was very painful, often fatal and, if the patient survived, the cancer almost always relapsed.

With use of a microscope, originally invented in the 17th century by Antoni van Leeuwenhoek, it became possible to see the difference between normal tissue and cancer tissue. This was a major step forward, since microscopic investigation of the edges of the tissue removed during an operation could tell whether the tumour had been removed completely, a process still performed by modern pathologists. Around 1900, with the discovery of X-rays, another type of cancer treatment emerged: radiotherapy. Thanks to continuous improvements of the instruments delivering the radiation, this therapy is now applied with high precision to destroy cancer cells while limiting the damage to surrounding normal tissue.

Up to about 1960, surgery and radiotherapy dominated the field of cancer therapy. Then, it became clear that the cure rates had reached a plateau, due to the presence of heretofore-unappreciated micrometastases. The use of a third type of treatment, chemotherapy, gained popularity. Although the term chemotherapy was already introduced early in the 20th century by Paul Ehrlich, people were hesitant in the use of chemicals to treat cancer. It was only after convincing evidence, like the remissions in lymphoma patients after administration of nitrogen mustard and remissions in children with acute lymphoblastic leukaemia following treatment with methotrexate, that the use of drugs in the treatment of cancer became widely accepted and that the field of anticancer drug development began to expand rapidly [2].

A main concern with anticancer agents was, and still is, their safety. Some patients experience severe side-effects, such as cardiotoxicity with the use of anthracyclines, nephrotoxicity with the use of cisplatin and peripheral neuropathy with the use of vincristine. Another point is that different patients may respond differently on a treatment. To better understand the underlying processes hereof and to be able to act upon that, there is a need to investigate what the body does to a drug (pharmacokinetics) and what a drug does to the body (pharmacodynamics).

This thesis focuses on a specific type of study that aims to determine the pharmacokinetics of a drug in the human body: the mass balance study. In a mass balance study, a radioactive label is incorporated in the drug molecule before the drug is administered to the patient.

The radioactivity facilitates the quantification of the drug and drug-related compounds in for example urine, faeces and blood samples collected from the patient. Moreover, the radioactivity can be used to calculate the balance between the administered dose and the dose recovered in excreta: the mass balance. Although it provides information about the total of drug-related materials (unchanged drug plus metabolites) in a sample, it gives no information on their structure. Quantification of only the unchanged drug or specific metabolites requires a more selective approach. A widely-accepted method hereof is high-performance liquid chromatography tandem mass spectrometry (LC-MS/MS). Using dedicated and validated LC-MS/MS assays, concentrations of drugs and known metabolites can be determined in various biological matrices. Then, when the total of drug-related material in a sample is known and the amounts of unchanged drug and known metabolites have been determined, again a balance can be made up to calculate the amount of unknown metabolites. To detect, quantify and structurally elucidate these metabolites, a combination of the previously mentioned techniques is generally applied.

As becomes clear, a mass balance study, if well designed and executed, is a wealthy source of information about the disposition (absorption, distribution, metabolism and excretion) of a drug. The analyses may identify and quantitatively describe metabolites that could contribute to the antitumour effect and/or toxicity profile. Variation between patients in the metabolism may affect outcome and safety and, thus, is important to understand. However, the development of quantitative assays and the analysis of samples are not always straightforward. In Chapter 1, we discuss bioanalytical issues that can arise during the support of a clinical mass balance study and provide practical solutions, based on own experience and mass balance studies described in the literature. The subsequent chapters each focus on a different anti-cancer drug and present the results that were obtained in a mass balance study of these agents.

The alkylating agent bendamustine is investigated in Chapter 2. Chapter 2.1 describes the development and validation of quantitative LC-MS/MS assays for bendamustine and some of its metabolites in human plasma and urine. These assays were successfully applied to support a clinical mass balance study with ^{14}C-radiolabeled bendamustine, which is described in Chapter 2.2. As it turned out that bendamustine was extensively metabolised and primarily excreted into urine, the next step was to investigate the metabolic profile of bendamustine in urine, presented in Chapter 2.3.

Chapter 3 focuses on the novel anticancer agent eribulin (E7389), a synthetic analogue of a natural product of a marine sponge. Very recently (2010-2011), this drug has been approved, among other countries, in the United States, Japan and Europe as a third-line treatment for metastatic breast cancer. Chapter 3.1 outlines the development and validation of quantitative LC-MS/MS assays for eribulin in human plasma, whole blood, urine and faeces. The clinical mass balance study of ^{14}C-eribulin, in which these assays were applied, is described in Chapter 3.2.

In Chapter 4, the drug under investigation is lenvatinib, an investigational multi-targeted tyrosine kinase inhibitor also known under the code E7080. The development and validation of assays that quantify lenvatinib and certain of its metabolites in human plasma, whole blood, urine and faeces is outlined in Chapter 4.1. Chapter 4.2 presents the results of the mass balance study that was performed with this compound.

Another tyrosine kinase inhibitor is the subject of Chapter 5. This chapter describes a clinical mass balance study, including the metabolism, of dovitinib, a compound currently tested in Phase II and III clinical trials against various types of cancer.

In the end, we all know that cancer is still affecting people's lives. Yet, we think that the knowledge obtained during these pharmacokinetic studies of promising anticancer agents can be used in the further assessment of their safety and efficacy. Moreover, this knowledge may be used, or has already been used to support their admission on the market, making them available for patients. In that way, we hope that the studies in this thesis contribute to a valuable treatment for at least some, but hopefully more, cancer patients.

References

[1] Breasted JH, The Edwin Smith Surgical papyrus (facsimile and hieroglyphic transliteration with translation and commentary, in two volumes)., The University of Chicago Press, Chicago, 1930.

[2] DeVita VT, Jr., Chu E, A history of cancer chemotherapy, *Cancer Res.*, **68** (2008) 8643-8653.

Chapter 1

Bioanalytical aspects of clinical mass balance studies in oncology

Chapter 1

Bioanalytical aspects of clinical mass balance studies in oncology

Anne-Charlotte Dubbelman, Hilde Rosing,
Jan H.M. Schellens, Jos H. Beijnen

Bioanalysis (2011) **3**:2637-2655

Abstract

Clinical mass balance studies aim to investigate the absorption, distribution, metabolism and elimination (ADME) of a(n) (often radiolabelled) drug, following a single administration to humans. They are perfectly suited to determine the disposition and major metabolic pathways of a drug, the exposure to the parent drug and its metabolites, and the rate and route of elimination. A mass balance study, however, poses interesting challenges to the analysis of parent drug and metabolites in different biological matrices. Using recent clinical mass balance studies in oncology as an example, this review focuses on the aspects of mass balance studies, from bioanalytical assay development, analysis of clinical samples to reporting of study results. Along the way, it discusses bioanalytical problems and practical solutions.

Introduction

Absorption, distribution, metabolism and excretion (ADME) are the main processes that determine the extent and duration of exposure to (the biological activity of) a drug. The ultimate study to investigate these processes in human is a mass balance study with a radiolabelled drug [1]. The information that can be extracted from a mass balance study is extensive and includes general insight into the drug disposition, the elimination routes and the major metabolic pathways. Additionally, it may help in the identification of pharmacologically active or toxic metabolites and the enzymes involved in biotransformation reactions. This knowledge is extremely valuable to predict or explain for instance drug-drug interactions, toxicities and the effects of the drug at normal dose on patients with impaired renal or liver function.

In the past, it was not uncommon that anticancer drugs were tested in clinical trials or were even registered with only limited prior pharmacokinetic data. This sometimes resulted in the late discovery of metabolites contributing to pharmacological or toxic effects, which was the case for the severely urotoxic metabolite acrolein, generated by the biotransformation of the alkylating agents cyclophosphamide and ifosfamide [2]. The use of mesna in combination with these chemotherapeutics to reduce the urotoxicity exemplifies how knowledge of metabolism and toxicity allows the development of strategies to circumvent side effects [3]. For anticancer drugs for which no mass balance study was performed before registration, or for which the mass balance results were far from complete, the elimination pathway(s) is/are still largely unknown. An example is the antineoplastic agent mitoxantrone, of which only 11 and 25% of the dose was recovered in urine and faeces, respectively, and for which the available data on metabolites is very limited [4]. Consequently, while being marketed for decades, limited data is available on drug interactions, on the pharmacokinetics of mitoxantrone in special populations, such as patients with renal impairment, or on the influence of gender and race on the pharmacokinetics of mitoxantrone [4].

Apart from the clinical pharmacological need to investigate the ADME properties of a drug, at least part of the information that can be gained from a mass balance study is nowadays required for regulatory filing. In this context, especially the quantification of metabolites has gained much attention over the last years, since the appearance of the guidances for Metabolites in Safety Testing (MIST guidelines). These guidances, issued by the Food and Drug Administration (FDA) [5] and the International Conference on Harmonisation (ICH) [6], recommend additional safety assessment for major metabolites that are present in humans at disproportionally higher levels than in any of the tested animal species.

A mass balance study should start with a thorough preparation. For the bioanalysis this often means that quantitative bioanalytical assays, including sample handling procedures need to be developed and validated. The clinical part of the mass balance study usually

starts with the administration of a single dose of the study drug, containing a radiolabel, to a small group of subjects. While various types of radiolabels (e.g. ^{3}H, ^{14}C, ^{32}P, ^{35}S) have been used for mass balance studies, there is agreement that the use of ^{14}C is preferred, for multiple reasons. Unlike ^{32}P and ^{35}S, ^{14}C has a long decay half-life and carbon atoms are far more common in drug molecules than phosphorus and sulphur. Furthermore, in contrast to hydrogen, carbon is unlikely to be exchanged with the environment, which would result in loss of the radiolabel [1;7]. This review therefore focuses on the use of ^{14}C as a tracer. After drug administration, blood samples and excreta (e.g. urine and faeces) are collected during a predefined period. The radioactivity in the collected samples represents the sum of the drug-related material, i.e. the parent drug and all metabolites containing the radiolabel. Theoretically, the mass balance is complete when 100% of the administered radioactivity is recovered in the excreta. The bioanalytical support of the clinical study consists of the analysis of the study samples, which are collected for three purposes:

- Quantitative analysis of total radioactivity (TRA). This is the total of the drug-related material used to construct time courses of the excretion of all drug-related material and to calculate the mass balance.
- Quantitative analysis of unchanged parent drug and (if desired) known metabolites. The validated bioanalytical assay, usually a liquid chromatography tandem mass spectrometry (LC-MS/MS) method, is applied and the measured concentrations are used to estimate pharmacokinetic parameters of the study drug. Additionally, the amount of metabolite(s) present in a sample may be derived by comparing the parent drug concentrations with TRA concentrations.
- Qualitative/quantitative analysis of metabolites. Samples are usually submitted to a highly selective chromatographic system to separate known and unknown metabolites from the parent, followed by detection and quantification based on the radioactivity and structural elucidation of the unknown metabolites, an approach frequently referred to as metabolite profiling.

Finally, the mass balance study is completed by reporting the results. The present review discusses the bioanalytical aspects in the different stages of a clinical mass balance study, from preparation to reporting. It focuses on anti-cancer drugs, and uses mass balance studies in oncology as illustrative examples in the discussion of bioanalytical problems and potential solutions.

Recent clinical mass balance studies in oncology

Mass balance studies of anticancer drugs pose some additional challenges to the study design when compared with most other drugs. Because many anticancer drugs are potentially mutagenic, carcinogenic or teratogenic, it is unethical to test these drugs in

Table 1: Overview of recent clinical mass balance studies in oncology with their main characteristics and the analysis methods used for total radioactivity (TRA) determination.

Compound	Subjects		Administration		Matrix assessed for TRA										Pretreatment			Analytical technique		Ref.
	Adv. cancer pts	Healthy humans	n	Dose (mg)	^{14}C- activity (μCi)	Plasma	Whole blood	Urine	Faeces	Vomitus	Bile	Expired air	Saliva	Tears	Solubilisation (and decolourization)	Oxidation (combustion)	Oxidation and reduction	LSC	AMS	
BIBF1120	-	√	8	100	70	√	√	√	√	-	-	-	-	-	?	?	?	√	-	[8]
BMS-690514	-	√	9	200	80	√	-	√	√	-	√	-	-	-	√	-	√	√	√[a]	[9]
Brivanib	√	-	4	800	100	√	√	√	√	-	-	-	-	-	?	?	√	√	√[a]	[10]
Eribulin	√	-	6	2	80	√	√	√	√	-	-	-	-	-	√	-	-	√	-	[11]
Imatinib	-	√	4	200	31.9	√	√	√	√	-	-	-	-	-	√	-	-	√	-	[12]
Irofulven	√	-	3+3[b]	0.55 mg/kg	100	√	√	√	√	-	-	√	√	√	√	-	-	√	-	[13]
Ixabepilone	√	-	8	70	0.080	√	-	√	√	-	-	-	-	-	-	-	√	-	√	[14]
Trabectedin	√	-	8	1.0	70	√	√	√	√	-	-	-	-	-	√	-	-	√	-	[15]
Vatalanib	√	-	7	1000	27.16	√	√	√	√	√	-	-	-	-	√	√	-	√	-	[16]
Vismodegib	-	√	6	150	1.000	√	√	√	√	-	-	-	-	-	-	√	√	√[c]	√	[17]

TRA: total radioactivity; Ref.: reference; Adv. cancer pts: advanced cancer patients; n: number of subjects; LSC: liquid scintillation counting; AMS: accelerator mass spectrometry. [a]Plasma samples only [b]Three patients received ^{14}C-irofulven and three patients received non-labelled irofulven [c]High concentration faeces samples only

healthy volunteers [1]. Instead, the subjects of mass balance studies in oncology are often cancer patients for whom no standard treatment options are available and who could benefit from the treatment. A secondary effect of the toxicity of most anticancer drugs is the increased importance of personal safety when handling not only study samples but also reference standards at the bioanalytical laboratory.

An extensive overview of mass balance studies of anti-cancer drugs that were reported up to 2004 has been published by Beumer *et al* [1]. The number of mass balance studies in oncology published afterwards, however, is limited. Table 1 lists mass balance studies employing a ^{14}C radiolabel that have been published since 2005 and that were not included in the review of Beumer *et al*, together with the methods they applied for total radioactivity determination. Table 2 summarizes the bioanalytical methods that these mass balance studies used to quantify the unchanged parent compound and known metabolites in the collected matrices. Finally, Table 3 describes the metabolite profiling techniques applied in these mass balance studies.

Bioanalytical assay development and validation

When a mass balance study of a compound is planned, it is advisable to develop (and to validate) the required bioanalytical assay for the compound before collection of the first clinical samples. This allows that the optimal collection and storage conditions, as determined during the validation, can actually be implemented in the clinical study.

Various bioanalytical techniques exist, but LC-MS/MS is nowadays common practice in pharmaceutical bioanalysis. To demonstrate, 8 out of the 10 bioanalytical methods summarized in Table 2 employed LC-MS/MS. Although the technique has some pitfalls, as will be discussed later, the better sensitivity and selectivity of the mass spectrometric detection as compared to UV detection and the wider applicability as compared to fluorescence detection makes LC-MS/MS a powerful tool for the quantitative analysis of anticancer agents (and other drugs) in biological matrices [18]. For this reason, the bioanalysis discussed in the present review is focussed on LC-MS/MS.

Samples from mass balance studies are often being collected up to one or more weeks after the administration of a single dose. Moreover, particularly in oncology, high potency agents have been developed, which are administered only in a few mg. Examples are the marine derived product trabectedin (recommended dose of 1.5 mg/m^2) [19] and the marine sponge product analogue eribulin (recommended dose of 1.4 mg/m^2) [20]. The extended collection times, as well as the low doses pose challenges to the sensitivity of the quantitative assays [21;22]. The bioanalytical development should therefore focus on high sensitivity and, since complex matrices are involved, on high selectivity.

Table 2: Overview of quantitative bioanalytical assays used in recent clinical mass balance studies in oncology of Table 1.

Parent [Metabolite]	Matrices	LLOQ (ng/mL)	Sample vol. (µL)	Internal Standard	Sample preparation	Analytical technique	Validated	Ref.
BIBF1120	Plasma	0.5	?	SIL BIBF 1120	SPE	HPLC-MS/MS	√	[8]
	Urine	1.0	?					
[BIBF1202]	Plasma	1.0	?	SIL BIBF 1202				
	Urine	1.0	?					
BMS-690514	Plasma	0.5	?	SIL BMS-690514	SPE	HPLC-ESI-MS/MS	√	[9]
	Urine	1.0	?					
Brivanib	Plasma	2.0	100	SIL-brivanib	SPE	HPLC-ESI-MS/MS	?	[10]
	Urine	1.0	50		ACN treatment			
Eribulin	Plasma	0.2	500	Structural analogue	LLE	HPLC-ESI-MS/MS	√	[22]
	Whole blood	0.5	500		LLE			
	Urine	0.5	500		LLE			
	Faeces	100	250		ACN treatment			
Imatinib	Plasma	4.0	200	SIL imatinib	PPT	HPLC-APCI-MS/MS	√	[12;23]
[CGP74588]	Plasma	4.0	200	SIL imatinib				
Irofulven	Plasma	2.5	?	?	?	HPLC-β-counter detection	√	[13]
	Urine	2.5	?					
Ixabepilone	Plasma	2.0	?	Structural analogue	PPT/LLE	HPLC-ESI-MS/MS	√	[14]
	Urine	2.0	?		PPT/LLE			
Trabectedin	Plasma	0.01	500	SIL trabectedin	SPE	HPLC-ESI-MS/MS	√	[21;24]
	Urine	0.01	500					
Vatalanib	Plasma	2.5	250	Structural analogue	LLE	HPLC-UV	√	[16;25]
Vismodegib	Plasma	5.0	200	SIL vismodegib	SPE	HPLC-ESI-MS/MS	√	[17;26]

LLOQ: lower limit of quantification; vol: volume; SIL: stable isotope labelled; SPE: solid phase extraction; HPLC: high performance liquid chromatography; MS/MS tandem mass spectrometry; ACN: acetonitrile; ESI: electrospray ionisation; PPT: protein precipitation; LLE: liquid-liquid extraction; APCI: atmospheric pressure chemical ionisation; UV: ultra violet

The FDA recommends a full validation if a bioanalytical method is developed and implemented for the first time or if metabolites are added to an existing method for quantification [27]. Therefore, the decision of which metabolites have to be quantified should be made before starting the validation procedures. Obviously, with metabolite identification as one of the main purposes of a mass balance study, the available information about metabolites is often limited at this point. Metabolites found in animal studies and in incubation experiments with human liver microsomes can guide the choice of which metabolites should be included in the bioanalytical assay.

In contrast to a full validation, a partial validation is considered sufficient when a validated bioanalytical method is applied on a different matrix from the same species [27]. The term partial validation is broad and can range from "as little as one intra-assay accuracy and precision determination to a nearly full validation" [27]. Apart from an accuracy and precision determination we suggest testing at least the analyte-stability, specificity and selectivity, and cross-analyte interference, if a method is applied to other biological matrices. An efficient approach can be to develop an assay in one of the matrices of major interest (usually plasma), with high attention to the sample clean-up and chromatographic separation between the analyte(s) and early eluting endogenous compounds. Subsequently, the applicability of the method for other matrices, like urine, whole blood or faeces can be tested. If the methods are applicable without major modifications, a logical step would be to fully validate the assay in plasma, and to partially validate the assay in the additional biological matrices.

Sample preparation optimization

Sample preparation is an essential part of a quantitative bioanalytical assay. It may differ from sample preparation for metabolite profiling as it aims to selectively isolate one or more known analytes from a matrix, rather than to clean up a sample using the mildest conditions possible, whereby preferential selection is kept to a minimum.

The standard sample preparation techniques liquid-liquid extraction (LLE), protein precipitation (PPT), solid phase extraction (SPE) and simple dilution have been extensively reviewed in literature [28;29]. As Table 2 shows, these methods are still commonly applied in quantitative assays for mass balance studies. If these conventional techniques fail to produce satisfactory results, a combination of techniques or more recent variations on these techniques may provide a solution. An example is the recently introduced HybridSPE-PPT technique. This method combines the simplicity of PPT with the selectivity of SPE and efficiently removes phospholipids, thereby minimizing the matrix effect [30]. It has successfully been applied in the development of a sensitive LC-MS/MS assay for the polar anti-cancer agent carboplatin [31]. The use of this and other modern sample preparation techniques have recently been reviewed by Kole *et al* [32].

The recent shift to high-throughput quantification and (semi-) automated techniques for sample preparation is less prominent in bioanalytical assays for mass balance studies. The

use of automated systems for liquid handling, PPT, LLE, on-line SPE or off-line SPE can result in a higher reproducibility, a smaller chance of random errors and a higher sample throughput, which is especially for routine analyses very advantageous [33]. However, the use of automated systems may result in systematic errors, they may be prone to technical malfunctions, and, which may explain their limited application in mass balance studies, they may not be cost-effective and time-saving if only a small number of samples is analysed. Mass balance studies are typically performed in a few subjects, meaning that the total number of samples is limited. However, if a drug appears successful in early clinical trials and if e.g. the plasma assay will also be applied for other pharmacokinetic studies, automation can be worthwhile. The availability of samples of a mass balance study or other early clinical studies may facilitate the development of a more routine assay, as they can provide information of suitable concentration ranges and can be used for incurred sample reproducibility and to check for interferences from potential metabolites of which no reference standards are available.

The advantage of automation when large numbers of samples need to be analysed is illustrated by Bakhtiar *et al* [23], who developed a semi-automated PPT method using a 96-well plate format, to prepare plasma samples for the analysis of imatinib and its main metabolite CGP 74588. With a capacity to process 2 to 4 plates a day (a sample preparation time of approximately 2 h per plate and a LC-MS/MS run-time of about 2.5 min per sample) thousands of clinical samples were analysed. Another example is the quantitative LC-MS/MS assay applied in the mass balance study of trabectedin [15]. The labour-intensity of the SPE method used for sample clean-up [21] was no limitation for the low number of samples from the mass balance study. However, when trabectedin progressed into Phase II clinical trials, the number of samples to be analyzed increased dramatically and the time-consuming sample preparation became disadvantageous. A new assay was then developed, whereby off-line PPT was combined with column switching to further clean-up and to concentrate the samples, reducing the sample preparation time by 10-fold. This new method was successfully used to support Phase II clinical studies [34].

Quantification of parent compound and metabolites

If little is known about the metabolism of a compound or only limited metabolism is expected, a quantitative bioanalytical assay, usually employing LC-MS/MS, of the parent compound only may be sufficient for a mass balance study. However, when a compound is known to be converted in one or more major or active metabolites, additional quantification of these metabolites may be desired. Generally, the difficulty of the development of an assay increases with an increasing number of analytes. Differences in polarity between the parent compound and the metabolites often complicate the development of a sample preparation method that yields adequate recoveries for all compounds. Also the design of a chromatographic method may be more difficult. This is exemplified in the assay development for the simultaneous quantification of the anticancer prodrug capecitabine, its intermediate biotransformation products 5'-deoxy-5-

fluorocytidine (5'-DFCR) and 5'-deoxy-5-fluorouridine (5'-DFUR), its bio-activation product 5-fluorouracil (5-FU) and the metabolite 5-fluorodihydrouracil (FUH_2) [35]. As precipitation with methanol or acetonitrile and LLE with various solvents failed to yield an acceptable and reproducible recovery for all analytes, finally a precipitation with 10% trichloroacetic acid was selected, resulting in recoveries between 70 and 88% with standard deviations below 15%. Reversed-phase (RP) chromatography was in this case hampered by the low affinity of the column for the most polar compounds 5-FU and FUH_2 combined with the high affinity for capecitabine. The remarkable, mixed retention mechanisms of a porous graphitic carbon column (Hypercarp) provided a solution here and, combined with 10 mM ammonium acetate in water and acetonitrile-2-propanol-tetrahydrofuran (1:3:2.25 v/v/v) as mobile phase, chromatographic separation was achieved within an acceptable run-time of 15 min [35].

Another approach to overcome the problems due to large differences in polarity between parent compound and metabolites is simply to develop two separate assays. An additional advantage is that when different concentration levels are expected for the parent and its metabolites (e.g. very high parent concentrations and very low metabolite concentrations), different concentration ranges can easily be applied for the separate assays. Obvious drawbacks of separate assays are that two assays may require more time for development, validation and analysis than a single assay and that more sample volume may be required if different sample preparation methods need to be applied. A few additional points should be considered when using separate assays for metabolites and parent compound. First of all, highly retained compounds may interfere with the quantitation of analytes in the next study sample. To overcome this, it is recommended to use gradient elution or to include washout steps to clean the column within the analytical run. Secondly, and this also applies to a single LC-MS/MS assay, the quantification of analytes with low concentrations in study samples may be disturbed by the high concentrations of a co-eluting analyte (e.g. the parent compound), due to ion suppression. Potential ion suppression or cross-analyte interference from the parent can remain unnoticed if the parent compound is not included in the calibration standard and quality control samples of the metabolites. Therefore, it is important to investigate interferences from the parent compound during the assay development and validation. If chromatographic separation between metabolites and parent is accomplished, high concentrations of the parent compound will no longer disturb the quantification, unless the metabolites are being quantified based on an internal standard co-eluting with the parent compound. Therefore, a proper choice of an internal standard for the metabolite quantification is very important. There is general agreement that use of a stable isotope for each analyte is preferred above any other type of internal standard [36]. Stable isotopically labelled internal standards behave very similar to their non-labelled analogues and can compensate for variations in matrix effect, sample preparation recovery and absorption on glassware or other surfaces during sample processing [37;38]. For metabolites of drugs in development, however, stable isotopes are often not available, due to difficulties with the synthesis and the associated costs. Use of the stable isotope of the

parent drug may seem an attractive alternative, but in presence of the parent compound the response of the stable isotope may be suppressed. This could lead to a serious overestimation of the metabolite concentrations as demonstrated by Jian et al. [37]. They compared in a case study the excreted amount of a metabolite B1 quantified using either (i) the stable isotope of the parent compound or (ii) the stable isotope of the metabolite. The deviation of the metabolite B1 concentration obtained with the first method relative to the second increased with increasing parent concentration to up to over 200%. To overcome ion suppression of the parent compound on its stable isotope, which is important if the latter is used to quantify metabolites, the study samples may be diluted or the concentration of the stable isotope may be increased. An alternative way to quantify metabolites without availability of a stable isotopically labelled internal standard is to use a structural analogue that preferably co-elutes with the metabolite [37].

Another issue to consider in assay development, especially of multiple-analyte systems, is cross-analyte interference. Various types of interferences between metabolites and parent drug have been described and chromatographic separation of the interfering analytes is often the only way to overcome this. First of all, isomeric metabolites, like zusammen (*Z*) and entgegen (*E*) isomers [39] or products of hydroxylation at different sites of the molecule will both give a response in the monitored transition, if they share a similar fragmentation pattern. This makes differentiation impossible if they are not separated. Similarly, isobaric metabolites, with the same nominal mass but a different elemental composition (e.g. R-OSO_3H instead of R-OPO_3H_2) can cause interference. Even if the molecular mass differs 1 Da (e.g. R-OH instead of R-NH_2) or 2 Da (e.g. R-OH instead of R-CH_3), interference can occur through a naturally occurring ^{13}C-, ^{15}N-, ^{37}Cl- or ^{81}Br-isotope of the analyte with the lower molecular mass [22;40;41]. In the latter two cases, whereby the elemental composition differs, high-resolution mass spectrometric detection provides an alternative solution to distinguish between the analytes [42].

Another type of interference arises when an analyte degrades in the ion source of a mass spectrometer. N-oxides, O-sulphates, acyl-, N- and O-glucuronides are typical examples of metabolites that can degrade to their parent compound due to in-source conversion [43], with an overestimation of the parent drug concentration as a potential consequence [44]. Again, this interference can be circumvented by separating the parent drug and its metabolites chromatographically. Alternatively, using ESI instead of APCI may decrease the analyte degradation as the ionization process of ESI is much less energetic than of APCI. Also the capillary temperature may influence the analyte degradation. Lowering the capillary tube temperature of ESI has been demonstrated to prevent deoxygenation of an N-oxide completely [45].

In conclusion, quantification of parent drug and metabolites may be complicated. Instead of separate assays for parent and metabolites, a single quantitative assay is often desired, as

it saves analysis time and requires validation of only one method instead of two. A few of the numerous examples of successful multi-analyte assays are provided by Srinivas [46].

Matrix specific aspects

Plasma is one of the most common used biological matrices for drug analysis. Because blood or plasma receives the drug from the site of administration and carries it to all organs, it is the most logical site to determine drug in the body [47]. Not surprisingly, plasma sample pretreatment for LC-MS/MS has been described extensively [29;32] and even a systematic methodology for the development of bioanalytical assays in plasma has been proposed [43]. For this review on mass balance studies, we will focus more on the less common matrices: urine, whole blood and faeces.

Urine

Quantification of drugs and their metabolites in urine is less widely applied in pharmacokinetic studies, but common for mass balance studies [1]. Seven of the recent mass balance studies in Table 2, included measurement of unchanged parent compound in urine. Bioanalysis in urine samples seems simple but the variability in pH and the high salt concentration may be complicating factors. Also non-specific binding of analytes in urine to the container wall can compromise adequate quantification [48], as the measured concentration will in this case underestimate the actual concentration. A simple test to diagnose an adsorption problem is to sequentially transfer part of a spiked urine volume into a series of empty tubes (allowing some time between each transfer) and to analyze the analyte concentration in each tube. A decreasing trend is indicative for adsorption to the container wall [48]. It is advised to perform such a test during the development of a urine assay. Any adsorption problems might be prevented by the addition of an anti-absorptive agent. In the recent mass balance studies included in Table 1, bovine serum albumin (BSA) was added to urine in one study to prevent adsorption [24] and in two studies, the urine samples were acidified after collection [8;9], which may also help preventing non-specific binding [48].

Whole blood

Quantitative analysis of unchanged parent compound in whole blood has only been reported in one of the studies in Table 2. Whole blood concentrations are useful to determine the distribution of a compound into red blood cells. Some anti-cancer agents, like the anthracyclines doxorubicin, epirubicin and daunorubicin, the alkylating agent ifosfamide and its metabolites and topoisomerase I inhibitor topotecan, are for a large part distributed into red blood cells, which appear to play an important role in their transport and clinical activity [49]. In practice, assays in whole blood are hard to perform and often hard to interpret. They require an extensive sample clean-up to remove interfering compounds and the interpretation may be hampered by a potential difference between spiked (calibration and quality control) samples and study samples in the partitioning of the analyte over plasma and red blood cells. This may be caused by incomplete equilibration of

the compound with the red blood cells before start of the sample preparation. The difference in partition could in turn result in a difference in quantification between the spiked samples and the study samples. To improve the similarity between spiked blank whole blood samples and frozen stored study samples, it is highly recommended to submit the blank whole blood to one freeze/thaw cycle and then prepare calibration and quality control samples instead of spiking the analytes of interest directly to 'fresh' whole blood. The red blood cells in study samples and blank whole blood after a freeze/thaw cycle will be haemolysed, as opposed to those in fresh whole blood. For plasma assays, differences in haemolysis may result in differences in quantification. Hughes *et al.* demonstrated that the presence of 1 or 2% haemolysed whole blood in plasma could result in altered method accuracy or even in non-quantifiable samples [50].

Faeces

Also the determination of unchanged drug in faeces is not common and was only performed in one of the mass balance studies listed in Table 2. From the mass balance studies tabulated by Beumer *et al* only 13% measured the concentration of unchanged parent drug in faeces [1]. From our experience, there are two major difficulties with bioanalytical assays for faeces, which are the large variability in faeces composition and the difference that may exist between a spiked sample and a study sample with the same concentration. The first results in a variability in sample preparation recovery and the second possibly in an underestimation of the actual concentration in study samples. Both phenomena remain unnoticed since even addition of a stable isotopically labelled internal standard can not correct for it, because the quantification is based on the assumption that study samples behave identically to spiked samples. The effect of these problems may be reduced by dilution with e.g. the addition of a large volume of water (or another appropriate solution) before homogenisation of the faeces sample; this however also results in a dilution of the analytes. In case of a radiolabeled compound, a way to assess the actual sample preparation recovery of study samples is to measure the radioactivity in the final solution for analysis and in the part of the sample that is discarded during the sample preparation (e.g. a pellet formed after extraction and centrifugation). Ideally, the ratio between the two should be similar between study samples and calibration samples that are spiked with a radiolabeled analyte. However, this method does not take into account the presence of potential non-extractable metabolites in the study samples. In the end, the difficulties encountered in the quantitative analysis of faeces samples are probably often the reason not to perform these determinations. This does not necessarily mean that the amount of unchanged drug excreted in faeces can not be determined at all. If a quantitative analysis of metabolites (metabolite profiling) in faeces is performed, whereby metabolites are separated from the parent and quantification is based on radioactivity, a good estimation of the excretion of unchanged parent in faeces can be made.

Sample handling

Before the start of a mass balance study, the required sample collection, aliquoting and storage conditions should be known to obtain a reliable quantification result when analysis occurs at a later time point. Additionally, if pooling of samples is applied, even if this takes place after storage and just before sample analysis, it is useful to develop a pooling strategy in advance, to avoid that the collected volumes are too small for the intended pooling method.

Collection

Sample collection conditions include the type of collection tubes and vials and the use of special conditions in the period immediately after collection, like cooling with ice-water, protection against full-spectrum light or addition of a stabilizing or anti-adsorptive agent. These conditions should have been established during the method validation.

Aliquoting

Sample aliquoting prevents the biological matrix undergoing multiple unnecessary freeze-thaw cycles. Therefore it is useful to prepare separate aliquots for the analysis of total radioactivity, the unchanged parent compound and for metabolite profiling. Faecal samples should be homogenized before aliquoting. To facilitate homogenization, often a 2-10 fold dilution with water, phosphate buffered saline or methanol is applied before mixing and aliquoting. Obviously, the exact dilution factor has to be recorded to calculate the mass balance in a later stage.

While small volumes (e.g. 0.2-5 mL aliquots) often suffice for the analysis of TRA and the determination of parent drug concentration, larger volumes (e.g. 4-6 mL for plasma and 20-100 mL aliquots for urine or faeces) are recommended for metabolite profiling to allow for a significant concentration of the analytes. If plasma metabolite profiling is only performed at a few selected time points, larger volumes of blood (e.g. 10-40 mL) are not uncommon [8;9]. Especially if a metabolite structure has to be confirmed using NMR analysis, a larger amount of metabolite, so a larger volume of the biomatrix is required. Obviously, from a bioanalytical point of view, large sample volumes divided over many aliquots of different sizes are ideal, however, storage space is often limited and the clinical sample handling should be kept to a minimum. Therefore, the design of the sample handling procedures should be a trade-off between bioanalytical and practical considerations.

Storage

The storage conditions of the samples may influence the stability of the compounds in the biomatrix. This is normally investigated during the development and validation of a bioanalytical assay and prior to sample storage. Even if stability is demonstrated at -20°C, additional stability testing at -70°C is advisable when samples are stored at this lower temperature, as potential denaturation or precipitation of matrix proteins may affect the ability to extract the compound from the matrix [36]. For aliquots meant for metabolite profiling, storage at temperatures at -70°C is recommended, as stability data of the

potential unknown metabolites is usually not available [1]. Storage conditions of aliquots intended for total radioactivity determination are less critical, since the total radioactivity is independent of the structure of the compounds.

Pooling

Pooling of plasma samples is not common for TRA analysis and quantitative analysis of parent and known metabolites, as these analyses aim to provide individual plasma-concentration time curves. For metabolite profiling, however, pooling can be very helpful. Three common pooling strategies are pooling across time points for each patient (AUC pooling), pooling across patients for each time point and a combination of both [7;51]. The first method, originally described by Hamilton and applied in the mass balance study of vatalanib [16], gives an estimation of the area under the plasma concentration-time curve (AUC) by measuring a single sample [52]. This method is very efficient to scan for the presence of major metabolites. It requires larger sample volumes at later time points, when the time periods between collections is longer, so the collection volumes might have to be adapted. The second approach, pooling across patients for each time point, is applied by eight studies in Table 3 and can be used if inter-individual variability is minimal. Equal volumes per time point of all subjects are mixed, and analysis of the samples gives a time profile of the metabolite concentrations. A combination of both methods, whereby the samples pooled between patients per time point are subsequently pooled across time points, is time-saving but less informative. If inter-individual variation is limited, this method can be useful to estimate the average AUC of metabolites and compare this between species [51].

Urine should preferably be collected over short time intervals (2-6 h) during the first 24 to 48 h after administration, but can be collected over 24-h periods thereafter [1], if the stability of the compound is assured. At the end of a collection interval the required urine aliquots can be withdrawn and the remainder discarded. These collections are suitable for total radioactivity and unchanged parent quantification. Pooling of faeces samples is usually done over 24-h periods. Collected portions can be combined and homogenized, followed by aliquoting samples for the different types of analysis.

For metabolite profiling additional pooling is timesaving. To be able to describe the total excreted radioactivity, the pool should represent the excreted concentrations over the total collection period. Therefore, the samples of different collection intervals should be pooled by combining volumes or masses proportional to the total excreted amount in each collection interval. However, care must be taken not to dilute the sample pool unnecessarily by including samples collected very late after dose administration containing very low radioactivity concentrations. As a compromise between analyzing as few samples as possible and avoiding excessive dilution, two or more pools can be created whereby the most concentrated samples (e.g. 0-24 h for urine or 0-72 h for faeces) are separated from

the remaining samples. Finally, to elucidate the structure of metabolites it is recommended to use the most concentrated urine or faeces sample instead of a pool over time.

Support of the clinical study

During and after the clinical study, the collected samples will be analysed for TRA (comprising parent drug and metabolites), for unchanged parent compound and known metabolites, and for metabolite profiling, usually in this order. The next sections discuss these procedures and provide some examples of unexpected problems that could arise during this phase of the mass balance study.

Analysis of total radioactivity (TRA)

To determine the pharmacokinetics of all drug-related material and to calculate the mass balance, the total radioactivity in plasma, whole blood and excreted samples are measured. Generally, it suffices to measure the activity in urine and faeces to complete the mass balance, but sometimes additional matrices, like tears, vomitus and expired air are analysed if indicated [13]. If large amounts of radioactivity are present in these samples, an incomplete recovery of the mass balance study may be explained.

Traditionally, total radioactivity is measured by liquid scintillation counting (LSC). In short, this technique, of which the basis was discovered by Kallmann and Reynolds [53;54], is based on the transfer of energy that is emitted due to radioactive decay via aromatic hydrocarbons and a scintillator in a scintillation cocktail into photons and subsequently into electrons which can be amplified and counted. To be analysed with this technique, a sample should be clear, colourless and homogenous. While for small volumes (<1 mL) of urine and plasma a minimally 10-fold dilution in a proper scintillation cocktail is usually sufficient for the determination of ^{14}C radioactivity, whole blood and faecal homogenates require more effort. As Table 1 shows, frequently applied methods are solubilisation followed by decolourization and combustion of the sample to form $^{14}CO_2$.

Similar to other bioanalytical assays a lower limit of quantification (LLOQ) should be determined for LSC measurements. In bioanalytical method validation the LLOQ should be reproducible with a precision of ≤ 20% and an accuracy within 80 and 120% [27]. Due to the statistical character of radioactive decay, the precision of a measurement can be expressed as a probability. As in a normal distribution, the probability that the number of observed counts is within ± 2 standard deviations (2s) of the mean value is 95.5%. For convenience, the 2s value is often expressed as a percentage of the net number of counts and referred to as %2s. A formula to calculate %2s is provided in equation (5) [55;56], which is derived from basic Poisson statistics (1), the number of counts (2,3) and the rule for propagation of error (4) [55]:

$$s = \sqrt{Counts_{total}} \tag{1}$$

$$Counts_{total} = CPM \cdot T \tag{2}$$

$$Counts_{total,n} = Counts_{total,s} - Counts_{total,b} \tag{3}$$

$$s_{Counts,total,n} = \sqrt{\left(s_{Counts,total,s}\right)^2 + \left(s_{Counts,total,b}\right)^2} \tag{4}$$

$$\%2s = \frac{200\sqrt{\left(CPM_s + CPM_b\right)/T}}{CPM_s - CPM_b} \tag{5}$$

The symbol s is herein the standard deviation, $Counts_{total}$ is the total number of counts, CPM is the abbreviation of counts per minute and T is the counting time in minutes. The subscripts n, s and b refer to net, sample and the background, respectively. Applying the precision requirements of bioanalytical method validation, the %2s value should be ≤ 20% for the LLOQ. As the counting time T can be chosen and the background CPM (CPM_b) observed from a blank control sample, the LLOQ in CPM can be calculated by solving equation (5) for CPM_s to obtain (6). Subsequent application of equations (2) and (3) and entering a %2s value of 20% gives (7):

$$CPM_s = CPM_b + \frac{20000}{T \cdot \%2s^2}\left(1 + \sqrt{1 + \frac{T \cdot \%2s^2 \cdot CPM_b}{5000}}\right) \tag{6}$$

$$CPM_{net}\left(LLOQ\right) = \frac{50}{T}\left(1 + \sqrt{1 + \frac{2 \cdot T \cdot CPM_b}{25}}\right) \tag{7}$$

Finally, CPM is related to the actual radioactivity expressed in the number of disintegrations per minute (DPM) by means of a counting efficiency (E) [57]:

$$DPM = \frac{CPM}{E} \cdot 100\% \tag{8}$$

This efficiency depends on the energy of the radioactive decay and the amount of quenching, but is for ^{14}C measurements of hardly quenched samples on a liquid scintillation counter typically in the range of 90%.

While LSC is still widely applied, and used in 9 of the studies of Table 1, a more recent technique to determine the ^{14}C-radioactivity is by means of accelerator mass spectrometry (AMS). This technique relies on determination of the $^{14}C/^{12}C$ isotope ratio [58;59] and can be up to a million-fold more sensitive than LSC [60]. Since the first publication of a biomedical application of AMS in 1990 [61], the technique has extensively been reviewed in literature [62-64] and also its application in human mass balance studies has been the subject of recent reviews [1;65]. From the recent mass balance studies in oncology listed in Table 1, four used AMS to calculate the total amount of drug related ^{14}C in at least part of the samples. Obviously, the high sensitivity of this technique is a major advantage, as it allows to perform a mass balance study by administration of a ^{14}C-labelled drug at an activity in the nCi instead of the μCi range [14]. For some compounds, use of such a low activity is necessitated. An example hereof is the anti-cancer agent ixabepilone, which appeared very unstable at an activity of 100 μCi due to autoradiolysis [14]. To date, wide application of AMS is still hampered by the high costs of the instrument. Other disadvantages of AMS include the complexity of the method and sample preparation procedures that are not amenable for automation [62].

Application of the bioanalytical assays

Even if a bioanalytical quantitative assay has been developed and validated prior to the start of a mass balance study, the practical application can give problems. A problem we experienced during the mass balance study of an anti-cancer agent (eribulin) was that for one of the treated patients the unchanged parent concentration in all faecal samples was below the LLOQ. The metabolite profiling of these samples, however, indicated the presence of unchanged parent as the most prominent radioactively labelled analyte. To explore the origin of this inconsistency, the total ion chromatogram of faeces samples of this patient were compared with those of other patients (Figure 1 A and B). A huge peak was observed, and the corresponding spectrum showed the specific repeating pattern of multiply-charged ions of a polymer (Figure 1C), which was identified as polyethylene glycol (PEG). Collection devices and preparation methods were excluded from being the source of the PEG, as they were identical for all patients. Therefore, the co-medication was investigated, which revealed daily use of macrogol-3350 as prophylaxis against constipation.

Orally administered macrogol-3350 or PEG-3350 is not absorbed and primarily excreted in faeces [66]. The m/z values 726, 735, 744 and 753 that have been used in a quantitative assay for PEG-3350 in faeces [66] are prominently present in the spectrum of Figure 1C. The presence of large amounts of PEG-3350 probably caused considerable ion suppression, impeding quantification of eribulin. This example demonstrates a potential effect of co-medication. Another possible effect of co-medication is a drug-drug interaction with the investigated compound. As this may result in altered ADME properties, it is extremely important to assess co-medication. For future assay development, the sample preparation or chromatography could be optimized to minimize possible ion suppression

of PEG-3350, but also the alternative solution, exclusion of patients using macrogol on a regular basis, should be considered.

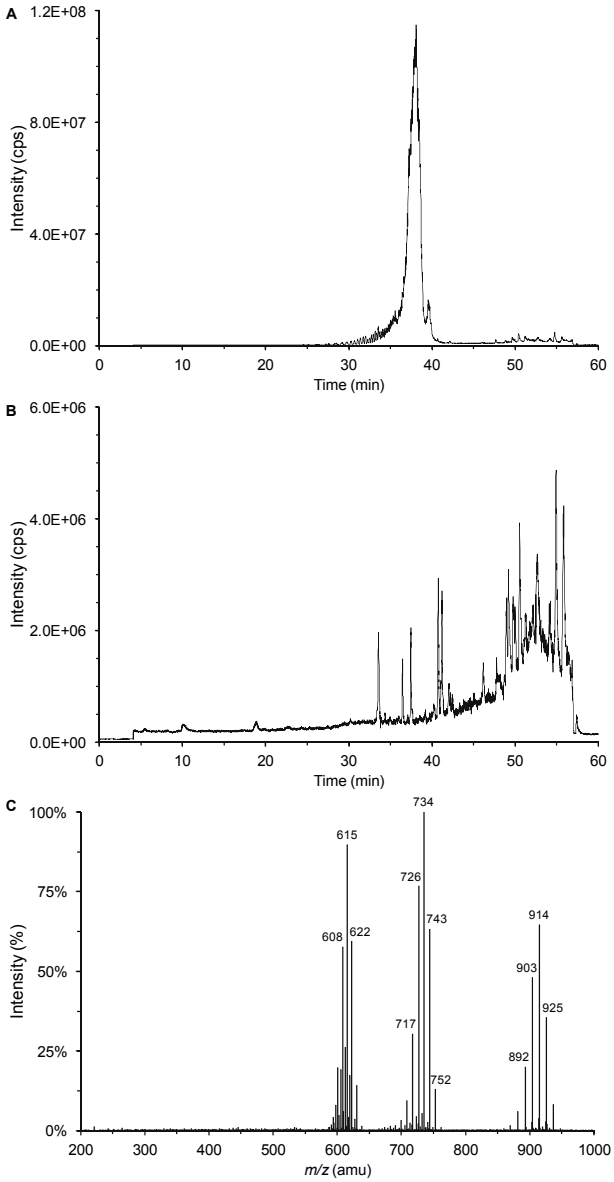

Figure 1: Total ion chromatogram of a faeces pool collected 72-168 h after administration of a single dose of ^{14}C-eribulin to a cancer patient who daily used macrogol-3350 as co-medication (A). Representative total ion chromatogram of a faeces collected 72-168 h after administration of a single dose of ^{14}C-eribulin to a cancer patient who did not use macrogol-3350 (B). Faeces samples were homogenised with water (1:3 m/v), extracted twice with acetonitrile (1:1 v/v) and diluted with water prior to injection. Panel C shows the mass spectrum of the peak in at 38 min Figure A, with m/z values typical for polyethylene glycol (PEG).

Another problem was observed during the mass balance study of trabectedin. In this study, patients received a flat dose of 1 mg trabectedin as a 24-h intravenous infusion [15]. An ultrasensitive LC-MS/MS assay (LLOQ 0.01 ng/mL) allowed quantitative analysis of unchanged trabectedin in the collected plasma samples for up to at least 48 h after start of the infusion [21]. However, after two patients, it was discovered that metabolite concentrations were too low for analysis. Therefore, it was decided to shorten the infusion time of the remaining patients to 3 h. The samples of these patients were later successfully used for metabolite profiling [24]. This example demonstrates the merit of analyzing samples during the study instead of waiting until all samples have been collected and then discovering that of the collected samples can not fully be exploited for their intended use.

Impact of the radiolabel on quantitative bioanalysis

A ^{14}C-radiolabelled dose prepared for a mass balance study is usually a mixture of radiolabelled and non-radiolabelled molecules. This may have to be accounted for in the quantification of the parent compound, as only the non-labelled molecules are normally quantified when using LC-MS/MS. When the dose is high and the molecular mass of the compound is low, the majority of the molecules is non-labelled. In this case, the presence of the labelled compound may often be neglected in the determination of the total drug concentration. However, at the other extreme, when a high-molecular mass molecule is administered in a low dose, a significant part of the molecules is radiolabelled. When LC-MS/MS is in this case applied to quantify the non-labelled parent compound, a correction should be applied to calculate the total drug concentration [11;15]. The proportion of the radiolabelled dose to the total dose may easily be calculated as described below.

An important input constant is the specific radioactivity of ^{14}C, which can be calculated using the general definition for radioactivity, the half-life of ^{14}C and the Avogadro constant. This results in a specific activity of ^{14}C of around 1.385 x10^{12} disintegrations per minute (dpm) per mol. In practice, the unit Curie (Ci) is often used to quantify radioactivity, giving 62.39 Ci/mol as specific activity of ^{14}C.

The theoretical percentage of labelled molecules can be calculated using equation (9), (10) and (11), provided that the administered dose and activity and number of ^{14}C-atoms per labelled molecule are known. First of all, the administered dose D (in g) is a combination of x mol non-labelled compound with an average molar mass $M_{w(non\text{-}labelled)}$ and y mol labelled compound with an average molar mass $M_{w(labelled)}$:

$$D = x \cdot M_{w(non-labelled)} + y \cdot M_{w(labelled)} \qquad (9)$$

Secondly, the administered activity A (in Ci) is the product of the amount of labelled compound y (in mol), the number of ^{14}C atoms per molecule (n) and the specific activity of ^{14}C (in Ci/mol):

$$A = y \cdot n \cdot A_{m(^{14}C)} \tag{10}$$

Now y can be calculated from (10) and entered in (9) to calculate x, as all other constants are known. The theoretical percentage of labelled molecules can then be calculated with (11):

$$Percentage_{labelled} = \frac{y}{x+y} \cdot 100\% \tag{11}$$

Taking the mass balance study of brivanib as an example [10], the values to enter in (9) and (10) are D = 0.80 g, $M_{w(non\text{-}labelled)}$ = 441.46 g/mol, $M_{w(labelled)}$= 443.45 g/mol, A = $100 \cdot 10^{-6}$ Ci, n = 1 and $A_{m(14C)}$ = 62.39 Ci/mol. This results in y = $1.6 \cdot 10^{-6}$ mol and x = $1.81 \cdot 10^{-3}$ mol, giving a theoretical percentage of labelled molecules of 0.088%. So, in this case the proportion of the labelled dose to the total dose is negligible and the concentrations can be determined by measuring the non-labelled parent compound. In contrast, the mass balance study of trabectedin is an example in which the contribution of the labelled compound cannot be neglected at all. For this study, the values would be D = $1.0 \cdot 10^{-3}$ g, $M_{w(non\text{-}labelled)}$ = 761.8 g/mol, $M_{w(labelled)}$= 763.8 g/mol, A = $70 \cdot 10^{-6}$ Ci, n = 1 and $A_{m(14C)}$ = 62.39 Ci/mol. The resulting y = $1.12 \cdot 10^{-6}$ mol and x = $0.188 \cdot 10^{-6}$ mol give a theoretical percentage of labelled molecules of 86%. It was very helpful to know this percentage beforehand, as the mass detector settings of the LC-MS/MS method to quantify trabectedin were for samples of this study adjusted to quantify ^{14}C-trabectedin and these concentrations were back-calculated to obtain the total concentrations of trabectedin [15].

Alternatively to the theoretical approach, the percentage of labelled molecules can be derived experimentally, using LC-MS [11]. If the percentage of labelled molecules is substantial, a correction factor should be applied to the result of quantification to obtain the concentrations of labelled and non-labelled compound combined.

Metabolite profiling

Metabolite profiling aims to detect, quantify and identify metabolites. This requires another tailored approach than standard quantitative bioanalytical analysis. In this section we will limit our focus on the techniques that were used for metabolite profiling in the recent mass balance studies (Table 3) and we will highlight a few points needing attention during metabolite profiling. For further reading on metabolite profiling, we refer to recent excellent reviews on this topic [67-69].

Metabolite profiling comprises sample pooling to limit the number of samples to analyze, sample preparation to make the sample compatible with the detection technique, separation to distinguish between metabolites and detection for structural elucidation of metabolites. The latter is often performed by combining several techniques, such as mass-

spectrometry, especially high-resolution mass spectrometry, NMR and enzyme incubation experiments with for example glucuronidases to aid identification of glucuronide metabolites. Table 3 summarises how the metabolite profiling was performed in the recent mass balance studies in oncology.

The first point of attention is the recovery of sample preparation. If samples are used for quantitative analysis, the loss of radioactivity during each step of the sample preparation should be monitored. This reveals if and where analyte loss occurs. Recovery of faeces sample preparation may be limited to 75-85% due to the inaccessible nature of the sample. To complete the mass balance, the sample preparation recovery should be taken into account. One approach to deal with an incomplete recovery is to treat the non-extracted radioactivity as a separate group. Alternatively, if a non-selective method is applied, the quantitative data can be corrected for the recovery. In case of extreme low faeces sample preparation recovery, like the 35% in the trabectedin mass balance study [24], additional investigation to find the source of the loss is recommended. In the case of trabectedin it was discovered that the recovery of radioactivity could be improved by treatment with acid, however, the recovery gained was lost during subsequent evaporation of the sample, implying the presence of small volatile compounds containing the ^{14}C label. Therefore, correction for the recovery would have given misleading quantitative results.

Also if a low recovery is observed for plasma, especially if a trend is observed over the collection time, extra caution is warranted. The low recovery might indicate the presence of (active) metabolites, covalently bound to plasma proteins. For example acyl glucuronides and thiol-group containing metabolites can bind with proteins [70;71]. The latter form disulfide conjugates with thiol-groups of proteins, such as from cysteine. A strategy to reveal this type of non-extractable metabolites is reduction of the disulfide bonds by incubation of plasma samples with a reducing agent like dithiotreitol (DTT) before further sample preparation [71].

As Table 3 shows, the separation of samples for metabolite profiling often requires a long run-time. This is one of the reasons to minimize the number of samples by pooling within or across subjects. The trend to use columns with sub-2 μm particles and ultra-performance liquid chromatography (UPLC) is not (yet) observed in the recent mass balance studies. This is probably because in case of off-line detection, enhanced peak resolution of an UPLC column is often not visible in the radiochromatogram as the resolution of the peaks depends on the size of the collected fractions. Particularly if LSC or AMS is applied to determine the radioactivity in the fractions, the fraction size is large. Additionally, each fraction should be prepared and counted individually, making the process very laborious. Probably this explains that the most popular method used to detect and to quantify metabolites is to collect HPLC-fractions with a 96-well plate suitable for microplate scintillation counting (HPLC-MSC). With this technique, the samples can be prepared by batch of 96 and counted by batches of 12 in a microplate scintillation counter,

thereby saving effort and time. Recently, a multi-microplate fraction collector has been evaluated which made it possible to collect fractions in up to 24 96-well or 384-well plates without manual intervention. Combined with UPLC this system provided high resolution radiochromatograms with minimum manual input [72]. Online radioflow detection (HPLC-RFD) also requires minimal manual input, but suffers from poor sensitivity due to the short residence times of the radioactive peaks in the detection cell [56]. Despite developments to increase the residence time and thereby the sensitivity, like stop-flow HPLC-RFD [73], or variable-flow HPLC-RFD [74] the application of radioflow detection in metabolite profiling is limited.

Another point of attention is the potential presence of metabolites that do not contain the radioactive label. When a radioactively labelled isotope is prepared, it is aimed to position the ^{14}C label at a metabolically stable site. Bioanalytical scientists or drug metabolism specialists should be involved to select a suitable site, which is often in the backbone of the molecular structure and may increase the synthetic complexity of the compound. As demonstrated by Lenz *et al*, who studied the metabolism of zibotentan in animals and human, a metabolically stable position is not always predictable. They had to repeat part of their study with double-labelled zibotentan after discovering that the ^{14}C label of the originally used single-labelled ^{14}C- zibotentan was lost as $^{14}CO_2$ in expired air from rats [75]. Another possibility is that a singly-labelled parent compound is metabolically split into two parts of similar size whereby only one part contains the label. In the mass balance study of E7070 (indisulam) this was anticipated and two ^{14}C-labeled isotopes of E7070 were prepared and used, with the ^{14}C-atom situated in different parts of the molecule [76]. While numerous methods exist to find metabolites without a radioactive label, like comparison of pre-dose and post-dose samples, knowledge-based prediction of metabolites and various data mining techniques, the quantification of these metabolites is problematic.

Reporting

The final step of a mass balance study is to report the results. The challenge in this is to combine the results that were obtained in order to fulfil the four purposes of sample analysis in a mass balance study: quantitative analysis of TRA, quantitative analysis of unchanged parent drug and known metabolites, qualitative/quantitative analysis of metabolites and structural elucidation of the unknown metabolites. As different techniques, each with their own analytical errors and shortcomings, are used for these analyses, inconsistencies may present. For example, if the LLOQ of the total radioactivity assay in urine or faeces is higher than the LLOQ of the unchanged parent compound assay and the formation of metabolites is limited, the calculated recovery of the unchanged parent compound can be more than the calculated recovery of the total radioactivity, which is not possible. In this case the accumulated radioactivity of samples below the LLOQ causes an underestimation of the recovered radioactivity. Also the reverse is possible, whereby the LLOQ of the unchanged parent compound assay is higher, resulting in an underestimation of the recovered parent compound [11;15].

Table 3: Overview of metabolite profiling techniques used in recent clinical mass balance studies in oncology

Parent	Mx.	Pooling strategy[a]						Sample preparation	
		Indiv. samples	Eq. vol. sel. time points	Over indicated period (h)	Across subj.	Prop. tot.	Other	Technique	Recovery (%)
BIBF1120	Pl		√		√			SPE/ lyoph./	89
	Ur			0-24				extraction	96
	Fa			0-72				Extraction	99
BMS-690514	Pl		√		√			Extraction	75-97
	Ur			0-192	√	√			
	Fa			0-192	√	√		Extraction	>100
	Bi			3-8	√[b]	√			
Brivanib	Pl		√		√			PPT/extraction	>90
	Ur			0-288		√		Extraction	
	Fa			0-192		√		Extraction	85-95
Eribulin	Pl	√	√		√			PPT	87.7
	Ur			0-24, 24-48, 48-72, 72-168		√		Direct injection	
	Fa			0-24, 24-48, 48-72, 72-168		√		Extraction	87.5
Imatinib	Pl		√		√			PPT	88.2-95.4
	Ur			0-24, 0-72	√			Centrifugation	100
	Fa			0-48, 0-168	√			Extraction	94-95
Irofulven	Pl	√						Extraction	?
	Ur	√						Extraction	?
Ixabepilone	Pl		√		√			PPT	73 and 76
	Ur			0-168	√	√		Direct injection	?
	Fa			0-168	√	√		Extractions	~77
Trabectedin	Ur			0-24	√[b]			Direct injection	
	Fa			0-120	√[b]			Extraction	~35
Vatalanib	Pl						√[c]	On-line clean-up	76-81
	Ur			0-48				On-line clean-up	76-81
	Fa			0-48				Extraction	68-83
Vismodegib	Pl		√		√			PPT/extraction	84.3
	Ur			0-312	√	√		Direct injection	
	Fa			0-72, 72-312	√	√		Extraction	84.7
Zibotentan	Pl						√[f]	PPT	89.9
	Ur			0-72		√		Lyophilisation	
	Fa			0-120		√		Extraction	76.2

Abbreviations: Mx: matrix; Quant.: quantification; Rf.: reference; Indiv.: individual; Eq. vol. sel. time points: equal volumes of selected time points; subj.: subjects; Prop. tot.: proportionally to total excreted amount; LSC: liquid scintillation counting; MSC: multiplate scintillation counting; AMS: accelerated mass spectrometry; T_{frac}.: time per fraction; RFD: radio flow detection; PDA: photo-diode array detection; HR-MS: high-resolution mass spectrometry; NMR: nuclear magnetic resonance; Ref. comp.: comparison with reference compounds; Pl: plasma; Ur: urine, Fa: faeces; SPE: solid phase extraction; lyoph.: lyophilisation; PPT: protein precipitation.

HPLC separation		Detection / Quantification	Metabolite structure elucidation								Rf.
Time (min)	Column		UV/PDA	MS	MS/MS	MS^n	HR-MS	NMR	Ref. comp.	Other	
>45	ProC18 HD, 5 µm, 150 x 4.6 mm I.D.	MSC (off-line) and RFD (online)				√	√	√	√		[8]
60	YMC ODS-AQ, 5 µm, 150 x 4.6 mm I.D.	MSC (off-line)				√			√		[9]
>69	Zorbax SB C18, 5 µm, 250 x 4.6 mm I.D.	MSC (off-line)				√		√	√		[82]
60	Synergi polar RP, 4 µm, 150 x 4.6 mm I.D.	LSC (off-line)				√	√		√		[11]
?	Symmetry C18, 3.5 µm, 150 x 4.6 mm I.D.	MSC (off-line) and UV (online)					√		√	√[c]	[12]
? / 30	Alltima C18, 5 µm, 250 x 4.6 mm I.D./ Uptisphere C18, 5 µm, 150 x 1 mm I.D.	UV (online)	√		√				√	√[d]	[13]
>50	Symmetry shield RP8, 3.5 µm, 150 x 4.6 mm I.D.	AMS (off-line)	√		√	√			√		[83]
>65	Kromasil C18, 5 µm, 250 x 4.6 mm I.D.	LSC (off-line)			√				√	√[d]	[24]
?	Xterra MS C18, 5 µm, 150 x 3.0 mm I.D.	MSC (off-line) and RFD (online)				√	√		√		[16]
100	Synergi Hydro RP 80A , 4 µm, 250 x 4.6 mm I.D.	AMS (off-line)				√	√				[17]
>35	Zorbax Rx-C18, 250 x 4.6 mm I.D.	RFD (online) and UV (online)		√							[75]

[a]Only pooling strategy and sample preparation procedures for metabolite detection/quantification is described. Other pooling strategies and sample preparation procedures may have been used for metabolite identification [b]Also for individual subjects [c]Hydrogen-deuterium exchange [d]β-glucuronidase incubation [e]AUC pool over 0.5-12 h [f]0-24 h, equal volumes from each subject

Another example of an inconsistency can arise due to difference in methods. As discussed previously, the correction for sample preparation recovery differs between the bioanalytical assay, whereby often an internal standard is used, and metabolite profiling, whereby the remaining radioactivity in discarded pellets is used. This may lead to a difference in the calculated recovered unchanged parent compound between the two methods. These and other type of inconsistencies lead to an either incomplete or "overcomplete" mass balance with recoveries below or above 100%, respectively. Therefore, the origin of such inconsistencies should be investigated and, if possible, an estimation of the true recovery should be made.

Now with all the data available, the results are normally presented as pharmacokinetic parameters, concentration-time curves, cumulative recovery curves, tables with quantitative or structural information of metabolites in the different matrices, and a metabolic scheme with the structures or descriptions of the metabolites. To simplify the direct understanding of the quantitative results, we propose to add a summarizing schematic overview, containing the main findings of the mass balance study. We will illustrate this using the hypothetical compound X as an example, and make two schemes containing the following data: the presence of compound X and its metabolites in plasma and the excretion balance of compound X (Figure 2).

Figure 2 presents an example of a summarising schematic overview of a hypothetical mass balance study. In this study, ^{14}C-compound X is administered to n subjects, followed by collection of blood samples and urine and faeces until a pre-specified time point. Total radioactivity is measured in all samples, compound X and its known metabolite X-M1 are quantified in plasma and urine using a validated bioanalytical assay. Metabolite profiling is performed on plasma samples pooled with the AUC method and on urine and faeces pools representative for the total amount of excreted urine and faeces. The mean plasma AUC of the total radioactivity, unchanged compound X and X-M1 were calculated from individual plasma samples and expressed in equivalents of compound X, to be able to compare the AUC values. In the AUC pooled plasma samples two new metabolites were identified, X-M2 and X-M3. It was further observed that the column recovery of the injected radioactivity was not 100% and there were some small peaks present in the radiochromatogram (below the limit of quantification) which were not attributed. A significant amount of radioactivity was not recovered during the sample preparation and covalent binding of metabolite(s) to plasma proteins was suspected. Therefore, a plasma incubation experiment with a reducing agent was performed, resulting in the discovery of another metabolite, X-M4, of which the AUC was estimated. A small portion of the radioactivity remained non-extractable. Regarding the excretion balance, total radioactivity measurements were used to assess the recovery in urine and faeces. The mean total amount of compound X and X-M1, converted to equivalents of compound X, were determined with the validated assay and expressed as a percentage of the administered dose. Metabolite

profiling of urine and faeces resulted in the identification of an additional part of the administered dose.

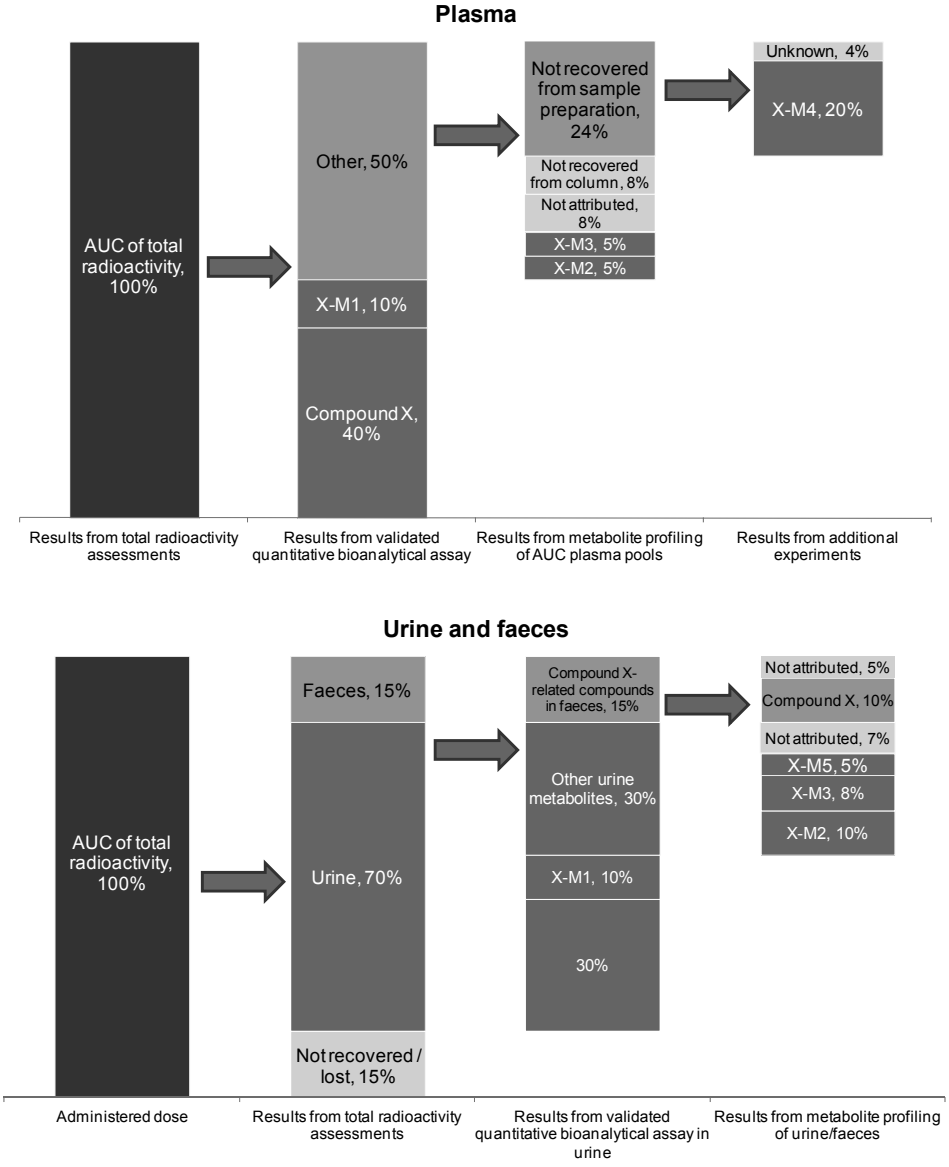

Figure 2: Example of a schematic overview that is helpful to present results of a mass balance study. These schemes summarise the results of a hypothetical mass balance study with compound X. The upper panel displays the composition of the total drug-related plasma area under the concentration-time curve (AUC). AUC values of X, its metabolites (X-M1, X-M2, etc.) and undefined compound-related material (other, not recovered, etc.) are expressed in percentage of the AUC of total radioactivity. The lower panel displays the excretion balance. In this panel all amounts are expressed in a percentage of the administered dose.

In practice, a mass balance study may be more complex and reveal many more metabolites of which the quantification is less straightforward, but if it is possible to present the results in schemes like or adapted from those in Figure 2, the results are clear and understandable in one view.

Future perspective

As a result of the rich information they provide, mass balance studies will continue to play an important role in drug development. Still, they have some drawbacks, like the exposure of volunteering subjects to radioactivity, the substantial investment to produce a radioactively labelled compound and the considerable amount of time and effort required to detect and elucidate the metabolites. Recent and future developments in bioanalysis aim to diminish these drawbacks.

The first development is the growing interest in the use of Phase 0 studies for mass balance purposes. In this type of study, a microdose of an investigational drug with a radioactivity in the nCi range is administered to humans, and the highly sensitive technique AMS is used used to quantify the low concentrations of total radioactivity and (in combination with HPLC) to produce radiochromatograms for metabolite profiling [62;65;77;78]. However, the costs, size and complexity of AMS will have to be reduced to make wide application possible.

The second direction may have more potential for the near future, as the investments required are less. This direction maintains the conventional radioactive doses of around 100 μCi, but uses high-resolution and high-throughput techniques, like the multi-microplate fraction collector combined with microplate scintillation counting for metabolite profiling [72], to reduce the labour-intensity of a mass balance study. Regarding the detection of unknown metabolites, data mining methods that can be applied to mass spectrometry data have high potency, especially in combination with high-resolution mass data. Methods like mass defect filtering, isotope pattern filtering and background subtraction make it much easier to detect metabolites in the huge amounts of data [68;79;80].

A final interesting development for the future of mass balance studies is the integration of the techniques used for the different purposes of the study samples. For example, when using high-resolution mass spectrometry for quantitative bioanalysis, the produced data may evenly be used to detect and identify metabolites, by application of a data mining method [81], likewise, when combining ULPC with off-line MSC and high resolution mass spectrometry with increasing collision energy (MS^E), detection, quantification and structural elucidation (by interpretation of the fragmentation spectra) can be realised within a single run.

Financial & competing interest disclosure

The authors have no relevant financial involvement with any organization or entity with a financial interest in or financial conflict with the subject matter or materials discussed in the manuscript. This includes employment, consultancies, honoraria, stock ownership or options, expert testimony, grants or patents received or pending, or royalties. No writing assistance was utilized in the production of this manuscript.

Executive summary

Mass balance studies

- Investigate the absorption, distribution, metabolism and elimination of a drug;
- Bring about some typical bioanalytical challenges and aspects: quantification of multiple analytes in various biological matrices, sample storage and pooling procedures, quantification of unchanged parent drug with a radiolabel and the combination of multiple analytical techniques;
- Provide a myriad of information but have as drawbacks the exposure of humans to radioactivity and the labour-intensity of the sample analysis, especially for metabolite profiling.

Future perspective

- Increase in the execution of mass balance studies as Phase 0 studies with a microdose and microtracer, using the ultrasensitive accelerator mass spectrometry (AMS) for sample analysis;
- Improvement of the throughput of sample analysis with new sample processing and data mining techniques.

References

[1] Beumer JH, Beijnen JH, Schellens JH, Mass balance studies, with a focus on anticancer drugs, *Clin.Pharmacokinet.*, **45** (2006) 33-58.
[2] Schellens JHM, in J.H.M.Schellens, H.L.McLeod, and D.R.Newell (Editors), Cancer Clinical Pharmacology, Oxford university press, 2005, p. 30.
[3] Giraud B, Hebert G, Deroussent A, Veal GJ, Vassal G, Paci A, Oxazaphosphorines: new therapeutic strategies for an old class of drugs, *Expert.Opin.Drug Metab Toxicol.*, **6** (2010) 919-938.
[4] US FDA, Mitoxantrone, www.drugs.com/pro/mitoxantrone.html, (2011), Accessed at: 4-8-2011
[5] US FDA, Department of Health and Human Services, Guidance for Industry, Safety testing of Drug Metabolites, www.fda.gov/downloads/Drugs/GuidanceComplianceRegulatoryInformation/Guidances/ucm079266.pdf, (2008), Accessed at: 4-8-2011
[6] ICH, Topic M 3 (R2), Non-Clinical Safety Studies for the Conduct of Human Clinical Trials and Marketing Authorization for Pharmaceuticals,

www.ema.europa.eu/docs/en_GB/document_library/Scientific_guideline/2009/09/WC500002720.pdf, (2009), Accessed at: 4-8-2011
[7] Penner N, Klunk LJ, Prakash C, Human radiolabeled mass balance studies: objectives, utilities and limitations, *Biopharm.Drug Dispos.*, **30** (2009) 185-203.
[8] Stopfer P, Rathgen K, Bischoff D, Ludtke S, Marzin K, Kaiser R, Wagner K, Ebner T, Pharmacokinetics and metabolism of BIBF 1120 after oral dosing to healthy male volunteers, *Xenobiotica*, **41** (2011) 297-311.
[9] Christopher LJ, Hong H, Vakkalagadda BJ, Clemens PL, Su H, Roongta V, Allentoff A, Sun H, Heller K, Harbison CT, Iyer RA, Humphreys WG, Wong T, Zhang S, Metabolism and disposition of [14C]BMS-690514, an ErbB/vascular endothelial growth factor receptor inhibitor, after oral administration to humans, *Drug Metab Dispos.*, **38** (2010) 2049-2059.
[10] Mekhail T, Masson E, Fischer BS, Gong J, Iyer R, Gan J, Pursley J, Patricia D, Williams D, Ganapathi R, Metabolism, excretion, and pharmacokinetics of oral brivanib in patients with advanced or metastatic solid tumors, *Drug Metab Dispos.*, **38** (2010) 1962-1966.
[11] Dubbelman AC, Rosing H, Jansen RS, Mergui-Roelvink M, Huitema ADR, Koetz B, Lymboura M, Reyderman L, Lopez-Anaya A, Schellens JHM, Beijnen JH, Mass balance study of 14C-eribulin in patients with advanced solid tumours, *Drug Metab Dispos.*, (2011).
[12] Gschwind HP, Pfaar U, Waldmeier F, Zollinger M, Sayer C, Zbinden P, Hayes M, Pokorny R, Seiberling M, Ben Am M, Peng B, Gross G, Metabolism and disposition of imatinib mesylate in healthy volunteers, *Drug Metab Dispos.*, **33** (2005) 1503-1512.
[13] Paci A, Rezai K, Deroussent A, De Valeriola D, Re M, Weill S, Cvitkovic E, Kahatt C, Shah A, Waters S, Weems G, Vassal G, Lokiec F, Pharmacokinetics, metabolism, and routes of excretion of intravenous irofulven in patients with advanced solid tumors, *Drug Metab Dispos.*, **34** (2006) 1918-1926.
[14] Beumer JH, Garner RC, Cohen MB, Galbraith S, Duncan GF, Griffin T, Beijnen JH, Schellens JH, Human mass balance study of the novel anticancer agent ixabepilone using accelerator mass spectrometry, *Invest New Drugs*, **25** (2007) 327-334.
[15] Beumer JH, Rademaker-Lakhai JM, Rosing H, Lopez-Lazaro L, Beijnen JH, Schellens JH, Trabectedin (Yondelis, formerly ET-743), a mass balance study in patients with advanced cancer, *Invest New Drugs*, **23** (2005) 429-436.
[16] Jost LM, Gschwind HP, Jalava T, Wang Y, Guenther C, Souppart C, Rottmann A, Denner K, Waldmeier F, Gross G, Masson E, Laurent D, Metabolism and disposition of vatalanib (PTK787/ZK-222584) in cancer patients, *Drug Metab Dispos.*, **34** (2006) 1817-1828.
[17] Graham RA, Lum BL, Morrison G, Chang I, Jorga K, Dean BJ, Shin Y, Yue Q, Mulder T, Malhi V, Xie M, Low J, Hop CE, A Single Dose Mass Balance Study of the Hedgehog Pathway Inhibitor Vismodegib (GDC-0449) in Humans Using Accelerator Mass Spectrometry, *Drug Metab Dispos.*, (2011).
[18] Stokvis E, Rosing H, Beijnen JH, Liquid chromatography-mass spectrometry for the quantitative bioanalysis of anticancer drugs, *Mass Spectrom.Rev.*, **24** (2005) 887-917.
[19] Chuk MK, Balis FM, Fox E, Trabectedin, *Oncologist.*, **14** (2009) 794-799.
[20] US FDA, Halaven, www.drugs.com/pro/halaven.html, (2010), Accessed at: 4-8-2011
[21] Rosing H, Hillebrand MJ, Jimeno JM, Gomez A, Floriano P, Faircloth G, Henrar RE, Vermorken JB, Cvitkovic E, Bult A, Beijnen JH, Quantitative determination of Ecteinascidin 743 in human plasma by miniaturized high-performance liquid chromatography coupled with electrospray ionization tandem mass spectrometry, *J.Mass Spectrom.*, **33** (1998) 1134-1140.
[22] Dubbelman AC, Rosing H, Thijssen B, Lucas L, Copalu W, Wanders J, Schellens JH, Beijnen JH, Validation of high-performance liquid chromatography-tandem mass spectrometry assays for the quantification of eribulin (E7389) in various biological matrices, *J.Chromatogr.B Analyt.Technol.Biomed.Life Sci.*, **879** (2011) 1149-1155.
[23] Bakhtiar R, Lohne J, Ramos L, Khemani L, Hayes M, Tse F, High-throughput quantification of the anti-leukemia drug STI571 (Gleevec) and its main metabolite (CGP 74588) in human plasma using liquid chromatography-tandem mass spectrometry, *J.Chromatogr.B Analyt.Technol.Biomed.Life Sci.*, **768** (2002) 325-340.

[24] Beumer JH, Rademaker-Lakhai JM, Rosing H, Hillebrand MJ, Bosch TM, Lopez-Lazaro L, Schellens JH, Beijnen JH, Metabolism of trabectedin (ET-743, Yondelis) in patients with advanced cancer, *Cancer Chemother.Pharmacol.*, **59** (2007) 825-837.
[25] Morgan B, Thomas AL, Drevs J, Hennig J, Buchert M, Jivan A, Horsfield MA, Mross K, Ball HA, Lee L, Mietlowski W, Fuxuis S, Unger C, O'Byrne K, Henry A, Cherryman GR, Laurent D, Dugan M, Marme D, Steward WP, Dynamic contrast-enhanced magnetic resonance imaging as a biomarker for the pharmacological response of PTK787/ZK 222584, an inhibitor of the vascular endothelial growth factor receptor tyrosine kinases, in patients with advanced colorectal cancer and liver metastases: results from two phase I studies, *J.Clin.Oncol.*, **21** (2003) 3955-3964.
[26] Ding X, Chou B, Graham RA, Cheeti S, Percey S, Matassa LC, Reuschel SA, Meng M, Liu S, Voelker T, Lum BL, Rudewicz PJ, Hop CE, Determination of GDC-0449, a small-molecule inhibitor of the Hedgehog signaling pathway, in human plasma by solid phase extraction-liquid chromatographic-tandem mass spectrometry, *J.Chromatogr.B Analyt.Technol.Biomed.Life Sci.*, **878** (2010) 785-790.
[27] US FDA, Department of Health and Human Services, Guidance for Industry, Bioanalytical Method Validation, www.fda.gov/downloads/Drugs/GuidanceComplianceRegulatoryInformation/Guidances/ucm070107.pdf, (2001), Accessed at: 9-1-2012
[28] Chang MS, Ji Q, Zhang J, El-Shourbagy TA, Historical review of sample preparation for chromatographic bioanalysis: pros and cons, *Drug Development Research*, **68** (2007) 107-133.
[29] Beijnen JH and Rosing H, in J.H.M.Schellens, H.L.McLeod, and D.R.Newell (Editors), Cancer Clinical Pharmacology, Oxford university press, 2005, p. 1.
[30] Pucci V, Di Palma S, Alfieri A, Bonelli F, Monteagudo E, A novel strategy for reducing phospholipids-based matrix effect in LC-ESI-MS bioanalysis by means of HybridSPE, *J.Pharm.Biomed.Anal.*, **50** (2009) 867-871.
[31] Jiang H, Zhang Y, Ida M, Lafayette A, Fast DM, Determination of carboplatin in human plasma using HybridSPE-precipitation along with liquid chromatography-tandem mass spectrometry, *J.Chromatogr.B Analyt.Technol.Biomed.Life Sci.*, **879** (2011) 2162-2170.
[32] Kole PL, Venkatesh G, Kotecha J, Sheshala R, Recent advances in sample preparation techniques for effective bioanalytical methods, *Biomed.Chromatogr.*, **25** (2011) 199-217.
[33] Vogeser M, Kirchhoff F, Progress in automation of LC-MS in laboratory medicine, *Clin.Biochem.*, **44** (2011) 4-13.
[34] Stokvis E, Rosing H, Lopez-Lazaro L, Beijnen JH, Simple and sensitive liquid chromatographic quantitative analysis of the novel marine anticancer drug Yondelis (ET-743, trabectedin) in human plasma using column switching and tandem mass spectrometric detection, *J.Mass Spectrom.*, **39** (2004) 431-436.
[35] Vainchtein LD, Rosing H, Schellens JH, Beijnen JH, A new, validated HPLC-MS/MS method for the simultaneous determination of the anti-cancer agent capecitabine and its metabolites: 5'-deoxy-5-fluorocytidine, 5'-deoxy-5-fluorouridine, 5-fluorouracil and 5-fluorodihydrouracil, in human plasma, *Biomed.Chromatogr.*, **24** (2010) 374-386.
[36] Viswanathan CT, Bansal S, Booth B, DeStefano AJ, Rose MJ, Sailstad J, Shah VP, Skelly JP, Swann PG, Weiner R, Quantitative bioanalytical methods validation and implementation: best practices for chromatographic and ligand binding assays, *Pharm.Res.*, **24** (2007) 1962-1973.
[37] Jian W, Edom RW, Xu Y, Gallagher J, Weng N, Potential bias and mitigations when using stable isotope labeled parent drug as internal standard for LC-MS/MS quantitation of metabolites, *J.Chromatogr.B Analyt.Technol.Biomed.Life Sci.*, **878** (2010) 3267-3276.
[38] Ciccimaro E, Blair IA, Stable-isotope dilution LC-MS for quantitative biomarker analysis, *Bioanalysis.*, **2** (2010) 311-341.
[39] Teunissen SF, Jager NG, Rosing H, Schinkel AH, Schellens JH, Beijnen JH, Development and validation of a quantitative assay for the determination of tamoxifen and its five main phase I metabolites in human serum using liquid chromatography coupled with tandem mass spectrometry, *J.Chromatogr.B Analyt.Technol.Biomed.Life Sci.*, **879** (2011) 1677-1685.
[40] Jansen RS, Rosing H, Schellens JH, Beijnen JH, Simultaneous quantification of 2',2'-difluorodeoxycytidine and 2',2'-difluorodeoxyuridine nucleosides and nucleotides in white

blood cells using porous graphitic carbon chromatography coupled with tandem mass spectrometry, *Rapid Commun.Mass Spectrom.*, **23** (2009) 3040-3050.
[41] Furlong MT, Wujcik CE, Ji C, Su Y, Identifying and overcoming bioanalytical challenges associated with chlorine-containing dehydrogenation metabolites, *Rapid Commun.Mass Spectrom.*, **24** (2010) 3092-3102.
[42] Zhang NR, Yu S, Tiller P, Yeh S, Mahan E, Emary WB, Quantitation of small molecules using high-resolution accurate mass spectrometers - a different approach for analysis of biological samples, *Rapid Commun.Mass Spectrom.*, **23** (2009) 1085-1094.
[43] Jemal M, Ouyang Z, Xia YQ, Systematic LC-MS/MS bioanalytical method development that incorporates plasma phospholipids risk avoidance, usage of incurred sample and well thought-out chromatography, *Biomed.Chromatogr.*, **24** (2010) 2-19.
[44] Kruger R, Vogeser M, Burghardt S, Vogelsberger R, Lackner KJ, Impact of glucuronide interferences on therapeutic drug monitoring of posaconazole by tandem mass spectrometry, *Clin.Chem.Lab Med.*, **48** (2010) 1723-1731.
[45] Tong W, Chowdhury SK, Chen JC, Zhong R, Alton KB, Patrick JE, Fragmentation of N-oxides (deoxygenation) in atmospheric pressure ionization: investigation of the activation process, *Rapid Commun.Mass Spectrom.*, **15** (2001) 2085-2090.
[46] Srinivas NR, Applicability of bioanalysis of multiple analytes in drug discovery and development: review of select case studies including assay development considerations, *Biomed.Chromatogr.*, **20** (2006) 383-414.
[47] Rowland M and Tozer TN, Clinical Pharmacokinetics: concepts and applications, Lippincott Williams & Wilkins, 1995, p. 11.
[48] Ji AJ, Jiang Z, Livson Y, Davis JA, Chu JX, Weng N, Challenges in urine bioanalytical assays: overcoming nonspecific binding, *Bioanalysis.*, **2** (2010) 1573-1586.
[49] Schrijvers D, Role of red blood cells in pharmacokinetics of chemotherapeutic agents, *Clin.Pharmacokinet.*, **42** (2003) 779-791.
[50] Hughes NC, Bajaj N, Fan J, Wong EY, Assessing the matrix effects of hemolyzed samples in bioanalysis, *Bioanalysis.*, **1** (2009) 1057-1066.
[51] Vishwanathan K, Babalola K, Wang J, Espina R, Yu L, Adedoyin A, Talaat R, Mutlib A, Scatina J, Obtaining exposures of metabolites in preclinical species through plasma pooling and quantitative NMR: addressing metabolites in safety testing (MIST) guidance without using radiolabeled compounds and chemically synthesized metabolite standards, *Chem.Res.Toxicol.*, **22** (2009) 311-322.
[52] Hamilton RA, Garnett WR, Kline BJ, Determination of mean valproic acid serum level by assay of a single pooled sample, *Clin.Pharmacol.Ther.*, **29** (1981) 408-413.
[53] Kallman H, Scintillation counting with solutions, *Phys.Rev.*, **78** (1950) 621-622.
[54] Reynolds GT, Harrison FB, Salvini G, Liquid scintillation counters, *Phys.Rev.*, **78** (1950) 488.
[55] Kessler MJ, in M.F.L'Annunziata (Editor), Handbook of radioactivity analysis, Academic Press, 1998, p. 387.
[56] Zhu M, Zhao W, Vazquez N, Mitroka JG, Analysis of low level radioactive metabolites in biological fluids using high-performance liquid chromatography with microplate scintillation counting: method validation and application, *J.Pharm.Biomed.Anal*, **39** (2005) 233-245.
[57] L'Annunziata MF and Kessler MJ, in M.F.L'Annunziata (Editor), Handbook of radioactivity analysis, Academic Press, 1998, p. 209.
[58] Nelson DE, Korteling RG, Stott WR, Carbon-14: direct detection at natural concentrations, *Science*, **198** (1977) 507-508.
[59] Bennett CL, Beukens RP, Clover MR, Gove HE, Liebert RB, Litherland AE, Purser KH, Sondheim WE, Radiocarbon dating using electrostatic accelerators: negative ions provide the key, *Science*, **198** (1977) 508-510.
[60] Garner RC, Barker J, Flavell C, Garner JV, Whattam M, Young GC, Cussans N, Jezequel S, Leong D, A validation study comparing accelerator MS and liquid scintillation counting for analysis of 14C-labelled drugs in plasma, urine and faecal extracts, *J.Pharm.Biomed.Anal.*, **24** (2000) 197-209.

[61] Turteltaub KW, Felton JS, Gledhill BL, Vogel JS, Southon JR, Caffee MW, Finkel RC, Nelson DE, Proctor ID, Davis JC, Accelerator mass spectrometry in biomedical dosimetry: relationship between low-level exposure and covalent binding of heterocyclic amine carcinogens to DNA, *Proc.Natl.Acad.Sci.U.S.A*, **87** (1990) 5288-5292.
[62] Arjomand A, Accelerator mass spectrometry-enabled studies: current status and future prospects, *Bioanalysis.*, **2** (2010) 519-541.
[63] Keck BD, Ognibene T, Vogel JS, Analytical validation of accelerator mass spectrometry for pharmaceutical development, *Bioanalysis.*, **2** (2010) 469-485.
[64] Vogel JS, Giacomo JA, Schulze-Konig T, Keck BD, Lohstroh P, Dueker S, Accelerator mass spectrometry best practices for accuracy and precision in bioanalytical (14)C measurements, *Bioanalysis.*, **2** (2010) 455-468.
[65] Dueker SR, Lohstroh PN, Giacomo JA, Le TV, Keck BD, Vogel JS, Early human ADME using microdoses and microtracers: bioanalytical considerations, *Bioanalysis.*, **2** (2010) 441-454.
[66] Pelham RW, Nix LC, Chavira RE, Cleveland MV, Stetson P, Clinical trial: single- and multiple-dose pharmacokinetics of polyethylene glycol (PEG-3350) in healthy young and elderly subjects, *Aliment.Pharmacol.Ther.*, **28** (2008) 256-265.
[67] Dear GJ, Beaumont C, Roberts A, Squillaci B, Thomas S, Nash M, Fraser D, Approaches for the rapid identification of drug metabolites in early clinical studies, *Bioanalysis.*, **3** (2011) 197-213.
[68] Zhu M, Zhang H, Humphreys WG, Drug Metabolite Profiling and Identification by High Resolution Mass Spectrometry, *J.Biol.Chem.*, (2011).
[69] Yu H, Bischoff D, Tweedie D, Challenges and solutions to metabolites in safety testing: impact of the International Conference on Harmonization M3(R2) guidance, *Expert.Opin.Drug Metab Toxicol.*, **6** (2010) 1539-1549.
[70] Skonberg C, Olsen J, Madsen KG, Hansen SH, Grillo MP, Metabolic activation of carboxylic acids, *Expert.Opin.Drug Metab Toxicol.*, **4** (2008) 425-438.
[71] Iyer RA, Malhotra B, Khan S, Mitroka J, Bonacorsi S Jr, Waller SC, Rinehart JK, Kripalani K, Comparative biotransformation of radiolabeled [(14)C]omapatrilat and stable-labeled [(13)C(2)]omapatrilat after oral administration to rats, dogs, and humans, *Drug Metab Dispos.*, **31** (2003) 67-75.
[72] Barros A, Jr., Ly VT, Chando TJ, Ruan Q, Donenfeld SL, Holub DP, Christopher LJ, Development and evaluation of a multiple-plate fraction collector for sample processing: application to radioprofiling in drug metabolism studies, *J.Pharm.Biomed.Anal.*, **54** (2011) 979-986.
[73] Nassar AE, Bjorge SM, Lee DY, On-line liquid chromatography-accurate radioisotope counting coupled with a radioactivity detector and mass spectrometer for metabolite identification in drug discovery and development, *Anal.Chem.*, **75** (2003) 785-790.
[74] Cuyckens F, Koppen V, Kembuegler R, Leclercq L, Improved liquid chromatography-Online radioactivity detection for metabolite profiling, *J.Chromatogr.A*, **1209** (2008) 128-135.
[75] Lenz EM, Kenyon A, Martin S, Temesi D, Clarkson-Jones J, Tomkinson H, The metabolism of [14C]-zibotentan (ZD4054) in rat, dog and human, the loss of the radiolabel and the identification of an anomalous peak, derived from the animal feed, *J.Pharm.Biomed.Anal.*, **55** (2011) 500-517.
[76] van den Bongard HJG, Pluim D, Rosing H, Nan-Offeringa L, Schot M, Ravic M, Schellens JH, Beijnen JH, An excretion balance and pharmacokinetic study of the novel anticancer agent E7070 in cancer patients, *Anticancer Drugs*, **13** (2002) 807-814.
[77] Tozuka Z, Kusuhara H, Nozawa K, Hamabe Y, Ikushima I, Ikeda T, Sugiyama Y, Microdose study of 14C-acetaminophen with accelerator mass spectrometry to examine pharmacokinetics of parent drug and metabolites in healthy subjects, *Clin.Pharmacol.Ther.*, **88** (2010) 824-830.
[78] Garner RC, Practical experience of using human microdosing with AMS analysis to obtain early human drug metabolism and PK data, *Bioanalysis.*, **2** (2010) 429-440.
[79] Zhu P, Tong W, Alton K, Chowdhury S, An accurate-mass-based spectral-averaging isotope-pattern-filtering algorithm for extraction of drug metabolites possessing a distinct isotope pattern from LC-MS data, *Anal.Chem.*, **81** (2009) 5910-5917.

[80] Zhang H, Zhang D, Ray K, Zhu M, Mass defect filter technique and its applications to drug metabolite identification by high-resolution mass spectrometry, *J.Mass Spectrom.*, **44** (2009) 999-1016.

[81] Ramanathan R, Jemal M, Ramagiri S, Xia YQ, Humpreys WG, Olah T, Korfmacher WA, It is time for a paradigm shift in drug discovery bioanalysis: from SRM to HRMS, *J.Mass Spectrom.*, **46** (2011) 595-601.

[82] Gong J, Gan J, Caceres-Cortes J, Christopher LJ, Arora V, Masson E, Williams D, Pursley J, Allentoff A, Lago M, Tran SB, Iyer RA, Metabolism and disposition of [14C]brivanib alaninate after oral administration to rats, monkeys, and humans, *Drug Metab Dispos.*, **39** (2011) 891-903.

[83] Comezoglu SN, Ly VT, Zhang D, Humphreys WG, Bonacorsi SJ, Everett DW, Cohen MB, Gan J, Beumer JH, Beijnen JH, Schellens HM, Lappin G, Biotransformation profiling of [(14)C]ixabepilone in human plasma, urine and feces samples using accelerator mass spectrometry (AMS), *Drug Metab Pharmacokinet.*, **24** (2009) 511-522.

Chapter 2

Bendamustine

Chapter 2.1

Development and validation of LC-MS/MS assays for the quantification of bendamustine and its metabolites in human plasma and urine

Anne-Charlotte Dubbelman, Matthijs Tibben, Hilde Rosing, Abadi Gebretensae, Lianda Nan, Steve H. Gorman, Philmore Robertson, Jr., Jan H.M. Schellens, Jos H. Beijnen

J Chromatogr B Analyt Technol Biomed Life Sci (2012) **893-894**:92-100

Abstract

A sensitive liquid chromatography tandem mass spectrometry (LC-MS/MS) assay is described for the quantification of the anti-cancer agent bendamustine and its phase I metabolites γ-hydroxy-bendamustine (M3) and N-des-methylbendamustine (M4) and for its product of two-fold hydrolysis, dihydroxy-bendamustine (HP2), in human plasma and urine.

Like most alkylating nitrogen mustards, bendamustine is prone to chemical hydrolysis in aqueous solution. To minimize degradation of bendamustine, urine samples were stabilized by a 100-fold dilution with human plasma and then processed identically to plasma samples. Sample aliquots of 200 μL were mixed with an internal standard solution and acidified before separation of the analytes from the biomatrix with solid phase extraction. Dried and reconstituted extracts were injected on a Synergi Hydro RP column for the analysis of bendamustine, M3 and M4 or a Synergi Polar RP column for the analysis of HP2. Gradient elution was applied using 5 mM ammonium formate with 0.1% formic acid in water and methanol as mobile phases. Analytes were ionized using an electrospray ionization source in positive mode and detected with a triple quadrupole mass spectrometer.

The quantifiable range for bendamustine, M3 and M4 was 0.5 - 500 ng/mL in plasma and 0.5 - 50 μg/mL in urine, and that for HP2 was 1 - 500 ng/mL in plasma and 0.1 - 50 μg/mL in urine. The assays were accurate and precise, with inter-assay and intra-assay accuracies within ± 20% of nominal and CV values below 20% at the lower limit of quantification and within ± 15% of nominal and below 15% at the other concentration levels tested. These methods were successfully applied to evaluate the pharmacokinetic profile of bendamustine and its metabolites in cancer patients treated with bendamustine.

Introduction

Bendamustine is an alkylating agent, comprising a nitrogen mustard moiety, a benzimidazole ring and an alkane carboxylic acid side chain. While it was already synthesized in 1963 by Ozegowski and Krebs [1] and in use for decades in Germany against a number of malignancies, it was only in 2008 that bendamustine was approved by the United States Food and Drug Administration (US FDA) for the treatment of chronic lymphocytic leukemia (CLL) and later for indolent B-cell non-Hodgkin's lymphoma (NHL) that has progressed during or following treatment with rituximab or a rituximab-containing regimen. To date, at least 80 clinical trials with bendamustine are active and recruiting patients [2], indicating that there is a lot of new interest in this rather old drug.

To support clinical trials, we developed and validated an LC-MS/MS method for the quantification of bendamustine in plasma and urine. To our knowledge, this article is the first describing the validation of a bioanalytical assay for this compound. Apart from unchanged bendamustine, the assay also allows quantification of γ-hydroxy-bendamustine (M3) and N-des-methylbendamustine (M4), the two known phase I metabolites of bendamustine, which have cytotoxic activity approximately equivalent to and five to ten times less than their parent, respectively [3]. Additionally, a separate assay is described to quantify the product of two-fold hydrolysis of bendamustine, dihydroxy-bendamustine (HP2), in the same samples.

The major challenge in the bioanalysis of bendamustine, similar to that of other, chemically-related nitrogen mustards like chlorambucil and melphalan, is its limited stability [4]. In presence of water, the 2-chloroethyl groups are prone to chemical hydrolysis, leading to the formation of monohydroxy-bendamustine (HP1), which in turn can degrade to HP2. The methods described herein for sample storage and treatment aimed to minimize undesired degradation.

Experimental

Chemicals and reagents

Bendamustine HCl, bendamustine metabolites γ-hydroxy-bendamustine (M3), N-des-methylbendamustine (M4) and dihydroxy-bendamustine (HP2) and a structural analogue of bendamustine (BM-IS), used as internal standard (IS) for the bendamustine assays, were manufactured by Carbogen Amcis AG (Bubendorf, Switzerland) and provided by Cephalon Inc. (West Chester, PA, USA). Sigma-Aldrich (St. Louis, MO, USA) supplied α-dansyl-L-arginine HCl (DLA), which served as IS for the HP2 assays. Methanol (Supra-Gradient grade) was obtained from Biosolve Ltd (Valkenswaard, the Netherlands) and formic acid (98%), ammonium formate and water (LiChrosolv) used to prepare the mobile phases were purchased from Merck (Darmstadt, Germany). Water (distilled) used for sample preparation originated from B. Braun Medical (Melsungen, Germany). Drug-free

control human K_2EDTA plasma was obtained from the Slotervaart Hospital (Amsterdam, the Netherlands) and control human urine from healthy volunteers.

Preparation of stock solutions, calibration standards (CS) and quality control (QC) samples

One mg/mL stock solutions for calibration standards and QC samples were prepared separately in methanol for each analyte: bendamustine, M3, M4 and HP2. They were further diluted with methanol to obtain working solutions with bendamustine, M3 and M4 combined and with HP2 exclusively, at several concentrations. Stock solutions of the internal standards BM-IS and DLA were prepared at a concentration of 10 µg/mL in methanol. The IS working solution contained 60 ng/mL BM-IS or 100 ng/mL DLA (or both for runs with study samples).

Stock solutions, working solutions and QC samples were stored at -70°C. The IS working solution and the calibration standards were freshly prepared for each analytical run.

CS and QC samples of the plasma assays

For the plasma assays, calibration standards were prepared by adding 10 µL working solution to 190 µL control human plasma, to give concentrations of 0.5, 1, 5, 10, 25, 125, 250, 400 and 500 ng/mL for bendamustine, M3 and M4 and of 1, 2, 5, 10, 25, 125, 250, 400 and 500 ng/mL for HP2.

The QC samples were prepared by spiking control human plasma with the appropriate QC working solution. Final concentrations at the lower limit of quantification (LLOQ), QC low, QC mid, QC high and QC above the upper limit of quantification (>ULOQ) were 0.5, 1.0, 20, 400 and 4000 ng/mL, respectively, for bendamustine, M3 and M4 and 1, 2, 20, 400 and 4000 ng/mL, respectively, for HP2.

CS and QC samples of the urine assays

To minimize the degradation of bendamustine in urine, samples were stabilized by 100-fold dilution in control human plasma. In this final matrix, to which we will refer as urine-plasma, a set of calibration standards with bendamustine, M3 and M4 concentrations of 5, 10, 25, 125, 250, 400 and 500 ng/mL was prepared, corresponding to concentrations in undiluted urine of 0.5 to 50 µg/mL. Calibration standards of HP2 in urine-plasma were prepared at concentrations of 1, 2, 5, 10, 25, 125, 250, 400 and 500 ng/mL, corresponding to undiluted urine concentrations of 0.1 to 50 µg/mL.

Because time and material would be saved if urine (i.e., urine-plasma) and plasma study samples could be analysed within a single analytical run with only CS curves of plasma samples, this option was also validated. To this end, calibration standards were made in plasma at the same concentrations as in urine-plasma and analyzed in combination with QC samples in urine-plasma.

These QC samples contained 5, 10, 50 and 400 ng/mL bendamustine, M3 and M4 (0.5 to 40 μg/mL in undiluted urine) or 1, 2, 40 and 400 ng/mL HP2 (0.1 to 40 μg/mL in undiluted urine) for the QC LLOQ, QC low, QC mid and QC high, respectively.

Sample preparation

Immediately after collection in the clinic, urine study samples were diluted with cooled (at 2-8°C) control human K_2EDTA plasma, at a 1:99 (urine : plasma, v/v) ratio, before storage at -70°C. The plasma samples and urine-plasma samples were processed identically, and the final extracts were used to quantify bendamustine, M3 and M4 and HP2.

Samples were thawed and kept in an ice-water bath pending processing. Ten μL of IS working solution and 800 μL of 5 mM ammonium formate with 0.1% formic acid in water were added to 200-μL sample aliquots. After vortex-mixing and centrifuging for 10 min at 4°C and 23,100 g, solid phase extraction (SPE) was performed using Oasis HLB 30 mg cartridges (Waters, Etten-Leur, the Netherlands). The cartridges were conditioned and equilibrated with 1.0 mL of methanol and 1.0 mL of water, respectively. Subsequently, the acidified samples were loaded, and the cartridges were washed with 1.0 mL of 5% methanol and vacuum dried for 1 min. The analytes were eluted with 1.0 mL of methanol and the eluates were evaporated to dryness under a gentle stream of nitrogen at 35°C. The residue was redissolved by adding 20 μL of methanol and vortex mixing for 1 min, followed by addition of 80 μL of mobile phase A. Samples were mixed for 5 min at 1,250 rpm and, after brief centrifugation, transferred to amber-coloured autosampler vials, which then were stored at 2-8°C pending analysis. The injection volumes of the assays for bendamustine, M3 and M4 and for HP2 were 10 and 4 μL, respectively.

Liquid chromatography-tandem mass spectrometry

The HPLC system comprised a HP1100 binary pump, a degasser, a HP1100 autosampler and a switching valve (Agilent technologies, Palo Alto, CA, USA). The autosampler temperature was kept at 4°C. Mobile phase A (5 mM ammonium formate with 0.1% formic acid in water), mobile phase B (methanol) and the flow rate (0.25 mL/min) were the same for both assays.

Bendamustine, M3 and M4 were separated on a Synergi Hydro RP column (150 x 2 mm I.D., particle size 4 μm; Phenomenex, Torrance, CA, USA) with the following mobile phase gradient: mobile phase B: 20% (0-0.2 min), from 20 to 50% (0.2-0.5 min), 50% (0.5-0.6 min), from 50 to 60% (0.6-6 min), 60% (6.0-8.0 min), from 60 to 20% (8.0-8.1 min) and 20% (8.0-11 min). The switching valve directed the flow eluting between 3 and 9.5 min into the mass spectrometer and the remainder to a waste container.

A Synergi Polar RP column (150 x 2 mm I.D., particle size 4 μm; Phenomenex) was used for the HP2 assay, with the following mobile phase gradient: mobile phase B: 15% (0-0.2

min), from 15 to 95% (0.2-3.2 min), 95% (3.2-5.2 min), from 95 to 15% (5.2-5.3 min) and 15% (5.3-8.0 min). The switching valve directed only the flow eluting between 4.5 and 6.8 min to the mass spectrometer.

Bendamustine, M3 and M4 were analysed on an API 3000 and HP2 on an API 4000 triple quadrupole mass spectrometer (MS) (AB Sciex, Thornhill, ON, Canada). Both instruments were equipped with a turbo ion spray interface, operating in positive mode and configured in multiple reaction monitoring (MRM).

LC-MS/MS data were acquired and processed using the software application Analyst™ (AB Sciex). Table 1 summarizes the MS operating parameters for both assays.

Table 1: Mass spectrometric parameters for the analysis of bendamustine, its metabolites M3, M4 and HP2 with the internal standards BM-IS and α-dansyl-L-arginine (DLA)

Mass spectrometer	**API 3000**				**API 4000**	
Ion source	ESI				ESI	
Ionization mode	positive				positive	
Ion spray voltage (kV)	3.5				3.5	
Turbo gas temperature (ºC)	350				550	
Turbo gas flow (L/min)	7				-	
Nebulizer gas (psi)	14				-	
Curtain gas (psi)	8				50	
Collision gas (psi)	5				7	
Gas 1 (Nebulizer gas, psi)	-				60	
Gas 2 (Turbo gas, psi)	-				70	
Analyte specific parameters	**Bendamustine**	**M3**	**M4**	**BM-IS**	**HP2**	**DLA**
Parent mass (*m/z*)	358	374	344	372	322	408
Product mass (*m/z*)	228	338	186	354	304	170
Declustering potential (V)	66	41	45	66	80	91
Focussing potential (V)	310	190	220	310	-	-
Entrance potential (V)	10	9	8.5	9	12	12
Collision energy (V)	51	35	59	37	40	43
Collision exit potential (V)	12	22	30	24	10	12
Dwell time (ms)	100	100	100	100	100	100
Typical retention time (min)	7.1	6.8	7.7	7.3	5.4	6.1

Validation procedures

The plasma assays were fully validated for calibration model, accuracy and precision, specificity and selectivity, recovery and matrix effect, carry-over and stability according to the FDA guidance of bioanalytical method validation [5;6]. A partial validation was performed for the assays in urine and included assessment of the calibration model, accuracy and precision, carry-over and stability.

Results and discussion

Method development

Sample collection and storage

Collection of urine samples for clinical pharmacokinetic studies often occurs over 24-h periods, whereby individual portions are pooled in a refrigerated container. Knowing, however, that compounds containing nitrogen mustard moieties may be unstable in aqueous solutions, it was questionable whether this approach would be suitable for urine collection for bendamustine analysis.

Stability tests in control human urine (n=6, pH range 6.5 to 7.6) confirmed that bendamustine is very unstable in aqueous solution. After 18 h of storage at 2-8 °C, 47 ± 20% (mean ± SD) of the bendamustine was lost. The degradation of bendamustine in urine appeared pH dependent: at pH 7.6 only 27% of the initial concentration was found while 75% was detected at pH 6.5.

Based on these and similar results, other possibilities for storage of urine samples containing bendamustine were investigated. Literature on the stability of nitrogen mustard-containing compounds like melphalan and chlorambucil describes that these compounds are more stable at a pH <3 [4], when treated on ice-water instead of at room temperature [7;8] and in the presence of 5% human serum albumin or human plasma as compared to aqueous buffers [9]. This led to the idea to stabilize bendamustine by a 100-fold dilution with human plasma. The additional advantage of this method is that the final biomatrix will be virtually identical to plasma, meaning that the urine-plasma samples can be processed and analysed in the same manner as plasma samples.

Sample preparation

To prevent analyte degradation, a low pH (obtained by addition of a low pH buffer or an acid solution), treatment on ice-water and amber-coloured vials were used as standard conditions during sample preparation. A method previously developed and validated at BASi (West Lafayette, IN, USA) served as a point of departure for the development and validation of the method for analysis of bendamustine, M3, and M4 in plasma.

During the development of the sample preparation procedure, five standard methods were systematically tested and the most sensitive method (high signal-to-noise ratio combined with a high recovery) was selected. Four plasma aliquots spiked with bendamustine, M3, M4 and HP2 and one blank plasma aliquot were all treated with the following methods: (i) protein precipitation (PPT) with perchloric acid, (ii) liquid-liquid extraction (LLE) with tert-butyl methyl ether (TBME), (iii) LLE with diethyl ether, (iv) SPE using Oasis Max cartridges and (v) SPE using Oasis HLB cartridges. A matrix-free dilution of a working solution was used as a reference to calculate the recovery. Signal-to-noise ratio was

calculated as the peak height of an analyte in the spiked plasma sample and the signal height at the same retention time in the blank plasma sample.

The results of these tests are visualised in the plots presented in Figure 1. The LLE methods appeared unsuitable to extract the polar compound HP2 from the plasma samples. Although the recovery and sensitivity of the simple PPT method was higher than of the LLE methods, the SPE methods resulted in the highest overall recovery. The signal-to-noise ratio of each compound was highest in the SPE method using the Oasis HLB cartridges; therefore, this method was selected.

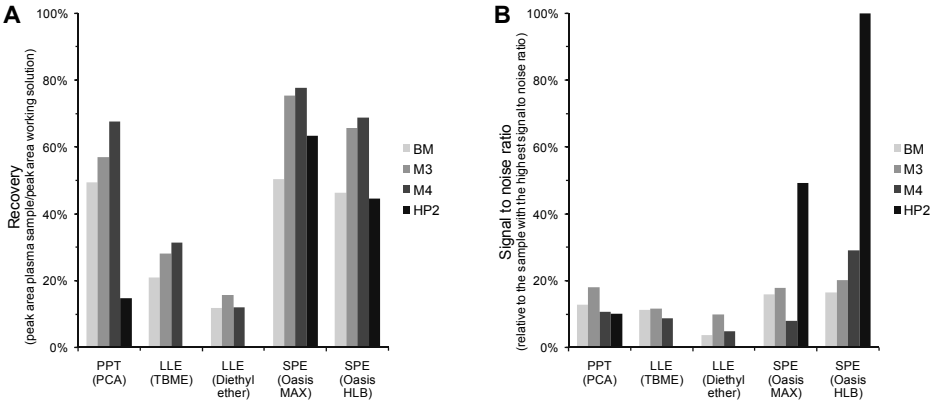

Figure 1: Sample preparation recovery of each analyte with different preparation procedures (A) and signal-to-noise ratio of each analyte compared to the sample with the highest signal-to-noise ratio (B). BM: bendamustine; PPT: protein precipitation; PCA: perchloric acid; LLE: liquid liquid extraction; TBME: tert-butyl methyl ether; SPE: solid phase extraction

Attempts to further decrease the conversion of bendamustine to HP2 during sample processing included evaporation at a lower temperature (25°C instead of 35°C), acidification with 1% perchloric acid instead of 5 mM ammonium formate with 0.1% formic acid in water, and addition of an excess of sodium chloride at the start of the sample preparation. None of these methods resulted in significant reduction in the formation of HP2. The SPE method using Oasis HLB cartridges (see section 2.3) was validated.

Liquid chromatography-tandem mass spectrometry

Simultaneous quantification of bendamustine, M3, M4 and HP2 was complicated by the high polarity of HP2 and by the absence of stable isotope-labelled internal standards. Initially, all analytes were combined in one chromatographic system; however, matrix effect caused a biased quantification of HP2. Attempts to compensate for this effect by use of alternative internal standards were not successful. Therefore, a separate chromatographic method for HP2 was developed. The Synergi Polar RP column was chosen for its ability to retain highly polar compounds. Using this column, HP2 quantification was less influenced by matrix effects; however, sensitivity was reduced. To accurately and precisely quantify HP2 at the target LLOQ of 1 ng/mL, the method was transferred to a more sensitive mass spectrometer (API 4000).

Table 2: Analytes with their selected mass transitions and proposed fragmentation pathways.

Compound	Transition	Proposed fragmentation
Bendamustine	358 → 228	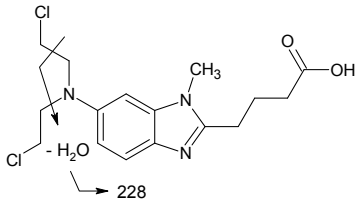
M3	374 → 338	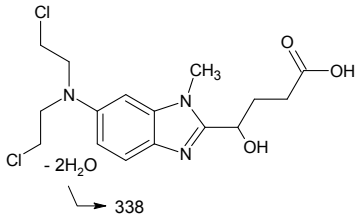
M4	344 →186	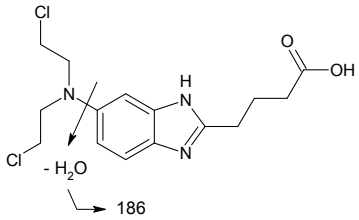
BM-IS	372 → 354	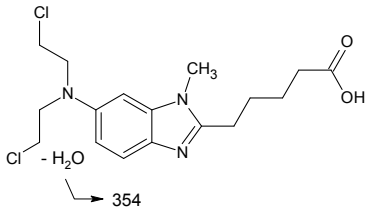
HP2	322 → 304	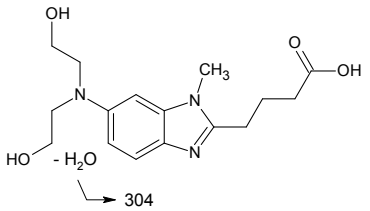
α-dansyl-L-arginine	407 → 170	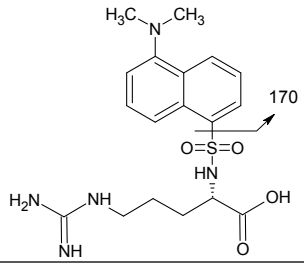

To optimize the mass spectrometric parameters and to find suitable product ions for multiple reaction monitoring, each analyte was infused directly into an electrospray ionization source. Settings for gasses and ion spray voltage were optimized by flow injection analysis. Table 2 shows the final transitions that were selected and their proposed fragmentation patterns. Figure 2 and 3 show representative chromatograms of bendamustine, M3, M4 and HP2 in a plasma QC LLOQ sample.

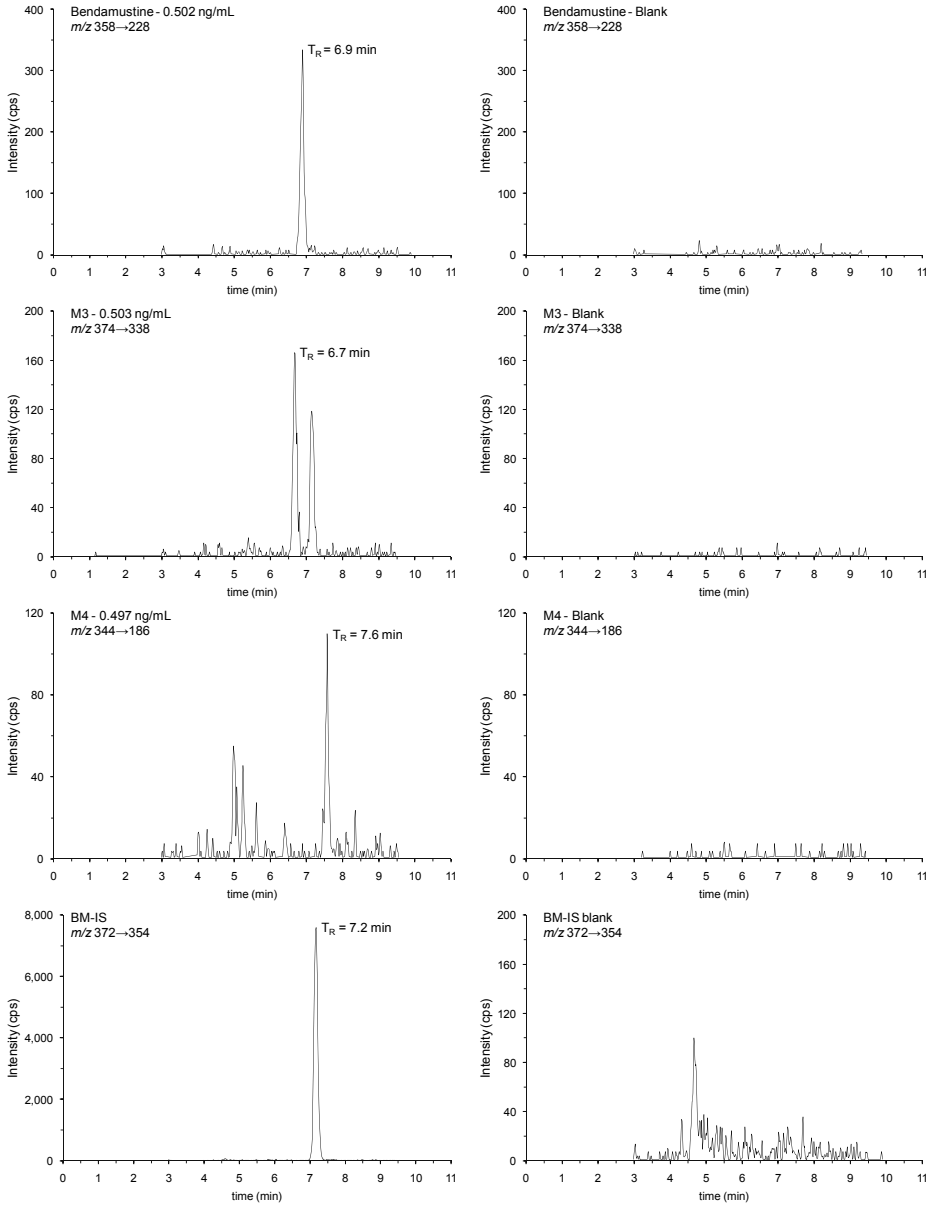

Figure 2: MRM chromatograms of bendamustine, M3, M4 and the internal standard BM-IS of a QC LLOQ (left) and a blank (right) plasma sample.

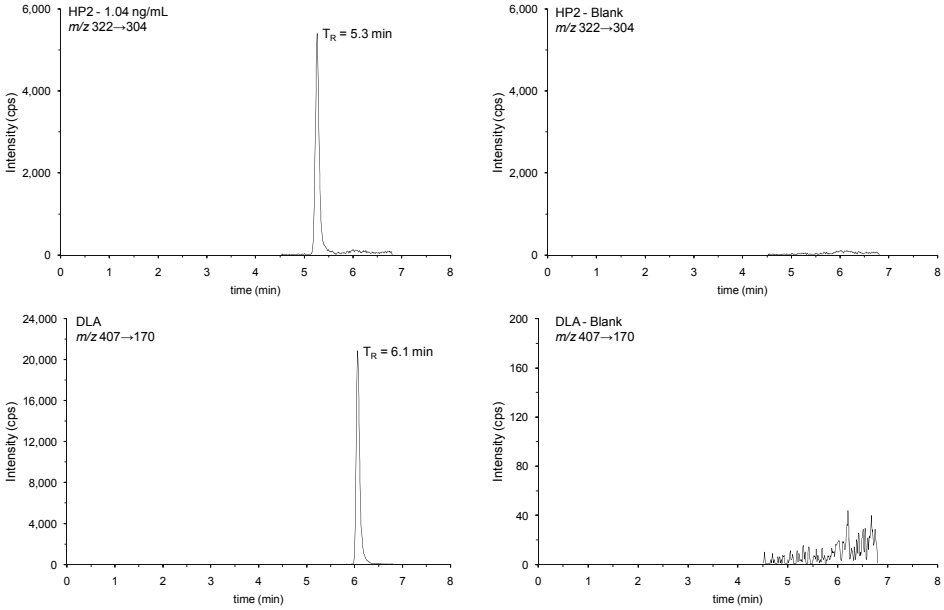

Figure 3: MRM chromatograms of HP2 and the internal standard α-dansyl-L-arginine (DLA) of a QC LLOQ (left) and a blank (right) plasma sample.

Validation procedures

Calibration model

For the bendamustine, M3 and M4 assay and the HP2 assay, 9 non-zero calibration standards were prepared and analysed in duplicate in three analytical runs. The simplest model that adequately described the concentration-response relationships for all analytes was a quadratic curve weighted with 1/x, whereby x is the concentration.

The calibration ranges of bendamustine, M3 and M4 were 0.5 - 500 ng/mL in plasma and 5 - 500 ng/mL in urine-plasma, corresponding to a 0.5 to 50 μg/mL range in undiluted urine. The HP2 calibration curve in both plasma and urine-plasma ranged from 1.0 to 500 ng/mL, corresponding to a 0.1 - 50 μg/mL range in undiluted urine.

Calibration curves were accepted if two-thirds of the non-zero calibration standards, including a LLOQ and an ULOQ, had a deviation within ± 15% of nominal (± 20% at the LLOQ) [5;6]. All calibration curves in plasma and urine-plasma met these acceptance criteria and had correlation coefficients (r^2) of 0.997 or better.

Accuracy and precision

To assess the accuracy and precision of the plasma assays, five replicates of the QC LLOQ, QC low, QC mid and QC high in plasma were analysed in 3 analytical runs with bendamustine, M3 and M4 and with HP2. The QC samples prepared in urine-plasma were analysed in one analytical run together with plasma and urine-plasma calibration standards.

Table 3: Assay performance data for the analysis of bendamustine, M3 and M4 and for the analysis of HP2 in human plasma

Analyte	Internal standard	QC	Nominal conc. (ng/mL)	Measured conc. (ng/mL)	Inter-assay accuracy (%)	Inter-assay precision (%)	n
Bendamustine	BM-IS	LLOQ	0.502	0.487	-3.07	16.2	14
		Low	1.00	0.952	-4.76	4.42	15
		Mid	20.1	17.9	-10.8	3.16	15
		High	402	379	-5.77	4.88	15
M3	BM-IS	LLOQ	0.503	0.517	2.85	15.6	14
		Low	1.01	0.974	-3.52	6.16	14
		Mid	20.1	17.5	-12.8	2.82	15
		High	402	373	-7.16	3.29	15
M4	BM-IS	LLOQ	0.497	0.490	-1.49	14.2	14
		Low	0.994	0.895	-10.0	10.0	15
		Mid	19.9	18.2	-8.54	3.69	15
		High	398	367	-7.74	3.44	15
HP2	DLA	LLOQ	1.04	1.01	-3.26	7.40	15
		Low	2.09	2.01	-3.64	5.71	15
		Mid	209	21.4	2.36	9.59	15
		High	417	420	0.719	5.23	15

Conc.: concentration; n: number of replicates

Table 4: Assay performance data for the analysis of bendamustine, M3 and M4 and for the analysis of HP2 in human urine : plasma (1 : 99 v/v) (referred to as urine-plasma), with respect to CS samples in urine-plasma and plasma.

			CS samples in urine-plasma			CS samples in plasma		
Analyte	QC	Nominal conc.[a] (ng/mL)	Measured conc.[a,b] (ng/mL)	Intra-assay accuracy (%)	Intra-assay precision (%)	Measured conc.[b] (ng/mL)	Intra-assay accuracy (%)	Intra-assay precision (%)
Benda-mustine	LLOQ	4.70	3.93	-16.3	4.77	4.07	-13.3	4.61
	Low	9.40	8.75	-6.87	4.64	8.90	-5.28	4.57
	Mid	47.0	45.1	-3.96	5.54	45.3	-3.57	5.55
	High	376	372	-1.12	4.18	373	-0.798	4.17
M3	LLOQ	5.47	4.50	-17.7	3.31	4.55	-16.8	3.21
	Low	10.9	10.7	-2.20	3.96	10.7	-2.20	3.96
	Mid	54.7	57.1	4.31	5.76	56.8	3.77	5.79
	High	437	434	-0.778	3.63	448	2.43	3.79
M4	LLOQ	4.63	4.48	-3.20	9.14	4.86	4.88	8.53
	Low	9.25	9.65	4.41	6.36	10.1	8.69	6.16
	Mid	46.3	51.9	12.1	3.80	52.6	13.6	3.75
	High	370	411	11.0	2.48	425	14.8	2.64
HP2	LLOQ	1.04	0.895	-13.9	1.77	0.904	-13.1	1.75
	Low	2.09	2.07	-1.05	1.30	2.06	-1.53	1.30
	Mid	20.9	23.4	12.2	2.08	23.1	10.7	2.11
	High	417	409	-1.92	4.51	414	-0.82	4.67

Conc.: concentration. [a]Reported concentrations are in urine-plasma instead of urine. [b]Samples were analyzed in five replicates

Table 3 summarizes the intra-assay accuracies (the percentage difference of the measured from the nominal concentration) and precisions (CV values) of the analytes in plasma. For the assays in urine-plasma, the QC samples were quantified using either calibration standards in urine-plasma or in plasma and for both cases the accuracy and precision data are tabulated in Table 4. Because the difference between the calculated concentrations of the two quantification methods was very small (2% on average), it was concluded that

study samples in urine-plasma can be quantified using calibration standards prepared in plasma.

The biases and precisions of all analytes were within the acceptance criteria (within ± 20% and ≤ 20%, respectively, at the LLOQ level and within ± 15% and ≤ 15% at the other QC levels) and the signal-to-noise ratios of the analytes at the LLOQ level were above 5 [5;6].

Five replicate samples of bendamustine, M3, M4 and HP2 at QC >ULOQ level that were diluted 10 and 100 fold with control plasma had a maximum deviation of -14.3% and a maximum CV of 6.06%, indicating that study samples with concentrations above the ULOQ can be diluted 10 and 100 fold with acceptable accuracy and precision values [5;6].

Specificity and selectivity

Six different batches of control plasma were spiked at the LLOQ level with either bendamustine, M3 and M4 or HP2 to investigate the selectivity. The mean deviations from the nominal concentrations were 0.4%, -3.6%, -13.3% and 7.5% with CV values of 3.2%, 11.3%, 12.1% and 5.0%, respectively. Peaks appearing in double-blank samples of these batches, caused by endogenous disturbances and co-eluting with an analyte, were maximally 14.6%, 13.8%, 13.2% and 10.1% of the LLOQ for bendamustine, M3, M4 and HP2, respectively, and no interferences were detected at the retention time of the internal standards BM-IS and DLA. Selectivity was therefore considered sufficient [5;6].

Cross-analyte interference was tested by spiking plasma with one of the analytes at the ULOQ level and analysing it with both the assay for bendamustine, M3 and M4 and the assay for HP2. In the assay of bendamustine, M3 and M4, the maximum cross-analyte interference that was observed originated from bendamustine, generating a peak of 2.66% of the LLOQ of M3 in the transition window of M3.

BM-IS produced a peak in the window of M3 (as shown in Fig. 2), probably resulting from the loss of $H^{35}Cl$ of a ^{37}Cl-isotope of the internal standard. However, the peak, which is baseline-separated from the M3 peak, will be essentially invariant because the BM-IS concentration is the same in all samples; this peak is not expected to impact the quantification of M3.

In the HP2 assay, the interferences of M3, M4, BM-IS and DLA on HP2 were less than 10% of the LLOQ of HP2, and no interference was observed in the transition window of DLA. The only significant interference that was observed was of bendamustine on HP2 quantification. The plasma sample spiked with bendamustine at 500 ng/mL gave a peak in the transition window of HP2 at the retention time of HP2 and with an area of 48% of the LLOQ of HP2, which was 1 ng/mL. As HP2 was not observed as a significant impurity in the stock solution of bendamustine, it was likely formed by chemical degradation during sample preparation and analysis. Because the sample preparation procedures were already

optimized to minimize degradation of bendamustine, we calculated in which cases this interference would adversely affect the results of study samples.

To this end, a maximum interference of 20% of the LLOQ level was considered acceptable and it was assumed that 0.1% (≈48% of 1 ng/mL per 500 ng/mL bendamustine) of the original bendamustine concentration is added to the HP2 concentration due to degradation during sample processing. In that case, a sample with original concentrations of 1 ng/mL HP2 and 200 ng/mL bendamustine would be quantified at 1.2 ng/mL HP2, which is the maximum accepted limit. The HP2 quantification results of study samples with a measured bendamustine : HP2 concentration ratio above 200 : 1.2 (i.e., 167 : 1) will be affected by the degradation of bendamustine during sample preparation and should be interpreted with caution. Considering the short half-life time of bendamustine and the plausibility of bendamustine to be converted into HP2 in the body, concentration ratios above 167 may occur during the infusion of bendamustine, but are not expected to persist.

Sample preparation recovery and matrix effect

The sample preparation recoveries of bendamustine, M3 and M4, determined in triplicate at three concentrations in plasma by comparing processed spiked samples with processed blank samples that had been spiked with working solutions, were consistent across the concentration range for the three analytes: 76.4 to 82.8%, 79.3 to 86.5% and 74.9 to 82.7%, respectively. The matrix effect was determined by comparing the latter samples to matrix-free working solutions and ranged from -32.2 to -6.4%, -18.7 to -1.2% and -23.3 to -2.4%, for bendamustine, M3 and M4, respectively. The sample preparation recovery of BM-IS was 79.6% and the matrix effect was -30.6%.

For HP2, the sample preparation recovery ranged from 81.4 to 83.9% and the matrix effect ranged from -31.3 to -18.5%. The sample preparation recovery of DLA was 89.2% and the matrix effect -19.1%.

Carry-over

Carry-over of bendamustine, M3 and M4 caused peaks in the first blank plasma sample after an ULOQ sample with an area of 49 to 89% of the LLOQs in plasma. In the second blank plasma sample, the carry-over was reduced to less than 20% of the LLOQ. As a consequence, a blank sample needs to be injected after ULOQ and QC high samples and between study samples with high expected concentrations of one or more of the analytes. No carry-over effect was observed for BM-IS with this assay. In urine-plasma, carry-over of bendamustine, M3 and M4 in the first blank was limited to ≤ 6.3% of the LLOQ with 0.95% carry-over of BM-IS.

The carry-over of HP2 was limited: 7.1% in the first blank plasma sample after an ULOQ sample and 10.1% in urine-plasma. No carry-over was observed for DLA.

Stability

Stability experiments were executed in triplicate at the concentration levels QC low and QC high. Biases were calculated against the initial concentrations and analytes were considered stable in a matrix if the difference was within ± 15%. For diluted stock solutions and working solutions of the analytes other than the internal standards, the maximum allowed deviation was ± 5%.

Stock solutions of bendamustine, M3, M4 and HP2 in methanol were stable for at least 12, 9, 12 and 7 months at -70ºC, respectively. The internal standards BM-IS and DLA were stable for at least 12 and 9 months, respectively, under the same storage conditions. The stability of the analyte stock solutions on ice-water (during sample preparation) was at least 3 h. Table 5 provides an overview of the stability of the analytes in methanol.

Table 5: Long-term and short-term stability of stock solutions of bendamustine, its metabolites and the internal standards in methanol.

Condition	Analyte	Nominal conc. (mg/mL)	Measured conc.[a] (mg/mL)	CV (%)	Dev. (%)
-70°C, 12 Mon	Bendamustine	1.02	1.06	1.10	4.57
-70°C, 9 Mon	M3	0.986	0.954	1.07	-3.23
-70°C, 12 Mon	M4	1.00	0.960	0.856	-4.03
-70°C, 7 Mon	HP2	1.04	1.07	1.39	3.03
-70°C, 12 Mon	BM-IS	0.106	0.117	1.26	10.4
-70°C, 9 Mon	DLA	0.105	0.0928	1.06	-9.09
Icewater, 3 h	Bendamustine	1.02	0.994	0.837	-2.56
Icewater, 3 h	M3	0.986	0.944	2.16	-4.29
Icewater, 4 h	M4	1.00	0.984	0.00	-1.58
Icewater, 6 h	HP2	1.04	1.03	1.37	-1.17

Conc.: concentration; CV: coefficient of variation; dev.: deviation; Mon: months; h: hours.
[a]Samples were analyzed in three replicates

Supplementary Tables 1 and 2 show the stability data for bendamustine and its metabolites in the biological matrices. When stored at -70ºC, bendamustine, M3 and M4 and HP2 were stable for at least 8 to 9 months in plasma and in urine-plasma. All analytes remained stable after three freeze-thaw cycles from -70ºC to ice-water in both plasma and urine-plasma, except for M4 in plasma, for which 2 cycles appeared to be the maximum. Stability of the analytes in plasma and urine-plasma on ice-water was demonstrated for 6 h, and the final extracts of plasma samples were stable for at least two days for bendamustine, M3 and M4 and 14 days for HP2 at 4ºC.

The stability of the analytes was also tested in undiluted urine at 4ºC, to mimic the situation of urine samples collected in the clinic and refrigerated but not instantly diluted with plasma. All analytes were stable for at least 2 hours under these conditions.

Supplementary Table 1: Stability data for bendamustine, M3 and M4 in plasma, urine and in human urine : plasma (1 : 99 v/v) (referred to as urine-plasma).

Condition	Analyte	Original Matrix	QC	Nominal conc. (ng/mL)
Spiked matrix, -70°C, 9 Mon	Bendamustine	Plasma	Low	1.00
			High	402
	M3	Plasma	Low	1.01
			High	402
	M4	Plasma	Low	0.994
			High	398
3 freeze-thaw cycles, -70°C	Bendamustine	Plasma	Low	1.00
			High	402
	M3	Plasma	Low	1.01
			High	402
	M4	Plasma	Low	0.994
			High	398
2 freeze-thaw cycles, -70°C	M4	Plasma	Low	1.01
			High	406
Spiked matrix, icewater, 6 h	Bendamustine	Plasma	Low	1.00
			High	402
	M3	Plasma	Low	1.01
			High	402
	M4	Plasma	Low	0.994
			High	398
Final extract, 4°C, 2 d	Bendamustine	Plasma	Low	1.01
			High	405
	M3	Plasma	Low	1.00
			High	399
	M4	Plasma	Low	1.01
			High	406
Spiked matrix, 4°C, 2 h	Bendamustine	Urine[a]	Low	9.40
			High	376
	M3	Urine[a]	Low	10.9
			High	437
	M4	Urine[a]	Low	9.25
			High	370
Spiked matrix, -70°C, 8.8 Mon	Bendamustine	Urine-plasma	Low	9.40
			High	376
	M3	Urine-plasma	Low	10.9
			High	437
	M4	Urine-plasma	Low	9.25
			High	370
Spiked matrix, icewater, 6 h	Bendamustine	Urine-plasma	Low	9.40
			High	376
	M3	Urine-plasma	Low	10.9
			High	437
	M4	Urine-plasma	Low	9.25
			High	370
3 freeze-thaw cycles, -70°C	Bendamustine	Urine-plasma	Low	9.40
			High	376
	M3	Urine-plasma	Low	10.9
			High	437
	M4	Urine-plasma	Low	9.25
			High	370

Conc.: concentration; CV: coefficient of variation; Dev.: deviation; Mon: months; d: days; h: hours.

Initial conc.[b] (ng/mL)	Measured conc.[b] (ng/mL)	CV (%)	Dev.[c] (%)
0.957	0.937	7.00	-2.02
380	397	2.43	4.29
0.941	0.870	24.5	-7.55
378	391	1.02	3.44
0.915	0.869	15.3	-4.99
366	372	1.57	1.64
0.846	0.872	1.38	3.07
383	373	1.88	-2.78
0.888	0.868	6.69	-2.21
377	357	2.81	-5.39
1.08	0.788	10.7	-27.2
379	355	2.89	-6.34
0.932	0.932	12.2	0.00
373	371	3.56	-0.537
0.910	0.855	2.23	-6.13
385	381	3.43	-1.12
0.959	0.988	11.7	3.06
371	363	1.2	-2.24
0.848	0.790	6.54	-6.94
364	376	2.94	3.48
1.09	1.06	2.50	-3.05
418	428	2.47	2.39
0.913	0.958	0.629	5.00
371	388	0.446	4.58
0.947	0.893	8.34	-5.70
396	358	2.74	-9.60
8.71	9.02	3.80	3.56
365	387	2.49	5.94
9.13	9.09	3.95	-0.438
402	424	5.97	5.56
10.1	9.75	7.96	-3.82
455	464	3.99	1.83
8.96	9.30	6.71	3.79
375	394	2.46	5.25
10.6	11.2	7.24	5.02
448	505	3.27	12.81
9.82	9.23	14.9	-6.01
427	393	0.294	-7.81
8.96	8.93	3.50	-0.372
375	374	6.37	-0.0890
10.6	10.6	3.77	-0.313
448	460	4.73	2.68
9.82	10.2	3.30	3.60
427	415	0.732	-2.73
11.4	10.7	3.27	-6.12
402	369	1.76	-8.05
11.7	11.1	3.12	-5.13
432	385	2.96	-11.0
12.3	12.1	3.79	-1.63
444	404	1.03	-9.00

[a]Reported concentrations are in urine-plasma instead of urine. [b]Samples were analyzed in three replicates. [c]Deviation is calculated against the initial concentration

Supplementary Table 2: Stability data for HP2 in plasma, urine and in human urine : plasma (1 : 99 v/v) (referred to as urine-plasma).

Condition	Analyte	Original Matrix	QC	Nominal conc. (ng/mL)	Initial conc.[b] (ng/mL)	Measured conc.[b] (ng/mL)	CV (%)	Dev.[c] (%)
Spiked matrix, -70°C, 8.6 Mon	HP2	Plasma	Low	2.09	NA	1.98	5.03	-5.10
			High	417	NA	447	3.36	7.11
3 freeze-thaw cycles, -70°C	HP2	Plasma	Low	2.09	2.09	1.90	1.85	-8.93
			High	417	409	416	3.13	-0.160
Spiked matrix, icewater, 6 h	HP2	Plasma	Low	2.09	2.06	2.13	3.54	1.91
			High	417	441	452	0.221	8.39
Final extract, 4°C, 14 d	HP2	Plasma	Low	2.09	2.09	1.88	2.68	-10.4
			High	417	409	387	2.55	-2.76
Spiked matrix, 4°C, 2 h	HP2	Urine[a]	Low	2.09	2.29	2.13	4.48	-6.99
			High	417	372	363	5.69	-2.42
Spiked matrix, -70°C, 8.3 Mon	HP2	Urine-plasma	Low	2.09	NA	2.20	8.10	5.10
			High	417	NA	479	3.74	14.8
Spiked matrix, icewater, 6 h	HP2	Urine-plasma	Low	2.09	2.03	1.96	7.09	-3.61
			High	417	418	417	8.62	-0.239
3 freeze-thaw cycles, -70°C	HP2	Urine-plasma	Low	2.09	2.03	2.09	3.89	2.95
			High	417	418	432	2.20	3.35

Conc.: concentration; CV: coefficient of variation; Dev.: deviation; Mon: months; d: days; h: hours

[a]Reported concentrations are in urine-plasma instead of urine. [b]Samples were analyzed in three replicates. [c]Deviation is calculated against the initial concentration, if available, otherwise against the nominal concentration.

Reinjection reproducibility

Reinjection of duplicate CS samples and triplicate QC samples of bendamustine, M3 and M4 in plasma was reproducible after 2 days storage at 4°C, as the results met the acceptance criteria of the calibration curve, accuracy and precision. For analysis of HP2, reinjection reproducibility was demonstrated after 24 h storage at 4°C.

Clinical application

The purpose of the validated assays was to support clinical pharmacokinetic studies of bendamustine. To demonstrate their applicability, we present the concentration profiles over time of bendamustine, M3, M4 and HP2 in plasma of a representative patient who had received bendamustine (Figure 4).

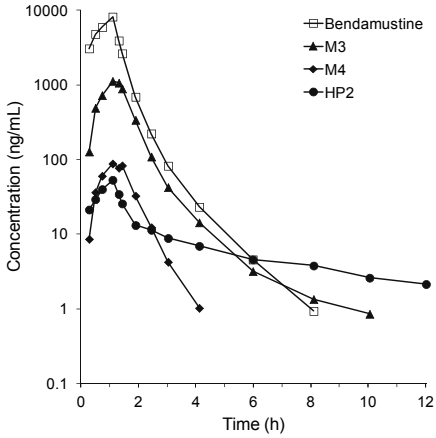

Figure 4: Representative plasma concentration-time curves of bendamustine and its metabolites M3, M4 and HP2 following a 1-h infusion with 120 mg/m² bendamustine in a cancer patient.

A 120 mg/m² dose of bendamustine was administered as a 1-h intravenous infusion to a cancer patient, as part of a clinical phase I study investigating the metabolism and excretion of bendamustine in patients with relapsed or refractory malignancies. Blood samples were collected at several time points using K_2EDTA tubes and put on ice. Within 30 min after collection, samples were centrifuged for 10 min at 1,200 g and 4°C; plasma was isolated and then stored at -70°C pending analysis. Figure 4 shows the plasma concentration-time curves for bendamustine and its metabolites in this patient. The maximum concentration of bendamustine was 8187 ng/mL, which was achieved at the end of the infusion. Concentrations then declined rapidly in a multiphasic manner. The phase I metabolites M3 and M4 showed a similar general time course as bendamustine, but reached much lower concentrations. The concentrations of HP2 early in the sampling period were much lower compared to those of bendamustine, but this metabolite had a longer elimination half-life

than the others. The maximum ratio between bendamustine and HP2 was 164 : 1, occurring halfway through the infusion; hence, the critical ratio (i.e., 167 : 1) above which degradation of bendamustine during sample processing would be predicted to affect HP2 quantification was barely achieved and only transiently.

Conclusion

By systematically comparing various sample preparation techniques and optimizing LC-MS/MS settings, we developed a sensitive assay for the quantification of bendamustine and its metabolites M3, M4 and HP2. The assays were validated according to the US FDA guidelines and applicable for human K_2EDTA plasma and for human urine that has been diluted with control plasma to minimize chemical hydrolysis of bendamustine. The assays were able to quantify bendamustine, M3 and M4 from 0.5 to 500 ng/mL and HP2 from 1 to 500 ng/mL in 200-μL plasma aliquots, with the possibility to dilute samples containing higher concentrations 10- or 100-fold with control plasma prior to analysis. The quantifiable range in urine was from 0.5 to 50 μg/mL for bendamustine, M3 and M4 and from 0.1 to 50 μg/mL for HP2. The assays are considered very suitable and are now in use to support clinical pharmacologic studies of bendamustine.

References

[1] Ozegowski W, Krebs D, w-[bis-(chlorethyl)-amino-benzimidazolyl-(2)]-propionic or butyric acids as potential cytostatic agents, *J Prakt Chem*, **20** (1963) 178-186.

[2] United States National Institutes of Health, http://clinicaltrials.gov/ct2/results?term=bendamustine&no_unk=Y, (2011), Accessed at: 1-11-2011

[3] Teichert J, Baumann F, Chao Q, Franklin C, Bailey B, Hennig L, Caca K, Schoppmeyer K, Patzak U, Preiss R, Characterization of two phase I metabolites of bendamustine in human liver microsomes and in cancer patients treated with bendamustine hydrochloride, *Cancer Chemother.Pharmacol.*, **59** (2007) 759-770.

[4] Bosanquet AG, Stability of solutions of antineoplastic agents during preparation and storage for in vitro assays. General considerations, the nitrosoureas and alkylating agents, *Cancer Chemother.Pharmacol.*, **14** (1985) 83-95.

[5] Rosing H, Man WY, Doyle E, Bult A, Beijnen JH, Bianalytical liquid chromatographic method validation. A review of current practices and procedures, *J.Liq.Chromatogr.Relat.Technol.*, **23** (2000) 329-354.

[6] US FDA, Department of Health and Human Services, Guidance for Industry, Bioanalytical Method Validation, www.fda.gov/downloads/Drugs/GuidanceComplianceRegulatoryInformation/Guidances/ucm070107.pdf, (2001), Accessed at: 9-1-2012

[7] Adair CG, Bridges JM, Desai ZR, Renal function in the elimination of oral melphalan in patients with multiple myeloma, *Cancer Chemother.Pharmacol.*, **17** (1986) 185-188.

[8] Mirkou A, Vignal B, Cohen S, Guillaumont M, Glehen O, Guitton J, Assays for the quantification of melphalan and its hydrolysis products in human plasma by liquid chromatography-tandem mass spectrometry, *J.Chromatogr.B Analyt.Technol.Biomed.Life Sci.*, **877** (2009) 3089-3096.

[9] Watson E, Dea P, Chan KK, Kinetics of phosphoramide mustard hydrolysis in aqueous solution, *J.Pharm.Sci.*, **74** (1985) 1283-1292.

Chapter 2.2

Pharmacokinetics and excretion of ^{14}C-bendamustine in patients with relapsed or refractory malignancy

Anne-Charlotte Dubbelman, Hilde Rosing, Mona Darwish, Denise D'Andrea, Mary Bond, Edward Hellriegel, Philmore Robertson, Jr., Jos H. Beijnen, Jan H.M. Schellens

Submitted for publication

Abstract

Background: Bendamustine is an alkylating agent with clinical activity against a variety of haematologic malignancies and solid tumours. To assess the roles of renal and hepatic drug elimination pathways in the excretion and metabolism of bendamustine, a mass balance study was performed in patients with relapsed or refractory malignancies.

Methods: A single 60-minute intravenous dose of 120 mg/m^2, 80–95 μCi ^{14}C-bendamustine hydrochloride was administered to 6 patients followed by collection of blood, urine and faecal samples at specified time points up to day 8 or until the radioactivity of the 24-hour urine and faecal collections was below 1% of the administered dose (whichever was longer). Total radioactivity (TRA) was measured in all samples and concentrations of unchanged bendamustine, and its metabolites γ-hydroxy-bendamustine (M3), *N*-desmethyl-bendamustine (M4) and dihydroxy bendamustine (HP2) were determined in plasma and urine using validated liquid chromatography-tandem mass spectrometry methods.

Results: The mean recovery of TRA in excreta was 76% of the radiochemical dose. Approximately half of the administered dose was recovered in urine and a quarter in faeces. Less than 5% of the administered dose was recovered in urine as unchanged bendamustine. Bendamustine clearance from plasma was rapid, with a half-life of ~40 minutes. Plasma concentrations of M3, M4 and HP2 were very low relative to the bendamustine concentrations. Plasma levels of TRA were higher and more sustained as compared with plasma concentrations of bendamustine, M3, M4 and HP2, suggesting the presence of 1 or more longer-lived ^{14}C-bendamustine–derived compounds. Bendamustine was well tolerated when administered at a dosage of 120 mg/m^2 for 2–3 cycles, with fatigue (50%) and vomiting (50%) as the most frequent treatment-related adverse events. A grade 3/4 absolute lymphocyte count occurred in all patients at some point during the study.

Conclusion: Bendamustine is extensively metabolised with subsequent excretion in both urine and faeces. Accumulation of bendamustine is not anticipated in cancer patients with renal or hepatic impairment due to the dose administration schedule and short half-life.

Introduction

Bendamustine is a unique alkylating agent that combines a nitrogen mustard moiety of mechlorethamine with a benzimidazole [1]. It has shown clinical activity against a variety of haematologic malignancies [2-5] and solid tumours [6;7] as a single agent or in combination with other anticancer agents. Bendamustine is indicated in the United States for the treatment of chronic lymphocytic leukaemia and for indolent B-cell non-Hodgkin's lymphoma that has progressed during or within 6 months of treatment with rituximab or a rituximab-containing regimen.

Similar to other alkylating agents, bendamustine causes cross-links between DNA bases, resulting in DNA damage. However, *in vitro* studies with human ovarian and breast cancer cell lines showed that the double-strand breaks caused by bendamustine are more extensive and durable than those produced by the alkylating agents cyclophosphamide and carmustine [8]. This, combined with unique mechanistic features, including activation of DNA damage stress response and apoptosis, inhibition of mitotic checkpoints and induction of mitotic catastrophe [1], may explain the activity of bendamustine in drug-resistant cells *in vitro* [8] and in patients with therapy-refractory lymphoma [3].

Bendamustine was generally well tolerated in patients with relapsed or refractory non-Hodgkin's lymphoma or mantle cell lymphoma [3;9-12]. The main toxicities observed were reversible myelosuppression including leukocytopenia, neutropenia, thrombocytopenia and anaemia. Nonhaematologic toxicities included mild gastrointestinal events and fatigue [3;10].

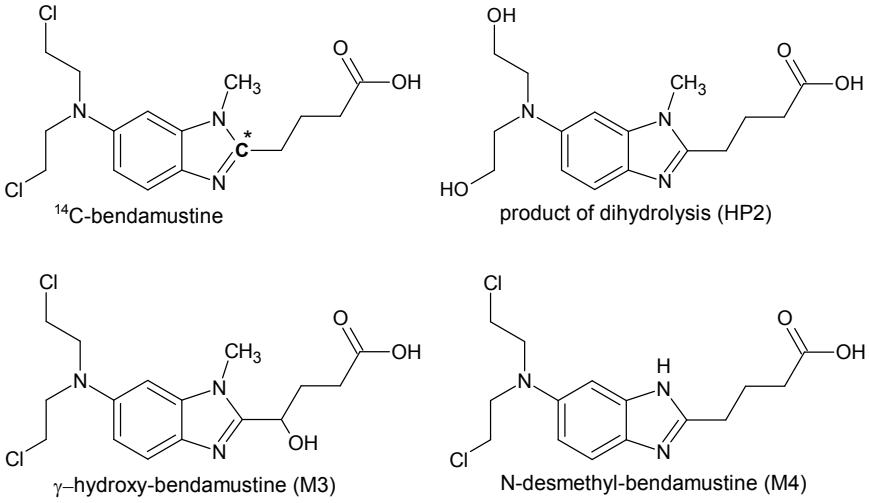

Figure 1: Chemical structure of bendamustine and its metabolites. Chemical structure of bendamustine and its metabolites γ-hydroxy-bendamustine (M3), *N*-desmethyl-bendamustine (M4) and dihydroxy bendamustine (HP2). The asterisk in the structure of bendamustine indicates the position of the ^{14}C-radiolabel.

A major route of bendamustine metabolism is hydrolysis to the inactive products monohydroxy bendamustine (HP1) and dihydroxy bendamustine (HP2), which make little or no contribution to the anti-cancer effects of bendamustine. Two phase I metabolites of bendamustine have been identified: γ-hydroxy-bendamustine (M3) and *N*-desmethyl-bendamustine (M4). Both are formed via the cytochrome P450 (CYP) 1A2 oxidative pathway, and they have a potency similar to (M3) or 5- to 10-fold lower (M4) than bendamustine [13].

In a mass balance study of ^{14}C-bendamustine performed in rats, approximately 90% of the dose was recovered in excreta after 7 days and substantial radioactivity (49%) was recovered in faeces [14]. Limited information, however, is available on the extent of renal and hepatic elimination of bendamustine in humans. Previously reported urinary pharmacokinetic data of bendamustine and its metabolites are characterised by a high variability, suspected to be caused by varying degrees of hydrolysis of bendamustine during sample handling and preparation [15;16].

The primary objective of the present study was to determine the pharmacokinetics and excretion of ^{14}C-bendamustine and its metabolites M3, M4 and HP2 (Figure 1) in humans. To this end, the mass balance of a single dose of 120 mg/m^2 (~80–95 μCi) ^{14}C-bendamustine was investigated in cancer patients by comparing the administered radioactivity with the radioactivity recovered in urine and faecal samples. Concentrations of bendamustine, M3, M4 and HP2 in plasma and urine were determined using validated liquid chromatography-tandem mass spectrometry (LC-MS/MS) assays, and special procedures were followed to minimise the chemical degradation of bendamustine in the study samples. A secondary objective was to further assess the safety profile of bendamustine.

Materials and Methods

Study design

This was a phase I, open-label, single-centre study, which enrolled 6 patients. The study was conducted in accordance with International Conference on Harmonisation guidelines for Good Clinical Practice; the code of Federal Regulations title 21, parts 50, 54, 56, 312 and 314; and the European Clinical Trials Directive (2001/20/EC). The protocol was approved by The Netherlands Cancer Institute Independent Ethics Committee.

The study was divided into 2 assessment periods: period A, during which the mass balance and pharmacokinetics of ^{14}C-bendamustine were investigated, and period B, an extended-use period of up to six 28-day cycles with nonlabelled bendamustine administration on days 1 and 2, during which safety continued to be assessed.

After giving written informed consent, patients received a 60-minute intravenous infusion containing a 120-mg/m^2 dose of ^{14}C-bendamustine HCl (~80–95 μCi) on day 1 and a 120-mg/m^2 dose of nonlabelled bendamustine on day 2. During days 1–8 of cycle 1, blood samples and excreta were collected while the patients remained hospitalised. In this period, patients received a high-fibre diet and adequate fluid intake (≥2 L/d). After day 8, the collection of excreta was continued on an outpatient basis until levels of radioactivity in the 24-hour urine and faecal collections were below 1% of the administered dose. Upon completion of period A, the patients were given the option to continue with period B.

Patients

Patients aged ≥18 years with a histologically or cytologically confirmed relapsed or refractory malignancy (haematologic or nonhaematologic except for uveal melanoma, sarcoma or primary brain tumours), considered unresponsive or poorly responsive to accepted treatment, were eligible for this study. Other eligibility criteria included World Health Organisation (WHO) performance status ≤2; estimated life expectancy ≥3 months; adequate bone marrow function (absolute neutrophil count ≥1.0 x 10^3/mm^3 and platelet count ≥1.0 x 10^6/mm^3); adequate hepatic function (bilirubin ≤1.5 times the upper limit of normal [ULN] and alanine aminotransferase [ALT] and aspartate aminotransferase [AST] ≤2.5 x ULN or ≤5 x ULN in the case of liver metastases); adequate renal function (creatinine clearance [CL_{CR}] >30 mL/min); and use of an approved method of birth control until ≥90 days after drug discontinuation. Patients were excluded if they smoked or used topical or oral nicotine preparations within 3 months; received mitomycin within 42 days, CYP1A2 inducers, chemotherapy, radiotherapy, radioimmunotherapy or immunotherapy within a month; or CYP1A2 inhibitors or haematopoietic growth factors within 14 days prior to the first study dose as well as if they required treatment with CYP1A2 inhibitors or inducers during days 1–8 of cycle 1 or if they had not recovered from adverse events (AEs) due to previously administered agents. Other reasons for exclusion included pregnancy or breastfeeding, known cerebral metastases, known positive human immunodeficiency virus status, serious infection or medical/psychiatric condition, other treatments for haematologic or nonhaematologic malignancy, previous treatment with bendamustine or significant constipation or obstruction of the urinary tract.

Study medication

Brown borosilicate glass vials containing 100 mg ^{14}C-bendamustine HCl (90–95μCi) were manufactured by Parenteral Medications Laboratories (Memphis, TN, USA), supplied by Teva Pharmaceutical Industries Ltd. (Frazer, PA, USA). They contained a mixture of ^{14}C-bendamustine (chemical and radiochemical purity >99.6%) and nonlabelled bendamustine (chemical purity 99.6%) as a lyophilised powder. Vials with 100 mg nonlabelled bendamustine HCl (chemical purity 99%) were provided by Pharmachemie BV (Haarlem, The Netherlands).

Individual aseptic preparations of ^{14}C-bendamustine infusions were prepared with 1 vial of ^{14}C-bendamustine and one or more vials with nonlabelled bendamustine to obtain a final dose of 120 mg/m^2. Each vial was reconstituted with 20 mL of Sterile Water for Injection. The complete volume of the vial with ^{14}C-bendamustine and the required volume of nonlabelled bendamustine were transferred to a 500-mL infusion bag with 0.9% sodium chloride. The actual administered radioactivity was calculated by determination of the total radioactivity (TRA), in the infusion bag before and after the administration.

Sample collection

Blood samples of 4 mL were collected in K_2EDTA tubes prior to the start of infusion as well as 15, 30, 45, 65 and 75 minutes and 1.5, 2, 2.5, 3, 4, 6, 8, 10, 12, 24, 36, 48, 72, 96, 120, 144 and 168 hours after the start of the ^{14}C-bendamustine infusion. Between collection and centrifugation (12,000 g, 4°C, 10 minutes), the tubes were placed on ice (maximally 30 minutes). An additional 1-mL whole blood sample was collected at the end of the infusion, at 168 hours after start of the infusion and optionally once every week thereafter.

Urine samples were collected before start of the ^{14}C-bendamustine infusion, as voided during specified time intervals (0–2, 2–4, 4–6, 6–8, 8–10, 10–12, 12–18, 18–24, 24–30, 30–36, 36–42, 42–48, 48–72, 72–96, 96–120, 120–144 and 144–168 hours) through 168 hours after the start of the infusion, and over additional 24-hour periods if collection was continued. Each urine sample was measured for TRA and several aliquots were prepared. For analysis of bendamustine, M3, M4 and HP2, 20-µL urine aliquots were mixed with 1980 µL of prechilled control human K_2EDTA plasma, to stabilise the compounds during storage and processing [17].

Faecal samples were collected per portion, prior to and then as voided through 168 hours following the start of the ^{14}C-bendamustine infusion, or longer if TRA represented ≥1% of the radiochemical dose in the 144- to 168-hour collection of faeces. The faecal portions were weighed, stored refrigerated, combined over 24-hour periods and homogenised after addition of water (1:3 w/v).

Plasma aliquots, urine aliquots, and whole blood samples were stored within the range of –70°C and –90°C.

Analysis of TRA

TRA in plasma, whole blood, urine and faecal samples was determined by liquid scintillation counting (LSC). Plasma (0.2 mL) and urine (1 mL) samples were directly mixed with 10 mL liquid scintillation cocktail (Ultima Gold™; PerkinElmer Inc.; Waltham, MA, USA). Whole blood samples (0.2 mL) and faecal homogenates (0.2 mL) were dissolved and decolourised first as described elsewhere [18], using Solvable™ (PerkinElmer Inc.), 30% hydrogen peroxide and either aqueous 0.1 M EDTA or isopropanol, respectively.

Samples were counted on a Tri-Carb® 2800TR LSC (PerkinElmer Inc.). Quench correction was applied with a calibration curve of quenched radioactive reference standards. Samples were counted to a sigma 2 counting error of 1% or for maximally 60 minutes.

Analysis of bendamustine, M3, M4 and HP2

Concentrations of bendamustine, M3, M4 and HP2 in plasma and urine samples obtained through 24 hours were determined with validated LC-MS/MS assays, described elsewhere [17]. Briefly, 200 µL plasma and 200 µL of urine fortified with control human plasma (1:99 v/v) were processed identically using solid-phase extraction after addition of an internal standard mixture. The assay for bendamustine, M3 and M4 used a Synergi™ Hydro-RP column and the assay for HP2, a Synergi™ Polar-RP column (Phenomenex, Inc; Torrance, CA, USA). On both columns, gradient elution was performed with 5 mM ammonium formate with 0.1% formic acid in water and methanol. The quantifiable ranges for bendamustine, M3 and M4 were 0.5–500 ng/mL in plasma and 0.5–50 µg/mL in urine, and for HP2 were 1–500 ng/mL in plasma and 0.1–50 µg/mL in urine. Quality control samples were prepared and analysed together with the study samples, and acceptance criteria for bioanalytical data during routine drug analysis, as described in the Food and Drug Administration (FDA) guidelines [19], were applied.

Pharmacokinetic analysis

Pharmacokinetic parameters for bendamustine, M3, M4, HP2 and TRA were estimated by noncompartmental analysis using WinNonlin™ software (version 4.1.a; Pharsight Corp; Mountain View, CA, USA). Parameters that were determined for all analytes included the maximum observed plasma concentration (C_{max}), the terminal phase half-life ($t_{½}$) and the area under the plasma concentration-time curve from zero to infinity (AUC_{∞}). Additionally, the plasma clearance (CL) and the apparent volume of distribution at steady state (V_{ss}) were determined for bendamustine and estimated for TRA, and the renal clearance (CL_R) was determined for bendamustine.

Safety assessments

The safety of bendamustine was assessed by evaluating AEs according to Common Terminology Criteria for AEs v3.0; serum chemistry, haematology and urinalysis test results; vital signs; 12-lead electrocardiograms (ECGs); body weight; physical examinations; and concomitant medication. ECGs were performed prior to study drug administration and at multiple time points on day 1 of cycle 1.

No formal statistical analysis was applied in this study; descriptive statistics were used when appropriate.

Results

Patients

Six patients with confirmed relapsed or refractory malignancy were enrolled (3 male and 3 female; all white), with a median age of 66 years (range, 48–75), a mean weight of 72.7 kg (range, 59–94), a mean height of 173.2 cm (range, 155–181) and a mean body surface area of 1.9 m^2 (range, 1.6–2.2). At the time of enrolment, 4 (67%) patients had a WHO performance status of 0, and 2 (33%) had a status of 1.

Pharmacokinetics

Plasma concentration-time curves of TRA, bendamustine, M3, M4 and HP2 during 24 hours after the start of the ^{14}C-bendamustine infusion are presented in Figure 2. Table 1 summarises the individual and mean pharmacokinetic parameters.

The maximum plasma concentrations of TRA, bendamustine and HP2 were typically observed in the first sample after completion of the infusion (median t_{max} = 1.10 hours), and the median t_{max} of M3 (1.26 hours) and M4 (1.28 hours) followed shortly thereafter. After reaching peak levels, the concentrations of bendamustine decreased in a multiphasic manner that was characterised by an initial rapid phase of decline, followed by a somewhat slower secondary phase with a mean apparent $t_{½}$ of 0.65 hours. The mean V_{SS} was 20.1 L and the CL 598.3 mL/min.

The active metabolite M3 showed a biphasic decline in concentration after reaching peak levels (mean terminal phase $t_{½}$ = 1.69 hours), whereas the decline of M4 appeared monophasic (mean $t_{½}$ = 0.52 hours). These metabolites had substantially lower concentrations than bendamustine. The concentrations of the dihydrolysis product HP2 were initially also much lower than the concentrations of bendamustine, but unlike the other analytes, small but measurable levels of HP2 were still present at 24 hours after start of the infusion, with a mean C_{24h} of 3.75 ng/mL.

The TRA concentrations were characterised by a very slow decrease after reaching peak levels. After 168 hours, the mean TRA concentration was still 2.29 μg Eq/mL, and the mean $t_{½}$ of the apparent terminal phase was estimated at 197 hours (Table 1). Bendamustine, M3, M4 and HP2 composed the bulk of the TRA early in the profile (almost 80%); however, their contribution to the TRA quickly declined to approximately 1% at 4 hours after start of the infusion.

The mean concentration ratio of TRA in plasma and in whole blood (Figure 3) was ~1.4 immediately after the end of infusion and approximately 1 at later time points.

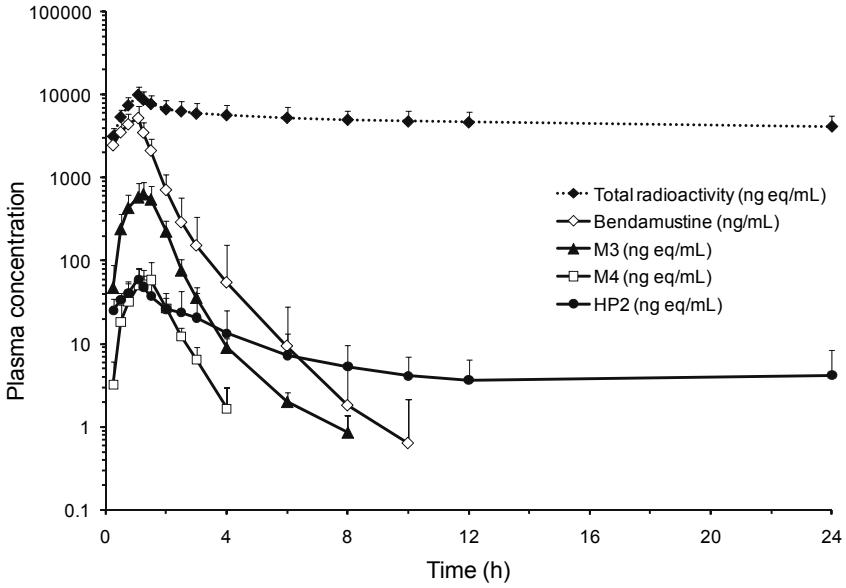

Figure 2: Mean log-linear plasma concentration-time curves. Mean (±SD, N = 6) log-linear plasma concentration-time curves of total radioactivity; unchanged bendamustine; and metabolites γ-hydroxy-bendamustine (M3), *N*-desmethyl-bendamustine (M4) and dihydroxy bendamustine (HP2) up to 24 h after start of a 60-minute (120 mg/m², 80−95 μCi) ^{14}C-bendamustine hydrochloride infusion.

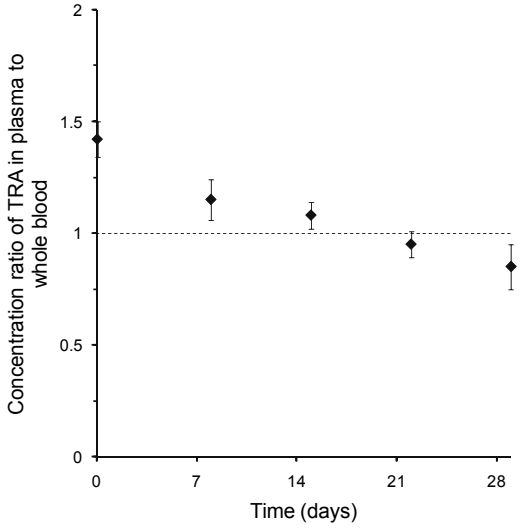

Figure 3: Mean plasma to whole blood concentration ratio of total radioactivity (TRA). Mean (±SD, n = 4–6) plasma to whole blood concentration ratio of TRA immediately after the end of a 60-minute (120 mg/m², 80−95 μCi) ^{14}C-bendamustine hydrochloride infusion and at weekly time points thereafter.

Table 1: Plasma pharmacokinetic parameters for TRA, bendamustine and its metabolites M3, M4 and HP2 following an intravenous 60-minute infusion of 120 mg/m² of ^{14}C-bendamustine hydrochloride

			TRA (Bendamustine equivalents)					Bendamustine			
Pt	BSA	Dose	C_{max}	AUC_∞	$t_{1/2}$	V_{ss}	CL	C_{max}	AUC_∞	$t_{1/2}$	V_{ss}
	m^2	mg[a]	µg/mL	µg·h/mL	h	L	mL/min	µg/mL	ng·h/mL	h	L
1	2.17	233	6.88	904	225	81.2	4.27	3.25	3963	0.57	27.1
2	1.84	198	12.4	1147	110	27.4	2.89	7.48	10619	0.96	15.3
3	1.85	197	9.31	1504	261	48.3	2.16	4.20	4906	0.58	24.4
4	1.6	172	12.1	695	171	59.2	4.13	8.19	8041	0.86	10.7
5	2.05	215	8.54	1403	222	49.6	2.56	3.60	4487	0.45	27.5
6	1.7	182	12.0	1571	193	31.3	1.92	5.20	6371	0.46	15.5
Mean	-	-	10.2	1204	197	49.5	2.99	5.32	6398	0.65	20.1
SD	-	-	2.29	351	52.5	19.6	1.00	2.07	2543	0.21	7.1

[a]Bendamustine free base (mg). AUC_∞: area under the plasma concentration-time curve from zero to infinity; BSA: body surface area; C_{max}: maximum observed plasma concentration; CL: clearance; CL_R: renal clearance; HP2: dihydroxy bendamustine; M3: γ-hydroxy-bendamustine; M4: *N*-desmethyl-bendamustine; NC: not calculable; Pt: patient number; SD: standard deviation; TRA: total radioactivity; $t_{½}$: terminal phase half-life; V_{ss}: apparent volume of distribution at steady state.

Table 2: Cumulative percentage (%) of excretion of bendamustine, M3, M4, HP2 and TRA in urine over 24 h and TRA in urine and faeces over 168 h and until the EoC, following an intravenous 60-minute infusion of 120 mg/m² of ^{14}C-bendamustine hydrochloride

	Urine					
Collection Period:	0−24 h					
Pt	Bendamustine	M3	M4	HP2	Sum[b]	TRA
1	1.46	0.64	0	8.65	10.75	36.36
2	5.17	0.36	0.12	4.09	9.74	36.08
3	1.65	0.5	0.08	4.18	6.41	36.53
4	1.85	0.7	0	8.25	10.8	34.77
5	3.74	0.76	0	2.12	6.62	32.83
6	5.98	1.42	0.27	2.04	9.71	43.1
Mean	3.31	0.73	0.08	4.89	9.01	36.61
SD	1.95	0.37	0.11	2.9	1.99	3.47

[a]The time at the EoC varied among patients and ranged from 168 to 504 h. [b] These values represent the sum of bendamustine, M3, M4 and HP2. EoC: end of collection period; HP2: dihydroxy bendamustine; M3: γ-hydroxy-bendamustine; M4: *N*-desmethyl-bendamustine; Pt: patient number; SD: standard deviation; TRA: total radioactivity.

BM (ctd.)		M3			M4			HP2		
CL mL/min	CL_R mL/min	C_{max} ng/mL	AUC_∞ ng·h/mL	$t_{1/2}$ h	C_{max} ng/mL	AUC_∞ ng·h/mL	$t_{1/2}$ h	C_{max} ng/mL	AUC_∞ ng·h/mL	$t_{1/2}$ h
977	14.3	644	829	3.58	38.7	59	0.48	35.0	NC	NC
313	16.1	264	389	0.82	29.8	61	0.8	73.3	NC	NC
666	11.0	714	975	1.41	50.1	81	0.48	43.2	188	15.4
358	6.6	1125	1428	2.14	87.9	119	0.44	53.1	153	14.1
800	29.9	550	792	1.09	28.5	43	0.45	40.8	215	23.8
476	28.5	816	1137	1.12	117	135	0.45	81.4	NC	NC
598	17.7	685	925	1.69	58.7	83	0.52	54.5	185	17.8
262	9.5	286	351	1.03	36.1	37	0.14	18.8	31	5.3

Urine		Faeces		Total	
0–168 h TRA	0–EoC[a] TRA	0–168 h TRA	0–EoC[a] TRA	0–168 h TRA	0–EoC[a] TRA
42.16	47.6	30.3	32.64	72.46	80.24
50.69	57.93	8.92	8.92	59.61	66.85
45.26	48.26	34.44	34.44	79.7	82.7
40.44	40.44	31.88	31.88	72.32	72.32
43.11	47.86	29.45	35.08	72.56	82.94
51.11	51.93	16.1	18.89	67.21	70.82
45.46	49.00	25.18	26.98	70.64	75.98
4.49	5.75	10.22	10.67	6.71	6.86

Excretion balance

For all 6 patients, urine and faecal samples were collected as planned during the first 168 hours after administration of ^{14}C-bendamustine. Thereafter, urine and faeces continued to be collected for longer periods in 5 and 3 patients, respectively, for up to 3 weeks.

Figure 4 shows the mean cumulative urinary, faecal and total recovery of TRA during 168 hours after ^{14}C-bendamustine administration. At this point, approximately half (45.5%) of the administered radioactivity was recovered in urine and a quarter (25.2%) in faeces, resulting in a total recovery of 70.6% after 168 hours. After the extended collection period, the total recovery was increased to 76.0%. Individual excretion values are tabulated in Table 2.

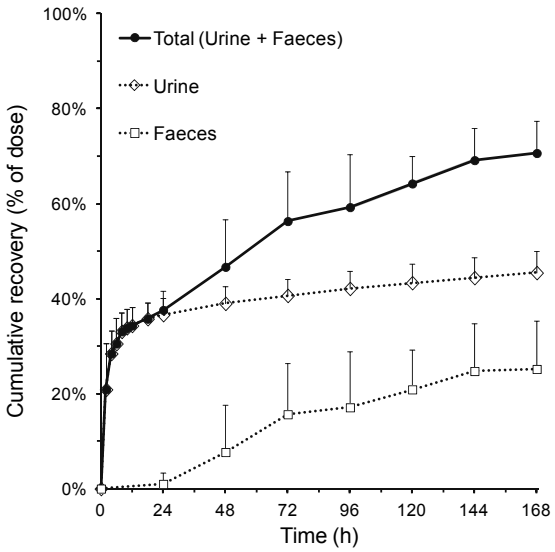

Figure 4. Mean cumulative recovery of ^{14}C-bendamustine-derived total radioactivity. Mean (±SD, N = 6) cumulative recovery of ^{14}C-bendamustine-derived total radioactivity in urine, faeces and in total during 7 days after a 60-minute (120 mg/m^2, 80–95 μCi) 14C-bendamustine hydrochloride infusion.

The mean cumulative urinary excretion of TRA and unchanged bendamustine, M3, M4 and HP2 during the first 24 hours is shown in Figure 5 and summarised per patient in Table 2. At 24 hours, approximately 3.3% of the dose was recovered in urine as bendamustine, <1% as M3 and M4 and <5% as HP2. Urinary recovery of bendamustine, M3, and M4 was predominantly in collections during the first 4 hours after the start of the infusion. After 8 hours, there were no measurable levels of these compounds in urine. The excretion of HP2 continued slowly, and low but quantifiable levels were still present in the urine samples of 16–24 hours.

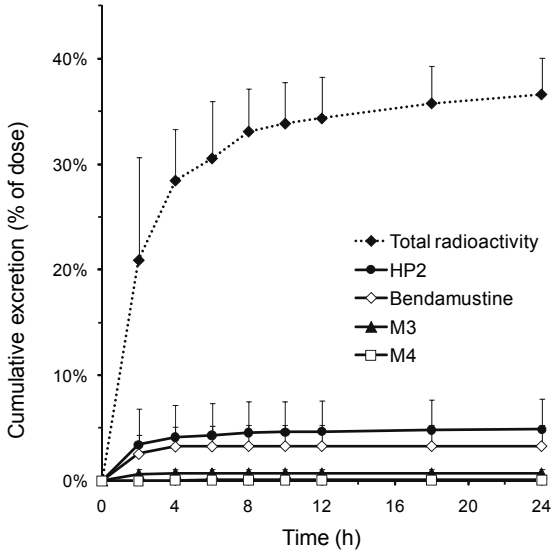

Figure 5. Mean cumulative urinary excretion. Mean (±SD, N = 6) cumulative urinary excretion of total radioactivity; unchanged bendamustine; and metabolites γ-hydroxy-bendamustine (M3), *N*-desmethyl-bendamustine (M4) and dihydroxy bendamustine (HP2) up to 24 h after start of a 60-minute (120 mg/m^2, 80−95 μCi) ^{14}C-bendamustine hydrochloride infusion.

Safety

All patients completed assessment period A, receiving a mean of 4 (range, 2–6) doses of bendamustine. All were withdrawn during assessment period B: 4 due to disease progression, 1 due to an AE (dyspnea) and 1 due to election to discontinue from the study.

During the treatment period, all 6 patients experienced at least 1 AE that was considered treatment-related. AEs occurring in 2 or more patients are shown in Table 3.

The most frequently occurring treatment-related AEs were fatigue (n = 3; 50%) and vomiting (n = 3; 50%). No deaths or treatment-related serious AEs occurred. One patient experienced a serious AE (constipation). Both this event and the AE of dyspnea in 1 patient, resulting in withdrawal of that patient from the study, appeared to be manifestations of the underlying medical condition and were considered unlikely to be related to bendamustine treatment.

There was no evidence of any drug-related trends in values of serum chemistry, urinalysis or vital signs, and no AEs were related to findings of physical examinations or ECG findings. A grade 3 or 4 absolute lymphocyte count decrease was observed in all 6 patients at some point during the study.

Table 3: Adverse events occurring in two or more patients

	Number (%) of Patients[a]		
System Organ Class MedDRA Preferred Term	**Grade 1**	**Grade 2**	**Grade 3**
Gastrointestinal disorders			
Abdominal pain	1 (17)	1 (17)	0
Constipation	1 (17)	3 (50)	0
Diarrhoea	1 (17)	0	1 (17)
Dry mouth	2 (33)	0	0
Nausea	3 (50)	1 (17)	0
Vomiting	1 (17)	2 (33)	0
General disorders and administration site conditions			
Chills	2 (33)	0	0
Fatigue	1 (17)	2 (33)	2 (33)
Pyrexia	3 (50)	1 (17)	0
Metabolism and nutrition disorders			
Anorexia	2 (33)	0	0
Musculoskeletal and connective tissue disorders			
Back pain	1 (17)	1 (17)	0
Nervous system disorders			
Dizziness	3 (50)	0	0
Headache	2 (33)	0	0
Respiratory, thoracic and mediastinal disorders			
Dyspnea	1 (17)	1 (17)	0

[a]Patients (n = 6) may have reported more than 1 adverse event (AE). MedDRA, Medical Dictionary for Regulatory Activities. NOTE: If a patient reported an AE more than once, the highest grade was presented for that AE. Patients were counted only once in each preferred term category, and only once in each system organ class category, at the highest grade for each.

Discussion

This study investigated the pharmacokinetics and excretion of ^{14}C-bendamustine in adult cancer patients. It was found that bendamustine is extensively metabolised with subsequent excretion in urine and faeces.

The short pharmacologically relevant half-life ($t_{½}$ = 0.65 hours), limited volume of distribution (V_{ss} = 20.1 L) and rapid CL (598 mL/min) of bendamustine are in line with results of previous studies [4;15;16;20]. However, a third, much slower elimination phase of bendamustine plasma concentrations, as reported by Owen and colleagues [20], was not observed in this study. The higher lower limit of quantification of the bendamustine assay used in the present study (0.5 versus 0.1 ng/mL) probably explains why the third phase was not detected. Nevertheless, the influence on the pharmacokinetic results is expected to be minimal because the AUC of the third (terminal) phase accounted for less than 1% of the total AUC, and the $t_{½}$ of the intermediate phase was considered to be the most pharmacologically relevant [20].

Consistent with the population pharmacokinetic models for the active metabolites M3 and M4 [20], the plasma elimination profiles of M3 and M4 were biphasic and monophasic,

respectively. The exposures to M3 and M4 were almost 1 and 2 orders of magnitude lower than those to bendamustine, respectively. This was also found in previous studies [4;13;16;20] and suggests a limited contribution of these active metabolites to the therapeutic activity of bendamustine. Additionally, the low plasma concentrations of M3 and M4 relative to the bendamustine concentration suggest a minor role of the CYP1A2 pathway, responsible for the formation of M3 and M4 [13], in the elimination of bendamustine. Consequently, the effect of concomitant treatment that influences CYP1A2 activity on the safety and efficacy of bendamustine is expected to be minimal.

The high and persistent plasma levels of TRA compared with the concentrations of bendamustine, M3, M4 and HP2 combined indicate the presence of 1 or more long-lived bendamustine-related compounds and emphasise the importance of metabolism in the elimination of bendamustine. The volume of distribution of bendamustine (V_{ss} = 20.1 L) implies that the drug is not extensively distributed into tissues. The apparent volume of distribution of TRA (V_{ss} = 49.5 L) seems slightly larger, but is overestimated since nearly half of the radiochemical dose was eliminated during the first 24 hours postdose, a period that represented only approximately 10% of the AUC for TRA. In addition, the plasma-to-whole blood ratio concentration ratios of TRA approximated unity at the later time points, suggesting no preferential association of bendamustine-related compounds with any specific blood components.

The incomplete recovery of TRA (~76%) is probably a result of the long elimination half-life of TRA (197 hours) and is not uncommon for an alkylating agent [21]. Measurable levels of TRA were still present in the last urine and faecal samples, even in those collected 3 weeks after the ^{14}C-bendamustine infusion, suggesting that a higher recovery could have been obtained if the collection time had been further extended. However, the added value of additional excretion data was, in this case, considered limited and did not outweigh the accompanying additional burden for the patients.

Urinary excretion of ^{14}C-bendamustine–derived radioactivity (49% of the administered dose) was more predominant than faecal excretion (27%). The urinary to faecal excretion ratio slightly differs from the ratio in rats, where ~49% of the administered dose was recovered in faeces, with a total recovery of ~90% [14]. Consistent with the rapid CL of bendamustine, M3 and M4 from plasma, these compounds were predominantly found in the 0- to 2-hour urine samples. Additionally, their relative amounts in urine were qualitatively the same as in plasma; ie, the amount of bendamustine >M3 >M4. In contrast, although HP2 concentrations in plasma were substantially lower than the bendamustine concentrations, the amount of HP2 recovered in urine is comparable to the recovered amount of bendamustine, indicating that hydrolysis of bendamustine facilitates renal excretion. The continuing recovery of low amounts of HP2 in urine correlates with the continuing low levels of HP2 that were measured in plasma.

The first 24-hour urine recovery values of unchanged bendamustine (3.31 ± 1.95%), M3 (0.73 ± 0.37%), M4 (0.08 ± 0.11%) and HP2 (4.89 ± 2.91%), adding up to a total of 9.01 ± 1.99%, are comparable to values seen in previous studies. Teichert and colleagues recovered 3.23 ± 3.69%, 0.30 ± 0.31%, 0.05 ± 0.03% and 0.94 ± 0.13% of the administered dose as bendamustine, M3, M4 and HP2, respectively, in the 0- to 24-hour urine samples after bendamustine infusion [13]. In two studies, Rasschaert and colleagues recovered 9.8% and 8.3% (range, 2.7%–26.0%) of the administered dose in the first micturition after a bendamustine infusion as bendamustine, M3, M4, HP1 and HP2 combined [15;16]. They further observed a high variation in the urine results; eg, the contribution of bendamustine to the total amount of bendamustine, M3, M4, HP1 and HP2 combined ranged between 0.8% and 50.2%. This result was explained as variable undesirable hydrolysis.

In the present study, extensive measures were applied to minimise degradation of bendamustine. Each urine void was processed individually and immediately; urine was diluted in prechilled control human plasma for stabilisation and immediately stored at -70°C pending bioanalysis, when samples were thawed on ice water and kept on ice water whenever possible during sample preparation. The stability of bendamustine was confirmed under these conditions [17]. Still, considerable variation was present in the urinary recovery of bendamustine. One cause may be the intrinsic variation of bendamustine elimination, which was also observed in plasma. Additionally, even though patients were asked to void their bladder every 2 hours during the first 12 hours, variable intravesical conversion of bendamustine may have contributed to variations in recovery and possibly to an underprediction of unchanged bendamustine excretion.

The relatively low recovery of bendamustine, M3, M4 and HP2 (combined 9.01% ± 1.99%) compared with the recovery of TRA (36.61% ± 3.47% after 24 hours) indicates the presence of additional metabolites. This finding is consistent with the metabolite profile in rat urine. Sixteen metabolites of bendamustine were detected in rat urine collected 0−4 hours after administration of ^{14}C-bendamustine to rats, and a major portion of the radioactivity in urine was accounted for by products of *N*-deethylation and *N*-acetylcysteine conjugates [14].

Bendamustine was well tolerated when administered at a dose of 120 mg/m^2 for 2 or 3 cycles. Bendamustine has been associated with myelosuppression, mild gastrointestinal events and fatigue [3;10;22]. The treatment-related AEs in the present study, with vomiting (50%) and fatigue (50%) as the most frequently reported, and lymphocytopenia, were consistent with the known safety profile of bendamustine. The short intermediate half-life and dosing schedule of bendamustine, in addition to the fact that bendamustine is extensively metabolised via multiple pathways, suggest accumulation is unlikely in patients with hepatic insufficiency. However, in a previous study [23], a longer intermediate half-life (47 versus 33 minutes) and lower CL (304 versus 639 mL/min) were demonstrated in

patients with severe hepatic impairment, leading to current labelling recommendations to use bendamustine with caution in mildly hepatically impaired patients and a contraindication for use in patients with moderate to severe impairment.

In conclusion, metabolism–in particular hydrolysis–has a major role in the elimination of bendamustine. Renal excretion of unchanged bendamustine is minor, representing only ~3% of the administered dose. Even though bendamustine excretion might be underestimated due to intravesical degradation, these results combined with the short $t_{½}$ of bendamustine and the dosing schedule of 2 consecutive days in 21- or 28-day cycles, suggest that renal impairment is also unlikely to have a substantial impact on systemic exposure to bendamustine. Treatment with bendamustine at a dose of 120 mg/m^2 for 2−3 cycles was tolerated with an acceptable level of toxicity in patients with confirmed relapsed or refractory malignancy. AEs and haematologic changes were consistent with the known safety profile of bendamustine. Additional research is being conducted to further elucidate the metabolic profile of bendamustine in humans.

References

[1] Leoni LM, Bailey B, Reifert J, Bendall HH, Zeller RW, Corbeil J, Elliott G, Niemeyer CC, Bendamustine (Treanda) displays a distinct pattern of cytotoxicity and unique mechanistic features compared with other alkylating agents, *Clin.Cancer Res.*, **14** (2008) 309-317.

[2] Fowler N, Kahl BS, Lee P, Matous JV, Cashen AF, Jacobs SA, Letzer J, Amin B, Williams ME, Smith S, Saleh A, Rosen P, Shi H, Parasuraman S, Cheson BD, Bortezomib, bendamustine, and rituximab in patients with relapsed or refractory follicular lymphoma: the phase II VERTICAL study, *J.Clin.Oncol.*, **29** (2011) 3389-3395.

[3] Friedberg JW, Cohen P, Chen L, Robinson KS, Forero-Torres A, La Casce AS, Fayad LE, Bessudo A, Camacho ES, Williams ME, Van der Jagt RH, Oliver JW, Cheson BD, Bendamustine in patients with rituximab-refractory indolent and transformed non-Hodgkin's lymphoma: results from a phase II multicenter, single-agent study, *J.Clin.Oncol.*, **26** (2008) 204-210.

[4] Ogura M, Uchida T, Taniwaki M, Ando K, Watanabe T, Kasai M, Matsumoto Y, Shimizu D, Ogawa Y, Ohmachi K, Yokoyama H, Tobinai K, Phase I and pharmacokinetic study of bendamustine hydrochloride in relapsed or refractory indolent B-cell non-Hodgkin lymphoma and mantle cell lymphoma, *Cancer Sci.*, **101** (2010) 2054-2058.

[5] Ponisch W, Rozanski M, Goldschmidt H, Hoffmann FA, Boldt T, Schwarzer A, Ritter U, Rohrberg R, Schwalbe E, Uhlig J, Zehrfeld T, Schirmer V, Haas A, Kreibich U, Niederwieser D, Combined bendamustine, prednisolone and thalidomide for refractory or relapsed multiple myeloma after autologous stem-cell transplantation or conventional chemotherapy: results of a Phase I clinical trial, *Br.J.Haematol.*, **143** (2008) 191-200.

[6] Eichbaum MH, Schuetz F, Khbeis T, Lauschner I, Foerster F, Sohn C, Schneeweiss A, Weekly administration of bendamustine as salvage therapy in metastatic breast cancer: final results of a phase II study, *Anticancer Drugs*, **18** (2007) 963-968.

[7] von Minckwitz G, Chernozemsky I, Sirakova L, Chilingirov P, Souchon R, Marschner N, Kleeberg U, Tsekov C, Fritze D, Thomssen C, Stuart N, Vermorken JB, Loibl S, Merkle K, Kaufmann M, Bendamustine prolongs progression-free survival in metastatic breast cancer (MBC): a phase III prospective, randomized, multicenter trial of bendamustine hydrochloride, methotrexate and 5-fluorouracil (BMF) versus cyclophosphamide, methotrexate and 5-fluorouracil (CMF) as first-line treatment of MBC, *Anticancer Drugs*, **16** (2005) 871-877.

[8] Strumberg D, Harstrick A, Doll K, Hoffmann B, Seeber S, Bendamustine hydrochloride activity against doxorubicin-resistant human breast carcinoma cell lines, *Anticancer Drugs*, **7** (1996) 415-421.
[9] Friedberg JW, Vose JM, Kelly JL, Young F, Bernstein SH, Peterson D, Rich L, Blumel S, Proia NK, Liesveld J, Fisher RI, Armitage JO, Grant S, Leonard JP, The combination of bendamustine, bortezomib, and rituximab for patients with relapsed/refractory indolent and mantle cell non-Hodgkin lymphoma, *Blood*, **117** (2011) 2807-2812.
[10] Ohmachi K, Ando K, Ogura M, Uchida T, Itoh K, Kubota N, Ishizawa K, Yamamoto J, Watanabe T, Uike N, Choi I, Terui Y, Usuki K, Nagai H, Uoshima N, Tobinai K, Multicenter phase II study of bendamustine for relapsed or refractory indolent B-cell non-Hodgkin lymphoma and mantle cell lymphoma, *Cancer Sci.*, **101** (2010) 2059-2064.
[11] Robinson KS, Williams ME, Van der Jagt RH, Cohen P, Herst JA, Tulpule A, Schwartzberg LS, Lemieux B, Cheson BD, Phase II multicenter study of bendamustine plus rituximab in patients with relapsed indolent B-cell and mantle cell non-Hodgkin's lymphoma, *J.Clin.Oncol.*, **26** (2008) 4473-4479.
[12] Rummel MJ, Al Batran SE, Kim SZ, Welslau M, Hecker R, Kofahl-Krause D, Josten KM, Durk H, Rost A, Neise M, von Grunhagen U, Chow KU, Hansmann ML, Hoelzer D, Mitrou PS, Bendamustine plus rituximab is effective and has a favorable toxicity profile in the treatment of mantle cell and low-grade non-Hodgkin's lymphoma, *J.Clin.Oncol.*, **23** (2005) 3383-3389.
[13] Teichert J, Baumann F, Chao Q, Franklin C, Bailey B, Hennig L, Caca K, Schoppmeyer K, Patzak U, Preiss R, Characterization of two phase I metabolites of bendamustine in human liver microsomes and in cancer patients treated with bendamustine hydrochloride, *Cancer Chemother.Pharmacol.*, **59** (2007) 759-770.
[14] Chovan JP, Li F, Yu E, Ring SC, Metabolic profile of [(14)C]bendamustine in rat urine and bile: preliminary structural identification of metabolites, *Drug Metab Dispos.*, **35** (2007) 1744-1753.
[15] Rasschaert M, Schrijvers D, Van den BJ, Dyck J, Bosmans J, Merkle K, Vermorken JB, A phase I study of bendamustine hydrochloride administered day 1+2 every 3 weeks in patients with solid tumours, *Br.J.Cancer*, **96** (2007) 1692-1698.
[16] Rasschaert M, Schrijvers D, Van den BJ, Dyck J, Bosmans J, Merkle K, Vermorken JB, A phase I study of bendamustine hydrochloride administered once every 3 weeks in patients with solid tumors, *Anticancer Drugs*, **18** (2007) 587-595.
[17] Dubbelman AC, Tibben M, Rosing H, Gebretensae A, Nan L, Gorman SH, Robertson P, Jr., Schellens JH, Beijnen JH, Development and validation of LC-MS/MS assays for the quantification of bendamustine and its metabolites in human plasma and urine, *J.Chromatogr.B Analyt.Technol.Biomed.Life Sci.*, (2012).
[18] Dubbelman AC, Rosing H, Jansen RS, Mergui-Roelvink M, Huitema AD, Koetz B, Lymboura M, Reyderman L, Lopez-Anaya A, Schellens JH, Beijnen JH, Mass balance study of [14C]eribulin in patients with advanced solid tumors, *Drug Metab Dispos.*, **40** (2012) 313-321.
[19] US FDA, Department of Health and Human Services, Guidance for Industry, Bioanalytical Method Validation, www.fda.gov/downloads/Drugs/GuidanceComplianceRegulatoryInformation/Guidances/ucm070107.pdf, (2001), Accessed at: 9-1-2012
[20] Owen JS, Melhem M, Passarell JA, D'Andrea D, Darwish M, Kahl B, Bendamustine pharmacokinetic profile and exposure-response relationships in patients with indolent non-Hodgkin's lymphoma, *Cancer Chemother.Pharmacol.*, **66** (2010) 1039-1049.
[21] Beumer JH, Beijnen JH, Schellens JH, Mass balance studies, with a focus on anticancer drugs, *Clin.Pharmacokinet.*, **45** (2006) 33-58.
[22] Knauf WU, Lissichkov T, Aldaoud A, Liberati A, Loscertales J, Herbrecht R, Juliusson G, Postner G, Gercheva L, Goranov S, Becker M, Fricke HJ, Huguet F, Del G, I, Klein P, Tremmel L, Merkle K, Montillo M, Phase III randomized study of bendamustine compared with chlorambucil in previously untreated patients with chronic lymphocytic leukemia, *J.Clin.Oncol.*, **27** (2009) 4378-4384.

[23] Preiss, R, Teichert, J, Athmani, A, Dollinger, M, Preiss, S, Schoppmeyer, K, and et al., Pharmacokinetics and toxicity profile of bendamustine in patients with impaired liver function, *Poster presented at: 2nd International Conference on Drug Discovery and Therapy; Dubai, United Arab Emirates*, (2010).

Chapter 2.3

Metabolite profiling of bendamustine in urine of cancer patients after administration of ^{14}C-bendamustine

Anne-Charlotte Dubbelman, Robert S. Jansen, Hilde Rosing, Mona Darwish, Edward Hellriegel, Philmore Robertson, Jr., Jan H.M. Schellens, Jos H. Beijnen

Drug Metabolism and Disposition (2012) April 4, epub ahead of print

Abstract

Bendamustine is an alkylating agent consisting of a mechlorethamine derivative, a benzimidazole group, and a butyric acid substituent. A human mass balance study showed that bendamustine is extensively metabolized and subsequently excreted in urine. Limited information, however, is available on the metabolite profile of bendamustine in human urine. The objective of this study was to elucidate the metabolic pathways of bendamustine in humans by identification of its metabolites excreted in urine. Human urine samples were collected up to 168 h after an intravenous infusion of 120 mg/m^2, 80–95 μCi ^{14}C-bendamustine. Metabolites of ^{14}C-bendamustine were identified using liquid chromatography (high resolution) tandem mass spectrometry with off-line radioactivity detection. Bendamustine and a total of 25 bendamustine-related compounds were detected. Observed metabolic conversions at the benzimidazole and butyric acid moiety were *N*-demethylation and γ-hydroxylation. Additionally, various other combinations of these conversions with modifications at the mechlorethamine moiety were observed, including hydrolysis (the primary metabolic pathway), cysteine conjugation and subsequent biotransformation to mercapturic acid and thiol derivatives, *N*-dealkylation, oxidation, and conjugation with phosphate, creatinine, and uric acid. Bendamustine-derived products containing phosphate, creatinine, and uric acid conjugates were also detected in control urine incubated with bendamustine. Metabolites that were excreted up to 168 h after the infusion included products of dihydrolysis and cysteine conjugation of bendamustine and γ-hydroxybendamustine. The range of metabolic reactions is generally consistent with those reported for rat urine and bile, suggesting that the overall processes involved in metabolic elimination are qualitatively the same in rats and humans.

Introduction

Bendamustine is an alkylating agent that is used for the treatment of chronic lymphocytic leukemia and indolent B-cell non-Hodgkin's lymphoma that has progressed during or following treatment with a rituximab-containing regimen. It consists of a bifunctional mechlorethamine derivative, a benzimidazole heterocyclic ring, and a butyric acid moiety (Table 1).

Clinical and preclinical studies showed that bendamustine is extensively metabolized in vivo [1-3]. Two phase 1 metabolites have been identified resulting from metabolic conversions at the benzimidazole/butyric acid moiety: γ-hydroxybendamustine and *N*-desmethylbendamustine [4]. All other metabolic conversions occurred at the mechlorethamine moiety. In human bile, cysteine *S*-conjugates, mercapturic acid, and mercapturic acid sulfoxide conjugates were detected, suggesting an important role of the glutathione conjugation pathway in the metabolism of bendamustine, although intact glutathione conjugates were not observed [3]. In contrast, intact glutathione conjugates were observed in rat urine. Among the metabolites detected in rat urine and bile, three metabolites were identified as glutathione conjugates and six as mercapturic acid conjugates. Additionally, products of *N*-dealkylation, oxidation, carboxylic acid formation, and sulphate conjugation were postulated [1]. Human urine has been investigated for the presence of cysteine *S*-conjugates [2], but the presence of other metabolites and the excretion of bendamustine metabolites over time have not been described.

Table 1: Chemical structure of bendamustine and its metabolites for which reference standards were available[a]

	Compound	R1	R2	R3	R4
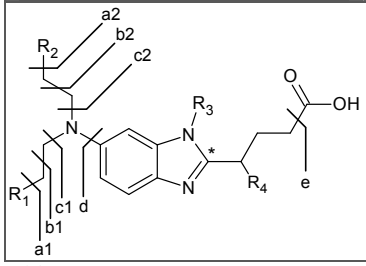	Bendamustine (BM)	Cl	Cl	CH_3	H
	γ-Hydroxybendamustine (M3)	Cl	Cl	CH_3	OH
	N-Desmethylbendamustine (M4)	Cl	Cl	H	H
	Product of monohydrolysis (HP1)	Cl	OH	CH_3	H

[a]The asterisk indicates the position of the ^{14}C-label. The letters a1, a2, b1…e indicate characteristic fragmentation points of bendamustine metabolites during MS^n and refer to Table 2.

The objective of this study was to elucidate the metabolic pathways of bendamustine in humans by identification of the chemical structures of its metabolites excreted in urine. In a mass balance study with ^{14}C-bendamustine in humans, 76% of the administered radiochemical dose was recovered in excreta collected in a period of up to three weeks after administration of a single 60-min intravenous dose of 120 mg/m^2, 80-95 μCi ^{14}C-bendamustine hydrochloride [5]. Approximately half of the radiochemical dose was

recovered in urine and approximately a quarter in faeces. Unchanged bendamustine in urine comprised only ~3% of the dose, indicating a major role of metabolism in the excretion of bendamustine. During the mass balance study, separate urine aliquots were prepared for metabolite profiling. From these aliquots, high concentration samples were selected to detect metabolites using a selective high-performance liquid chromatography (HPLC) method, followed by off-line radioactivity detection and characterisation with a linear ion trap mass spectrometer. Using existing knowledge of bendamustine metabolism and high-resolution mass spectrometry (MS), the metabolites were tentatively identified. Additionally, their presence in urine was investigated over time, up to 168 h after the ^{14}C-bendamustine infusion.

2 Materials and Methods

Reference standards and chemicals.

Reference standards of bendamustine (4-[5-[bis(2-chloroethyl)amino]-1-methyl-benzoimidazol-2-yl]butyric acid hydrochloride), *N*-desmethylbendamustine (M4) and the product of monohydrolysis (HP1) were synthesized by Carbogen AMCIS AG (Bubendorf, Switzerland). Cephalon Inc. (Now a wholly owned subsidiary of Teva Pharmaceutical Industries Ltd., Frazer, PA) manufactured γ-hydroxybendamustine (M3) and Salmedix Inc. (San Diego, CA) manufactured the product of dihydrolysis (HP2). Cephalon Inc. kindly provided all reference compounds. An overview of their structures is provided in Table 1.

Methanol (Supra-Gradient grade) and acetonitrile (Supra-Gradient grade) were obtained from Biosolve Ltd (Valkenswaard, the Netherlands). Formic acid (≥98%) and water (LiChrosolv) were purchased from Merck (Darmstadt, Germany) and Ultima Gold liquid scintillation cocktail from Perkin Elmer (Waltham, MA).

Samples

The urine samples used in this study were collected during a human mass balance study with ^{14}C-bendamustine [5]. Each void was collected individually and aliquots were stored at nominally –70°C. Upon analysis of a sample, one urine aliquot was thawed on ice water and divided over autosampler vials. One autosampler vial was used for immediate analysis and the others were refrozen for additional analyses.

All patients gave their informed consent before participation to the mass balance study and the study was conducted in accordance with the guidelines for Good Clinical Practice, the code of Federal Regulations title 21 (parts 50, 54, 56, 312, and 314), and the European Clinical Trials Directive (2001/20/EC).

Metabolite detection

Urine samples collected 2 h after the start of the infusion of ^{14}C-bendamustine (which was the urine portion with the highest radioactive concentration for 5 out of 6 patients) were submitted to a 180-min HPLC with off-line radiodetection by liquid scintillation counting (LSC) and mass spectrometric detection (liquid chromatography [LC]-LSC-MS^n). The predose urine samples were analysed using this method as well; however, no radiodetection was performed.

Individual urine aliquots, stored at –70°C, were thawed, vortex mixed, and analysed immediately. An Accela autosampler (Thermo Fisher Scientific, Waltham, MA), thermostatted at 4°C, loaded sample volumes of 50 µL onto a Synergi Polar RP column (4.6 mm i.d. x 150 mm, 4 µm particle size, Phenomenex, Torrance, CA) preceded by an in-line filter (0.2 µm, Upchurch Scientific, Oak Harbor, WA). The HPLC pump (Accela, Thermo Fisher Scientific) maintained a flow rate of 1.0 mL/min and started a gradient elution with 100% of 0.1% formic acid in water, followed by a slow linear increase of organic solvent (acetonitrile) to reach 12.5% acetonitrile at 75 min, 50% at 150 min and 80% at 180 min.

A post-column accurate flow splitter (LC Packings, Sunnyvale, CA) directed ¼ of the flow to an LTQ XL linear ion trap mass spectrometer (Thermo Fisher Scientific) and ¾ to a fraction collector (LKB-FRAC-100, Pharmacia, Amersham Biosciences, Uppsala, Sweden).

During the first 4 minutes, the MS eluent was directed to waste using a switching valve. The mass spectrometer was equipped with an electrospray ionization probe and operated in the positive ion mode, with a spray voltage of 5.4 kV, a capillary temperature of 300ºC, and a capillary voltage of 6.5 V. The sheath, auxiliary, and sweep gas flows were optimized to 60, 10, and 5 arbitrary units, respectively. Wideband activation was enabled, the scan range was 100–1100 atomic mass units, the isolation width was 2.0, and the normalized collision energy used for collision-induced dissociation was 35%. Data-dependent acquisition of MS^2 and MS^3 spectra was based on a predefined parent list containing m/z values of known bendamustine metabolites.

The eluent directed to the fraction collector was collected in 6-mL plastic LSC vials at a rate of 1 min/vial. After the addition of 4 mL of liquid scintillation cocktail, the total radioactivity per fraction was determined with a Tri-Carb 2800TR liquid scintillation counter (Perkin Elmer). A calibration curve of quenched radioactive reference standards was used to correct for quenching. Samples were counted to a sigma 2 error of 1% with a maximum of 20 min.

Radiochromatograms were constructed by plotting the radioactivity (after background subtraction) against the retention time. Fractions containing at least 1% of the total radioactivity in a chromatogram in one or more urine samples were selected for further characterization. At the retention time of these peaks, the mass spectra of predose and

postdose samples were compared, in order to find ions that were present in the postdose samples and absent in the predose samples. These molecular ion masses were added to the parent list, which was used for the data-dependent analysis of all following LC-MS measurements.

Metabolite identification

Metabolite identification was performed by analysis of the LC-MS^n data. Several tools were employed to facilitate the identification:

- Investigation of isotope pattern in the full MS spectrum for the presence of 1 or 2 chlorine atoms. The presence of 1 chlorine atom was recognized by the typical isotope pattern of two ions 2 Da apart (from the ^{35}Cl and ^{37}Cl isotopes) with a proportion of 3:1. The presence of 2 chlorine atoms was recognized by the typical isotope pattern consisting of three ions 2 Da apart with a proportion of 9:6:1.
- Comparison of detected molecular masses with masses in a list of possible metabolites. Using literature on metabolites of bendamustine [1;3], a list was made with the $[M+H]^+$ values of potential combinations of bendamustine, γ-hydroxybendamustine, and *N*-desmethylbendamustine with reactions at the mechlorethamine moiety.
- Retention times and fragmentation patterns of potential metabolites were compared with those of the available reference standards (Table 1 and Figure 1). To obtain the γ-hydroxy (M3) and *N*-desmethyl (M4) equivalents of monohydrolyzed bendamustine (HP1) and dihydrolyzed bendamustine (HP2), reference standards of M3 and M4 were incubated for 1 h at 60°C in water.

The elemental composition of the proposed structures was confirmed by the analysis of high-resolution MS and MS^2 data. Additionally, the high-resolution data were used to propose an elemental composition and, if possible, a structure for metabolites that were not identified with the normal resolution data.

High-resolution MS was performed on selected samples using an LTQ Orbitrap XL, preceded by a Finnigan Surveyor MS Pump Plus (Thermo Fisher Scientific). The 180-min chromatographic method and instrumental settings were identical to those described in the section *Metabolite Detection*, except for the normalized collision energy, which was set at 40% and the data-dependent acquisition settings, which were adapted to collect high-resolution MS^2 data of the most intense and the second most intense ion of the parent mass list. The resolution was set at 60,000.

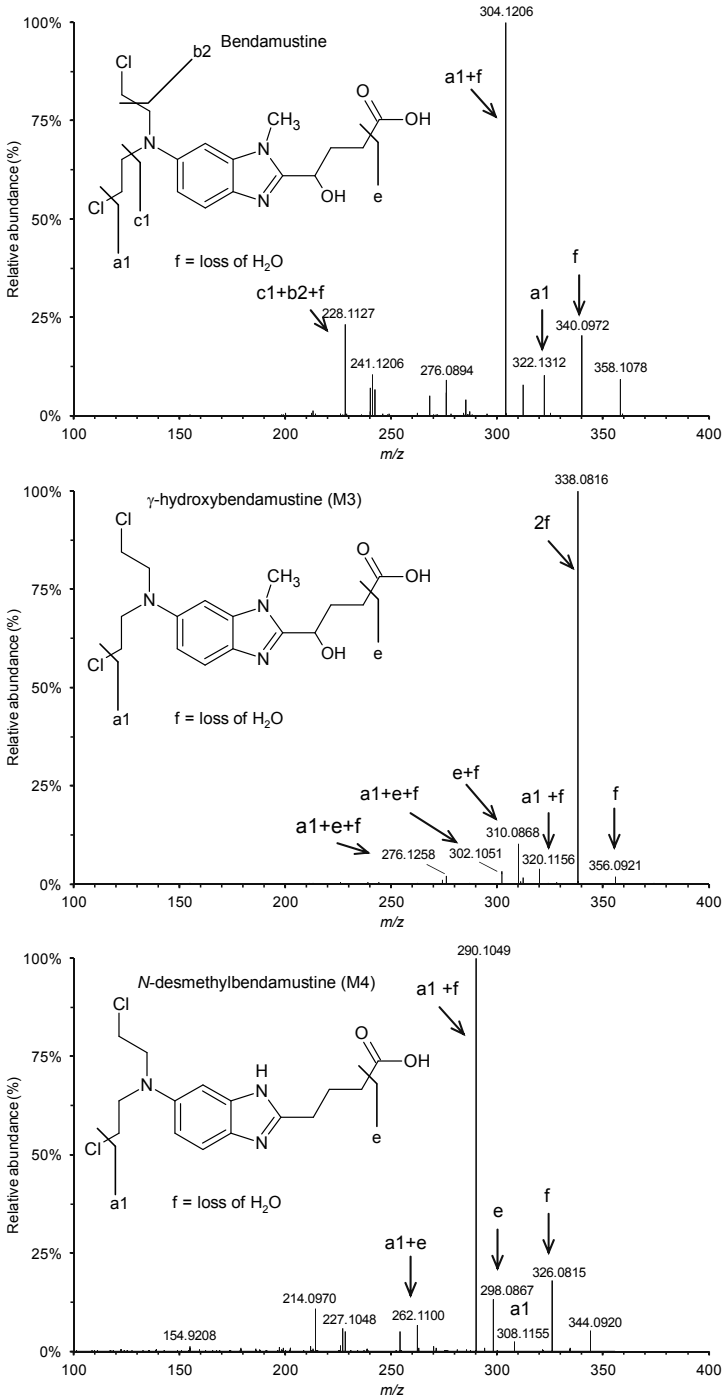

Figure 1: High-resolution MS² spectra and proposed fragmentation of the reference standards of bendamustine, γ-hydroxybendamustine, and *N*-desmethylbendamustine.

Time course

To determine the bendamustine metabolite profile over time, urine samples of each patient collected at 2, 6, 24, 48, 96, and 168 h after the start of the ^{14}C-bendamustine infusion were analysed using a 60-min LC-LSC-MS^n method. The instrumental settings were identical to those described for the 180-min LC-LSC-MS^n runs, except for the gradient composition. The gradient started with 95% of 0.1% formic acid in water and 5% of acetonitrile for 5 min. The acetonitrile percentage was increased to reach 10% at 15 min, 20% at 25 min, 40% at 35 min, 60% at 45 min, and 80% at 50 min. This composition was maintained for 4.9 min, followed by a return to the initial condition of 5% acetonitrile, which was held for 5 min.

Intravesical formation of metabolites

Since a previous study showed that the stability of bendamustine in urine is limited [6], an additional experiment was carried out to test for potential intravesical conversion of bendamustine. Hereto, a control urine sample was spiked with bendamustine to a final concentration of 25 µg/mL and analysed immediately (time zero) and after incubation for 1 h at 37°C, whereby the 60-minute chromatographic method was applied without fraction collection. The presence of metabolites was qualitatively assessed in both aliquots by LC-tandem MS (LC-MS/MS).

Results

Metabolite detection and identification

The radiochromatograms of the 180-min LC-LSC-MS^n runs revealed 25 peaks that had a radioactivity of more than 1% of the total radioactivity in the sample of one or more patients. These peaks were bendamustine (26) and bendamustine-related compounds, assigned Met2 to Met25. Figure 2 shows a representative radiochromatogram of a 2-h urine sample. Radiochromatograms of the 2-h urine samples of all six patients are provided in the Supplemental Data (Supplemental Figure 1). One additional early-eluting peak (Met1) was detected in the 60-min radiochromatograms of urine samples collected at later time points (Figure 3). For each compound, the retention time on both the 180-min and 60-min HPLC method, the proposed elemental composition, theoretical and observed $[M+H]^+$ value, the major or characteristic product ions with their proposed origin, and proposed identification are summarized in Table 2. The proposed chemical structures can be found in Table 3.

Met1 was not prominently present (i.e., >1% of the total radioactivity) in any of the 2-h urine samples; however, this metabolite became prevalent over time (Figure 3). In the 60-min HPLC run, the retention time was between 3 and 5 min. A molecular ion was not identified by LC-MS analysis and therefore, the structure of Met1 was not determined.

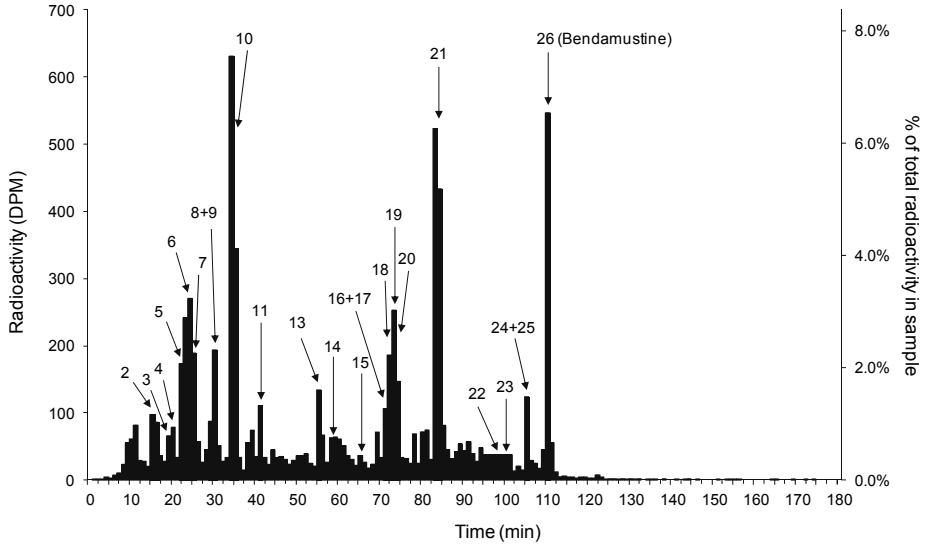

Figure 2: Radiochromatogram of a urine sample collected from a cancer patient 2 h after start of a 1-h infusion with ^{14}C-bendamustine (120 mg/m^2, ~95 μCi), using a selective chromatographic method.

The molecular ion of Met2 was detected at *m/z* 418 and comparison with the list of potential metabolites suggested a sulphate conjugate of didechlorinated γ-hydroxybendamustine. However, this was not confirmed by the high-resolution data. The high-resolution *m/z* of 418.1363 suggested an elemental composition of $C_{16}H_{24}N_3O_8P$. Major product ions were 338.1075 (–79.9658 Da, loss of HPO_3), 320.1600 (–97.9763 Da, loss of H_3PO_4), and 302.1495 (–115.9868 Da, loss of H_3PO_4 and water). The MS^3 spectrum of the product ion at *m/z* 338 (see Figure 3) was identical to the MS^2 spectrum of the dihydrolysis product of γ-hydroxybendamustine obtained by degradation of M3. Met2 was therefore proposed to be a phosphate conjugate of didechlorinated γ-hydroxybendamustine.

Met3 had a retention time of 10.9 min and 18.7 min on the 60-min and 180-min HPLC runs, respectively. The retention times and the MS^2 spectrum were identical to those of the product of dihydrolysis of *N*-desmethylbendamustine obtained by degradation of M4, which was therefore the proposed identity of Met3. This was confirmed with the high-resolution data.

Met4, with a protonated ion at *m/z* 441, was tentatively identified as a cysteine conjugate of didechlorinated γ-hydroxybendamustine, based on the list of potential metabolites. This proposed structure was supported by the high-resolution *m/z* value and by the product ions at *m/z* 352.1320 (-89.047 Da, loss of alanine) and *m/z* 294.1444 (–147.0346 Da, loss of ethylcysteine).

The ion of Met5 at m/z 402 suggested a sulphate conjugate of didechlorinated bendamustine. However, the high-resolution mass pointed to an elemental composition of $C_{16}H_{24}N_3O_7P$. The same neutral losses were observed as for Met2: at m/z 322.1756 (–79.9659 Da, loss of HPO_3), m/z 304.1650 (–97.9765 Da, loss of H_3PO_4), and 286.1545 (–115.9870 Da, loss of H_3PO_4 and water). Since the MS^3 spectrum of the product ion at m/z 322 showed the same fragmentation pattern as the MS^2 spectrum of the reference standard of dihydrolyzed bendamustine, the proposed structure of Met5 was a phosphate conjugate of didechlorinated bendamustine.

Metabolite Met6 had a retention time of 13.3 min and 23.8 min on the 60-min and 180-min HPLC runs, respectively. The retention times, MS^n spectra and high-resolution data were identical to those of the product of dihydrolysis of γ-hydroxybendamustine (obtained by thermal degradation of M3), which was therefore the proposed identity of Met6.

The protonated ion of Met7, found at m/z 417 (417.2234 with high-resolution MS), was not present in the list of potential metabolites. The most abundant product ion at m/z 304.1651 (–113.0583 Da) fragmented identically to the fragment at m/z 304 in the MS^2 spectrum of dihydrolyzed bendamustine, suggesting that Met7 was a 113.0583-Da conjugate of didechlorinated bendamustine. The proposed elemental composition of the conjugate was $C_4H_7N_3O$ (113.0584 Da; Δppm = –0.88), which corresponds with the endogenous compound creatinine. Met7 was therefore proposed to be a creatinine conjugate of didechlorinated bendamustine.

The m/z value of the protonated ion of Met8 (m/z 425) corresponded with a cysteine conjugate of didechlorinated bendamustine in the list of potential metabolites. This identification was supported by the high-resolution m/z value and the neutral losses that were similar to Met4: at m/z 336.1371 (–89.047 Da, loss of alanine) and 278.1494 (–147.0347 Da, loss of ethylcysteine).

The m/z value of the protonated ion of Met9 (m/z 276) corresponded with oxidized *N*-dealkylated bendamustine in the list of potential metabolites. The identification was supported by the high-resolution m/z value and the major product ions 258.1232 (–18.0104 Da, loss of water), 230.1283 (–46.0053 Da, loss of carboxyl moiety), and 217.0972 (–59.0364, loss of aminoacetaldehyde), which are consistent with those reported for this compound in rat urine [1].

Met10 eluted at 17.6 min and 33.7 min when applying the 60-min and 180-min chromatography, respectively. Based on comparison of the retention times, MS^n spectra, and the high-resolution data of Met10 with the available reference standards, Met10 was identified as dihydrolyzed bendamustine (HP2).

The protonated ion of Met11, found at m/z 472 (472.1923 with high-resolution MS), was not in the potential metabolites list. The presence of product ions at m/z 304.1651 and

278.1494, which were also detected in the MS^2 spectrum of HP2, and the absence of a ^{37}Cl isotope suggested that Met11 was a 168.0272-Da conjugate of didechlorinated bendamustine. The proposed elemental composition of the conjugate was $C_5H_4N_4O_3$ (168.0278 Da; Δppm = –3.57), which corresponds with the endogenous compound uric acid. Neutral loss of 43 Da (HCON), followed by loss of 28 Da (CO), is frequently observed for uric acid derivatives [7] and also occurred for Met11, supporting the proposed identification of this compound as a uric acid conjugate of didechlorinated bendamustine.

The protonated ion of Met12, detected at *m/z* 454 (454.1805 with high-resolution MS), was also not present in the potential metabolites list and, similar to Met11, the presence of the HP2-related product ions at *m/z* 304.1651 and 278.1495 and the absence of a ^{37}Cl isotope suggested that Met12 was a 150.0154-Da conjugate of didechlorinated bendamustine. However, the structure of the conjugate was not identified.

The protonated ion of Met13, found at *m/z* 435 (435.1894 with high-resolution MS), was not in the list of potential metabolites. The isotope pattern indicated presence of 1 chlorine atom. The most abundant product ion was *m/z* 322.1311, which was equal to the fragment ion of bendamustine originating from loss of HCl. The corresponding neutral loss (–113.0583 Da) was identical to the neutral loss observed for Met7, therefore the proposed identity of Met13 is a creatinine conjugate of bendamustine.

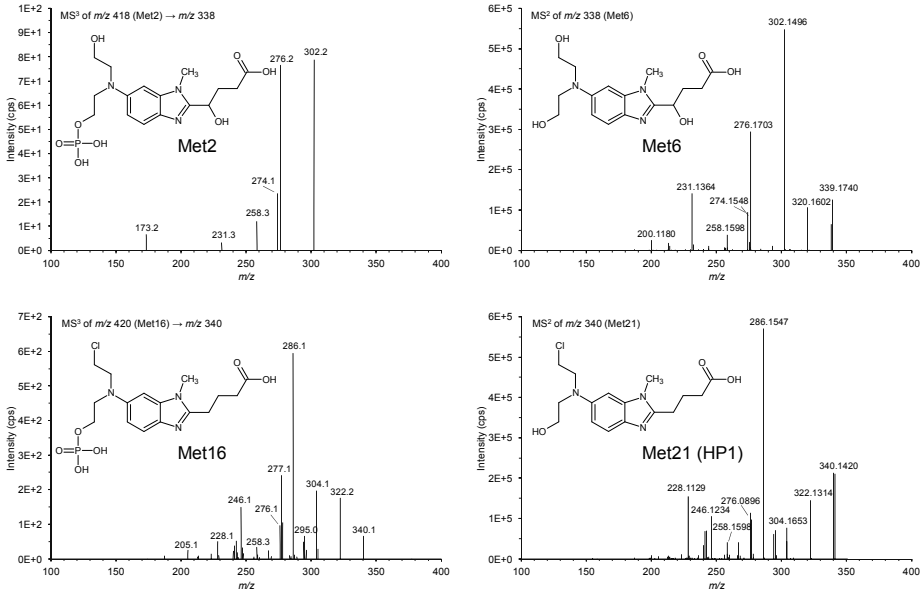

Figure 3: The MS^3 spectrum of the product ion at m/z 338 (loss of HPO_3) of Met2 (upper left) is identical to the MS^2 spectrum of Met6 (upper right). Similarly, the MS^3 spectrum of the product ion at m/z 340 (loss of HPO_3) of Met16 (lower left) is identical to the MS^2 spectrum of Met21 (lower right).

Table 2: Overview of structural information obtained by LC-MS^n for bendamustine metabolites detected in human urine

Peak identification	T_R[a] (min)	T_R[b] (min)	Proposed elemental comp.	$[M+H]^+$ theoretical	$[M+H]^+$ observed	Δppm
1	-	3-5[d]	Unknown	-	-	-
2	14.7	7.9	$C_{16}H_{24}N_3O_8P$	418.1374	418.1363	-2.63
3	18.7	10.9	$C_{15}H_{21}N_3O_4$	308.1605	308.16	-1.62
4	19.7	11.0	$C_{19}H_{28}N_4O_6S$	441.1802	441.179	-2.72
5	22.0	12.1	$C_{16}H_{24}N_3O_7P$	402.1425	402.1415	-2.49
6	23.8	13.3	$C_{16}H_{23}N_3O_5$	338.1710	338.1704	-1.77
7	24.2	13.9	$C_{20}H_{28}N_6O_4$	417.2245	417.2234	-2.64
8	29.0	15.8	$C_{19}H_{28}N_4O_5S$	425.1853	425.1841	-2.82
9	29.4	16.9	$C_{14}H_{17}N_3O_3$	276.1343	276.1336	-2.53
10 (HP2)	33.7	17.6	$C_{16}H_{23}N_3O_4$	322.1761	322.1754	-2.17
11	40.7	18.9	$C_{21}H_{25}N_7O_6$	472.1939	472.1923	-3.39
12	50.2	19.9	$C_{20}H_{27}N_3O_9$	454.1820	454.1805	-3.30
13	54.6	23.1	$C_{20}H_{27}N_6O_3Cl$	435.1906	435.1894	-2.76
14	57.3	25.4	$C_{14}H_{18}N_3O_3Cl$	312.1109	312.1103	-1.92
15	64.4	24.2	$C_{16}H_{23}N_3O_3S$	338.1533	338.1525	-2.37
16	70.7	26.1	$C_{16}H_{23}N_3O_6PCl$	420.1086	420.1076	-2.38
17	71.1	25.9	$C_{23}H_{36}N_4O_3Cl$	483.2363[c]	483.2353[c]	-2.07
18	71.3	27.1	$C_{16}H_{22}N_3O_4Cl$	356.1372	356.1362	-2.81
19	72.5	28.6	$C_{14}H_{18}N_3O_2Cl$	296.1160	296.1153	-2.36
20	73.7	26.5	$C_{19}H_{27}N_4O_4SCl$	443.1514	443.1503	-2.48
21 (HP1)	82.7	29.2	$C_{16}H_{22}N_3O_3Cl$	340.1422	340.1416	-1.76
22	97.6	32.2	$C_{21}H_{29}N_4O_5SCl$	485.1620	485.1605	-3.09
23	99.4	35.1	$C_{16}H_{22}N_3O_2SCl$	356.1194	356.119	-1.12
24 (M3)	104.5	35.1	$C_{16}H_{21}N_3O_3Cl_2$	374.1033	374.1023	-2.67
25 (M4)	105.1	35.3	$C_{15}H_{19}N_3O_2Cl_2$	344.0927	344.0919	-2.32
26 (Bendamustine)	109.2	36.3	$C_{16}H_{21}N_3O_2Cl_2$	358.1084	358.1076	-2.23

[a] Retention time on the 180-min HPLC method. [b] Retention time on the 60-min HPLC method. [c] The most abundant product ions are displayed in bold. The letters between parentheses indicate the proposed fragmentation. The letters a1, a2, b1, b2, c1, c2, d, and e correspond with the fragmentations indicated with these letters in Table 1. The other letters have the following proposed fragmentations: f = loss of H_2O: g = loss of HPO_3; h = loss of alanine; i = loss of OCNH, j = loss of CO; k = loss of HCOOH; l = loss of C_3H_9N; m = loss of $C_6H_{11}NO_2$; n = loss of N-acetyl-2-iminopropionic acid. [d] Retention time in radiochromatogram [e] $[M]^+$ instead of $[M+H]^+$ value if conjugate is carnitine as hypothesized in the discussion.

Major or specific product ions $[M+H]^{+}$ [c]	Proposed metabolic conversions at:		
	Chloroethyl moiety 1	Chloroethyl moiety 2	Benzimidazole/ butyric acid moiety
-	Unknown	Unknown	Unknown
338.1705 (g), **320.1600 (g+f)**, 302.1495 (g+2f)	Phosphate conjugation	Hydrolysis	γ-Hydroxylation
263.1260 (c1), 214.0971 (c1+b2+f)	Hydrolysis	Hydrolysis	*N*-Demethylation
352.1320 (h), **294.1444 (c1)**, 276.1338 (c1+f)	Cysteine conjugation	Hydrolysis	γ-Hydroxylation
322.1756 (g), **304.1650 (g+f)**	Phosphate conjugation	Hydrolysis	-
302.1496 (2f), 276.1703 (e+f)	Hydrolysis	Hydrolysis	γ-Hydroxylation
304.1651 (a1), 278.1495 (c1)	Creatinine conjugation	Hydrolysis	-
336.1371 (h), **278.1494 (c1)**, 260.1389 (c1+f)	Cysteine conjugation	Hydrolysis	-
258.1232 (f), **230.1283 (e)**, 217.0967 (d)	*N*-Dealkylation	Oxidation	-
304.1653 (f), **277.1418 (c1)**, 246.1234 (c1+b2)	Hydrolysis	Hydrolysis	-
429.1871 (i), **411.1766 (i+f)**, 385.1975 (i+j), 304.1651 (a1), 278.1494 (c1), 260.1389 (c1+f)	Uric acid conjugation	Hydrolysis	-
408.1757 (k), **304.1651 (a1)**, 286.1545 (a1+f)	Conjugation with 150.0154 Da	Hydrolysis	-
322.1311 (a1), 296.1155 (c1)	Creatinine conjugation	-	-
276.0894 (2f), 248.0945 (e+f)	*N*-Dealkylation	-	γ-Hydroxylation
278.1494 (c1), 260.1388 (c1+f)	Thiol conjugation	Hydrolysis	-
340.1418 (g), **322.1313 (g+f)**, 304.1207 (g+2f)	Phosphate conjugation	-	-
424.1624 (l), 354.1572 (m), 336.1468 (m+f), 322.1311 (a1), 304.1206 (a1+f)	Hydrolysis	-	Conjugation with 161.1042 Da
320.1155 (2f), 294.1363 (e)	Hydrolysis	-	γ-Hydroxylation
278.1049 (f), 250.1100 (e), **242.1283 (a2+f)**	*N*-Dealkylation	-	-
354.1034 (h), **296.1157 (c1)**, 278.1052 (c1+f)	Cysteine conjugation	-	-
322.1314 (f), **286.1547 (a2+f)**, 246.1234 (c1+b2)	Hydrolysis	-	-
356.1187 (n), **296.1155 (c1)**, 278.1049 (c1+f)	*N*-Acetylcysteine conjugation	-	-
302.1320 (a2+f), 296.1160 (c1)	Thiol conjugation	-	-
338.0816 (2f), 310.0868 (e+f)	-	-	γ-Hydroxylation
326.0815 (f), 298.0867 (e), **290.1049 (a1+f)**	-	-	*N*-Demethylation
304.1206 (a1+f), 228.1127 (c1+b2+f)	-	-	-

The m/z value of the protonated ion of Met14 (m/z 312) corresponded with *N*-dealkylated γ-hydroxybendamustine in the list of potential metabolites. This identification was supported by the specific isotope pattern of 1 chlorine atom and the high-resolution m/z value.

The similarity of the MS^2 spectrum of Met15 (protonated ion at m/z 338) with the MS^2 spectrum of Met8 suggested that Met15 was a part of Met8, and the proposed identity was a thiol conjugate of didechlorinated bendamustine. This was supported by the absence of a ^{37}Cl isotope and the high-resolution m/z value.

Table 3: Proposed structures of bendamustine metabolites in human urine, formed by the main metabolic conversions and arranged by structure of the benzimidazole/butyric acid moiety

Metabolic conversion	Bendamustine 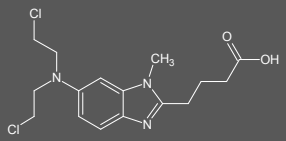 26 (BM)	
Hydrolysis	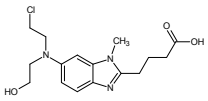 Met21 (HP1)	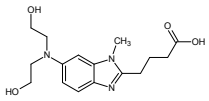 Met10 (HP2)
Cysteine and cysteine-derived conjugations	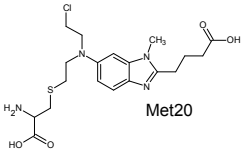 Met20 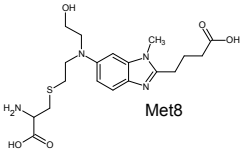 Met8 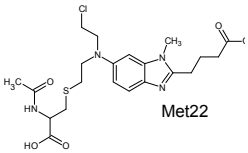 Met22 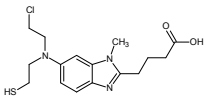 Met23 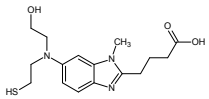 Met15	
N-dealkylation/oxidation	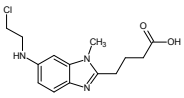 Met19	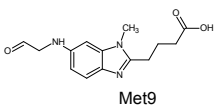 Met9
Phosphate conjugation	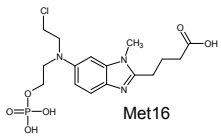 Met16	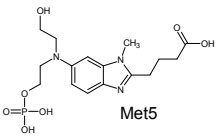 Met5
Creatinine/uric acid conjugation	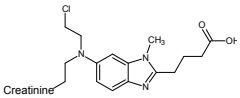 Creatinine Met13	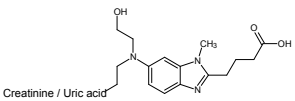 Creatinine / Uric acid Met7 / Met11

	γ-hydroxybendamustine	*N*-desmethylbendamustine
	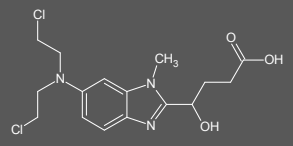 Met24 (M3)	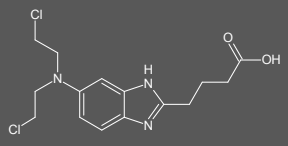 Met25 (M4)
	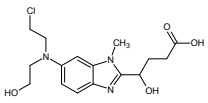 Met18	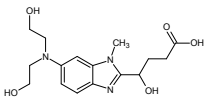 Met6	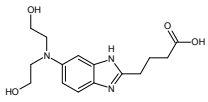 Met3
		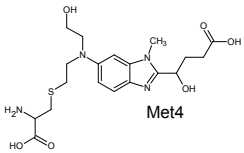 Met4	
	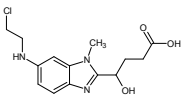 Met14	
		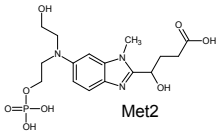 Met2	

The protonated ion of Met16 at m/z 420 suggested a sulphate conjugate of bendamustine. The MS^3 spectrum of the product ion at m/z 340 was identical to the MS^2 spectrum of monohydrolyzed bendamustine (Figure 3). However, in line with Met5 and Met2, the high-resolution mass and the neutral losses of the most abundant product ions at m/z 340.1418 (–79.9658 Da, loss of HPO_3), 322.1313 (–97.9763 Da, loss of H_3PO_4), and 304.1207 (–115.9869 Da, loss of H_3PO_4 and water) pointed to a phosphate conjugate of bendamustine.

Met17 had a retention time of 25.9 min and 71.1 min on the 60-min and 180-min HPLC method, respectively. The protonated ion, detected at m/z 483 (483.2353 with high-resolution MS), was not in the list of potential metabolites. The presence of a product ion at m/z 322.1311, which was also detected in the MS^2 spectrum of HP1, and the isotope pattern specific for 1 chlorine atom suggested that Met17 was a monodechlorinated 161.1042-Da conjugate of bendamustine. A complete structure, however, was not determined.

Met18 had a retention time of 27.1 min and 71.3 min on the 60-min and 180-min HPLC method, respectively. The retention times, MS^n spectra, and high-resolution data were identical to those of the product of monohydrolysis of γ-hydroxybendamustine, which was therefore the proposed identity of Met18.

The m/z value of the protonated ion of Met19 (m/z 296) corresponded with *N*-dealkylated bendamustine in the list of potential metabolites. The high-resolution m/z value supported this identification.

The m/z value of the protonated ion of Met20 (m/z 443) corresponded with a cysteine conjugate of bendamustine in the potential metabolites list. This identification was supported by the high-resolution m/z value and by the neutral losses that were similar to Met4 and Met8: at m/z 354.1034 (–89.0469 Da, loss of alanine) and 296.1157 (–147.0347 Da, loss of ethylcysteine).

Met21 eluted at 29.2 min and 82.7 min when applying the 60-min and 180-min chromatography, respectively. Since the retention times, MS^n spectra, and high-resolution data of this metabolite were equal to those of the reference standard of HP1, Met21 was identified as monohydrolyzed bendamustine (HP1).

The m/z value of the protonated ion of Met22 (m/z 485) corresponded with an *N*-acetylcysteine (mercapturic acid) conjugate of bendamustine in the list of potential metabolites. This identification was supported by the high-resolution m/z value and the neutral losses of the most abundant product ions at m/z 356.1187 (–129.0418 Da, loss of *N*-acetyl-2-iminopropionic acid) and 296.1155 (–189.045 Da, loss of *N*-acetyl-*S*-ethylcysteine).

The protonated ion of Met23, detected at m/z 356, was not included in the list of potential metabolites. The similarity of the MS^2 spectrum of this metabolite with the MS^2 spectrum of Met22 suggested that Met23 was a part of Met22, and the proposed identity was a thiol conjugate of bendamustine, which was supported by the presence of one ^{37}Cl isotope and the high-resolution m/z value.

Based on comparison of the retention times, MS^n fragmentation patterns, and high-resolution data with reference standards, the compounds designated Met24, Met25, and 26 were identified as γ-hydroxybendamustine (M3), *N*-desmethylbendamustine (M4), and bendamustine, respectively.

Table 4: Excretion of bendamustine and its metabolites over time in human urine and metabolites potentially formed by intravesical conversion of bendamustine

	Percentage of patients (n = 6) in which this metabolite was detected[a] in urine at specified time point						Detected[a] metabolites in control urine spiked with bendamustine and incubated at 37°C	
	2 h	6 h	24 h	48 h	96 h	168 h	Time zero	1 h
Met1	NA	NA	NA	NA	NA	NA	NA	NA
Met2	83	33	0	0	0	0		
Met3	100	100	0	0	0	0		
Met4	100	100	50	100	100	83		
Met5	100	67	0	0	0	0		✓
Met6	100	100	50	100	100	100		
Met7	100	67	0	0	0	0		✓
Met8	100	100	83	100	100	100		
Met9	100	100	0	0	0	0		
Met10 (HP2)	100	100	100	100	100	100		✓
Met11	100	50	17	0	0	0		✓
Met12	67	17	0	0	0	0		
Met13	100	17	0	0	0	0		✓
Met14	100	100	0	0	0	0		
Met15	100	33	0	0	0	0		
Met16	100	17	0	0	0	0		✓
Met17	100	17	0	0	0	0		
Met18	100	83	0	17	0	0		
Met19	100	100	0	0	0	0		
Met20	100	67	0	0	0	0		
Met21 (HP1)	100	100	17	17	0	0	✓	✓
Met22	100	100	67	83	17	0		
Met23	100	0	0	0	0	0		
Met24 (M3)	100	83	0	0	0	0		
Met25 (M4)	100	50	0	0	0	0		
26 (BM)	100	83	0	0	0	0	✓	✓

[a]A metabolite was considered detected if its presence was confirmed with an MS/MS scan.

Time course

The radiochromatograms showing the metabolite profile of bendamustine in urine over time from a representative patient are provided in Figure 4. The designation of the peaks was based on the detection and retention time in LC-MS/MS chromatograms. Table 4 summarizes for each metabolite and all analysed time points in how many patients the metabolite was detected.

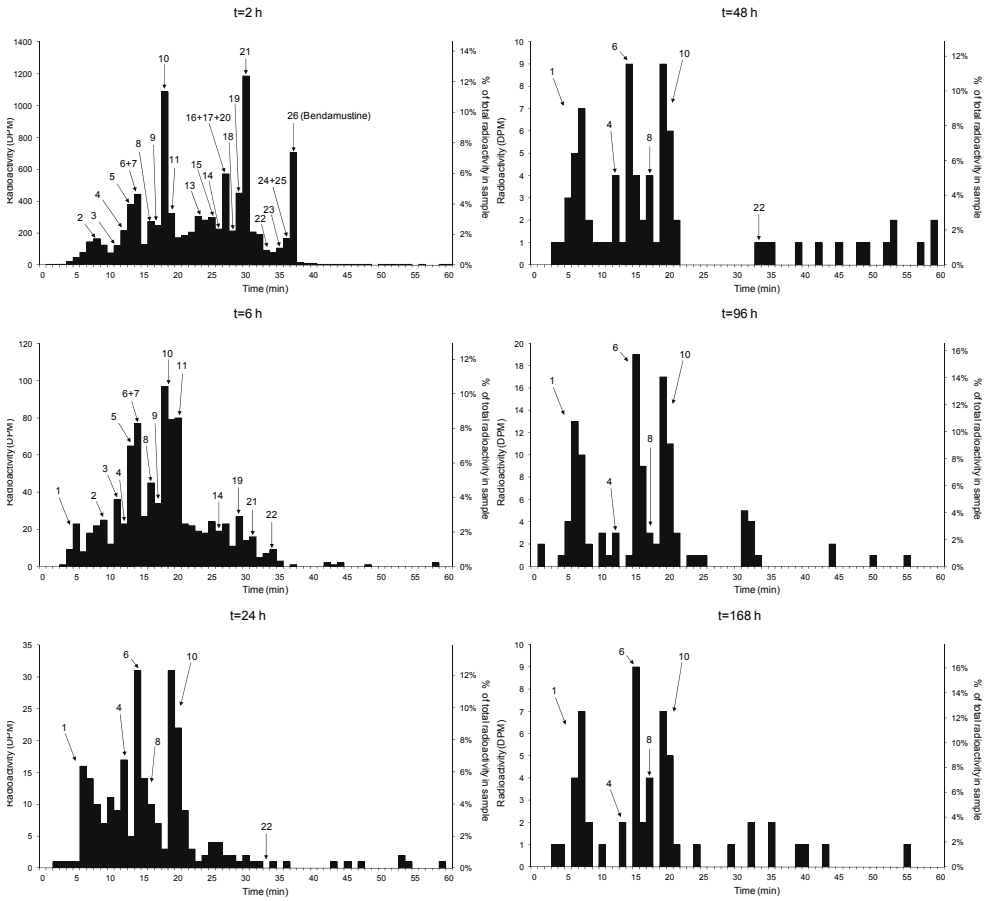

Figure 4: Radiochromatograms of urine samples collected from a cancer patient at different time points after start of a 1-h infusion with ^{14}C-bendamustine (120 mg/m^2, ~95 µCi). Designation of the peaks was based on LC-MS^n data.

The metabolite profiles show a rapid conversion of bendamustine (26) into more polar metabolites. Low but detectable levels of five metabolites were present in most late urine samples, collected up to 168 h after the administration of the radiolabelled bendamustine. Apart from the unidentified metabolite (Met1), these were the dihydrolysis products of bendamustine (Met10) and γ-hydroxybendamustine (Met6) and the cysteine conjugates of didechlorinated bendamustine (Met8) and γ-hydroxybendamustine (Met4).

Intravesical formation of metabolites

Table 4 shows the metabolites formed after 1-h incubation at 37°C of urine spiked with bendamustine. In addition to from hydrolysis, which was known to occur in urine, conjugation with phosphate, creatinine, and uric acid also occurred.

Discussion

This study investigated the metabolite profile of bendamustine in urine of patients with relapsed or refractory malignancies to whom ^{14}C-bendamustine had been administered via intravenous infusion. A total of 25 bendamustine-related compounds were detected in addition to the parent drug. Observed metabolic conversions at the benzimidazole and butyric acid moiety were *N*-demethylation and γ-hydroxylation. Additionally, various combinations of these conversions with modifications at the mechlorethamine moiety were observed, including hydrolysis, cysteine conjugation and subsequent biotransformation to mercapturic acid and thiol derivatives, *N*-dealkylation, oxidation, and conjugation with, among others, phosphate, creatinine, and uric acid. Most metabolites were predominantly present in early collections of excreta, except for five: one unidentified metabolite (Met1) and the products of dihydrolysis and of cysteine conjugation of bendamustine (Met10 and Met8) and γ-hydroxybendamustine (Met6 and Met4), which were excreted up to 168 h after the infusion. Additionally, two minor other metabolic conversions were tentatively identified as products of conjugation with partially identified compounds (Met12 and Met17). Although bendamustine primarily activates base excision repair pathways [8], repaired DNA adducts of bendamustine have not been identified in the urine samples.

Use of knowledge-based prediction of metabolites proved to be very helpful in this study. More than half of the 25 bendamustine-derived compounds were included in the list of potential metabolites, a list that was made beforehand, consisting of $[M+H]^+$ values of potential combinations of known and theoretical metabolic conversions of bendamustine. Based on this list, however, three metabolites were initially thought to be sulphate conjugates. Sulphate conjugation was assumed in rat urine [1] and, moreover, the normal resolution MS^2 spectra of these metabolites showed intense product ions resulting from loss of 80 Da, which is characteristic for sulphate conjugates [9]. Evaluation of the elemental composition of the proposed metabolite structures with high-resolution MS revealed, however, that the mass deviations of the three postulated sulphate conjugates (around 20 ppm) were substantially higher than deviations of the other metabolites (range, –1 to –3 ppm). This led to their tentative identification as phosphate conjugates. This is an excellent example of the additional value of high-resolution MS above normal resolution MS for metabolite identification.

The types of metabolites that were observed in this study were generally consistent with those previously reported for rat [1]. The most abundant metabolite in rat urine and bile was a mercapturic acid conjugate of bendamustine, corresponding with Met22 in this study.

The similarities between the bendamustine metabolites found in rat and human suggest that the overall process involved in metabolic elimination of bendamustine is qualitatively similar for the two species. The origin of the cysteine-related metabolites, however, may be different. Glutathione conjugation was suggested to be a major detoxification pathway in rats, based on the observation of glutathione conjugates and possible biotransfomation products thereof (mercapturic acid conjugates) in rat urine and bile. In human bile, glutathione conjugates were not observed and this was explained by a higher hepatic activity of γ-glutamyltransferase in human as compared to rat [3]. This study showed that cysteine-related metabolites continued to be excreted in urine up to 168 h after bendamustine administration. However, cysteine-related metabolites originating from glutathione conjugation would be expected to be excreted quickly. Therefore, while the early excreted cysteine-conjugates may theoretically be derived from glutathione conjugation, another potential source of the long-lived cysteine conjugates may be their release during catabolism of alkylated proteins. Also, the other long-lived metabolites, the dihydrolysis products of bendamustine and γ-hydroxybendamustine, may be derived from slow hydrolysis of alkylated products. A similar origin may apply to the highly polar metabolite Met1, of which the identity was not elucidated.

Metabolic products of bendamustine that were not observed in previous studies in rat and/or human were thiol derivatives; phosphate, creatinine, and uric acid conjugates; and two conjugates with unidentified moieties. Similar to mercapturic acid conjugates, thiol derivatives are common biotransformation products of cysteine conjugates [9], which can explain their presence in urine. Phosphate, creatinine, and uric acid conjugates are less commonly observed. Apart from study samples, corresponding conjugates of bendamustine were detected in control urine after incubation with bendamustine. This shows that the bendamustine-derived products containing phosphate, creatinine, and uric acid conjugates can be formed by reaction with urinary components. Although the results do not preclude that these products were formed systemically, at least in part, they indicate that intravesical formation may be an explanation for their unexpected presence in the metabolite profile of bendamustine. Analysis of time points at which metabolites were detected in patients also indicates that their conjugation in the control urine may be primarily of bendamustine, since they were only detected in urine samples of the early time points, when bendamustine was also being excreted. Renal impairment would not affect the elimination of bendamustine as because much of it is metabolized, primarily via hydrolysis, but it may decrease the intravesical formation of conjugated products and it would affect the elimination of metabolites as much of them are excreted by the kidneys.

The two metabolites with unidentified conjugations were Met12 and Met17. Met12 was a minor metabolite, only detected in the 2-h urine samples of 4 out of the 6 patients and in one 6-h urine sample. The high-resolution mass of the conjugate (150.0154 Da) indicates an elemental composition of $C_4H_6O_6$ (150.0159 Da; Δppm = –3.20). The product ion at m/z 408.1757 (loss of CHOOH) probably did not result from fragmentation at site e in

Table 1, since the major product ion in the MS^3 spectrum of m/z 408 was identified as bendamustine, split at site a1. Therefore, a carboxyl group may be expected in the conjugate. The complete structure, however, has not been elucidated. The high-resolution mass of the conjugate of Met17 (161.1046 Da) led to a proposed elemental composition of $C_7H_{15}NO_3$ (161.1046 Da; Δppm = –2.48), a molecular formula corresponding with carnitine. This quarternary ammonium compound can be endogenously formed and is required for transport of long-chain fatty acids across intracellular membranes, which is facilitated by oxidation of the fatty acids into acylcarnitines [10]. The suggestion of Met17 being a carnitine conjugate of bendamustine is supported by the most abundant product ion at m/z 424.1624, since the loss of 59.0729 Da (loss of trimethylamine) is characteristic for carnitine and acylcarnitine conjugates [11]. Although the mass spectra give no definite answer on the site of the conjugation, it is hypothesized that Met17 may be monohydrolyzed bendamustine, conjugated with carnitine at the butyric acid moiety to form an acylcarnitine derivative. This would be in line with the acylcarnitine conjugates that have been observed for other carboxylic acid-containing drugs [12;13].

In conclusion, this study showed that bendamustine is extensively metabolized in humans via hydrolytic, oxidative, and conjugative pathways. These metabolic reactions are similar to those identified in rats. In addition, products were observed that are consistent with intravesical reaction of bendamustine and certain of its metabolites with uric acid, creatinine, and phosphate.

Footnotes

This work was supported by Teva Pharmaceutical Industries Ltd.

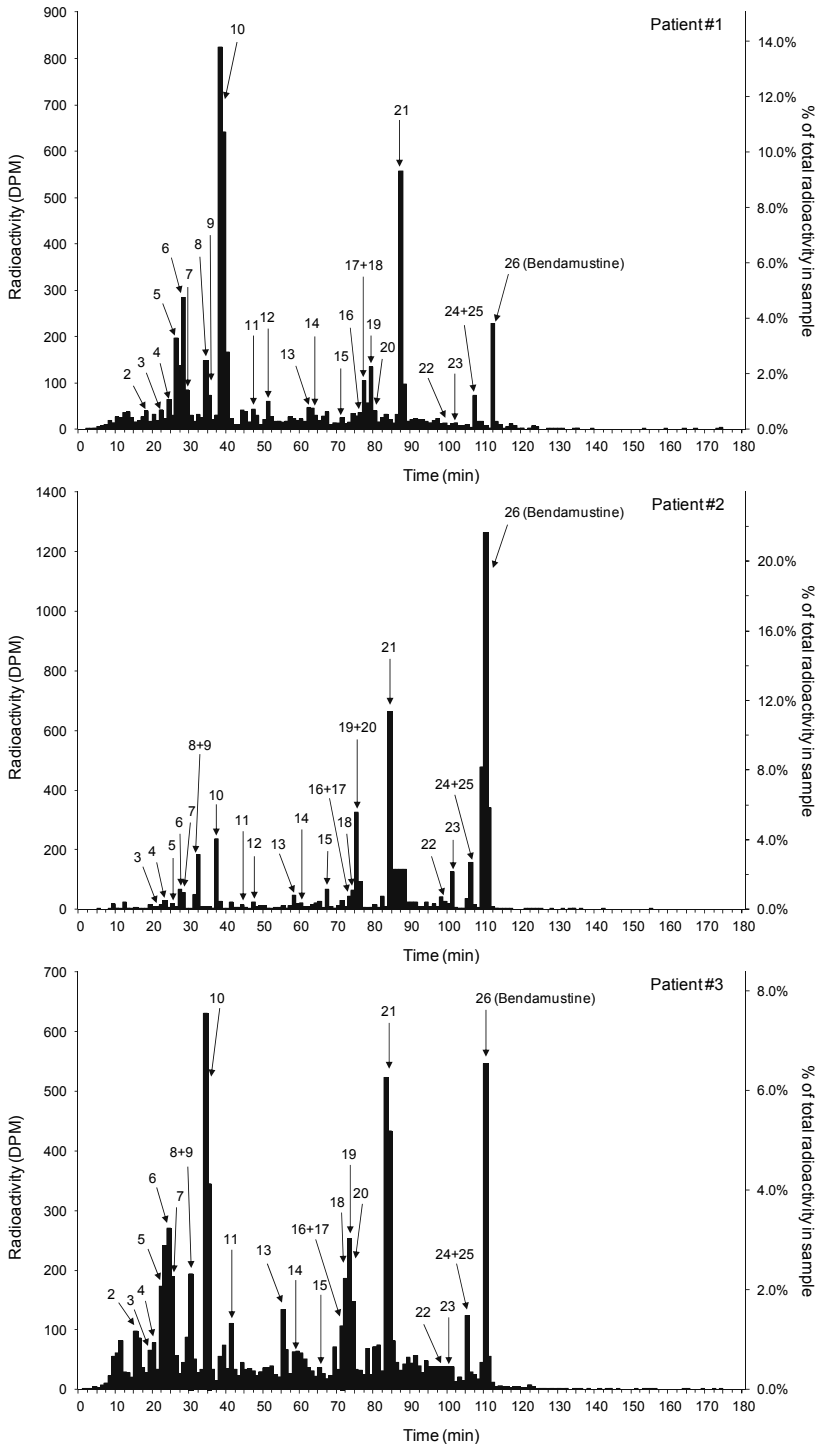

Supplemental Figure 1 (part 1 of 2): Radiochromatograms of the urine samples of six cancer patients, collected 2 h after start of a 1-h infusion with ^{14}C-bendamustine (120 mg/m^2, ~95 μCi).

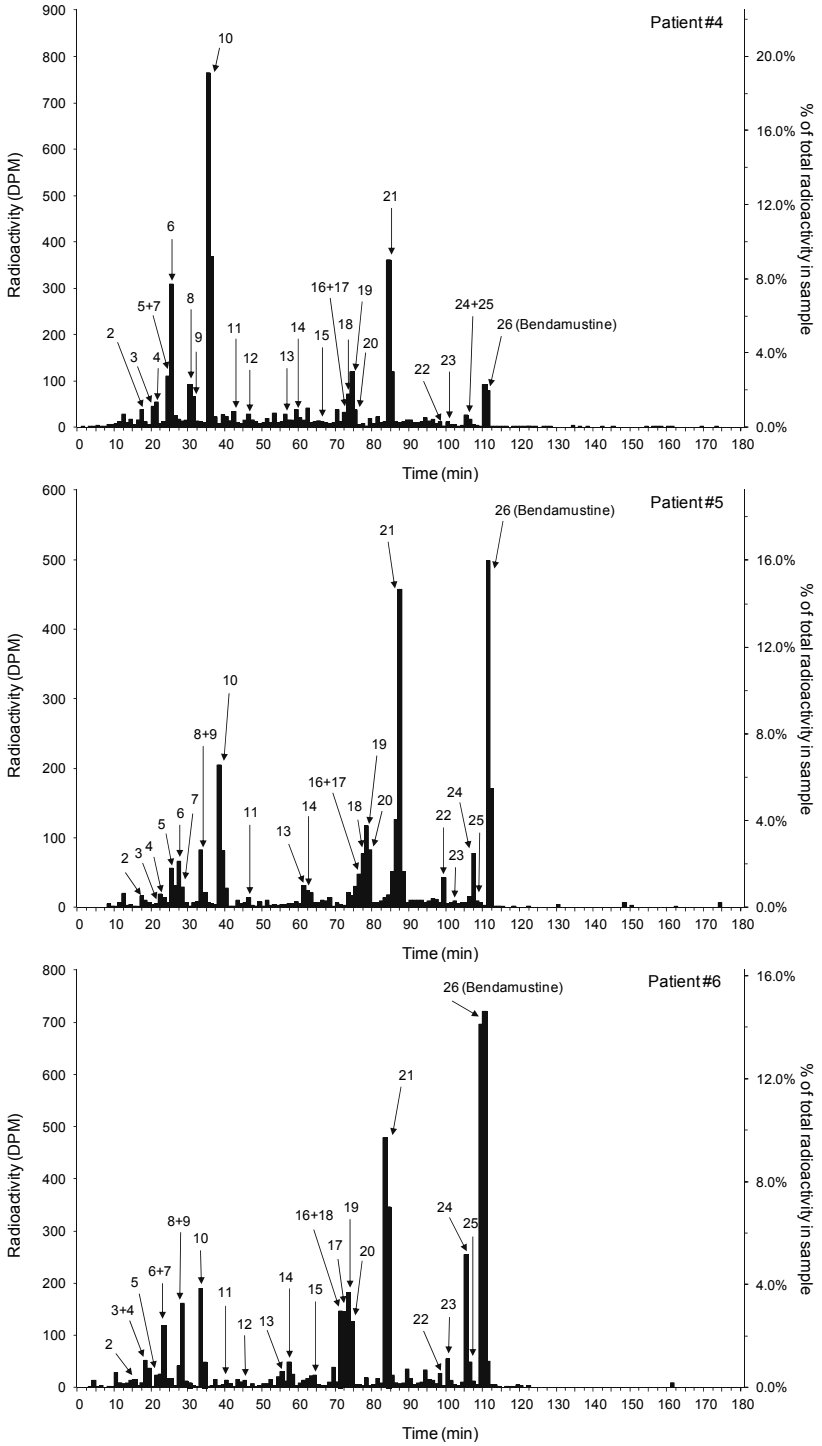

Supplemental Figure 1 (part 2 of 2): Radiochromatograms of the urine samples of six cancer patients, collected 2 h after start of a 1-h infusion with ^{14}C-bendamustine (120 mg/m^2, ~95 μCi).

References

[1] Chovan JP, Li F, Yu E, Ring SC, Metabolic profile of [(14)C]bendamustine in rat urine and bile: preliminary structural identification of metabolites, *Drug Metab Dispos.*, **35** (2007) 1744-1753.

[2] Teichert J, Sohr R, Baumann F, Hennig L, Merkle K, Caca K, Preiss R, Synthesis and characterization of some new phase II metabolites of the alkylator bendamustine and their identification in human bile, urine, and plasma from patients with cholangiocarcinoma, *Drug Metab Dispos.*, **33** (2005) 984-992.

[3] Teichert J, Sohr R, Hennig L, Baumann F, Schoppmeyer K, Patzak U, Preiss R, Identification and quantitation of the N-acetyl-L-cysteine S-conjugates of bendamustine and its sulfoxides in human bile after administration of bendamustine hydrochloride, *Drug Metab Dispos.*, **37** (2009) 292-301.

[4] Teichert J, Baumann F, Chao Q, Franklin C, Bailey B, Hennig L, Caca K, Schoppmeyer K, Patzak U, Preiss R, Characterization of two phase I metabolites of bendamustine in human liver microsomes and in cancer patients treated with bendamustine hydrochloride, *Cancer Chemother.Pharmacol.*, **59** (2007) 759-770.

[5] Dubbelman, AC, Rosing, H, Darwish, M, D'Andrea, D, Bond, M, Hellriegel, ET, Beijnen, JH, and Schellens, JHM, An Open-Label Phase I Pharmacokinetic Study of [14C]bendamustine in patients with relapsed or refractory malignancy, *Blood*, **118** (2011),

[6] Dubbelman AC, Tibben M, Rosing H, Gebretensae A, Nan L, Gorman SH, Robertson Jr. P, Schellens JHM, Beijnen JH, Development and validation of LC-MS/MS assays for the quantification of bendamustine and its metabolites in human plasma and urine, *Submitted for publication*, (2012).

[7] Bianco G, Abate S, Labella C, Cataldi TR, Identification and fragmentation pathways of caffeine metabolites in urine samples via liquid chromatography with positive electrospray ionization coupled to a hybrid quadrupole linear ion trap (LTQ) and Fourier transform ion cyclotron resonance mass spectrometry and tandem mass spectrometry, *Rapid Commun.Mass Spectrom.*, **23** (2009) 1065-1074.

[8] Leoni LM, Bailey B, Reifert J, Bendall HH, Zeller RW, Corbeil J, Elliott G, Niemeyer CC, Bendamustine (Treanda) displays a distinct pattern of cytotoxicity and unique mechanistic features compared with other alkylating agents, *Clin.Cancer Res.*, **14** (2008) 309-317.

[9] Levsen K, Schiebel HM, Behnke B, Dotzer R, Dreher W, Elend M, Thiele H, Structure elucidation of phase II metabolites by tandem mass spectrometry: an overview, *J.Chromatogr.A*, **1067** (2005) 55-72.

[10] Strijbis K, Vaz FM, Distel B, Enzymology of the carnitine biosynthesis pathway, *IUBMB.Life*, **62** (2010) 357-362.

[11] Minkler PE, Ingalls ST, Hoppel CL, Strategy for the isolation, derivatization, chromatographic separation, and detection of carnitine and acylcarnitines, *Anal.Chem.*, **77** (2005) 1448-1457.

[12] Millington DS, Bohan TP, Roe CR, Yergey AL, Liberato DJ, Valproylcarnitine: a novel drug metabolite identified by fast atom bombardment and thermospray liquid chromatography-mass spectrometry, *Clin.Chim.Acta*, **145** (1985) 69-76.

[13] Olsen J, Li C, Bjornsdottir I, Sidenius U, Hansen SH, Benet LZ, In vitro and in vivo studies on acyl-coenzyme A-dependent bioactivation of zomepirac in rats, *Chem.Res.Toxicol.*, **18** (2005) 1729-1736.

Chapter 3

Eribulin

Chapter 3.1

Validation of high-performance liquid chromatography-tandem mass spectrometry assays for the quantification of eribulin (E7389) in various biological matrices

Anne-Charlotte Dubbelman, Hilde Rosing, Bas Thijssen, Luc Lucas, William Copalu, Jantien Wanders, Jan H.M. Schellens, Jos H. Beijnen

J Chromatogr B Analyt Technol Biomed Life Sci (2011) **879**:1149-1155.

Abstract

This paper presents specific and sensitive high-performance liquid chromatography coupled with tandem mass spectrometry (HPLC-MS/MS) assays for the quantification of the novel anticancer agent eribulin in human plasma, whole blood, urine and faeces. These assays, developed to support clinical pharmacological studies with the drug, quantify eribulin concentration ranges of 0.2 – 100 ng/mL for plasma, 0.5 – 100 ng/mL for whole blood and urine and 0.1 – 25 μg/g for faeces, using sample volumes of 500 μL or 250 μg (faeces).

Samples were prepared with liquid-liquid extraction, separated on a C18 column with gradient elution and analysed with a triple quadrupole MS, in positive ion mode. A structural analogue of eribulin was used as internal standard for the quantification.

The assays were linear with correlation coefficients (r^2) of 0.99 and better, whereby the deviation from nominal concentrations ranged from -8.2 to 8.9% with CV values of maximally 14.2%. Stability assessments demonstrated that eribulin is stable at -20 °C in plasma, whole blood, urine and faeces for at least 38, 4, 10.5 and 5 months, respectively. In conclusion, the validation results show that the assays are specific and accurate and can therefore adequately be applied to support clinical studies of eribulin.

Introduction

Eribulin mesylate (E7389) (Figure 1A) is a nontaxane microtubule dynamics inhibitor with a distinct mode of action. While it is still being investigated in clinical trials, eribulin has recently been approved by the United States Food and Drug Administration (FDA) for treatment of patients with metastatic breast cancer, who have previously received at least two chemotherapeutic regimens, including an anthracycline and a taxane [1].

Like most anti-mitotic drugs, eribulin affects the microtubule dynamics, resulting in a cell cycle block, leading to apoptosis [2]. Unlike other tubulin-targeted agents, eribulin only inhibits the growth and not the shortening of microtubules and it induces the formation of tubulin aggregates [3]. These distinct modes of action may contribute to the results of phase II studies wherein eribulin shows activity in patients who had received previous therapy with taxanes and anthracyclines [4].

To support clinical pharmacological studies of eribulin, and especially mass balance studies, it was essential to develop and validate quantitative bioanalytical assays of eribulin in plasma, whole blood, urine and faeces. The quantification of eribulin in human plasma and urine described by Desjardins *et al.* [5] served as a starting point for the development of the plasma assay in this paper. As our attempts to reproduce their method resulted in an insufficient separation between eribulin and the internal standard, we further optimized the chromatographic conditions. Additionally, we present methods for quantification of eribulin in whole blood and faeces, for which thus far no methods have been published. The described validations were performed according to the FDA guidelines for bioanalytical method validation [6;7].

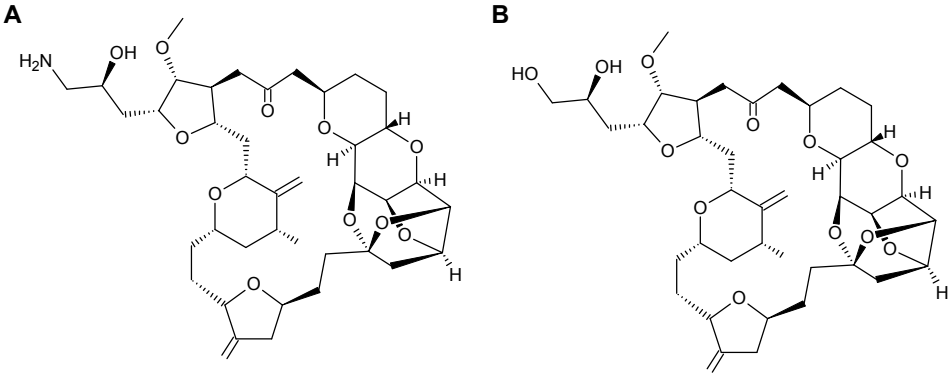

Figure 1: Chemical structures of eribulin (A) and the internal standard ER-076349 (B).

Experimental

Chemicals and reagents

Eribulin methanesulfonic acid salt and its internal standard ER-076349 (Figure 1B) were provided by Eisai Co., Ltd, Japan. Methanol (Supra-Gradient grade), ethanol absolute (HPLC-grade) and acetonitrile (ACN, Supra-Gradient grade) were obtained from Biosolve Ltd, Valkenswaard, The Netherlands. Ethyl acetate (LiChrosolv), sodium hydroxide (NaOH) (>99%) and formic acid (98%) were purchased from Merck, Darmstadt, Germany. Water (distilled) used for sample preparation originated from B. Braun Medical, Melsungen, Germany and water (LiChrosolv) used to prepare eluentia from Merck. Drug-free control human lithium heparinized plasma was obtained from Sanquin, Amsterdam, the Netherlands and Bioreclamations, Hicksville, USA. Control human lithium heparinized whole blood, urine and faeces originated from healthy volunteers.

Preparation of stock solutions, calibration standard (CS) and quality control (QC) samples

Stock solutions of eribulin (1 mg/mL) and the internal standard (IS) (0.1 mg/mL) were prepared in methanol and diluted in methanol:water (1:1, v/v) to obtain CS and QC or IS working solutions. IS working solutions of 500 ng/mL, 2.5 µg/mL and 10 µg/mL were used for the plasma, urine and whole blood and faeces assay, respectively.

Calibration standard and QC samples were prepared by diluting the corresponding working solutions with control human plasma, whole blood (with at least 1 freeze-thaw cycle at -20 °C), urine or faecal homogenate in water (1:3, w/v). The final concentrations of the CS samples were 0.2, 0.5, 1, 2, 5, 10, 50 and 100 ng/mL for plasma, 0.5, 1, 2.5, 10, 25, 50, 75 and 100 ng/mL for whole blood and urine and 0.1, 0.25, 1, 2.5, 5, 12.5 and 25 µg/g (undiluted faeces) for faeces. Final concentration of the QC samples at the lower limit of quantification (LLOQ), QC low, QC mid, QC high and QC above the upper limit of quantification (>ULOQ, for plasma only) were 0.2, 0.6, 5, 80 and 500 ng/mL for plasma, 0.5, 1.5, 10 and 80 for whole blood and urine and 0.1, 0.25, 2.5 and 20 µg/g for faeces.

Stock and working solutions were stored at nominally 4 °C, QC samples were stored at nominally -20 °C and CS samples were freshly prepared before each validation run.

Processing of samples

Plasma, whole blood and urine samples were prepared following the procedure of [5], with the modification that urine samples were diluted with 500 µL control human plasma instead of water. After liquid-liquid extraction (LLE), followed by evaporation of the organic layer, reconstitution and filtration, 20 µL of the final extract were injected.

Faecal samples were homogenized with water (1:3 w/v). Since CS and QC samples for faeces were prepared by adding 50 µL working solution to 1.00 mL of faecal homogenate,

50 µL of MeOH:water (1:1 v/v) was added to patient samples of 1.00 mL of faecal homogenate.

Subsequently, 50 µL IS working solution and 2 mL acetonitrile were added. Samples were vortex mixed for 30 s, shaken at 1,250 rpm for 10 min and centrifuged for 5 min at around 2,250 g. The supernatant was filtered using 0.2 µm micro-spin filters (Alltech, Deerfield, IL, USA) and after centrifuging for 5 minutes at 10,300 g, 3 µL of the filtrate were injected.

Liquid chromatography

The assay in plasma was conducted on a HPLC system comprising a LC-20AD Prominence binary solvent delivery system with a column oven, a SiL-HTc autosampler and a DGU-20A3 online degasser (Shimadzu, Kyoto, Japan). The HPLC system used for the other assays consisted of a HP1100 binary pump, a degasser and a HP1100 autosampler (Agilent technologies, Palo Alto, CA, USA).

For all four assays, separation was achieved within 10 min on a Polaris® C18-A column (30 x 2.0 mm, particle size 3.0 µm; Varian Inc, Palo Alto, CA, USA), thermostatted at 30 °C, like in [5], but with different mobile phases. Eluent A consisted of 0.1% formic acid in (Lichrosolv) water and B of 0.1% formic acid in acetonitril at a flow rate of 0.3 mL/min. For the plasma assay, the mobile phase composition was as follows: mobile phase B: 20% (0-1 min), from 20 to 40% (1-5.5 min), from 40 to 80% (5.5-6 min), 80% (6-7 min), from 80 to 20% (7-7.5 min) and 20% (7.5-10 min). For the other assays, it consisted of: mobile phase B: 18% (0-1.7 min), 33% (1.7-6.5 min), 80% (6.5-7.5 min) and 18% (7.5-10 min). The autosampler temperature was kept at 4 °C for the plasma assay and at room temperature for the other assays.

Mass spectrometry

For all four assays, a triple quadrupole mass spectrometer was used, operating with an electrospray ionization (ESI) source in positive mode and configured in multiple reaction monitoring (MRM). Mass spectrometric parameters were optimized for the transitions of m/z 730.5 → 712.5 (eribulin) and 731.5 → 681 (IS).

A Finnigan TSQ Quantum Ultra (Thermo Fisher Scientific, Waltham MA, USA) was used for the assay in plasma. The optimized instrument parameters were as follows: capillary temperature, 375 °C; ion spray voltage, 4.75 kV; sheath gas, 47 mTorr; auxiliary gas, 16 mTorr; ion sweep gas, 1.5 mTorr; source CID collision energy, 8 V; Q2 collision gas pressure, 1.5 mTorr; collision energy, 32 V (eribulin) and 25 V (IS); tube lens voltage, 137 V (eribulin) and 90 V (IS) and scan time, 100 ms.

The whole blood, urine and faeces assays were performed on an API 3000 triple quadrupole with a turbo ion spray interface (AB Sciex, Thornhill, ON, Canada) using the following settings: turbo ionspray temperature, 550 °C; ionspray voltage, 2 kV; turbo gas

flow, 7 L/min; nebulizer gas; 13 psi; curtain gas, 6 psi; collision gas, 8 psi; dwell time 250 ms (eribulin) and 100 ms (IS).

Validation procedures

A full validation according to the FDA guidelines [6;7] was performed for the quantification of eribulin in human heparinized plasma, including linearity, intra-assay and inter-assay accuracy and precision, dilution test, specificity and selectivity, recovery and matrix effect, carry-over and stability.

The other assays are modifications of the plasma assay and validation of these assays covered linearity, intra-assay accuracy and precision, carry-over and stability. Additionally, specificity and selectivity were assessed in whole blood and urine, matrix effect was determined in urine and recovery was tested in both urine and faeces.

Results and discussion

Method development

Sample pretreatment

The apolar nature of eribulin theoretically makes it a good substrate for LLE with an organic solvent. Ethyl acetate only or in combination with methanol and ethanol (90:5:5 v/v/v) and tert-butyl methyl ether were tested. Extraction with the ethyl acetate, methanol and ethanol combination resulted in clean extracts and reproducible recoveries and was chosen as pretreatment method.

Because whole blood study samples collected from patients are stored frozen, and thereby haemolysed, it was decided to use only control whole blood that had undergone at least 1 freeze-thaw cycle for the preparation of CS and QC samples.

Application of the plasma sample processing method to urine resulted in diverging calibration curves and QC samples being incompatible with the calibration curves. High pH variation between individual urine batches, even after the addition of NaOH, and a varying matrix effect were suspected to cause the observed problems. Therefore, to neutralize the effect of urine as a matrix, the 500 μL of water -that was added to the plasma samples before LLE- was for the urine samples replaced with control human plasma.

A simple extraction method was applied on faecal samples, excluding the snap-freezing and concentration step of the other assays. The disadvantage of this method is that the samples are being diluted; on the other hand, the expected concentrations in faeces are much higher than in the other matrices. Thus, sensitivity was not critical for this assay.

Liquid chromatography

Starting point of the development of the chromatographic system of the plasma assay were the conditions used by DesJardins *et al.* [5]. However, this system resulted in an insufficient separation between eribulin and the internal standard. Although full separation between analytes is generally not required for LC-MS/MS quantification in MRM mode, in this case, with an IS molecular mass differing only 1 Da from eribulin itself, cross-interference between the analytes would arise. Namely, the transition of the ^{13}C-isotope peak of the internal standard and its unspecific loss of water would be indistinguishable from the transition of eribulin. Furthermore, a significant amount of noise dominated the chromatograms obtained using chromatographic system of [5]. As THF is generally not recommended for mass spectrometry [8], the first step was to eliminate this solvent from the eluent. With the alternative eluentia 0.1% formic acid in water and 0.1% formic acid in ACN, the gradient was optimized until acceptable baseline separation between eribulin and the IS was established, without prolonging the total runtime. The final chromatographic system for the plasma assay was also tested for the urine assay, however, for this matrix, a stable chromatography could not be accomplished. Consequently, other gradients were tested, resulting in the selected step-wise gradient, which turned out to be equally applicable for the whole blood and faeces assay. Figure 2 shows the MRM chromatograms of eribulin and the IS of a LLOQ and a blank sample of each matrix.

Mass spectrometry

Mass spectrometric parameters were optimized with direct infusion and flow injection analysis. The positive ionization mode resulted in higher ion counts than the negative mode and was therefore selected. The full-scan mass spectrum of eribulin (Figure 3A) showed the protonated ions $[M+H]^+$ and $[M+Na]^+$ at m/z 730 and 752, respectively. The product ion (PI) spectrum (Figure 3B) demonstrated that eribulin is hardly fragmented. Product ions were observed at m/z 712 (loss of H_2O), 698 (loss of the methoxy group, CH_3OH) and 680 (loss of both CH_3OH and H_2O). Since maximum sensitivity was aimed for, the most abundant product ion was selected for quantification. Therefore, although loss of water is generally an unspecific and variable transition, this particular transition of m/z 730.5 → 712.5 was used.

The full-scan spectrum of the IS (Figure 3C) showed protonated ions $[M+H]^+$ and $[M+Na]^+$ with nominal m/z values of 731 and 753, respectively. Again, the most abundant product ion from the PI spectrum (Figure 3D), m/z 681, was monitored for quantification.

Validation procedures

Linearity, accuracy and precision

Linearity in plasma and whole blood was assessed in three analytical runs and in urine and faeces in two runs. Using a $1/x^2$ weighting factor, differences between back-calculated and nominal concentrations were minimized. The assays were linear over concentration ranges

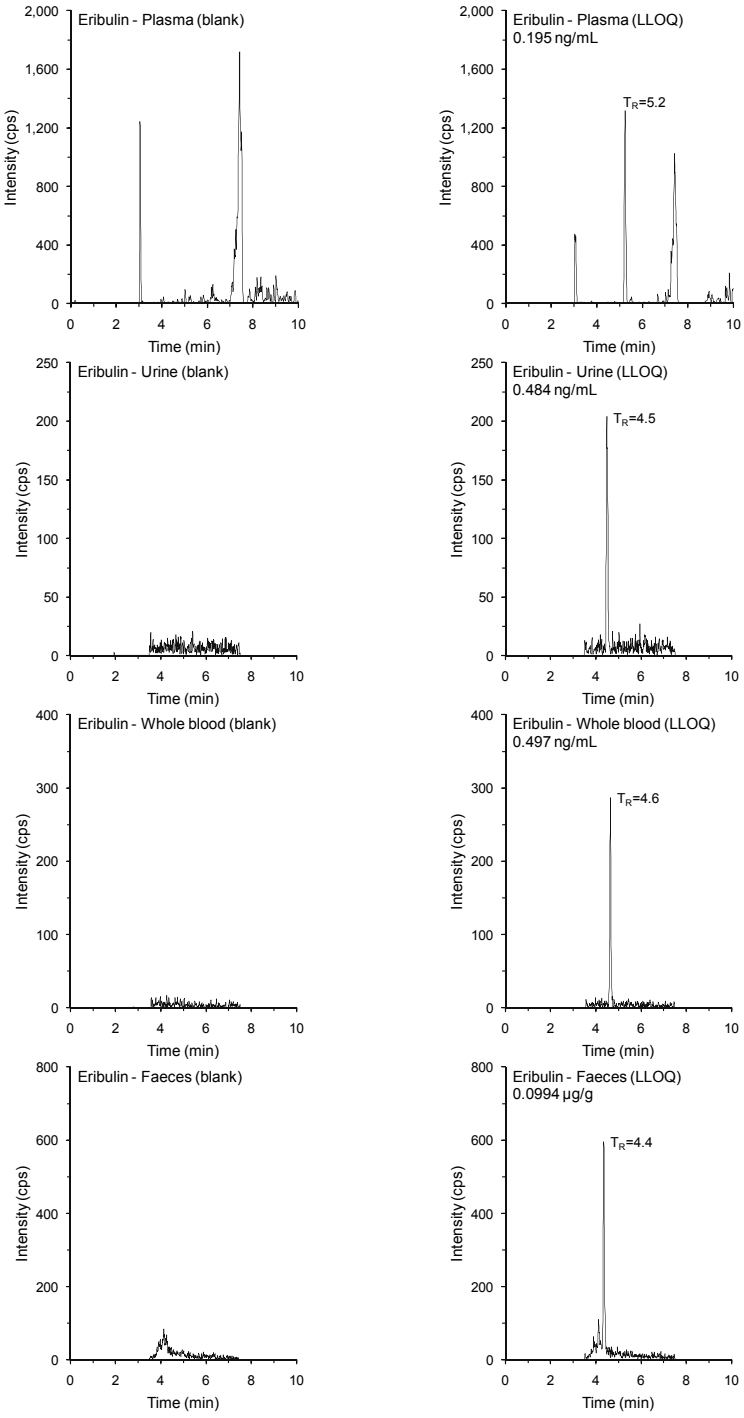

Figure 2: MRM chromatograms of eribulin (left, m/z 730.5→712.5) and the internal standard (right, m/z 731.5→681) of blank samples and QC LLOQ samples, in plasma (upper row), urine (second row), whole blood (third row) and faeces (lower row).

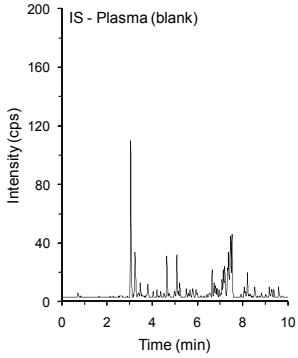
IS - Plasma (blank)
Intensity (cps)
Time (min)

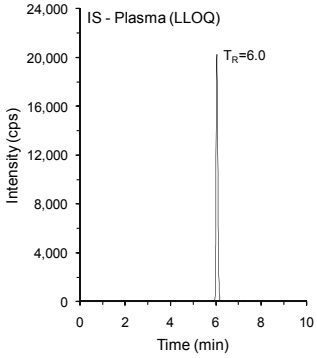
IS - Plasma (LLOQ)
T_R=6.0
Intensity (cps)
Time (min)

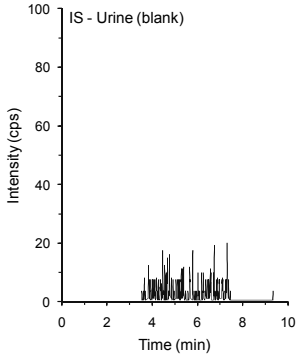
IS - Urine (blank)
Intensity (cps)
Time (min)

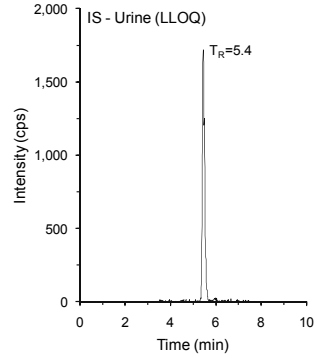
IS - Urine (LLOQ)
T_R=5.4
Intensity (cps)
Time (min)

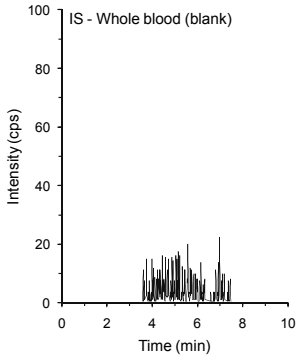
IS - Whole blood (blank)
Intensity (cps)
Time (min)

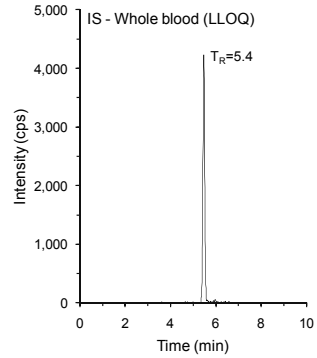
IS - Whole blood (LLOQ)
T_R=5.4
Intensity (cps)
Time (min)

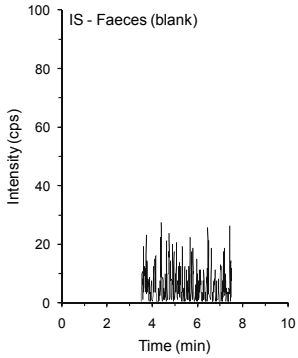
IS - Faeces (blank)
Intensity (cps)
Time (min)

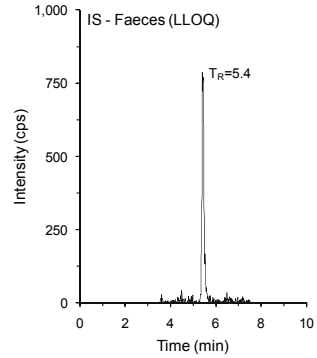
IS - Faeces (LLOQ)
T_R=5.4
Intensity (cps)
Time (min)

of 0.2 – 100 ng/mL for plasma, 0.5 – 100 ng/mL for urine and whole blood and 0.1 – 25 µg/g for faeces with correlation coefficients (r^2) of 0.99 or better. Deviations from the nominal concentrations were -5.29 to 4.81% for all concentrations in plasma, -1.72 to 4.03% in whole blood, -8.25 to 3.92% in urine and -4.23 to 8.87% in faeces, with CV values less than 10.7, 14.2, 8.14 and 9.12%, respectively. Since also the signal to noise ratios at the LLOQ were above 5, the selected ranges comply with the criteria for linearity. Moreover, plasma samples can be diluted 10 times, as the accuracy and precision of six analysed diluted replicates were 5.15 and 8.78%, respectively.

Also the accuracies and precisions met the criteria of the FDA guidelines [7]. Table 1 summarizes the intra-assay accuracies and precisions. The plasma inter-assay accuracy over three runs ranged from -3.18 to 2.77% with an inter-assay precision ≤13.0%.

Table 1: Assay performance data for eribulin in plasma, whole blood, urine and faeces

Matrix	Nominal conc.[a]	Measured conc.[a]	Intra-assay accuracy (%)	Intra-assay precision (%)	Number of replicates
Plasma	Run 1				
	0.195	0.180	-7.95	9.38	6
	0.586	0.604	3.10	6.73	6
	4.88	5.14	5.40	2.73	6
	78.1	76.6	-1.98	4.97	6
	Run 2				
	0.195	0.218	11.6	8.25	6
	0.586	0.647	10.4	11.1	6
	4.88	5.41	10.8	4.55	6
	78.1	80.1	2.54	2.69	6
	Run 3				
	0.195	0.174	-10.7	6.17	6
	0.586	0.535	-8.65	8.85	6
	4.88	4.49	-7.92	4.03	6
	78.1	70.2	-10.1	3.02	6
Whole blood	0.484	0.497	2.77	7.93	5
	1.45	1.61	11.2	2.46	5
	9.68	10.4	7.85	2.21	5
	77.5	85.1	9.86	2.28	5
Urine	0.484	0.470	-3.00	9.35	6
	1.45	1.51	4.37	4.99	6
	9.68	9.34	-3.51	4.13	6
	77.5	77.0	-0.688	6.00	6
Faeces	0.0968	0.0963	-0.475	5.11	5
	0.242	0.248	2.48	3.28	5
	2.42	2.55	5.45	4.13	5
	19.4	20.2	4.02	3.33	5

Conc.: concentration. [a]Concentrations are in ng/mL for plasma, whole blood and urine and in µg/g for faeces

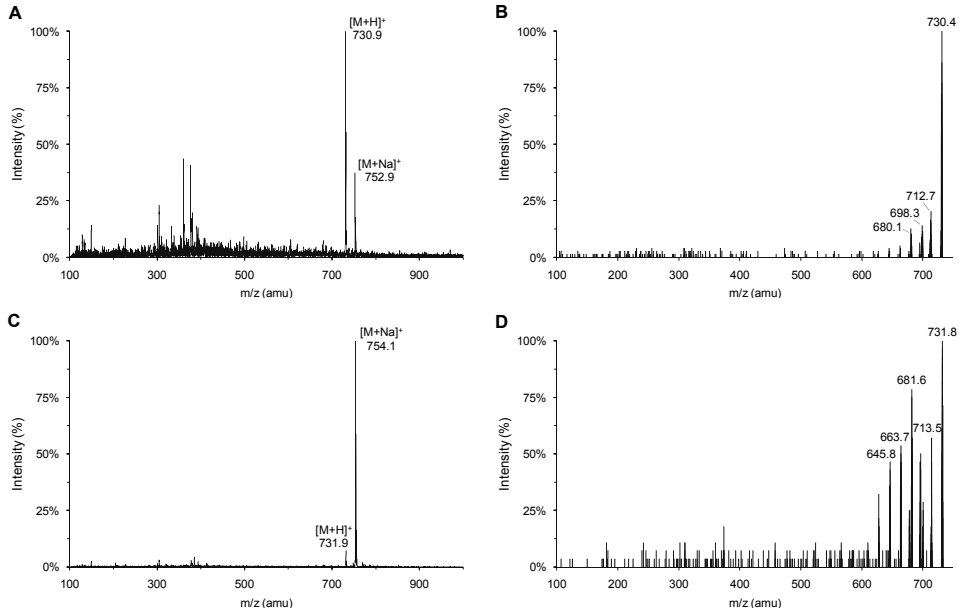

Figure 3: Full-scan positive ion mass spectrum of eribulin (A) and the internal standard ER-076349 (C) and the corresponding product ion spectra (B and D).

Specificity, selectivity and carry-over

Six individual batches, spiked with eribulin at the LLOQ level showed deviations between -18.9 and 18.0% for plasma, between 3.72 and 19.0% for whole blood and between -7.23 and 12.4% for urine. Co-eluting peaks with areas >20% of the LLOQ were not observed in the MRM chromatograms of 6 individual batches of blank controls of the tested matrices, neither were peaks >5% of and co-eluting with the IS. The same applied for the blank samples injected after ULOQ samples for the carry-over test. Thus, the specified criteria for specificity and carry-over were fulfilled.

Matrix effect and total recovery

The total recoveries (including sample pretreatment and matrix effect) of eribulin were 63.7±3.8% (mean ± SD) in plasma, 68.8±3.4% in urine and 114±1.0% in faeces. The matrix effect of plasma ranged from -8.4 to 2.9%, for urine this was between 13.3 and 18.1% (ion enhancement). The recovery of eribulin from the LLE of plasma and urine samples was 65.0±0.7% and 59.2±2.1%, respectively.

The total recovery of the IS was 79.4% in plasma, 90.0% in urine and 111% in faeces, with a matrix effect of 2.2% in plasma and 20.2% in urine and a LLE recovery of 77.7% in plasma and 74.8% in urine.

A total recovery of >100%, as observed for eribulin and its IS in faeces, may be due to ion enhancement, which was also demonstrated for urine, or can be caused by analyte loss in the absence of matrix during analysis [9].

Table 2: Stability data for eribulin. All experiments were performed in triplicate.

Condition	Sample type	Nominal conc.[a]	Initial conc.[a]	Measured conc.[a]	CV (%)	Dev.[b] (%)
Stock/working solutions in MeOH						
Ambient, 6 h	Eribulin solution	-	1.00E+06	1.04E+06	1.24	4.05
Ambient, 6 h	IS solution	-	1.00E+05	1.03E+05	1.00	2.88
2-8^{0}C, 7.5 m	IS solution	-	9.96E+04	1.04E+05	8.29	4.64
2-8^{0}C, 8 m	IS solution	-	473	530	5.54	12.0
2-8^{0}C, 18.5 m	IS solution	-	498	558	4.79	12.0
Plasma						
3 freeze (-20^{0}C) - thaw cycles	Biomatrix	0.616 82.1	0.561 75.5	0.639 74.5	7.96 3.56	13.8 -1.32
Ambient, 24 h	Biomatrix	0.586 78.1	0.574 71.3	0.571 70.6[c]	5.89 4.51	-0.465 -1.10
2-8^{0}C, 7 days	Dried extract	0.586 78.1	0.553 77.6	0.553 75.5	8.06 10.9	-0.120 -2.71
Ambient, 5 days	Processed	0.586 4.88 78.1	0.583 5.05 77.4	0.529 5.08 79.5	11.3 4.95 0.856	-9.27 0.462 2.80
2-8^{0}C, 7 days	Processed	0.598 79.8	0.592 72.8	0.604 79.1	7.37 7.73	1.97 8.66
-20^{0}C, 38.5 m	Biomatrix	0.616 82.1	0.561 75.5	0.623 69.2	2.58 3.01	11.1 -8.35
Whole blood						
3 freeze (-20^{0}C) - thaw cycles	Biomatrix	1.45 77.5	NA NA	1.58 85.1	12.8 9.29	8.74 9.81
Ambient, 24 h	Biomatrix	1.45 77.5	NA NA	1.44 68.8	3.82 4.71	-0.460 -11.2
2-8^{0}C, 9 days	Dried extract	1.45 77.5	NA NA	1.39 74.0	9.13 7.43	-4.37 -4.52
Ambient, 9 days	Processed	1.45 77.5	NA NA	1.60 87.1	0.720 3.17	10.6 12.3
-20^{0}C, 4 m	Biomatrix	1.45 77.5	NA NA	1.59 74.2	11.4 2.09	9.89 -4.30
Urine						
Ambient, 16h	Biomatrix	1.45 77.5	1.50 74.4	1.57 82.4	5.21 7.70	4.67 10.7
2-8^{0}C, 28 days	Dried extract	1.45 77.5	1.40 66.2	1.19 57.0	4.13 2.62	-14.8 -13.9
Ambient, 28 days	Processed	1.45 77.5	1.40 66.2	1.20 63.8	3.63 3.68	-14.3 -3.63
-20^{0}C, 10.5 m	Biomatrix	1.50 79.8	NA NA	1.54 75.9	5.77 1.79	2.67 -4.93
Faeces						
3 freeze (-20^{0}C)- thaw cycles	Biomatrix	0.242 19.4	0.245 19.9	0.273 19.7	5.22 7.05	11.1 -1.17
Ambient, 20 h	Biomatrix	0.242 19.4	0.254 19.8	0.277 22.5	2.41 14.8	8.92 13.8
Ambient, 8 days	Processed	0.242 19.4	0.245 19.9	0.281 18.9	8.00 3.61	14.7 -5.2
-20^{0}C, 5 m	Biomatrix	0.242 19.4	NA NA	0.269 19.2	13.5 5.46	11.0 -0.859

Conc.: concentration; CV: coefficient of variation; Dev.: deviation; MeOH: methanol; h: hours; m: months; NA: not available. [a]Concentrations are in ng/mL for MeOH, plasma, whole blood and urine and in µg/g for faeces. [b]Deviation is calculated against the initial concentration if available, otherwise against the nominal concentration. [c]Experiment was performed in duplicate instead of triplicate.

Stability

Results of the stability experiments are displayed in table 2. Eribulin is a relatively stable compound, with a demonstrated stability at -20 °C in plasma, whole blood, urine and faeces of at least 38, 4, 10.5 and 5 months, respectively. In whole blood and plasma eribulin is stable for at least 24 h at ambient temperature, indicating that no specific stability precautions are required during sample handling at the clinical site.

Reinjection reproducibility experiments demonstrated that runs with plasma and urine can be reinjected after 24 h and with faeces after 5 days residence in the autosampler at ambient temperature.

Conclusion

For the quantification of eribulin in human plasma, whole blood, urine and faeces, sensitive and accurate LC-MS/MS assays are presented. Using sample volumes of 500 µL of plasma, whole blood and urine and 250 µg faeces, linear ranges from 0.2 – 100 ng/mL for plasma, 0.5 – 100 ng/mL for whole blood and urine and 0.1 – 25 µg/g for faeces were validated. The assays have successfully been used to support clinical studies. Especially in mass balance studies they can play a major role, making it possible to quantify concentrations and excreted amounts of unchanged drugs.

References

[1] US FDA, Halaven, www.drugs.com/pro/halaven.html, (2010), Accessed at: 4-8-2011

[2] Kuznetsov G, Towle MJ, Cheng H, Kawamura T, TenDyke K, Liu D, Kishi Y, Yu MJ, Littlefield BA, Induction of morphological and biochemical apoptosis following prolonged mitotic blockage by halichondrin B macrocyclic ketone analog E7389, *Cancer Res.*, **64** (2004) 5760-5766.

[3] Jordan MA, Kamath K, Manna T, Okouneva T, Miller HP, Davis C, Littlefield BA, Wilson L, The primary antimitotic mechanism of action of the synthetic halichondrin E7389 is suppression of microtubule growth, *Mol.Cancer Ther.*, **4** (2005) 1086-1095.

[4] Vahdat LT, Pruitt B, Fabian CJ, Rivera RR, Smith DA, Tan-Chiu E, Wright J, Tan AR, Dacosta NA, Chuang E, Smith J, O'Shaughnessy J, Shuster DE, Meneses NL, Chandrawansa K, Fang F, Cole PE, Ashworth S, Blum JL, Phase II study of eribulin mesylate, a halichondrin B analog, in patients with metastatic breast cancer previously treated with an anthracycline and a taxane, *J.Clin.Oncol.*, **27** (2009) 2954-2961.

[5] Desjardins C, Saxton P, Lu SX, Li X, Rowbottom C, Wong YN, A high-performance liquid chromatography-tandem mass spectrometry method for the clinical combination study of carboplatin and anti-tumor agent eribulin mesylate (E7389) in human plasma, *J.Chromatogr.B Analyt.Technol.Biomed.Life Sci.*, **875** (2008) 373-382.

[6] Rosing H, Man WY, Doyle E, Bult A, Beijnen JH, Bianalytical liquid chromatographic method validation. A review of current practices and procedures, *J.Liq.Chromatogr.Relat.Technol.*, **23** (2000) 329-354.

[7] US FDA, Department of Health and Human Services, Guidance for Industry, Bioanalytical Method Validation, www.fda.gov/downloads/Drugs/GuidanceComplianceRegulatoryInformation/Guidances/ucm070107.pdf, (2001), Accessed at: 9-1-2012

[8] Niessen WMA, Liquid chromatography -- mass spectrometry, CRC Press, Taylor & Francis Group, 2006, p. 3.
[9] Viswanathan CT, Bansal S, Booth B, DeStefano AJ, Rose MJ, Sailstad J, Shah VP, Skelly JP, Swann PG, Weiner R, Quantitative bioanalytical methods validation and implementation: best practices for chromatographic and ligand binding assays, *Pharm.Res.*, **24** (2007) 1962-1973.

Chapter 3.2

Mass balance study of ^{14}C-eribulin in patients with advanced solid tumours

Anne-Charlotte Dubbelman, Hilde Rosing,
Robert S. Jansen, Marja Mergui-Roelvink,
Alwin D.R. Huitema, Barbara Koetz, Margarita Lymboura,
Larisa Reyderman, Arturo Lopez-Anaya,
Jan H.M. Schellens, Jos H. Beijnen

Drug Metab Dispos. (2012) **40**:313-321.

Abstract

This mass balance study investigated the metabolism and excretion of eribulin, a non-taxane microtubule dynamics inhibitor with a novel mechanism of action, in patients with advanced solid tumours. A single ~2 mg (~80 μCi) dose of ^{14}C-eribulin acetate was administered as a 2–5 min bolus injection to 6 patients on day 1. Blood, urine, and faecal samples were collected at specified time points on days 1–8 or until sample radioactivity was ≤1% of the administered dose. Mean plasma eribulin exposure (627 ng.h/mL) was comparable to that of total radioactivity (568 ng eq.h/mL). Time-matched concentration ratios of eribulin to total radioactivity approached unity in blood and plasma indicating that unchanged parent compound constituted almost all eribulin-derived radioactivity. Only minor metabolites were detected in plasma samples up to 60 min post-dose, pooled across patients, each metabolite representing ≤0.6% of eribulin. Elimination half-lives for eribulin (45.6 h) and total radioactivity (42.3 h) were comparable. Eribulin-derived radioactivity excreted in faeces was 81.5% and that of unchanged eribulin was 61.9%. Renal clearance (0.301 L/h) was a minor component of total eribulin clearance (3.93 L/h). Eribulin-derived radioactivity excreted in urine was comparable (8.9%) to that of unchanged eribulin (8.1%) indicating minimal excretion of metabolite(s) in urine. Total recovery of the radioactive dose was 90.4% in urine and faeces. Overall, no major metabolites of eribulin were detected in plasma. Eribulin is primarily eliminated unchanged in faeces, while urine constitutes a minor route of elimination.

Introduction

Eribulin (Fig. 1) is a synthetic analogue of Halichondrin B, a complex polyether macrolide, first isolated from the marine sponge *Halichondria okadai* Kadota by Hirata and Uemura [1]. In human tumour cell lines, Halichondrin B proved to be highly cytotoxic, causing mitotic cell cycle arrest by inhibiting polymerization of tubulin and microtubule assembly [2]. The naturally low abundance of the molecule led to the development of complex methods for total synthesis and eventually to the discovery of eribulin [3], a structurally simplified Halichondrin B analogue with similar or identical anti-cancer properties in pre-clinical models [4]. In clinical studies, eribulin has demonstrated anti-tumour activity in extensively pre-treated patients who had advanced or metastatic breast cancer (MBC), with manageable tolerability [5-7]. A multicentre, randomised, Phase III study involving heavily pre-treated patients with metastatic breast cancer (MBC) showed a significant improvement in median overall survival by 2.5 months for patients treated with eribulin (n=508) compared with patients who received treatment of physician's choice (n=254) [8]. Eribulin mesylate was recently approved in the United States for the treatment of patients with metastatic breast cancer who have previously received at least two chemotherapeutic regimens for the treatment of metastatic disease. Prior therapy should have included an anthracycline and a taxane in either the adjuvant or metastatic setting.

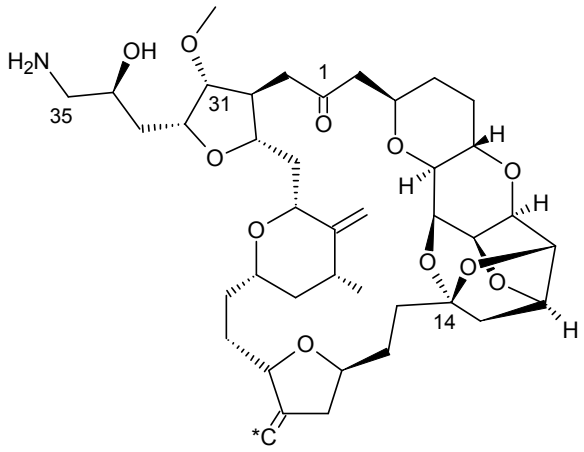

Figure 1: Chemical structure of ^{14}C-eribulin. The asterisk indicates the position of the ^{14}C-label.

Knowledge about the metabolism and excretion of a new drug are essential for its approval. Over the past few years, the interest in drug metabolism has increased rapidly due to discussion on the potential contribution of drug metabolites to toxicity. Within this scope, the U.S. Food and Drug Administration (FDA) and the International Conference on Harmonisation (ICH) recently issued guidances for Metabolites in Safety Testing (MIST), recommending additional safety assessments for major metabolites [9;10]. Major metabolites are herein defined as metabolites with a systemic exposure greater than 10% of

the parent (FDA) or the total drug-related (ICH) exposure that are either identified only in human plasma or present at disproportionally higher levels in humans than in any preclinical test species.

Knowledge about drug excretion is particularly important in treatment of patients with impaired renal or liver function, as clinical implications of urinary or biliary excreted drugs may be more pronounced for these patients, with potential need for dosage adjustments.

Pre-clinical studies showed that eribulin is predominantly metabolized by CYP3A4 [11]. In clinical studies, eribulin was found to be minimally eliminated as unchanged form in urine [12;13]. The objective of this study was to determine the metabolism and excretion of eribulin after a single dose of ^{14}C-eribulin in patients with advanced solid tumours. Pharmacokinetics and excretion of both unchanged drug and total radioactivity (comprising parent-drug and metabolites) were determined using validated liquid chromatography tandem mass spectrometry (LC-MS/MS) assays and liquid scintillation counting (LSC), respectively. Radiochromatography and high-resolution mass spectrometry were combined to detect and identify eribulin metabolites.

Methods

Compounds and reagents

^{14}C-eribulin acetate was manufactured by GE Healthcare UK limited (Chalfont St Giles, UK) and provided by Eisai Ltd. (Hatfield, Hertfordshire, UK). Sterile water for injection, normal saline (0.9% NaCl) and distilled water for sample preparation originated from B. Braun (Melsungen, Germany). All solvents for sample preparation and high performance liquid chromatography (HPLC) were analytical or HPLC grade. Methanol (MeOH) and acetonitrile (ACN) were obtained from Biosolve Ltd. (Valkenswaard, the Netherlands). Ammonium acetate was purchased from Fluka (Zwijndrecht, the Netherlands) and water for mobile phase preparation (LiChrosolv), isopropanol, EDTA, 30% hydrogen peroxide (w/w) and acetic acid originated from Merck (Darmstadt, Germany). Solvable and Ultima Gold liquid scintillation cocktail were obtained from Perkin Elmer (Waltham, MA, USA).

Patients

Patients aged at least 18 years with a histologically or cytologically confirmed advanced solid tumour, that had progressed following standard therapy or for which no standard therapy existed, were eligible for this study. Prior chemotherapy other than eribulin, mitomycin C or nitrosourea was allowed, as was radiation or biological therapy, provided that the last treatment was at least 3 weeks prior to study entry (4 weeks for investigational drugs and alternative therapies). Other eligibility criteria included: Eastern Cooperative Oncology Group performance status (ECOG-PS) $\leq$ 2, adequate renal function (serum creatinine $\leq$ 135 μmol/L ($\leq$ 1.5 mg/dL) or creatinine clearance $\geq$40 mL/min), adequate

bone marrow function (absolute neutrophil count ≥1.5 x 10^9/L and platelet count ≥100 x 10^9/L), adequate hepatic function (bilirubin ≤1.5 times the upper limit of normal (ULN) and alkaline phosphatase, alanine aminotransferase, and aspartate aminotransferase ≤3 x ULN or ≤5 x ULN in the case of liver metastases) and resolution of all chemotherapy or radiotherapy related toxicities to ≤ grade 1, except for stable sensory neuropathy ≤ grade 2 and alopecia.

Exclusion criteria included presence of severe intercurrent illness or infection, significant cardiovascular impairment, known positive human immunodeficiency virus status, major surgery within 4 weeks before treatment start, pulmonary dysfunction requiring active treatment, treatment with warfarin or related compounds other than for line patency, pregnancy and breast-feeding, meningeal carcinomatosis, pre-existing neuropathy > grade 2, organ allografts requiring immunosuppression, radiation therapy that encompassed > 30% of marrow and active brain metastases.

Study design

Six patients with advanced solid tumours were enrolled into this Phase I, open-label, non-randomised, single centre (the Netherlands Cancer Institute, Amsterdam, the Netherlands) study. Patients received a 2 mg flat dose of ^{14}C-eribulin acetate (approximately 80 to 90 μCi) on Day 1, Cycle 1 after pre-dose evaluations (medical/surgical history, tumour assessment, complete physical examination, vital signs, ECG and clinical laboratory tests for safety) were completed. During the study phase (day 1-8), the patients remained hospitalised for collection of blood samples and excreta. Collection of urine and faeces was continued until the radioactivity levels of 24 h collections were below 1% of the administered dose. Patients received 1.4 mg/m^2 unlabelled eribulin mesylate on Day 8 of Cycle 1. If, however, sample collection was continued beyond day 8, the Day 8 dose was delayed until completion of the sample collection. From cycle 2 onwards, patients could enter the extension phase of the trial and receive 1.4 mg/m^2 unlabelled eribulin mesylate on Days 1 and 8 of each subsequent 21-day cycle. Patients were permitted to continue their participation in the study and receive eribulin treatment if they had stable disease, partial or complete response to treatment, assessed according to response evaluation criteria in solid tumours (RECIST).

The safety of eribulin was assessed by measuring vital signs, laboratory testing, physical examinations and by documenting concomitant medication and adverse events.

The study was conducted in accordance with the ICH guidelines for Good Clinical Practice (CPMP/ICH/135/95), the European Clinical Trials Directive (2001/20/EC) and the Declaration of Helsinki. The protocol was approved by the Netherlands Cancer Institute Independent Ethics Committee.

^{14}C-Eribulin drug formulation and administration

Individual aseptic preparations of ^{14}C-eribulin infusions were prepared in a laminar flow cabinet, situated in a laboratory suited for handling radio-labelled drugs. ^{14}C-eribulin acetate was provided in vials containing 0.5 mL ethanol with 10 mg/mL eribulin acetate, at a specific activity of 40 μCi/mg (chemical and radiochemical purity >99.6%). A volume of 0.2 mL was extracted from the vial, added to 5 mL of sterile water for injection and combined with 45 mL normal saline (0.9% NaCl). The solution was filtered through a 0.22 μm syringe filter (Millipore Millex, Billerica, MA, USA). A 0.5 mL aliquot was separated from the final dosing solution for analysis, and two 200 μL aliquots thereof were mixed with 10 mL liquid scintillation cocktail, analysed using liquid scintillation counting and used to calculate the total radioactivity of the final dosing solution. The final dosing solution was administered to the patient by a syringe pump as a 2-5 min bolus infusion, which was followed by administration of normal saline to flush the lines. Remaining radioactivity was determined in both tubing and syringe. This was done by flushing them with a known volume of normal saline and analysis of a 1 mL aliquot for total radioactivity. The actual administered activity was calculated by subtracting the radioactivity remaining in the dosing system from the radioactivity in the final solution.

Sample collection

Venous blood samples (6 mL) were collected pre-dose, at the end of the 2-5 min ^{14}C-eribulin infusion (EoI) and at 5 min, 15 min, 30 min, 1, 2, 4, 6, 8, 10, 24, 48, 72, 96, 120, 144 and 168 h after EoI. The blood samples were collected in lithium heparinised tubes, inverted gently and centrifuged at 2,000 g and 4ºC for 15 min. Two 0.2 mL aliquots of the plasma layer were transferred to scintillation vials for total radioactivity (TRA) determination and the remainder was divided over 2 labelled polypropylene (PP) tubes for quantitative bioanalysis and for metabolite profiling and identification.

Whole blood samples (4 mL) were collected pre-dose, at EoI and 5 min, 15 min, 30 min, 1, 2, 4, 8, 24, 72 and 168 h after EoI. Two 0.2 mL aliquots were transferred to scintillation vials to measure TRA and the remainder was divided over 2 labelled PP tubes for quantitative bioanalysis.

Urine samples were collected before ^{14}C-eribulin administration, over 6 h periods for the first 48 h after administration and then over 24 h periods until day 8 or longer, i.e. until the daily urinary recovery was <1% of the administered activity. Total mass and collection time were recorded, a 1 mL aliquot was transferred to a scintillation vial to determine TRA and 5 and 25 mL aliquots were stored for quantitative bioanalysis and for metabolite profiling and identification.

Pre-dose faecal samples were collected and all faecal portions produced after administration were individually collected in pre-weighed containers until day 8 or longer, i.e. until the daily faecal recovery was <1% of the administered activity. Samples were

stored refrigerated until homogenisation with water in a 1:3 (w/v) ratio. Three aliquots of 0.2 mL were used to determine TRA, 1, 5 and 25 mL aliquots were stored for quantitative bioanalysis and for metabolite profiling and identification.

All samples were stored at nominally -70ºC. The samples were collected for: (i) measurement of TRA with LSC (to determine concentrations of all eribulin-related ^{14}C-labelled compounds combined), (ii) quantitative bioanalysis with LC-MS/MS (to determine concentrations of unchanged eribulin), (iii) metabolite profiling with LC-LSC-MS/MS (to detect and quantitate eribulin metabolites) and (iv) metabolite identification with LC-LTQ Orbitrap MS.

Total radioactivity

After recording the exact sample sizes by mass, radioactivity was determined by liquid scintillation counting. Before adding scintillation cocktail, whole blood and faecal homogenate samples were prepared (dissolved and decolourized) similar to the procedures described in [14]. One mL Solvable™, 1 mL isopropanol and 0.4 mL 30% hydrogen peroxide were added to faecal homogenates (triplicate) and 1 mL Solvable™, 100 µL 0.1 M EDTA and 0.5 mL 30% hydrogen peroxide were added to whole blood samples (duplicate). Subsequently, both faecal homogenates and whole blood samples, the latter only after at least 1 h storage in the dark at room temperature, were gently shaken in a water bath (Salm en Kipp, Breukelen, the Netherlands) at 40-45ºC until decolourization. After cooling down, these samples were treated identically to plasma (duplicate) and urine (singular) samples: 10 mL liquid scintillation cocktail was added and samples were stored in the dark for at least 1 h.

Counting was then performed on a Tri-Carb 2800TR liquid scintillation counter (Perkin Elmer), employing a ^{14}C counting protocol with automatic quench correction and a maximum counting time of 60 min per sample.

Quantitative bioanalysis

Concentrations of unchanged eribulin in plasma, whole blood, urine and faeces were measured using validated LC-MS/MS assays as described elsewhere [15]. Briefly, liquid-liquid extraction was used for sample clean-up. Supernatants of plasma, whole blood and urine were concentrated and extracts of all matrices were filtered. Final extracts were injected onto a C18 column and eluted using a gradient with 0.1% formic acid in water and ACN. An electrospray ionisation source produced positive ions that were detected with a triple quadrupole MS. Using multiple reaction monitoring, the mass transition of m/z 730 → 712 was recorded for eribulin and 731 → 681 for the internal standard ER-076349. The validated ranges were 0.2 – 100 ng/mL for plasma, 0.5 – 100 ng/mL for urine and whole blood and 0.1 – 25 µg/g (undiluted faeces) for faeces. Quality control samples were prepared and assayed together with the study samples. Criteria for the acceptance of

bioanalytical data during routine drug analysis, as described in the FDA guidelines [16], were applied.

The ratio of ^{14}C-eribulin to ^{12}C-eribulin in the dosing solution, as determined by LC-MS, was 1.03. As only ^{12}C-eribulin was quantitated with these bioanalytical assays, the concentrations were multiplied by 2.03 to obtain the total eribulin concentrations.

Metabolite profiling and metabolite identification

Sample preparation

To check for the presence of major metabolites, plasma samples collected up to 60 min after EoI were pooled across patients, to obtain a single 300 µL plasma sample for each time point, containing equal volumes from each patient.

Additionally, plasma samples of individual patients from EoI and 5 min, 15 min, 60 min, 2, 6, 24, 72 and 144 h after EoI were processed and analysed if the radioactivity in the extracts was considered sufficient for radiochromatography. Both urine and faecal samples were pooled within patients over from 0-24 h, 24-48 h, 48-72 h and 72-168 h, in proportion to the total mass of the excreta.

To process plasma samples for metabolite profiling, proteins were precipitated by adding 900 µL of MeOH:ACN (50:50, v/v) to 300 µL plasma. The mixture was vortex mixed for 30 s and centrifuged for 10 min at 23,100 g. The clear supernatant was transferred to a clean 1.5 mL vial, evaporated to dryness under a gentle nitrogen stream at 40ºC and reconstituted in 100 µL of 20 mM ammonium acetate pH 5:ACN (70:30, v/v) by vortex mixing for 10 s, followed by sonication for 1 h. After centrifuging for 10 min at 23,100 g, a 10 µL aliquot of the final supernatant was mixed with 4 mL scintillation cocktail and assayed for radioactivity using LSC, to calculate the recovery of the sample preparation. The remaining supernatant was transferred to an autosampler vial and used for LC-LSC-MS/MS analysis (described later). Additionally, for each sample, the pellets formed after the first and second centrifugation step were mixed with 1 mL Solvable™, dissolved by sonication for 1 h and analysed for TRA.

For metabolite profiling, pooled urine samples were injected directly without sample preparation. For metabolite identification, a single urine sample, collected 0-6 h after infusion, was lyophilised. To this end, a 25 mL sample of frozen urine was transferred to a freeze-dryer (Snijders, Tilburg, The Netherlands) operating at -80ºC. Vacuum was applied until the sample was totally dehydrated. The dried sample was reconstituted in 1 mL water. After centrifugation for 10 min at 23,100 g, the supernatant was used for LC-LTQ Orbitrap MS.

Faecal homogenates were prepared for metabolite profiling by extracting 100 µL aliquots of faecal homogenates with 100 µL ACN. The mixtures were then vortex mixed for 30 s,

shaken for 10 min at 1,250 rpm on an automatic shaker (Labinco, Breda, the Netherlands), vortex mixed another 30 s and centrifuged for 10 min at 23,100 g. This process was repeated with the pellet remaining after transfer of the clean supernatants to empty vials. After the second extraction, the pellet was dissolved and analyzed for radioactivity, identically to the plasma pellets. The supernatants of the first and second extraction were combined and vortex mixed after addition of 300 µL water. An aliquot of 50 µL was mixed with 4 mL scintillation cocktail and radioactivity was determined to calculate the recovery of the sample preparation. The remainder was distributed over autosampler vials for metabolite profiling. For metabolite identification, the faecal homogenate with the highest radioactive concentration was further concentrated by evaporation. Two 500 µL aliquots of faecal homogenate were mixed with 500 µL ACN and shaken and centrifuged identically to the other faecal homogenates. In 4 h, the supernatants were partially evaporated at 45ºC in a SpeedVac (SPD1010, Thermo Scientific, Waltham, MA, USA). After centrifuging for 5 min at 23,100 g, the clear supernatants were combined and the volume was adjusted to 500 µL with ACN.

LC-LSC-MS/MS and LC-LTQ Orbitrap MS

For both metabolite profiling and metabolite identification, chromatography was performed using a 1 h gradient containing 2 mobile phases (A and B) on a Synergi Polar RP column (150 x 4.6 mm, particle size 4 µm) (Phenomenex, Torrance, CA, USA) preceded by an in-line filter (0.2 µm, Upchurch scientific, Oak Harbor, WA, USA). Mobile phase A consisted of 20 mM ammonium acetate at pH 5 and mobile phase B of 100% ACN. Starting at 3% B, the percentage B linearly increased to reach 5% at 5.0 min, 10% at 15.0 min, 20% at 25 min, 40% at 35 min, 60% at 45 min, and 80% at 50 min, where it was maintained until 54.9 min. From 55 to 60 min, the column was re-equilibrated at 3% B. The flow rate was set to 1.0 mL/min, the injection volume to 50 µL (20 µL for the high resolution mass spectrometry) and during the first 4 minutes the eluent was directed to waste.

The system used for metabolite profiling consisted of an Accela HPLC pump coupled to a LTQ XL linear ion trap mass spectrometer equipped with an electrospray ionisation probe (Thermo Fisher Scientific, Waltham, MA, USA). The mass spectrometer operated in positive ion mode, with a spray voltage of 5.4 kV, a capillary temperature of 300ºC and a capillary voltage of 6.5 V. The sheath, auxiliary and sweep gas flow were optimised to 60, 10 and 5 arbitrary units, respectively. Wideband activation was enabled, the scan range was 100-1100 amu, the isolation width 2.0 and the normalised collision energy used for collision induced dissociation was 35%. To collect MS^2 and MS^3 spectra, data dependent acquisition was performed based on a parent list. This list contained masses of eribulin and hypothetical metabolites (e.g. products of single or multiple hydroxylation) and was expanded when additional potential metabolites were found.

Radiochromatograms were generated using HPLC coupled to a post-column accurate flow splitter (LC Packings, Sunnyvale, CA, USA), directing ¼ of the flow to a linear ion trap MS and ¾ to a fraction collector (LKB-FRAC-100, Pharmacia, Amersham Biosciences, Uppsala, Sweden) to collect fractions for radioactivity measurement using LSC. The fraction collector collected the eluent in 6 mL plastic LSC vials, at a rate of 1 min/vial (or in 20 mL vials at a rate of 5 min/vial in regions containing low radioactivity levels). After addition of 4 mL (or 10 mL) liquid scintillation cocktail, the fractions were assayed for TRA for 20 min per vial with LSC. Radiochromatographic profiles were prepared by plotting the net disintegrations per minute against the time after injection.

For metabolite identification, high-resolution mass spectrometry was applied to the concentrated urine and faecal samples. The equipment used for these samples consisted of a Finnigan Surveyor MS pump Plus which was coupled to a LTQ Orbitrap XL mass spectrometer (Thermo Fisher Scientific). Pump and mass spectrometer settings were identical to those described above, except for the normalised collision energy, which was set at 40%. Additionally, the resolution was set on 60,000.

Calculations

The metabolite concentrations in plasma and total amounts excreted in urine and faeces were derived from the radiochromatograms. Concentrations were calculated by dividing the activity of the fraction presenting the metabolite (in disintegrations per minute, dpm) by the injection volume (50 x 10^{-3} mL), the split ratio (¾), the specific activity (88.8 dpm/ng eribulin, corresponding with 40 μCi/mg eribulin), the sample preparation recovery (only for plasma and faeces, 100% for urine) and the concentration factor (3 for plasma, 1 for urine and 1/6 for faecal homogenates). To obtain the total amounts, the concentrations in urine and faecal homogenates were multiplied with the total volume of the pooled urine and pooled faecal homogenate, respectively.

The limit of detection (LOD) and lower limit of quantitation (LLOQ) of the LSC results were based on the formulas described by Currie [17;18], using a maximum counting error of 5% for total radioactivity measurements and 20% for metabolite profiling. The LLOQ for TRA determination was 0.304 ng eq/mL in urine and 1.52 ng eq/mL in plasma, whole blood and faeces. The LOD and LLOQ for metabolite profiling were 4 and 14 dpm per collected fraction, respectively.

Pharmacokinetic analysis

Pharmacokinetic parameters of eribulin and total radioactivity were calculated using non-compartmental analysis with WinNonlin™ Professional (version 5.1.1, Pharsight Corp, Mountain View, CA, USA). For plasma radioactivity, the pharmacokinetic parameters determined included maximum concentration (C_{max}), the terminal phase half-life ($t_{½}$) and the area under the plasma concentration time curve (AUC). For eribulin in plasma also the

clearance (CL), the renal clearance (CL_r) and the apparent volume of distribution (V_z) were determined.

Results

Patients

Four male and two female patients were enrolled in this study. All patients were Caucasian, had an ECOG-PS of 0 or 1, a median age of 60.5 years (range 34 - 70), a median weight of 70.5 kg (range 55.0 - 175), a median height of 172.5 cm (range 162.0 - 210.0) and a median body surface area of 1.9 m^2 (range 1.6 - 3.2). The patients had metastatic cancer with the primary tumour in one of the following locations: lung, testis, nasopharynx, ovaries, esophagus and prostate.

Total radioactivity and quantitative bioanalysis

Pharmacokinetics

Plasma concentration/time curves of unchanged eribulin and TRA are presented in Figure 2 and Table 1 summarises the pharmacokinetic parameters. Since the actual administered dose ranged from 1.75 to 3.01 mg, the dose-normalised values for C_{max}, AUC_{0-t} and $AUC_{0-\infty}$ were also calculated and presented in Table 1.

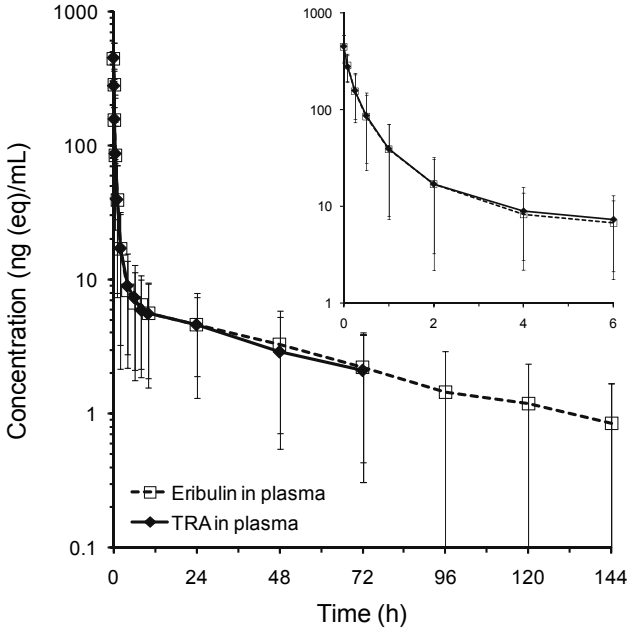

Figure 2: Mean (± SD) log-linear plasma concentration-time curves of total radioactivity (TRA, by LSC) and eribulin (by LC-MS/MS) in plasma up to 144 h after the end of a 2-5 min IV infusion of ~2 mg (~80 μCi) ^{14}C-eribulin in cancer patients. Inset: first 6 hours.

Table 1: Administered doses and pharmacokinetic parameters (mean ± SD) of eribulin and total radioactivity in cancer patients (n=6) after a 2-5-min bolus injection of ~2 mg (~80 μCi) of ^{14}C-eribulin.

Actual administered doses				
Dose	2.14 ± 0.44	mg		
Activity	85.5 ± 17.9	μCi		
Pharmacokinetic parameters				
	Eribulin		Total radioactivity	
C_{max}	444 ± 144	ng/mL	449 ± 137	ng eq/mL
$t_{½}$	45.6 ± 8.68		42.3 ± 17.2[a]	h
AUC_{0-t}	627 ± 386	ng.h/mL	568 ± 392	ng eq.h/mL
$AUC_{0-\infty}$	681 ± 425	ng.h/mL	753 ± 403[a]	ng eq.h/mL
CL	3.93 ± 2.10	L/h	-	
CL_r	0.30 ± 0.13	L/h	-	
V_z	247 ± 123	L	-	
Dose-normalized parameters				
	Eribulin		Total radioactivity	
C_{max}	222 ± 76.4	ng/mL/mg	224 ± 74.1	ng eq/mL/mg
AUC_{0-t}	301 ± 165	ng.h/mL/mg	269 ± 153	ng eq.h/mL/mg
$AUC_{0-\infty}$	328 ± 189	ng.h/mL/mg	357 ± 148	ng eq.h/mL/mg

Data are presented as mean ± SD. eq: equivalents; C_{max}: maximum observed plasma concentration; $t_{½}$: terminal half-life; AUC_{0-t}: area under the plasma concentration-time curve; $AUC_{0-\infty}$: area under the plasma concentration-time curve from zero to infinity; CL: clearance; CL_r: renal clearance; V_z: apparent volume of distribution in the terminal phase. [a]n=5 (for one patient too few data points were above the limit of quantification to estimate an terminal disposition rate constant for the total radioactivity, therefore $t_{½}$ and $AUC_{0-\infty}$ could not be calculated for this patient).

To obtain a standard infusion time of 5 min, the dosing solution was administered at a flow of 10 mL/min. T_{max} was typically observed at the end of infusion. The values for dose-normalised C_{max} and exposure ($AUC_{0-\infty}$) to unchanged eribulin (222 ng/mL/mg and 328 ng.h/mL/mg, respectively) were comparable to those of TRA (224 ng eq/mL/mg and 357 ng eq.h/mL/mg, respectively). The $t_{½}$ value for eribulin (45.6 h) was similar to that of the total radioactivity (42.3 h). Figure 3 shows the time courses of eribulin and TRA distribution as the whole blood to plasma ratios. For eribulin as well as TRA, the whole blood to plasma ratio approximated unity.

Excretion

For all six patients, urine and faeces was collected as planned during the first 168 h after administration of ^{14}C-eribulin. Thereafter, four of the patients continued collecting faeces for up to a maximum of 312 h, until the daily recovery of radioactivity in faeces was <1% of the administered radioactivity.

Figure 4 shows the cumulative excretion of unchanged eribulin and TRA in urine and faeces. The mean (± SD) recovery of total radioactivity in the combined excreta (faeces and urine) after 312 h was 90.4 ± 11.7% of the administered activity (81.5 ± 13.4% in faeces

and 8.9 ± 4.0% in urine). The total contribution of unchanged eribulin was 68.6 ± 14.1% of the administered dose.

Within 168 h, the minimal excreta collection period for all patients, 86.5 ± 16.4% of the administered activity was excreted, with unchanged eribulin accounting for 68.0 ± 13.1%. Most of the administered radioactivity (77.6 ± 19.0%) was excreted via faeces and a minor part (8.9 ± 4.0%) via urine.

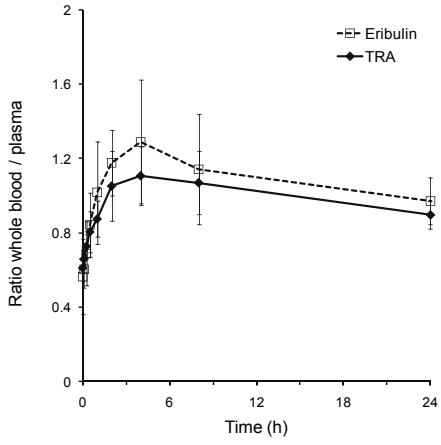

Figure 3: Mean (± SD, n=6) whole blood to plasma concentration ratio of total radioactivity (TRA, by LSC) and eribulin (by LC-MS/MS), after a single IV dose of ~2 mg (~80 μCi) ^{14}C-eribulin to cancer patients.

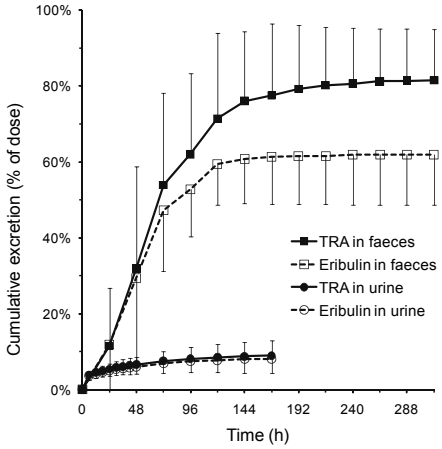

Figure 4: Mean (± SD) cumulative urinary and faecal excretion of eribulin (by LC-MS/MS) and ^{14}C-eribulin derived radioactivity (by LSC) of cancer patients after a single IV dose of ~2 mg (~80 μCi) ^{14}C-eribulin. n=6, only for eribulin in faeces n=5, as the results of one patient were excluded due to LC-MS/MS interference with co-medication (macrogol)

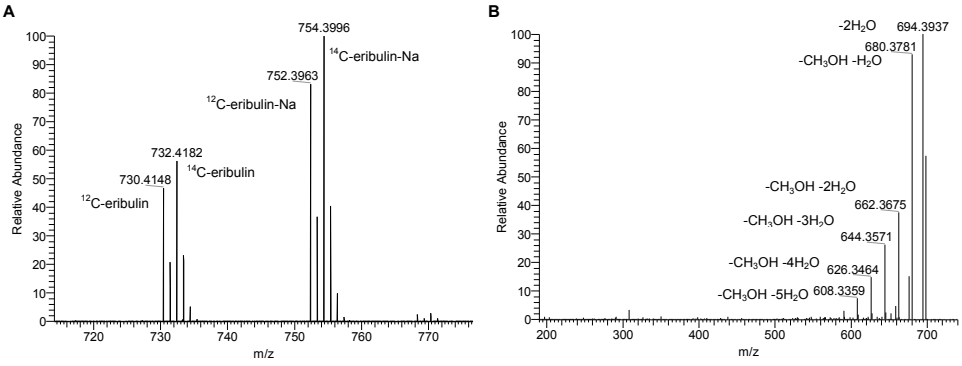

Figure 5: Mass spectrum of radiolabelled eribulin, showing the typical pattern of the ^{12}C- and ^{14}C-eribulin peaks and their Na-adduct peaks (A) and MS^2 spectrum of eribulin (m/z 730) (B).

Metabolite profiling

Plasma

The mean sample pre-treatment recovery of radioactivity in pooled and individual plasma extracts used for metabolite profiling was 87.7 ± 4.6%. Similar amounts of non-extractable radioactivity were found in the first (4.3 ± 1.8%) and second (4.1 ± 1.9%) pellet that were formed during sample preparation.

Radiochromatograms of the pooled plasma samples collected up to 1 h after EoI revealed the presence of a single major radioactive component, accounting for over 90% of the injected radioactivity (data not shown). The mass spectrum at this retention time showed a protonated molecular ion at m/z 730 with a ^{14}C isotope peak at m/z 732 (Fig. 5 A) that was not present in the pre-dose plasma sample. MS^2 fragmentation of this ion was identical to the fragmentation pattern of the reference standard (not shown) of eribulin (Fig. 5 B), and therefore this peak was identified as eribulin. Major metabolites were not present in these samples, as other radioactivity containing fractions constituted only a maximum of 0.6% of the eribulin peak.

In the individual plasma extracts, the radioactivity of the samples collected at 48 and 72 h after EoI was below LLOQ for all and below LOD for most patients. Therefore, only samples collected up to 24 h after EoI were analyzed with LC-LSC-MS/MS. Eribulin represented the main peak of the radiochromatogram of all these samples (representative example Fig. 6 A). Small amounts of radioactivity eluted shortly before and after eribulin, mainly in samples drawn at EoI and 5 min after EoI. Four elution fractions contained a radioactivity level above the LLOQ in one or more patient samples and were designated as eribulin metabolites MP1 to MP4. Table 2 provides an overview of these metabolites, summarising the retention times, the number of patients in which the metabolites were detected in plasma, the time points at which the metabolites were detected and the maximum relative and absolute concentrations that were detected in a sample. The most prominent metabolites were MP2 and MP3, observed in plasma of 5 and 4 patients, respectively, and both representing maximally ≤1% of the eribulin concentration.

Urine

The radiochromatograms of the urine samples, of which Fig. 6 B is a representative example, show very little metabolism, similar to the plasma samples. The main radioactive peak eluted after 43-44 min and was identified as eribulin based on the MS and MS^2 spectra. Only a single radioactive peak other than eribulin was above the LLOQ in two patients within the 0-24 h urine pools. This peak, designated MU1, had a maximum of 3.48% of the eribulin peak and accounted for a maximum of 0.42% of the administered dose (see Fig. 7).

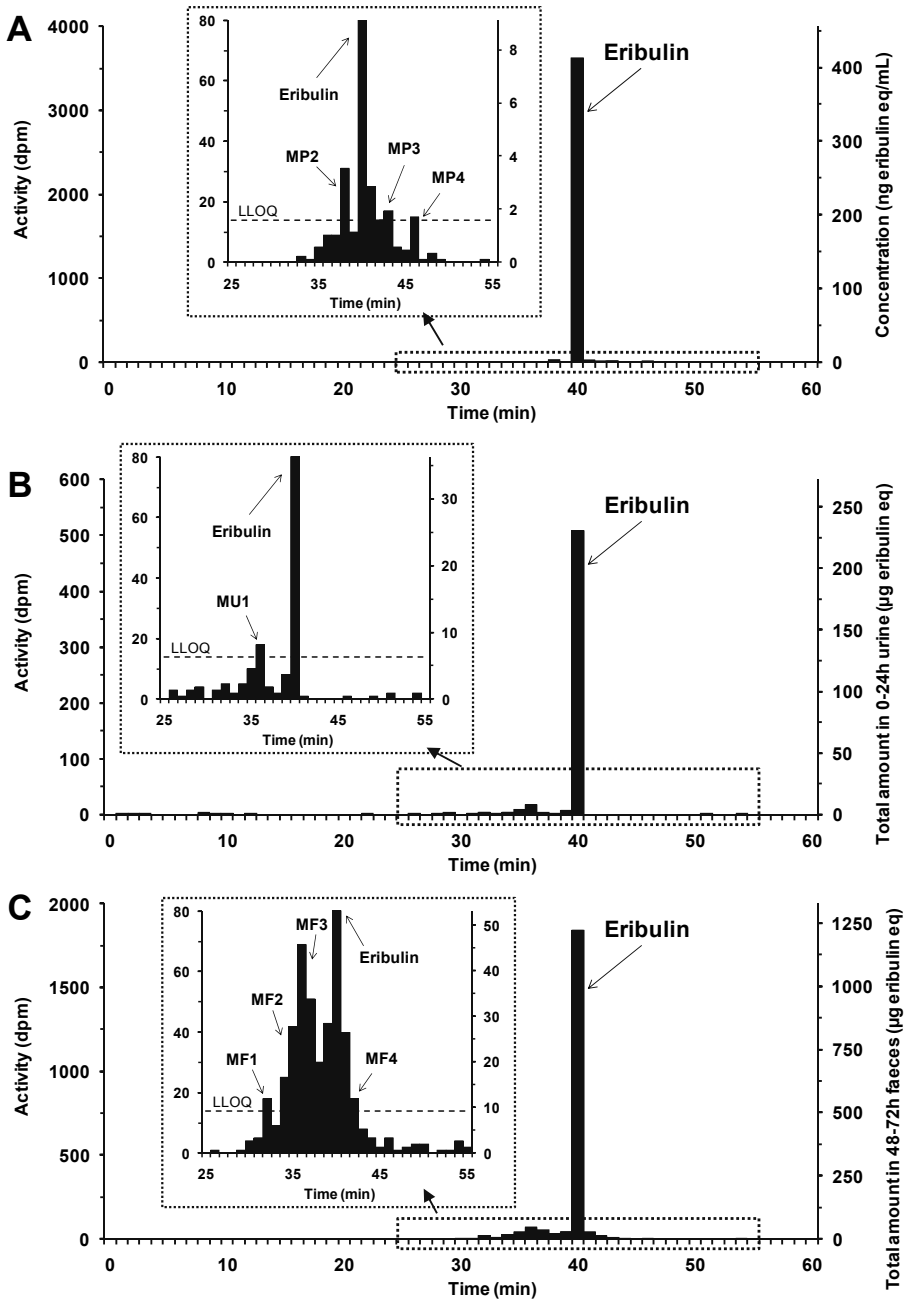

Figure 6: Representative radiochromatograms of a 5 min after EoI plasma sample (A), a 0-24 h urine sample (B) and a 48-72 h faecal sample (C), collected after administration of ~2 mg ^{14}C-eribulin (~80 µCi) to a cancer patient. The left vertical axes display the activity of the fraction and the right axes the corresponding concentration in ng eribulin equivalents/mL (for plasma) or the total amount excreted in that sample pool in µg eribulin equivalents (for urine and faeces). The insets show an enlargement of the region of metabolite elution, the lower limit of quantitation (LLOQ) is marked with a dashed line.

Table 2: Eribulin metabolites detected in plasma samples of individual patients

Peak ID	Retention time (min)	n	Timepoints	Max. relative concentration (% of eribulin peak)	Max. absolute concentration (ng eq/mL (% of eribulin))
MP1	35-36	1	EoI	0.31%	2.12 (0.31 %)
MP2	37-38	5	Upto 15 min after EoI	1.04%	3.64 (0.48 %)
MP3	42-43	4	Upto 15 min after EoI	0.99%	4.28 (0.56 %)
MP4	45-46	1	Upto 15 min after EoI	0.70%	2.15 (0.70 %)

n: number of patients for which this metabolite was observed in plasma; Max. relative concentration: maximum peak area of the metabolite relative to the eribulin peak area in the same radiochromatogram; Max. absolute concentration: maximum absolute concentration of the metabolite in a plasma sample, with corresponding relative concentration between parentheses

Faeces

Sample preparation of faecal homogenates with an evaporation and reconstitution step, similar to plasma samples, resulted in <80% recovery. It was not feasible to resolve the analytes from the dried residue using a solution compatible with the LC system. Therefore, faecal homogenates were extracted using a minimal extraction volume and the supernatant was further diluted with water until the final composition was compatible with the LC system. This approach increased recovery to 87.5 ± 6.0%.

Only small amounts of radioactivity corresponding to metabolites were present in faecal homogenates (representative example Fig. 6 C), with the largest peak in all samples identified as eribulin. The metabolite peaks were not resolved, complicating their designation. At least four metabolites appeared to be present. These were designated MF1 to MF4 and accounted for a maximum of 0.61, 0.85, 2.79 and 0.61% of the administered dose (Fig. 7).

Metabolite identification

To identify the m/z value of the metabolites, LC-MS spectra of pre-dose and post-dose samples were compared at the retention time of each radioactive peak. Post-dose samples were also scanned for the specific isotope pattern (Fig. 5 A) of two peaks of equal intensity with a difference of 2 in m/z value (due to the ^{14}C-isotope).

Plasma samples were concentrated by a factor 3 for plasma profiling, which resulted in insufficient concentration to obtain MS signals for metabolite identification. Therefore, the identity of the metabolites MP1 to MP4, each with a maximum concentration ≤1% of the eribulin concentration, was unresolved.

Since a large volume of urine was available for each collection interval, a considerable concentration step (25 times) was required for sufficient MS response. The urine sample with the highest MU1 concentration was concentrated 25 times and analyzed using LC-LTQ Orbitrap MS. At the retention time of MU1, the MS spectrum showed the specific $^{12}C/^{14}C$-eribulin related pattern, with a parent m/z value of 748.4244. The MS^2 spectrum of

MU1 showed the same fragmentation pattern as eribulin, with subsequent losses of water and methanol, however with an 18 Da shift to the right. Based on the high-resolution mass determinations, this metabolite was identified as eribulin+H_2O. Further elucidation of the molecular structure was not possible due to the unspecific fragmentation.

The faecal homogenate containing the highest radioactivity level was concentrated twice. The concentration of MF1 was still insufficient for MS detection, but MF2, MF3 and MF4 were detected. Based on the high-resolution mass determinations, they were identified as eribulin+O, eribulin+O and eribulin+H_2O, respectively. Similar to MU1, the MS^2 spectra of MF2, MF3 and MF4 showed the same pattern as eribulin (Fig. 5 B), with a mass shift of 16, 16 and 18 Da, respectively. Also for these metabolites the unspecific fragmentation in the MS^2 spectrum impeded further structural elucidation. Table 3 summarises the main characteristics of the metabolites detected in urine and faeces: retention times, number of patients in which the metabolites were detected, time periods in which they were detected, maximum percentage of administered dose recovered as this metabolite (compared between the 6 patients), m/z value, proposed identity, theoretical m/z value of the proposed identity and the difference between the theoretical and measured m/z values.

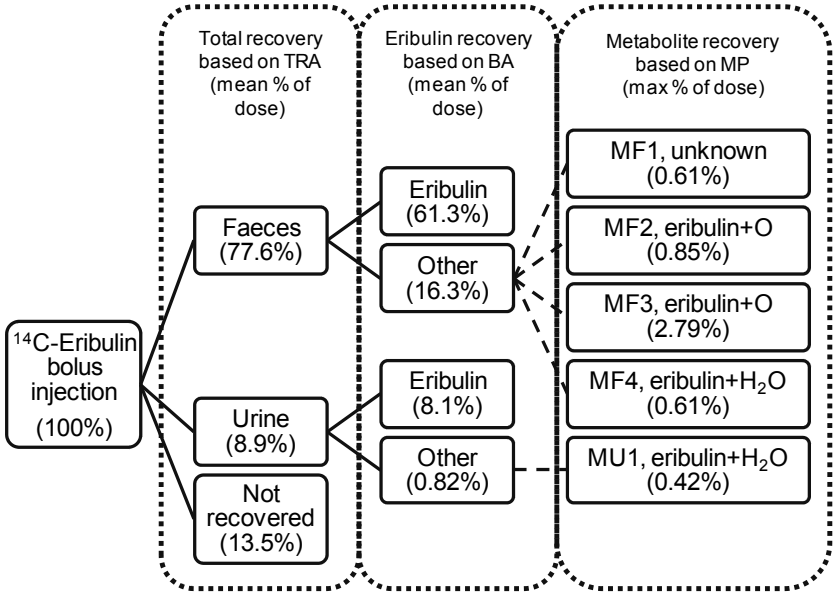

Figure 7: Overview of the average mass balance of ^{14}C-eribulin in 5 or 6 patients with advanced solid tumours during 168 h excreta collection after an IV-bolus injection of ~2 mg (~80 μCi) ^{14}C-eribulin. TRA: total radioactivity; BA: quantitative bioanalysis using LC-MS/MS, MP: metabolite profiling using LC-LSC. Max % of dose: maximum percentage of the administered dose that was excreted for a patient as this metabolite (assuming that excretion recovery was proportional for all radioactive material).

Safety

The ^{14}C-eribulin dose was generally well tolerated. A total of 4/6 patients experienced at least one treatment-related adverse event (AE) during the study phase. The most common AE reported as treatment-related was fatigue (n=3). The majority of AEs were of grade 1 or 2; grade 3 AEs were reported for one patient. There were no deaths or serious adverse events, no dose reductions or delays due to AEs and no patients were withdrawn from study treatment due to an AE. No significant abnormalities in laboratory parameters or obvious changes in vital signs were observed. Five patients continued treatment with eribulin mesylate after the study phase at a dose of 1.4 mg/m^2 on day 1 and 8 of 21-day cycles; one patient discontinued after completion of the assessments of the study phase and prior to entering cycle 2.

Table 3: Eribulin metabolites detected in urine and faeces.

Peak ID	Retention time (min)	n	Time periods	Max. contribution (% of adm. dose)	Accurate mass ($[M+H]^+$)	Proposed ID	Theoretical mass ($[M+H]^+$)	Δ ppm
MU1	35-36	2	0-24 h	0.42%	748.4244	Eribulin+H_2O	748.4267	-3.07
MF1	31-32	1	48-72 h	0.61%	unk	-	-	-
MF2	33-34	1	48-72 h	0.85%	746.4116	Eribulin+O	746.4110	0.80
MF3	35-37	2	24-72 h	2.79%	746.4111	Eribulin+O	746.4110	0.13
MF4	41-42	1	48-72 h	0.61%	748.4272	Eribulin+H_2O	748.4267	0.67

n: number of patients for which this metabolite was observed in urine / faeces; Max. contribution: maximum percentage of administered dose recovered as this metabolite (compared among the 6 patients); Δ ppm: deviation of accurate mass from theoretical mass in parts-per-million; unk: unknown.

Discussion

This study investigated the metabolism and excretion of eribulin in humans. It was found that eribulin undergoes limited metabolism and is primarily excreted unchanged via faeces (61.3% within 168 h). Four minor metabolites were detected in plasma, one in urine and four in faeces. Those that were identified had mass differences of +16 (+O) and +18 (+H_2O) relative to unchanged eribulin.

The plasma pharmacokinetic properties of eribulin are comparable to those reported in previous Phase I studies [12;13]. The plasma concentration-time curve shows that both total radioactivity and unchanged eribulin are rapidly distributed and then slowly eliminated. This profile, as well as the extensive volume of distribution, was demonstrated before [12]. Also the average $t_{½}$ of 45.6 h for eribulin was within the range of previously reported values for terminal half-life of 36 to 48 h [19]. Additionally, the recovery of unchanged eribulin in urine (8.1% after 168 h, Figure 7) is consistent with other Phase I studies, wherein 5 to 6% [12] and 7% [13] of the administered eribulin was recovered unchanged within 72 h after a single dose.

The plasma to whole blood ratio of both TRA and unchanged eribulin approximates unity, suggesting no preferential distribution of eribulin or eribulin-derived compounds to either red blood cells or plasma compartments. The comparable pharmacokinetics for eribulin and total radioactivity is indicative of limited metabolism. This was confirmed by the metabolic profile of eribulin in plasma: metabolites constituted ≤0.6% of the parent compound concentration in pooled plasma samples following 60 min after EoI and individual plasma samples revealed only four minor metabolites, MP1 to MP4, of which the most abundant comprised maximally 1% of the eribulin concentration. The low concentrations of the plasma metabolites impeded detection with LC-MS/MS; consequently, definite identification was not possible. Based on retention time only, MP1 could be identical to the urine metabolite MU1, and MP3 to the faecal metabolite MF4. Since the plasma metabolites were only detected in a few samples collected up to 15 min after the end of infusion and had a concentration of maximally 1% of the eribulin concentration in one patient, their overall systemic exposure does not exceed 10% of the parent compound, neither 10% of the total drug related exposure. This means that further tests to evaluate the safety of the metabolites may not be required according to the MIST guidelines [9;10].

The total recovery of the administered radioactivity, 86.5% at day 8 (168 h) slowly increasing to 90.4% at day 14 (312 h), is generally acceptable for a mass balance study [20]. Expired air was not analysed for the presence of $^{14}CO_2$, but considering the stability of eribulin, it is not expected that the production of $^{14}CO_2$ has contributed significantly to the loss of radioactivity, even though the ^{14}C-label was not incorporated in the ring structure of eribulin.

The quantitation of unchanged eribulin in faeces samples of one patient was not possible due to interference with large amounts of polyethylene glycol (PEG) in the samples. The PEG caused a dramatic ion suppression of eribulin in the quantitative LC-MS/MS assay, hampering reliable quantitation. The source of the PEG was probably macrogol, which was used daily by this patient to prevent constipation. Because of the interference, the LC-MS/MS results for eribulin in faeces of this patient were not included to calculate mean recoveries. PEG did not interfere with the quantitation of eribulin in plasma and urine of this patient since it appeared to be unabsorbed.

The total radioactivity that was recovered in faeces after 168 h (77.6% of the administered dose) is not completely accounted by the presence of unchanged eribulin (61.3% of the dose) and the identified metabolites MF1 to MF4 (<5% of the dose) (Figure 7). This difference can be explained by at least four factors: (i) unattributed radioactivity in the radiochromatograms, (ii) difference in LLOQ between bioanalysis and TRA analysis, (iii) incomplete recovery of eribulin during bioanalysis and (iv) presence of non-extractable metabolites. We will shortly discuss these factors and their quantitative impact.

First, not all radioactivity in the radiochromatograms of faecal samples was attributed to eribulin or one of the four identified metabolites. As the peaks were not completely resolved, a part of the unattributed radioactivity could be eribulin, MF1, MF2, MF3 and/or MF4. The other part comprises cumulative amounts of radioactivity below the LLOQ and could contain additional metabolites. On average, 5% of the administered dose was recovered in faeces, but unattributed.

Second, the LLOQ for the (LC-MS/MS) quantitation of unchanged eribulin (0.1 μg/g) was higher than the LLOQ for total radioactivity (LSC, 1.52 ng eq/g) in faeces. Consequently, samples with a concentration just below the LLOQ for quantitative bioanalysis were included to calculate TRA, but excluded when calculating the total amount of unchanged eribulin. Due to this difference in LLOQ, the underestimation of unchanged eribulin recovery in faeces would on average be 2% of the administered dose, assumed that the ratio of unchanged eribulin to TRA was equal for all samples of the same patient.

Third, the recovery of unchanged eribulin during the bioanalysis of faeces samples may have been incomplete, which may also have resulted in an underestimation of the unchanged eribulin recovery. This would be the case if faeces samples spiked with eribulin during assay validation have a higher extraction recovery than real-life patient samples or if the extraction recovery was dependent on the substance of the original non-homogenized faecal samples. At least the latter was suspected, as it was observed that for metabolite profiling, the highest extraction recoveries were obtained from watery faeces samples, while originally dry and hard faeces samples resulted in lower extraction recoveries. To obtain an indication of the underestimation of unchanged eribulin recovery in faeces due to incomplete eribulin recovery, the highest extraction recovery across patients and the extraction recoveries of individual patients were used. This resulted in an average potential underestimation of 6% of the administered dose.

Finally, the faeces samples could have contained unknown non-extractable metabolites. However, if these were present, their quantitative contribution was limited, as the three above mentioned factors already explained the main difference between TRA in faeces and unchanged eribulin plus metabolites MF1 to MF4.

The metabolites detected in urine and faeces differed by 16 and 18 mass units from eribulin. High-resolution mass analysis indicated incorporation of O and H_2O, respectively, in eribulin. Metabolites MF2 and MF3, with molecular masses of eribulin+16, may be products of hydroxylation. Eribulin metabolites with the same molecular masses were previously reported by Zhang *et al.* in an *in vitro* study with human liver microsomes [11]. That study showed that eribulin was primarily metabolized by CYP3A4, resulting in the formation of at least four mono-oxygenated metabolites. The described product ion spectra were similar to those we found for MF2 and MF3 in this study and, likewise, only comprised fragments formed by loss of water and/or loss of methanol. Due to the limited information provided by the MS^2 spectra, further structural elucidation was impossible.

The metabolites MU1 and MF4, with a mass of eribulin+18, may be products of hydration of an alkene group or products of hydroxylation with reduction of the ketone at the C-1 position. Alternatively, they may have been formed by hydrolysis of the ketal at the C-14 position. The exact structure of these metabolites remains undetermined.

The results of the present study may help to explain findings in other clinical studies. For example, the limited contribution of metabolism to the elimination of eribulin can explain that although eribulin is predominantly metabolized by CYP3A4 *in vitro* [11], co-administration of the CYP3A4 inhibitor ketoconazole with eribulin to patients has no effect on eribulin exposure [21], and neither do CYP3A4 inducers or inhibitors on eribulin systemic clearance [22]. Furthermore, the small contribution of urinary excretion to total excretion of eribulin may help to explain that eribulin is well tolerated at full dose in patients with moderate and severe renal dysfunction [23]. Similarly, the important role of biliary excretion may explain that in patients with moderate hepatic impairment, dose reductions of eribulin are supported by a population pharmacokinetic / adverse event model based on data from Phase 1 and 2 studies [24]. Hepatic impairment prolonged the elimination half-life of eribulin and the dose-normalised exposure ($AUC_{0-\infty}$) of patients with mild and moderate hepatic impairment was higher by 1.75-fold and 2.79-fold, respectively, compared with normal hepatic function [24].

In conclusion, eribulin was rapidly distributed and slowly eliminated following a 2-5 min IV bolus injection of ~2 mg (~80 μCi) ^{14}C-eribulin. Eribulin was primarily excreted unchanged in faeces and metabolism played only a minor role in the elimination. Renal clearance represented a minor component (<10%) in eribulin clearance. No major metabolites were found in plasma; each metabolite represented ≤0.6% of eribulin in pooled plasma samples.

Acknowledgements

The authors thank Sanquin (Amsterdam, the Netherlands) for providing the opportunity to use the LTQ Orbitrap. We acknowledge Luc Lucas and Bas Thijssen for their bioanalytical support to this study. Most importantly, we would like to thank the patients who gave their valuable time to participate in this study.

Footnotes

This study was supported by Eisai Inc. Part of this work was previously presented as follows: Dubbelman AC, Mergui-Roelvink M, Koetz B, Lymboura M, Reyderman L, Lopez-Anaya A, Rosing H, Marchetti S, Beijnen JH, Schellens JHM (2011) Metabolism and excretion of eribulin in patients with advanced solid tumors. *102nd annual meeting of the American Association for Cancer Research*, Orlando Florida, April 2-6, 2011, Abstract 1294.

References

[1] Hirata Y, Uemura D, Halichondrins - antitumor polyether macrolides from a marine sponge, *Pure & Appl.Chem.*, **58** (1986) 701-710.

[2] Bai RL, Paull KD, Herald CL, Malspeis L, Pettit GR, Hamel E, Halichondrin B and homohalichondrin B, marine natural products binding in the vinca domain of tubulin. Discovery of tubulin-based mechanism of action by analysis of differential cytotoxicity data, *J.Biol.Chem.*, **266** (1991) 15882-15889.

[3] Jackson KL, Henderson JA, Phillips AJ, The halichondrins and E7389, *Chem.Rev.*, **109** (2009) 3044-3079.

[4] Towle MJ, Salvato KA, Budrow J, Wels BF, Kuznetsov G, Aalfs KK, Welsh S, Zheng W, Seletsk BM, Palme MH, Habgood GJ, Singer LA, DiPietro LV, Wang Y, Chen JJ, Quincy DA, Davis A, Yoshimatsu K, Kishi Y, Yu MJ, Littlefield BA, In vitro and in vivo anticancer activities of synthetic macrocyclic ketone analogues of halichondrin B, *Cancer Res.*, **61** (2001) 1013-1021.

[5] Cortes J, Vahdat L, Blum JL, Twelves C, Campone M, Roche H, Bachelot T, Awada A, Paridaens R, Goncalves A, Shuster DE, Wanders J, Fang F, Gurnani R, Richmond E, Cole PE, Ashworth S, Allison MA, Phase II study of the halichondrin B analog eribulin mesylate in patients with locally advanced or metastatic breast cancer previously treated with an anthracycline, a taxane, and capecitabine, *J.Clin.Oncol.*, **28** (2010) 3922-3928.

[6] Vahdat, LT, Twelves, C, Allison, MK, Cortes, JA, Campone, M, Shuster, DE, Wanders, J, Fang, F, Gurnani, RD, and Blum, JL, Phase II study of eribulin mesylate (E7389) in patients (pts) with locally advanced or metastatic breast cancer (MBC) previously treated with anthracycline, taxane, and capecitabine therapy. [abstr 1084], *J Clin Oncol*, **26** (2008),

[7] Vahdat LT, Pruitt B, Fabian CJ, Rivera RR, Smith DA, Tan-Chiu E, Wright J, Tan AR, Dacosta NA, Chuang E, Smith J, O'Shaughnessy J, Shuster DE, Meneses NL, Chandrawansa K, Fang F, Cole PE, Ashworth S, Blum JL, Phase II study of eribulin mesylate, a halichondrin B analog, in patients with metastatic breast cancer previously treated with an anthracycline and a taxane, *J.Clin.Oncol.*, **27** (2009) 2954-2961.

[8] Cortes J, O'Shaughnessy J, Loesch D, Blum JL, Vahdat LT, Petrakova K, Chollet P, Manikas A, Dieras V, Delozier T, Vladimirov V, Cardoso F, Koh H, Bougnoux P, Dutcus CE, Seegobin S, Mir D, Meneses N, Wanders J, Twelves C, Eribulin monotherapy versus treatment of physician's choice in patients with metastatic breast cancer (EMBRACE): a phase 3 open-label randomised study, *Lancet*, **377** (2011) 914-923.

[9] ICH, Topic M 3 (R2), Non-Clinical Safety Studies for the Conduct of Human Clinical Trials and Marketing Authorization for Pharmaceuticals, www.ema.europa.eu/docs/en_GB/document_library/Scientific_guideline/2009/09/WC500002720.pdf, (2009), Accessed at: 4-8-2011

[10] US FDA, Department of Health and Human Services, Guidance for Industry, Safety testing of Drug Metabolites, www.fda.gov/downloads/Drugs/GuidanceComplianceRegulatoryInformation/Guidances/ucm079266.pdf, (2008), Accessed at: 4-8-2011

[11] Zhang ZY, King BM, Pelletier RD, Wong YN, Delineation of the interactions between the chemotherapeutic agent eribulin mesylate (E7389) and human CYP3A4, *Cancer Chemother.Pharmacol.*, **62** (2008) 707-716.

[12] Goel S, Mita AC, Mita M, Rowinsky EK, Chu QS, Wong N, Desjardins C, Fang F, Jansen M, Shuster DE, Mani S, Takimoto CH, A phase I study of eribulin mesylate (E7389), a mechanistically novel inhibitor of microtubule dynamics, in patients with advanced solid malignancies, *Clin.Cancer Res.*, **15** (2009) 4207-4212.

[13] Tan AR, Rubin EH, Walton DC, Shuster DE, Wong YN, Fang F, Ashworth S, Rosen LS, Phase I study of eribulin mesylate administered once every 21 days in patients with advanced solid tumors, *Clin.Cancer Res.*, **15** (2009) 4213-4219.

[14] van den Bongard HJG, Pluim D, Rosing H, Nan-Offeringa L, Schot M, Ravic M, Schellens JH, Beijnen JH, An excretion balance and pharmacokinetic study of the novel anticancer agent E7070 in cancer patients, *Anticancer Drugs*, **13** (2002) 807-814.

[15] Dubbelman AC, Rosing H, Thijssen B, Lucas L, Copalu W, Wanders J, Schellens JH, Beijnen JH, Validation of high-performance liquid chromatography-tandem mass spectrometry assays for the quantification of eribulin (E7389) in various biological matrices, *J.Chromatogr.B Analyt.Technol.Biomed.Life Sci.*, **879** (2011) 1149-1155.
[16] FDA, U.S. Department of Health and Human Services, Food and Drug Administration, Guidance for Industry, Bioanalytical Method Validation, http://www.fda.gov/downloads/Drugs/GuidanceComplianceRegulatoryInformation/Guidances/ucm070107.pdf, (2001), Accessed at: 9-1-2012
[17] Currie LA, Limits for Qualitative Detection and Quantitative Determination: Application to Radiochemistry, *Anal Chem*, **40** (1968) 586-593.
[18] Zhu M, Zhao W, Vazquez N, Mitroka JG, Analysis of low level radioactive metabolites in biological fluids using high-performance liquid chromatography with microplate scintillation counting: method validation and application, *J.Pharm.Biomed.Anal*, **39** (2005) 233-245.
[19] Cigler T, Vahdat LT, Eribulin mesylate for the treatment of breast cancer, *Expert.Opin.Pharmacother.*, **11** (2010) 1587-1593.
[20] Beumer JH, Beijnen JH, Schellens JH, Mass balance studies, with a focus on anticancer drugs, *Clin.Pharmacokinet.*, **45** (2006) 33-58.
[21] Devriese, L, Wanders, J, Jenner, A, Edwards, G, Reyderman, L, Copalu, W, Peng, F, Marchetti, S, Beijnen, J, and Schellens, J, Eribulin mesylate pharmacokinetics in patients with solid tumors receiving repeated oral ketoconazole, *Poster presented at EORTC-NCI-AACR Symposium, Berlin, Germany*, (2011),
[22] Reyderman, L, Gupta, A, Pelletier, RD, and Wong, N, Eribulin and cytochrome P450 effectors: in vitro studies and population pharmacokinetic–pharmacodynamic analysis, *Poster presented at EORTC-NCI-AACR Symposium, Berlin, Germany*, (2011),
[23] Synold, T, Tsao-Wei, D, Quinn, D, Groshen, S, Aparicio, A, Twardowski, P, Stadler, W, Gandara, D, Lara Jr., P, and Newman, E, Phase I and pharmacokinetic (PK) study of eribulin (E7389) in patients (pts) with renal dysfunction (RD) and advanced urothelial cancer (UC): A California Cancer Consortium Trial, *J Clin Oncol 28:15s, 2010 (suppl; abstr 2527)*, (2010),
[24] Devriese, L, Witteveen, P, Voest, E, Overkleeft, EN, Langenberg, M, Beijnen, JH, Reyderman, L, Wanders, J, Mould, DR, Gupta, A, Hussein, Z, and Schellens, JHM, Eribulin dosing in patients with advanced solid tumors and hepatic impairment, *J Clin Oncol 29: 2011 (suppl abstr 2544)*, (2011),

Chapter 4

Lenvatinib

Chapter 4.1

Development and validation of LC-MS/MS assays for the quantification of E7080 and metabolites in various human biological matrices

Anne-Charlotte Dubbelman, Hilde Rosing, Bas Thijssen, Abadi Gebretensae, Luc Lucas, Huachun Chen, Robert Shumaker, Jan H.M. Schellens, Jos H. Beijnen

J Chromatogr B Analyt Technol Biomed Life Sci (2012) **887-888**:25-34.

Abstract

To support clinical pharmacokinetic studies with the anticancer agent E7080 (lenvatinib), liquid chromatography tandem mass spectrometry (LC-MS/MS) methods were developed for the quantification of E7080 and four of its metabolites in human plasma, urine and faeces and of E7080 in whole blood.

Cross-analyte interferences between metabolites and parent compound were expected and therefore accounted for early in the method development. Plasma, urine and faeces samples were extracted with acetonitrile. Chromatographic separation was achieved on a 50 x 2.1 mm I.D. XTerra MS C18 column, with a 0.2 mL/min flow and gradient elution starting with 100% formic acid in water, followed by an increasing percentage of acetonitrile. Whole blood samples were extracted with diethyl ether and extracts were injected on a 150 x 2.1 mm I.D. Symmetry Shield RP8 column. Detection was performed using an API3000 triple quadrupole mass spectrometer, with a turbo ion spray interface, operating in positive ion mode.

Using 250 µL of plasma, E7080 and its metabolites could be quantified between 0.25 and 50.0 ng/mL. The quantifiable ranges of E7080 in whole blood, urine and faeces were 0.25 to 500 ng/mL, 1.00 to 500 ng/mL and 0.1 to 25 µg/g, using sample volumes of 250 µL, 200 µL and 250 mg, respectively. Calibration curves in all matrices were linear with a correlation coefficient (r^2) of 0.994 or better. At the lower limit of quantification, accuracies were within ± 20% of the nominal concentration with CV values less than 20%. At the other concentrations the accuracies were within ± 15% of the nominal concentration with CV values below 15%. The developed methods have successfully been applied in a mass balance study of E7080.

Introduction

E7080 (lenvatinib) is an investigational orally active inhibitor of multiple receptor tyrosine kinases, including vascular endothelial growth factor (VEGF), fibroblast growth factor (FGF), platelet derived growth factor (PDGF) and stem cell factor (SCF) receptors [1]. It has demonstrated potent antitumour effects in xenograft models of various human cancer cell lines by inhibition of angiogenesis [2;3]. Currently, E7080 is being tested in several phase I and phase II studies and has shown promising signs of anticancer activity [4;5].

To support clinical pharmacokinetic studies of E7080, robust quantification methods in different biological matrices are required. Thus far, no validated method for the quantification of E7080 and/or its metabolites has been published. This article describes the development and validation of high performance liquid chromatography tandem mass spectrometry (LC-MS/MS) assays for the quantification of E7080 and four of its metabolites in human plasma, urine and faeces and of E7080 in whole blood. The metabolites are products of decyclopropylation (M1), demethylation (M2), N-oxidation (M3) and O-dearylation (M5). The assays have been validated according to the FDA guidelines for bioanalytical method validation [6;7] and have been used to support a mass balance study with E7080.

Experimental

Chemicals and reagents

E7080 methanesulphonic acid salt, E7080 metabolites M1, M2, M3 and M5 and the internal standard ER-227326-00 (see Table 3 for the chemical structures) were provided by Eisai Co. Ltd, Tsukuba, Japan. Methanol (MeOH, Supra-Gradient grade), diethyl ether (HPLC-grade) and acetonitrile (ACN, Supra-Gradient grade) were obtained from Biosolve Ltd., Valkenswaard, the Netherlands. Dimethyl sulphoxide (DMSO), disodium hydrogenphosphate.2H_2O (>99.5%), ammonium acetate (>98%), phosphoric acid (85%), acetic acid (100%) and formic acid (98%) were purchased from Merck, Darmstadt, Germany. Water (distilled) used for sample preparation originated from B. Braun Medical, Melsungen, Germany and water (LiChrosolv) from Merck was used to prepare the mobile phases. Drug-free control human sodium heparinized plasma was obtained from Bioreclamations, Hicksville, NY, USA. Control human sodium heparinized whole blood, urine and faeces originated from healthy volunteers.

Preparation of stock solutions, calibration standard (CS) and quality control (QC) samples

Two independent stock solutions were made for each analyte: E7080, M1, M2, M3 and M5. One stock solution was used for the preparation of CS samples and the other for QC samples. All stock solutions were corrected for purity and salt. To prepare the 0.5 mg/mL

E7080 stock solutions, approximately 5.0 mg E7080 was weighed accurately and dissolved in 10.0 mL MeOH-water (1:1, v/v). Stock solutions containing 0.1 mg/mL M1, M2 or M3 were prepared by weighing approximately 2.0 mg of the analyte accurately, adding 3.0 mL DMSO to dissolve it and adding MeOH to a final volume of 20.0 mL. The 0.1 mg/mL M5 stock solutions were prepared by dissolving 2.0 mg M5 in 20.0 mL MeOH.

Stock solutions of different analytes were mixed and diluted with MeOH to obtain CS and QC working solutions for plasma, whole blood, urine and faeces. Subsequently, CS and QC samples in the biological matrices were prepared by diluting the corresponding working solutions with drug-free human sodium heparinized plasma, urine, faecal homogenate in water (1:3, w/v) and sodium heparinized whole blood (with at least 1 freeze /thaw cycle at -20 °C). Plasma and urine working solutions were diluted at least 20-fold. Calibration standards and QC samples for faeces and whole blood were prepared by addition of 250 µL and 10 µL of a mixture of working solution and MeOH to 1.00 mL and 200 µL faeces homogenate and whole blood, respectively. Table 1 lists the target concentrations of the CS and QC samples.

Table 1: Target concentrations of E7080 and its metabolites M1, M2, M3 and M5 in the calibration standard (CS) and quality control (QC) samples of the different biological matrices

Matrix	Plasma	Urine			Faeces		Whole blood
Sample type	Conc. (ng/mL)	Conc. (ng/mL)			Conc. (µg/g undiluted faeces)		Conc. (ng/mL)
	E7080, M1-M3, M5	E7080	M1-M3	M5	E7080	M1-M3, M5	E7080
CS 0/0	0	0	0	0	0	0	0
CS 0	0	0	0	0	0	0	0
CS 1	0.250	1.00	1.00	2.50	0.100	0.0200	0.250
CS 2	0.500	2.00	2.00	5.00	0.250	0.0500	0.500
CS 3	1.00	5.00	5.00	12.5	1.00	0.200	2.00
CS 4	2.50	10.0	10.0	25.0	2.50	0.500	10.0
CS 5	5.00	25.0	25.0	40.0	5.00	1.00	25.0
CS 6	10.0	100	50.0	80.0	12.5	2.50	100
CS 7	25.0	250	100	160	25.0	5.00	250
CS 8	50.0	500	200	200			500
QC LLOQ	0.250	1.00	1.00	2.50	0.100	0.0200	0.250
QC Low	0.750	3.00	3.00	7.50	0.250	0.0500	0.750
QC Mid	5.00	125	50.0	50.0	2.50	0.500	10.0
QC High	37.5	375	150	150	20.0	4.00	375
QC > ULOQ	250	2000	800	800			2500

Conc.: concentration; LLOQ: lower limit of quantification; ULOQ: upper limit of quantification

Stock solutions of the internal standard ER-227326-00 (IS) were prepared by weighing 5.0 mg (corrected for salt and purity) of the reference standard. For the plasma and faeces

assay, the compound was dissolved in 4 mL MeOH, after which 4 mL water was added and the volume was adjusted to 10.0 mL with MeOH. For the whole blood assay, the compound was dissolved in 7 mL MeOH, after which the volume was adjusted to 10.0 mL with water. IS working solutions (100 ng/mL and 1.0 μg/mL) were obtained by diluting the stock solution with MeOH-water (1:1, v/v).

All stock and working solutions were stored at nominally -20 °C, except for the stock solution of E7080 and the IS stock and working solutions, which were stored at -70 and 2-8°C, respectively. The QC samples were stored at nominally -20 °C and CS samples were freshly prepared before each validation run.

Sample preparation

Plasma

Plasma samples were prepared by protein precipitation. To a 250 μL aliquot of plasma, 20 μL internal standard working solution (100 ng/mL) and 500 μL ACN were added. After 10 min shaking at 1,250 rpm on an automatic shaker, the sample was centrifuged for 5 min at 23,100 g. The supernatant was transferred to a clean tube and evaporated to dryness under a gentle stream of nitrogen at 40 °C. The dried extract was reconstituted in 100 μL ACN-0.1% formic acid in water (25:75, v/v), by vortex mixing for 30 s. After centrifuging for 5 min at 23,100 g, the clear supernatant was transferred to an autosampler vial and a volume of 5 μL was injected onto the HPLC column.

Urine

A volume of 600 μL ACN was added to a 200 μL aliquot of urine. Subsequently, the sample was vortex mixed for 20 s, centrifuged for 10 s at 900 g and evaporated to dryness under nitrogen at 40 °C. The dried extract was reconstituted in 100 μL ACN-0.1% formic acid in water (25:75, v/v) by vortex mixing for 30 s, and then the sample was filtered through a 0.2 μm micro-spin filter (Alltech, Deerfield, IL, USA) by centrifuging for 10 min at 8,300 g. The filtrate was transferred to an autosampler vial and 5 μL was injected.

Faeces

Faecal samples were homogenized with water (1:3, w/v). Since CS and QC samples for faeces were prepared by adding MeOH and a working solution with a combined volume of 250 μL to 1.00 mL of faecal homogenate, 250 μL of MeOH was added to patient samples (1.00 mL faecal homogenate). Then, 50 μL IS working solution (1.0 μg/mL) and 2.00 mL ACN were added to the samples. After vortex mixing for 30 s, followed by automatic shaking at 1,250 rpm for 10 min, the samples were centrifuged for 5 min at 2,250 g. The supernatant was filtered using the same micro-spin filters as for urine and after centrifuging for 5 minutes at 10,300 g, the filtrate was transferred to an autosampler vial. The injection volume was 3 μL.

Whole blood

Whole blood samples were prepared by liquid-liquid extraction under alkaline conditions. For the same reason as described for faecal homogenates, a volume of 10 µL MeOH was added to the 200 µL whole blood aliquots of patient samples. Next, 20 µL IS working solution (100 ng/mL), 50 µL 0.5 M Na_2HPO_4 solution at pH 8 and 1.5 mL diethyl ether were added to all samples. Following vortex mixing for 30 s and centrifuging for 5 min at 900 g, the aqueous layer was snap-frozen in a dry-ice ethanol bath. The organic layer was transferred to a clean 2 mL tube and evaporated to dryness under nitrogen at 35 °C. Samples were reconstituted with 500 µL MeOH-water (50:50, v/v) by vortex mixing for 30 s. After centrifuging for 5 min at 11,300 g, 200 µL of the supernatant was transferred to an autosampler vial. The injection volume was between 7 and 20 µL to obtain a signal-to-noise ratio of at least 5 at the LLOQ.

Liquid chromatography

The HPLC system used consisted of a HP1100 binary pump, a degasser, a HP1100 autosampler and a column oven (Agilent technologies, Palo Alto, CA, USA). The assays for E7080 and metabolites in plasma, urine and faeces had a total run time of 21 min, and gradient chromatography was performed at 35 °C on a XTerra MS C18 column (50 x 2.1 mm I.D., particle size 2.5 µm; Waters, Milford, MA, USA), using 0.1% formic acid in (LiChrosolv) water as mobile phase A and 0.1% formic acid in ACN as mobile phase B. The flow rate was 0.2 mL/min and started with 100% A, which was maintained for 1.5 min. The percentage B increased slowly to reach 50% at 12 min and then quickly to reach 95% at 12.5 min, where it was kept for 1 min. Subsequently, the percentage B decreased to 0% within 0.5 min and the column was equilibrated at 100% A until 21 min.

For the E7080 in whole blood assay a Symmetry Shield RP8 column (150 x 2.1 mm I.D., particle size 3.5 µm; Waters) was used, which was preceded by a Phenomenex C8 guard column (4.0 x 2.0 mm I.D.). Mobile phase A consisted of 2 mM ammonium acetate pH 4 and ACN (60:40 v/v) and mobile phase B of 100% ACN. With the oven temperature at 40 °C and a flow rate of 0.2 mL/min, a gradient was applied from 0 to 100% B in 6.5 min, returning to 0% B in 0.75 min, where it was kept until the end of the run (12 min).

For the plasma and urine assays, the autosampler temperature was set at 10 °C and for the faeces and whole blood assays at room temperature.

Mass spectrometry

The LC eluate was directed into an API 3000 triple quadrupole mass spectrometer (MS) (AB Sciex, Foster City, CA, USA), equipped with a turbo ion spray interface, operating in positive mode and configured in multiple reaction monitoring (MRM) mode. LC-MS/MS data were acquired and processed using the software application Analyst™ version 1.2 (AB Sciex). The general MS settings and analyte specific parameters for each assay are summarized in Table 2.

Table 2: General settings and analyte specific parameters for the analysis of E7080, its metabolites M1, M2, M3 and M5 and an internal standard using an API3000 triple quadrupole MS with electrospray ionization source, operating in positive ion mode.

General settings	Plasma, urine, faeces						Whole blood	
Ion spray voltage (kV)	5.5						5.5	
Turbo gas temperature (°C)	550						450	
Turbo gas flow (L/min)	7						7	
Nebulizer gas (psi)	13						12	
Curtain gas (psi)	8						8	
Collision gas (psi)	3						2	
Analyte specific parameters	**E7080**	**M1**	**M2**	**M3**	**M5**	**IS[a]**	**E7080**	**IS**
Parent mass (m/z)	427	387	413	443	219	429	427	429
Product mass (m/z)	370	370	339	386	202	370	370	370
Declustering potential (V)	71	68	66	76	66	66	71	66
Focussing potential (V)	260	280	270	350	230	250	260	250
Entrance potential (V)	10	9	9	10	10	10	10	10
Collision energy (V)	37	37	46	38	29	37	37	37
Collision exit potential (V)	26	24	21	25	13	12	26	12
Dwell time (ms)	150	150	150	150	150	150	600	300
Typical retention time (min)	9.6	8.3	9.6	10.7	7.3	10.0	4.0	5.1

IS: internal standard. [a]Not included in the urine assay

Validation procedures

The quantitative assays for E7080 in human sodium heparinized plasma and in human urine were fully validated according to the FDA guidance [6;7] by testing linearity, accuracy and precision, specificity and selectivity, total recovery (and matrix effect for plasma), carry-over and stability under various conditions. Since partial validation is advised by the FDA guidance for change in matrix within species [7], the faeces and whole blood assay were partially validated, covering linearity, accuracy and precision and stability. Additionally, total recovery and carry-over were tested in faeces and specificity and selectivity in whole blood.

Results and discussion

Method development

Sample preparation

A quantitative assay for the analysis of E7080 only in plasma was already in use in our laboratory. Sample preparation of this assay was optimized to achieve maximum recovery of E7080, which was obtained using liquid-liquid extraction (LLE) with diethyl ether under alkaline conditions. For whole blood this LLE method was applicable, since only E7080 was aimed to be quantified. However, when this method was applied to quantify E7080 and its metabolites in the other matrices, M3 and M5 were poorly extracted from the aqueous phase, resulting in a poor sensitivity for these compounds. More generic

preparation methods were therefore required to quantify both E7080 and the metabolites, explaining why a simple protein precipitation was chosen to treat plasma samples.

For urine, the response of the analytes was compared between spiked urine samples that were either not diluted or diluted 1:1 (v/v) with ACN or diluted 1:1 (v/v) with ACN, centrifuged, transferred, evaporated and reconstituted in one out of various mixtures of water with ACN, MeOH or DMSO. As the response of the analytes in undiluted urine was up to 8 times lower than in diluted urine and even up to 10 times lower than in reconstituted urine samples, we choose the latter method for further analyses. Reconstitution in 50% ACN resulted in a higher recovery than reconstitution in 50% DMSO or 75% MeOH, but the peak shape was distorted. To minimize this solvent effect, the concentration ACN was reduced to 25% and mixed with mobile phase A and the injection volume was set at 5 μL.

A similar approach was used for preparation of faecal samples, with the exception that the aimed sensitivity of 0.02 μg/g for the metabolites was already obtained when samples were diluted with ACN without the evaporation and reconstitution step. The potential solvent effect caused by the higher concentration of organic modifier in the final extracts was circumvented by adjusting the injection volume to 3 μL.

Mass spectrometry

Mass spectrometric parameters were optimized by performing direct infusion and flow injection analysis of each analyte. In order to achieve high specificity and sensitivity, the MRM scan mode was applied to monitor for each analyte the mass transition to the product ion with the highest abundance in the product ion scan. Table 3 shows the selected transitions and the proposed corresponding fragmentation pathways.

In-source conversion related cross-analyte interference

It is known for LC-MS/MS analysis that metabolites of the target analyte can be an important source of interference. For example glucuronides and N-oxides can be converted back to the parent drug due to degradation in the ion source, thereby leading to cross-analyte interference in the transition window of the parent drug when these analytes are not chromatographically separated [8]. When reference standards of metabolites are available, like in this case, it is advisable to check for possible cross-analyte interferences caused by in-source conversion early in the method development phase. Since this type of interference can be circumvented by chromatographic separation of the analytes, early detection of it avoids having to start over the chromatography optimization after concluding from a validation run that the interference is disturbing the quantification.

Table 3: Analytes with their selected mass transitions and proposed fragmentation pathways.

Compound	Transition	Proposed fragmentation
E7080	427 → 370	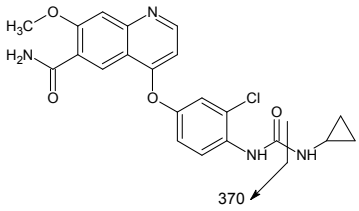
M1	387 → 370	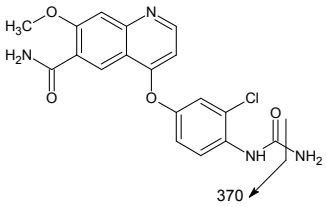
M2	413 → 339	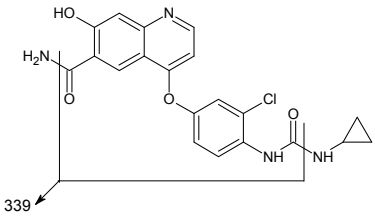
M3	434 → 386	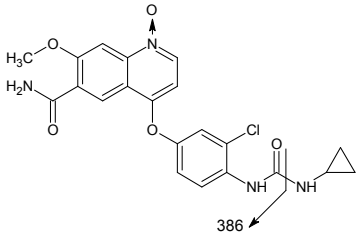
M5	219 → 202	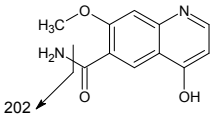
Internal standard	429 → 370	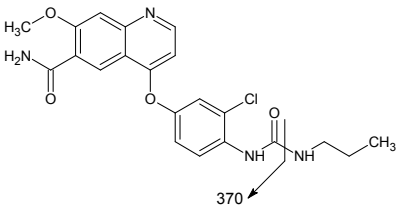

With a single experiment, which can generally be applied in the development of quantitative assays of a compound and its metabolites, we estimated the cross-analyte interference. Stock solutions of the analytes and the internal standard were diluted with 50% MeOH to 1000 ng/mL (the ULOQ for this experiment), and analysed individually, whereby the transitions of all analytes were monitored. Using the peak height of the ULOQ sample, and assuming that a linear calibration curve could describe the concentration-response relationship over a 500-fold range, the theoretical peak heights at 2 ng/mL (the LLOQ for this experiment) were calculated. For the internal standard the theoretical peak height of a concentration in-between the range (250 ng/mL) was calculated.

Table 4: A. Estimated cross-analyte interference of the injected analyte at the ULOQ relative to a 500-fold smaller LLOQ of the other transitions. The highlighted combinations (≥ 20%) require chromatographic separation. B. Resolution (Rs) of each analyte peak relative to the other peaks in the final chromatography used for the plasma, urine and faeces assay. A Rs ≥ 2 is desirable for separation.

A

Transition / Injected analyte	E7080 m/z 427 → 370	M1 m/z 387 → 370	M2 m/z 413 → 339	M3 m/z 434 → 386	M5 m/z 219 → 202	IS m/z 429 → 370
E7080	-	20%	0%	0%	68%	0%
M1	0%	-	0%	0%	75%	0%
M2	0%	0%	-	0%	0%	0%
M3	100%	0%	0%	-	0%	0%
M5	0%	0%	0%	0%	-	0%
IS	3%	28%	0%	0%	25%	-

B

Analyte / Analyte	E7080	M1	M2	M3	M5	IS
E7080	0.0	2.8	0.0	2.3	4.5	0.7
M1	2.8	0.0	2.7	5.1	1.8	3.4
M2	0.0	2.7	0.0	2.3	4.5	0.7
M3	2.3	5.1	2.3	0.0	6.8	1.6
M5	4.5	1.8	4.5	6.8	0.0	5.2
IS	0.7	3.4	0.7	1.6	5.2	0.0

Then, for all analytes, the cross interference was expressed as a percentage of the theoretical peak height at the LLOQ (Table 4A). For example, when M3 was injected at the ULOQ level, not only the transition window of M3 showed a peak, but also the transition window of E7080. The peak height of the latter was approximately equal to (so 100% of)

the theroretical peak height of the LLOQ of E7080. Since M3 is an N-oxide of E7080, this interference was expected, but also other interferences were observed. Table 4A summarizes the interference of each combination of analyte and transition. Combinations causing an interference ≥ 20% of the LLOQ are highlighted; these analytes had to be chromatographically separated in the final method.

Then, we focussed on the retention time of the injected analyte and expressed the peak heights of all other transitions as percentage of their theoretical peak height at the LLOQ. For example, when M3 was injected at the ULOQ level, at the retention time of M3, the transition used for E7080 had a peak height of 1,120 cps which was approximately equal to, so 100% of, the theoretical peak height of the LLOQ of E7080 (which was 1,122 cps). Since M3 is an N-oxide of E7080, this interference was expected, but also other interferences were observed. Table 4A summarizes the interference of each combination of analyte and transition. Combinations causing an interference ≥ 20% of the LLOQ are highlighted; these analytes had to be chromatographically separated in the final method. Apart from the described interferences, also small impurities of reference standards by other reference standards were observed.

HPLC

The cross-analyte interference experiment posed a number of requirements on the chromatography. Combined with the difference in polarity between M5 and the other analytes, a relatively long runtime was inevitable.

Various combinations of mobile phases, columns and gradients were explored. A Symmetry Shield RP8 (150 x 2.1 mm I.D., particle size 3.5 μm) and a XTerra MS C18 (50 x 2.1 mm I.D., particle size 2.5 μm) column were combined with ACN as mobile phase B, and 2 mM ammonium acetate (NH_4Ac) either at pH 4 in 40% ACN, or at pH 8 in 20% ACN or at pH 4 in 20% ACN as mobile phase A. One of the combinations (see section 2.4) separated E7080 from the IS within an acceptable runtime of 12 min. This method, of which Figure 1 shows representative MRM chromatograms, was selected for the whole blood assay. The small peak (signal to noise ratio around 2) that is present in the blank whole blood sample at the retention time of E7080 was probable due to a memory effect of the analytical column. The height of this peak remained peak remained always <20% of the LLOQ.

Neither this system, nor the other combinations could give the compound M5 retention, so the organic content of the in the eluent was lowered for the assays of the other matrices. Using the XTerra MS C18 column and starting the gradient with 100% of 0.1% formic acid in water, M5 had sufficient retention and the other analytes were separated as required. Figure 2 shows the resulting MRM chromatograms of a plasma sample spiked at the LLOQ level. To check the quality of the separation, the resolution (R_s) was calculated for each combination of peaks with the formula [9]:

$$R_S = \frac{2\left(t_{R(i)} - t_{R(j)}\right)}{W_i + W_j}$$

The retention times of peak i ($t_{R(i)}$) and j ($t_{R(j)}$) of Figure 2 were used and the baseline widths for peak i (W_i) and j (W_j) were safely set at 0.5 min. While symmetrical peaks are separated on baseline if $R_s \geq 1.5$, a $R_s \geq 2$ is desirable to allow for some tailing [9]. Table 4B shows the R_s for each combination of peaks in the final chromatography, whereby the combinations requiring separation are again highlighted. Of these combinations, only M1 and M5 have a R_s below 2. As M5, the first peak in the chromatogram, normally had a baseline width of less than 0.5 min, this resolution was acceptable.

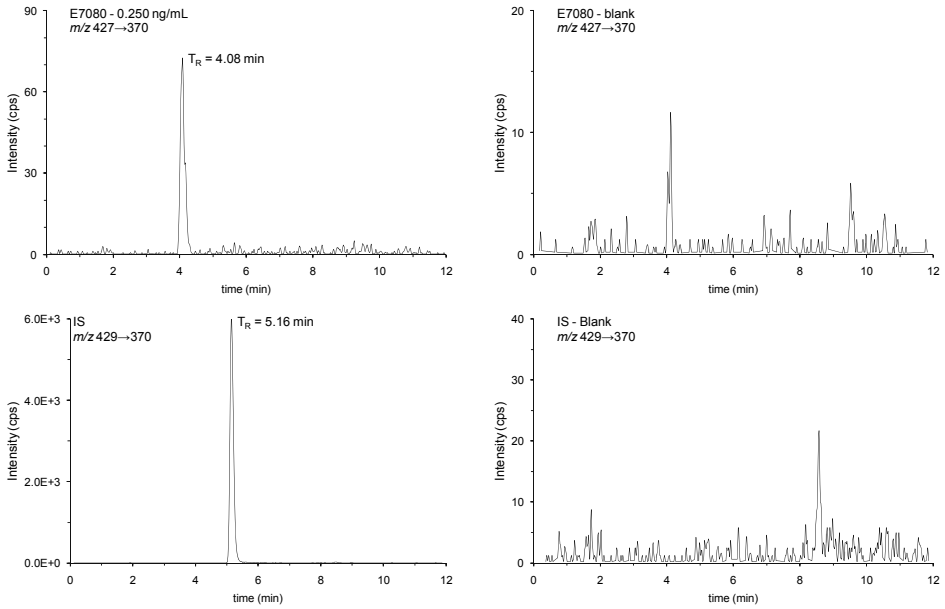

Figure 1: MRM chromatograms of E7080 and the internal standard (IS) of a QC LLOQ (left) and a blank (right) whole blood sample.

Validation procedures

Linearity

The linearity of the assays was assessed by preparing and analysing 8 (plasma, urine and whole blood) or 7 (faeces) non-zero calibration standard (CS) samples in duplicate, in four (plasma) or three (urine, whole blood and faeces) independent analytical runs.

Least-squares linear regression was applied to describe the relationship between either the peak area ratio with the internal standard ER-227326-00 (plasma, whole blood and faeces) or the absolute peak area (urine) *versus* the nominal concentration. A weighting factor of $1/x^2$ on the calibration data was chosen since it resulted in smaller differences between the

back-calculated and the nominal concentrations than a weighting factor of 1/x or no weighting factor.

It is generally agreed that stable-isotopically labelled internal standards are preferred above any other type of internal standard [10], however, these were not available for the analytes in the present study. Therefore, a structural analogue was chosen, which corrected well for all analytes in plasma, whole blood and faeces. In the urine assay, however, the IS failed to correct properly for the analyte concentrations. Therefore, the quantification in urine was based on the absolute areas of the analytes. Although not often applied, direct quantification in complex biological matrices without spiking with matched internal standards is possible, provided that the sample processing and LC-MS platform are highly reproducible [11]. The main concern that is raised when no stable-isotopically labelled IS is used, is that the quantification may disturbed by a matrix effect and that it remains unnoticed. The matrix effect was further investigated by analysis of 6 different batches of control matrix spiked at the LLOQ level (section 3.2.3) and comparison of response of diluted stock solutions and processed control samples reconstituted with diluted stock solutions (section 3.2.4).

The correlation coefficients (r^2) of the calibration curves of the analytes in all matrices were 0.994 or better. The linear range varied per analyte and per matrix but was in all cases between the corresponding concentration of the LLOQ and the highest CS sample, as depicted in Table 1.

At all concentration levels, the deviations of the back-calculated concentrations were within ± 15% of the nominal concentrations with a CV below 15%. Also five replicates of QC>ULOQ samples that were diluted 10 and 100 times in blank human plasma, urine and whole blood had deviations within ± 15% and CV values below 15%. This means that dilution integrity is demonstrated and that plasma, urine or whole blood samples can be diluted 10 and 100 times with blank control matrix, if the analyte concentration is above the ULOQ [6;7].

Accuracy and precision

To test the accuracy and precision of the assays, 5 replicates of the QC samples QC LLOQ, QC low, QC mid and QC high were analysed together with a set of CS samples in 3 (plasma and urine) or 1 (whole blood and faeces) analytical run(s). Accuracies (deviations from the nominal concentration) and precisions (CV values) were within ± 15% and below 15%, respectively, except for the intra-assay accuracy of M5 in urine at the LLOQ level, which was maximally -20.0%, and the precisions of M2 and M5 in faeces at the LLOQ level, which were maximally 16.7%. Additionally, in all matrices, the signal to noise ratio of the analytes at the LLOQ level was above 5. In conclusion, the acceptance criteria for accuracy and precision were met [6;7]. The assay performance data, comprising the intra-assay accuracy and precision and for plasma and urine also the inter-assay accuracy and precision, are summarized in Supplementary Table 1.

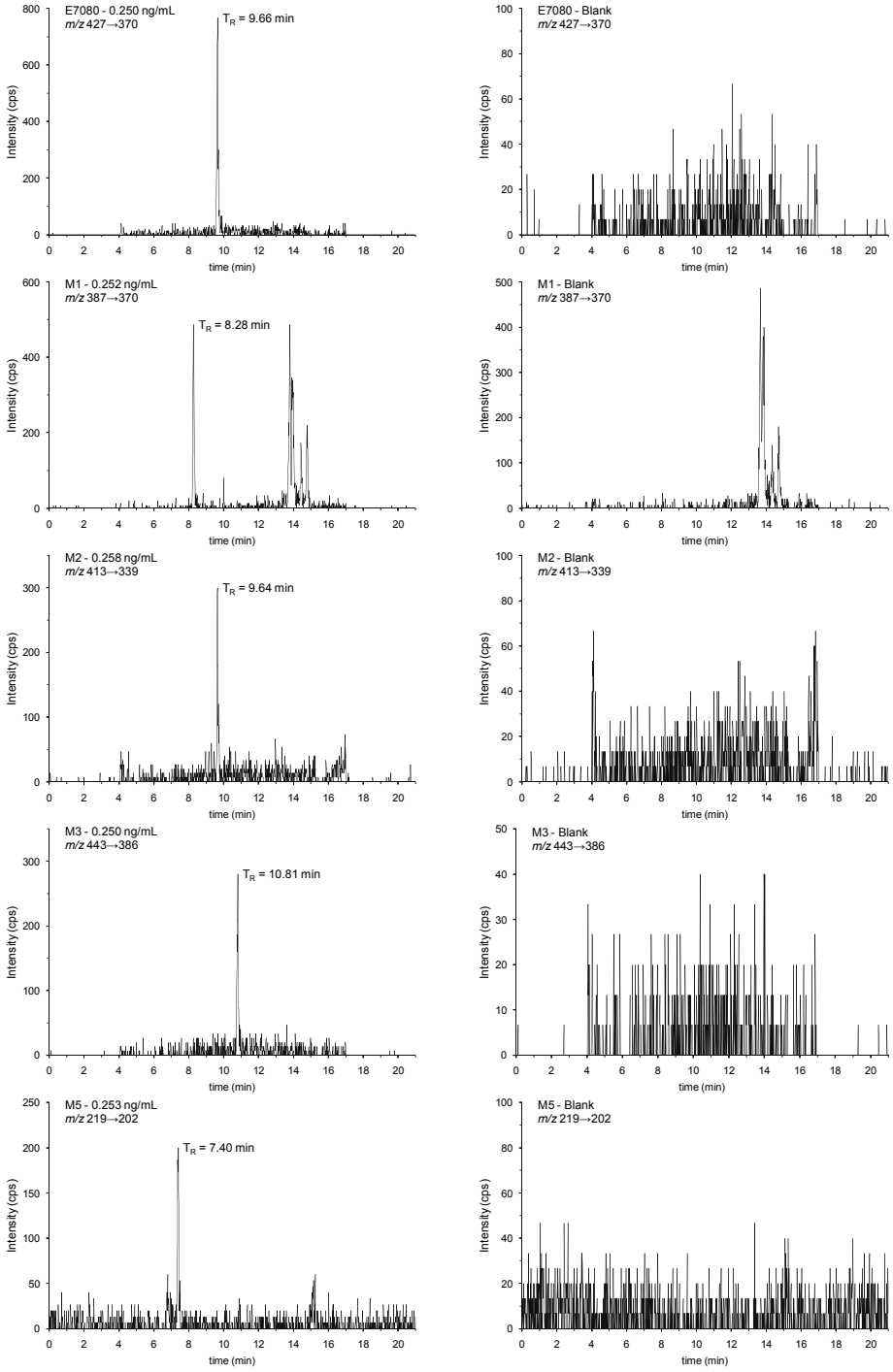

Figure 2: MRM chromatograms of E7080, its metabolites M1, M2, M3 and M5 and the internal standard (IS) of a QC LLOQ (left) and a blank (right) plasma sample.

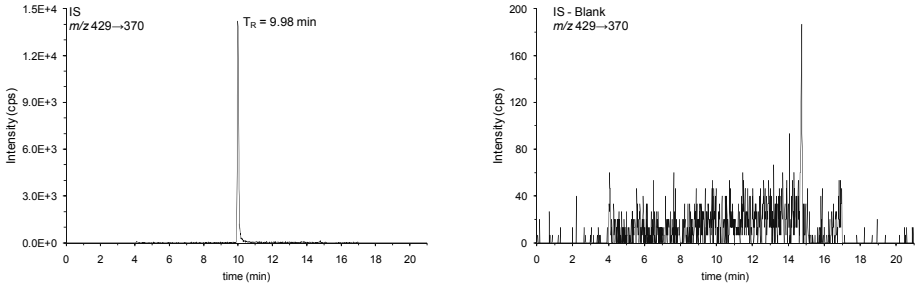

Figure 2 (continued): MRM chromatograms of E7080, its metabolites M1, M2, M3 and M5 and the internal standard (IS) of a QC LLOQ (left) and a blank (right) plasma sample.

Specificity and selectivity

The selectivity of the assays in plasma, urine and whole blood was tested by analysis of double blank samples (containing neither analyte nor internal standard) and LLOQ samples, prepared in 6 individual batches of blank control matrix.

None of the MRM chromatograms of the double blank samples showed peaks co-eluting with an analyte and with an area of >20% of the LLOQ. Furthermore, no peaks of >5% of and co-eluting with the internal standard were present in plasma and whole blood. The deviations from the 6 plasma, urine and whole blood batches spiked with all analytes at the LLOQ level ranged from -18.1 to 19.6%. Based on these results we concluded that the selectivity was sufficient, meaning that quantification of E7080 and its metabolites in plasma, urine and whole blood was not disturbed by endogenous interferences.

Cross-analyte interference was preliminary investigated with dilutions of stock solutions during the development (see section 3.1.3), and included as a validation procedure for plasma and urine, to check for degradation or conversion of analytes during sample preparation. Samples spiked with only one of the analytes at the ULOQ level produced peaks with areas of maximally 3.42% of the ULOQ of one of the other analytes. This was due to small amounts of impurities in the reference standards. As it thereby only influences the CS and QC samples and not the study samples, this was acceptable.

Total recovery and matrix effect

The total recovery, comprising both sample preparation recovery and matrix effect, was determined in triplicate at three concentration levels in plasma, urine and faeces. For the IS, only one concentration level was investigated. For plasma samples, also the matrix effect was estimated, by comparing the response of diluted stock solutions with processed blank plasma samples that were reconstituted with dilutions of the stock solution. As mentioned before, especially for the urine assay a reproducible recovery was important, as the quantification in this assay is not aided by an internal standard which can correct for variations in recovery.

In plasma, the mean total recoveries of E7080, M1, M2, M3 and M5 ranged from 43.2 to 52.8%, with standard deviation (SD) values from 1.4 to 8.0%. E7080 had the lowest recovery and SD and M3 the highest. The relatively low total recovery was mainly caused by loss during sample preparation, as the mean matrix effect ranged between -2.4 and 5.8% for all compounds. This small matrix effect is advantageous, since no stable isotope of the analytes was available to use as an internal standard and to correct for the matrix effect. The total recovery of the internal standard in plasma was 45.4%.

In urine, the total recovery of E7080 was very reproducible, with a mean of 84.6% and a SD of 2.6%. The total recoveries of the metabolites varied somewhat more, but were considered acceptable with (mean ± SD) values of 82.1 ± 7.3%, 86.9 ± 4.4%, 132 ± 7.2% and 102 ± 10% for M1, M2, M3 and M5, respectively.

In faeces, the mean total recoveries of E7080, M1, M2, M3 and M5 were 102 ± 2.1%, 94 ± 2.7%, 102 ± 3.5%, 108 ± 4.6% and 113 ± 1.5%, respectively. The low SD values indicate a good reproducibility. The total recovery of the internal standard in faeces was 104%.

A total recovery of >100%, as observed for M3 and M5 in urine and for part of the analytes in faeces, may be due to ion enhancement, or can be caused by analyte loss in the absence of matrix during analysis [10].

4

Carry-over

Carry-over was tested in plasma, urine and faeces by injecting a blank sample after an ULOQ sample. The response of the blank sample at the retention time of E7080, M1, M2, M3 and M5 was limited to <20% of the corresponding peak area in a LLOQ sample and the response of the internal standard was <2% of the normal response. Carry-over was therefore considered acceptable.

Stability

The stability of the E7080 stock solution was first tested at 2-8 °C. After 2 months, however, the deviation against a fresh solution was already -20.3%, therefore this stock solution was from then stored at -70 °C. At this condition, the solution was stable for at least 5 months. Stock solutions of the metabolites were stable for at least 10 months at -20 °C. Table 5 shows the results of the stock stability tests.

Supplementary Table 2 summarizes the stability data for E7080, M1, M2, M3 and M5 in the biological matrices. The stability experiments were executed in triplicate at the concentration levels QC low and QC high. Deviations were calculated against the initial concentrations or, in case of long-term stability in plasma, against concentrations of freshly prepared QC-samples. For long-term stability in whole blood, urine and faeces, the deviation was calculated against the nominal concentration. Analytes are considered stable in a matrix if the deviation is within ± 15%.

At -20 °C, E7080 and its metabolites were stable in plasma and faeces for 6 months, in urine for 8 months and in whole blood for 8.5 months.

Table 5: Long term stability of stock solutions of E7080 and metabolites. All experiments were performed in triplicate.

Condition	Matrix	Analyte	Nominal conc. (ng/mL)	Mean measured conc. (ng/mL)	CV (%)	Dev. (%)
-70°C, 5 m	DMSO : MeOH (15:85, v/v)	E7080	5.01E+04	4.91E+04	0.850%	-1.92%
-20°C, 10 m	DMSO : MeOH (15:85, v/v)	M1	1.01E+05	1.02E+05	0.136%	0.265%
-20°C, 10 m	DMSO : MeOH (15:85, v/v)	M2	1.04E+05	1.03E+05	1.80%	-1.00%
-20°C, 10 m	DMSO : MeOH (15:85, v/v)	M3	9.89E+04	9.80E+04	1.41%	-0.929%
-20°C, 10 m	MeOH	M5	9.97E+04	1.01E+05	0.571%	1.23%

Conc.: concentration; CV: coefficient of variation; dev.: deviation; m: months; DMSO: dimethyl sulphoxide; MeOH: methanol

Stability was demonstrated after three freeze / thaw cycles for all analytes in all matrices, except for M2 in plasma (as the QC high had a deviation of 19.4% from the initial concentration) and urine (as the QC low and QC high had a deviation of 24.7% and 18.0% from the initial concentration). Nevertheless, the deviation of M2 in plasma was accepted, because the initial concentration was unexpectedly low and the deviation of the measured concentration from the nominal concentration was only -6.7%. The same pattern was observed for M2 in urine, but as in this case both concentrations exceeded the acceptation limit, the stability of M2 after 2 freeze / thaw cycles in urine was also analysed and considered acceptable with a maximum deviation of 8.15%.

The plasma, urine and faeces spiked samples were stable for at least 6 h at room temperature, with a maximum deviation of 14.0% from the initial concentration for M5 in urine. Dried plasma and whole blood extracts were stable for at least 26 days at 2-8 °C and final plasma extracts for at least 14 days.

Reinjection reproducibility

Reinjection reproducibility was tested for all matrices by reinjecting the CS samples of the calibration curve, the QC low, QC mid, and the QC high samples in duplicate at least 24 h after the original analysis. Based on fulfilment of the acceptance criteria of linearity, accuracy and precision [6;7], analytical runs with plasma can be reinjected up to 4 days, and with whole blood and faeces up to 6 days after the start of the original run, when stored at ambient temperature. The reinjection reproducibility of analytical runs in urine was evaluated at 2-10 °C and it was demonstrated that reinjection is possible up to 13 days after the first analysis.

Clinical application

The validated assays aimed to support a human mass balance study and other clinical pharmacokinetic studies of E7080. Figure 3 provides an example of the application of one of the assays. A 23.5 mg oral dose of E7080 was administered to a cancer patient, as part of a clinical Phase I study investigating the metabolism and excretion of E7080 in patients with advanced solid tumours. The study was conducted in accordance with the International Conference on Harmonisation guidelines for Good Clinical Practice and the Declaration of Helsinki. The protocol was approved by the Netherlands Cancer Institute Independent Ethics Committee. Blood samples were collected at several time points using sodium heparinized tubes and, after centrifugation, plasma was removed and stored frozen until analysis. The plasma concentration-time curve of E7080 and its metabolites in Figure 3 shows that E7080 reached the maximum concentration one hour after intake. Furthermore, in this patient, the circulating concentrations of M2 and M5 were below 1 ng/mL and quantifiable levels of M1 and M3 were not reached.

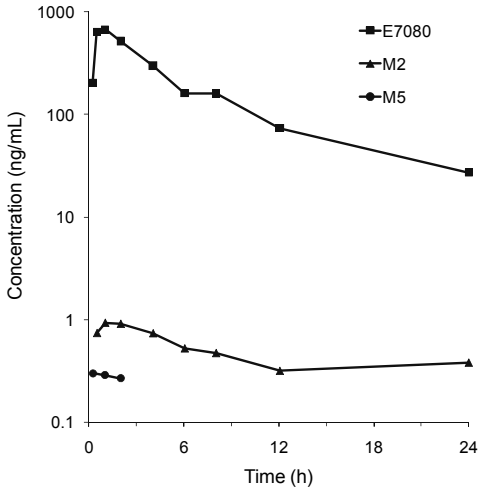

Figure 3: Concentrations of E7080 and metabolites in plasma of a cancer patient, up to 24 h after oral administration of 23.5 mg E7080.

Conclusion

Sensitive and specific LC-MS/MS assays for the quantification of E7080 in human whole blood and E7080 and four of its metabolites in human plasma, urine and faeces have been developed and validated to meet the FDA guidelines. Using 250 μL aliquots, the plasma and whole blood assays quantify a range from 0.25 ng/mL to 50.0 ng/mL (plasma) and 500 ng/mL (whole blood). In 200 μL aliquots of urine, the validated ranges of E7080, the three metabolites M1, M2 and M3, and the metabolite M5 are from 1.00 to 500 ng/mL,

from 1.00 to 200 ng/mL and from 2.50 to 200 ng/mL, respectively. E7080 in 1 mL faecal homogenate is quantifiable between 0.1 and 25 µg/g faeces, and the metabolites M1, M2, M3 and M5 between 0.02 and 5.0 µg/g faeces. These assays have been applied to support a mass balance study of E7080.

Supplementary table 1: Assay performance data for the analysis of E7080, M1, M2, M3 and M5 in human plasma, urine, faeces and whole blood

Matrix	Analyte (linear range)	Nom. conc.[a]	n	Intra-assay		Inter-assay	
				Accuracy[b] (%)	Precision[b] (%)	Accuracy (%)	Precision (%)
Plasma	E7080	0.25	3 x 5	-3.12 – -2.80	6.10 – 9.61	-3.09	7.57
	(0.25 – 50	0.751	3 x 5	1.49 – 8.58	1.26 – 3.80	4.69	3.75
	ng/mL)	5.01	3 x 5	-2.32 – 4.43	1.71 – 3.63	2.16	3.99
		37.5	3 x 5	-6.45 – -0.267	1.72 – 2.55	-2.79	3.42
	M1	0.252	3 x 5	-0.317 – 2.14	2.81 – 8.56	0.582	5.49
	(0.25 – 50	0.756	3 x 5	0.0265 – 5.03	1.63 – 4.94	3.17	4.16
	ng/mL)	5.04	3 x 5	-5.12 – 4.68	2.21 – 2.68	0.278	4.80
		37.8	3 x 5	-8.84 – -0.370	1.49 – 2.64	-4.67	4.30
	M2	0.258	3 x 5	-13.9 – 4.03	7.45 – 8.67	-5.09	10.9
	(0.25 – 50	0.774	3 x 5	1.14 – 4.94	3.83 – 6.80	3.37	5.74
	ng/mL)	5.16	3 x 5	-5.74 – 5.50	0.857 – 3.16	1.29	5.60
		38.7	3 x 5	-8.17 – 0.930	0.482 – 3.34	-2.33	4.85
	M3	0.250	3 x 5	0.240 – 13.3	3.61 – 10.7	8.69	9.73
	(0.25 – 50	0.751	3 x 5	4.10 – 9.13	5.22 – 6.97	6.14	6.18
	ng/mL)	5.00	3 x 5	0.800 – 9.48	2.55 – 3.24	5.97	4.50
		37.5	3 x 5	-2.83 – 4.11	1.85 – 2.25	1.17	3.57
	M5	0.253	3 x 5	-11.9 – 7.43	5.29 – 6.66	-1.11	10.0
	(0.25 – 50	0.758	3 x 5	-1.37 – 11.3	4.51 – 5.85	3.78	7.18
	ng/mL)	5.05	3 x 5	-3.33 – 6.46	3.31 – 3.87	3.04	5.66
		37.9	3 x 5	-7.23 – 1.53	2.14 – 4.20	-1.92	5.02
Urine	E7080	0.999	3 x 5	-14.8 – 2.24	6.51 – 9.65	-6.37	10.5
	(1 – 500	3.00	3 x 5	-13.8 – 1.53	4.26 – 6.94	-5.29	8.84
	ng/mL)	125	3 x 5	-12.6 – 3.36	1.64 – 3.07	-2.72	7.84
		375	3 x 5	-13.0 – 3.63	1.23 – 8.06	-3.08	8.68
	M1	1.00	3 x 5	-10.9 – 3.36	2.85 – 5.57	-3.35	7.55
	(1 – 200	3.01	3 x 5	-4.72 – 1.33	3.52 – 6.95	-1.66	5.70
	ng/mL)	50.4	3 x 5	-4.01 – -1.59	2.44 – 3.13	-2.87	2.73
		151	3 x 5	-6.09 – -1.59	1.88 – 6.33	-3.44	4.24
	M2	1.03	3 x 5	-4.87 – 13.2	3.60 – 13.8	2.75	11.9
	(1 – 200	3.09	3 x 5	-14.7 – 8.80	1.95 – 10.0	-2.46	11.6
	ng/mL)	51.6	3 x 5	2.17 – 10.0	1.06 – 4.96	5.66	4.34
		155	3 x 5	-11.1 – 9.03	1.23 – 7.46	-1.33	10.1
	M3	1.03	3 x 5	-3.17 – 9.71	3.96 – 5.74	2.75	7.16
	(1 – 200	3.09	3 x 5	-0.388 – 3.43	2.07 – 3.91	1.29	3.36
	ng/mL)	50.0	3 x 5	5.12 – 5.92	1.33 – 2.59	5.48	1.84
		150	3 x 5	2.13 – 5.73	0.795 – 6.49	3.51	3.94
	M5	2.54	3 x 5	-20.0 – 1.16	2.15 – 5.18	-9.29	9.23
	(2.5 – 200	7.61	3 x 5	-6.23 – 8.41	1.42 – 7.28	-1.31	6.80
	ng/mL)	50.5	3 x 5	-2.73 – 1.91	2.03 – 4.32	-2.05	5.22
		152	3 x 5	-5.53 – 11.4	1.44 – 11.3	-0.307	8.12

Conc.: concentration; n: number of replicates. [a] Concentrations are in ng/mL for plasma, whole blood and urine and in µg/g for faeces. [b]If multiple validation runs were performed, the range of accuracies and precisions was listed.

Supplementary table 1 (continued): Assay performance data for the analysis of E7080, M1, M2, M3 and M5 in human plasma, urine, faeces and whole blood

Matrix	Analyte (linear range)	Nom. conc.[a]	n	Intra-assay		Inter-assay	
				Accuracy[b] (%)	Precision[b] (%)	Accuracy (%)	Precision (%)
Faeces	E7080	0.100	5	-2.00	4.41		
	(0.1 – 25	0.250	5	-2.88	5.20		
	µg/g)	2.50	5	0.00	3.83		
		20.0	5	-0.500	2.01		
	M1	0.0202	5	-2.18	2.96		
	(0.02 – 5	0.0504	5	-4.17	6.26		
	µg/g)	0.504	5	1.31	3.91		
		4.03	5	1.74	2.66		
	M2	0.0206	5	5.63	16.7		
	(0.02 – 5	0.0516	5	-8.49	9.90		
	µg/g)	0.516	5	-3.95	3.19		
		4.13	5	-3.83	2.38		
	M3	0.0200	5	-4.20	14.6		
	(0.02 – 5	0.0500	5	-4.00	10.2		
	µg/g)	0.500	5	-0.0800	6.76		
		4.00	5	2.15	2.71		
	M5	0.0202	5	-10.5	15.8		
	(0.02 – 5	0.0505	5	-6.85	8.83		
	µg/g)	0.505	5	-3.60	5.21		
		4.04	5	-2.52	1.72		
Whole blood	E7080	0.250	5	10.8	5.20		
	(0.25 – 500	0.750	5	8.32	5.46		
	ng/mL)	10.0	5	5.00	1.90		
		375	5	0.480	1.12		

Conc.: concentration; n: number of replicates. [a] Concentrations are in ng/mL for plasma, whole blood and urine and in µg/g for faeces. [b]If multiple validation runs were performed, the range of accuracies and precisions was listed.

Supplementary table 2: Stability data for E7080 and metabolites in plasma, urine, faeces and whole blood. All experiments were performed in triplicate.

Condition	Matrix	Analyte	Nominal/initial conc.[1]	Measured conc.[a]	CV (%)	Dev. (%)
Spiked matrix 6 months						
-20 °C	Plasma	E7080	0.761	0.782	1.22	2.80
			35.6	36.1	0.320	1.50
		M1	0.696	0.676	2.74	-2.83
			33.8	32.3	1.35	-4.44
		M2	0.761	0.720	4.75	-5.47
			37.6	35.9	0.643	-4.35
		M3	0.709	0.667	2.63	-5.97
			33.8	33.0	1.77	-2.27
		M5	0.661	0.713	9.04	7.92
			31.0	29.9	1.67	-3.55
3 freeze / thaw cycles						
-20 °C	Plasma	E7080	0.794	0.785	3.83	-1.18
			36.0	36.3	5.33	0.648
		M1	0.771	0.761	3.68	-1.30
			34.6	35.0	4.39	1.25
		M2	0.711	0.718	6.15	0.937
			30.2	36.1	5.04	19.4
		M3	0.847	0.840	4.05	-0.787
			35.9	36.9	5.23	2.88
		M5	0.806	0.803	4.20	-0.372
			36.1	35.9	5.66	-0.646
Sample (preparation) 6 h						
Ambient temp.	Plasma	E7080	0.758	0.747	4.59	-1.36
			35.7	34.8	1.91	-2.52
		M1	0.767	0.741	2.38	-3.30
			34.7	33.8	1.23	-2.78
		M2	0.807	0.758	14.5	-5.99
			36.0	37.2	0.821	3.52
		M3	0.821	0.808	4.25	-1.58
			36.6	36.5	2.24	-0.182
		M5	0.765	0.699	6.49	-8.62
			35.5	34.0	0.340	-4.23
Dried extracts 26 days						
-20 °C	Plasma	E7080	0.793	0.794	4.11	0.168
			35.3	36.0	2.08	1.98
		M1	0.768	0.771	3.47	0.304
			34.3	34.6	1.50	0.973
		M2	0.788	0.711	6.43	-9.77
			35.1	30.2	1.63	-13.9
		M3	0.794	0.847	1.78	6.63
			36.3	35.9	1.43	-1.19
		M5	0.785	0.806	4.55	2.63
			35.3	36.1	0.960	2.36
Final extract 14 days						
2-8 °C	Plasma	E7080	0.758	0.737	3.33	-2.73
			35.7	34.4	1.70	-3.64
		M1	0.767	0.723	3.86	-5.70
			34.7	33.1	1.67	-4.80
		M2	0.807	0.754	12.0	-6.49
			36.0	33.5	1.53	-6.77
		M3	0.821	0.799	5.97	-2.60
			36.6	36.6	2.60	0.00
		M5	0.765	0.657	1.45	-14.2
			35.5	35.6	4.10	0.282

Conc.: concentration; CV: coefficient of variation; Dev.: deviation; h: hours; temp.: temperature. [a]Concentrations are mean values in ng/mL for plasma, whole blood and urine and in μg/g for faeces

Supplementary table 2 (continued): Stability data for E7080 and metabolites in plasma, urine, faeces and whole blood. All experiments were performed in triplicate.

Condition	Matrix	Analyte	Nominal/initial conc.[1]	Measured conc.[a]	CV (%)	Dev. (%)
Spiked matrix 8 months						
	Urine	E7080	3.00	3.10	2.82	3.44
			375	405	3.57	7.91
		M1	3.02	3.23	7.16	6.84
			151	161	4.35	6.62
		M2	3.00	2.57	12.5	-14.3
			150	154	2.99	2.89
		M3	2.90	2.48	10.6	-14.4
			145	130	1.18	-10.6
		M5	7.33	7.41	2.17	1.09
			147	153	0.377	4.31
3 freeze / thaw cycles						
-20 °C	Urine	E7080	2.94	3.35	3.67	13.8
			370	409	1.60	10.4
		M1	3.06	3.11	3.22	1.63
			164	164	3.36	0.00
		M2	2.58	3.22	8.72	24.7
			135	159	3.22	18.0
		M3	2.88	3.09	1.23	7.18
			151	146	2.09	-3.09
		M5	6.85	7.30	10.5	6.52
			173	169	7.41	-2.69
2 freeze / thaw cycles						
-20 °C	Urine	M2	2.58	2.76	1.47	6.85
			135	146	2.37	8.15
Sample (pre-treatment) 6 h						
Ambient temp.	Urine	E7080	2.94	3.19	1.44	8.38
			370	391	2.88	5.58
		M1	3.06	3.49	2.98	13.9
			164	175	5.73	6.50
		M2	3.03	3.07	2.87	1.32
			150	156	1.62	4.01
		M3	2.88	3.17	2.21	10.1
			151	156	0.371	3.09
		M5	6.85	7.81	9.97	14.0
			173	165	3.21	-4.81
Spiked matrix 6 months						
-20 °C	Faeces	E7080	0.250	0.236	2.17	-5.47
			20.0	18.7	1.12	-6.67
		M1	0.0504	0.0539	3.12	7.01
			4.03	4.20	2.39	4.14
		M2	0.0500	0.0480	8.55	-3.93
			4.00	3.87	1.44	-3.25
		M3	0.0484	0.0536	5.48	10.7
			3.87	4.17	1.18	7.67
		M5	0.0489	0.0445	4.59	-9.07
			3.91	4.08	2.09	4.26

Conc.: concentration; CV: coefficient of variation; Dev.: deviation; h: hours; temp.: temperature
[a]Concentrations are mean values in ng/mL for plasma, whole blood and urine and in µg/g for faeces

Supplementary table 2 (continued): Stability data for E7080 and metabolites in plasma, urine, faeces and whole blood. All experiments were performed in triplicate.

Condition	Matrix	Analyte	Nominal/initial conc.[1]	Measured conc.[a]	CV (%)	Dev. (%)
3 freeze / thaw cycles						
-20 °C	Faeces	E7080	0.247	0.239	1.05	-3.50
			19.8	18.5	1.43	-6.57
		M1	0.0477	0.0467	3.54	-2.17
			4.09	3.79	1.12	-7.26
		M2	0.0499	0.0425	2.92	-14.7
			4.04	3.47	3.04	-14.0
		M3	0.0475	0.0468	5.73	-1.47
			3.89	3.91	1.82	0.515
		M5	0.0442	0.0399	6.77	-9.74
			4.04	3.81	2.05	-5.69
Sample (pre-treatment) 6 h						
Ambient temp.	Faeces	E7080	0.238	0.243	2.18	2.24
			19.0	19.1	0.798	0.702
		M1	0.0467	0.0469	5.03	0.571
			3.86	3.90	1.27	0.950
		M2	0.0451	0.0464	5.94	2.96
			3.92	3.82	0.400	-2.47
		M3	0.0501	0.0512	2.88	2.20
			3.92	4.04	0.870	2.89
		M5	0.0447	0.0508	14.7	13.6
			3.66	3.75	0.616	2.46
Spiked matrix 8.5 months						
-20 °C	Whole	E7080	0.752	0.650	16.5	-13.6
	blood		376	320	2.84	-15.0
3 freeze / thaw cycles						
-20 °C	Whole	E7080	0.826	0.817	5.69	-1.09
	blood		376	387	2.91	2.83
Dried extracts 26 days						
-20 °C	Whole	E7080	0.826	0.864	14.4	4.60
	blood		376	380	1.69	1.06

Conc.: concentration; CV: coefficient of variation; Dev.: deviation; h: hours; temp.: temperature
[a]Concentrations are mean values in ng/mL for plasma, whole blood and urine and in µg/g for faeces

References

[1] Matsui J, Yamamoto Y, Funahashi Y, Tsuruoka A, Watanabe T, Wakabayashi T, Uenaka T, Asada M, E7080, a novel inhibitor that targets multiple kinases, has potent antitumor activities against stem cell factor producing human small cell lung cancer H146, based on angiogenesis inhibition, *Int.J.Cancer*, **122** (2008) 664-671.

[2] Ikuta K, Yano S, Trung VT, Hanibuchi M, Goto H, Li Q, Wang W, Yamada T, Ogino H, Kakiuchi S, Uehara H, Sekido Y, Uenaka T, Nishioka Y, Sone S, E7080, a multi-tyrosine kinase inhibitor, suppresses the progression of malignant pleural mesothelioma with different proangiogenic cytokine production profiles, *Clin.Cancer Res.*, **15** (2009) 7229-7237.

[3] Matsui J, Funahashi Y, Uenaka T, Watanabe T, Tsuruoka A, Asada M, Multi-kinase inhibitor E7080 suppresses lymph node and lung metastases of human mammary breast tumor MDA-MB-231 via inhibition of vascular endothelial growth factor-receptor (VEGF-R) 2 and VEGF-R3 kinase, *Clin.Cancer Res.*, **14** (2008) 5459-5465.

[4] Glen, H, Boss, DR, Morrison, R, Roelvink, M, Wanders, J, Mazur, A, Gupta, A, Das, A, Evans, TR, and Schellens, JH, A phase I study of E7080 in patients (pts) with advanced malignancies, *J Clin Oncol*, **26** (2008),

[5] Sherman, S, Jarzab, B, Cabanillas, M, Licitra, L, Pacini, F, Martins, R, Robinson, B, Ball, D, McCaffrey, J, Shah, M, Bodenner, D, Allison, R, Newbold, K, Elisei, R, O'Brien, J, and

Schlumberger, M, A phase II trial of the multitargeted kinase inhibitor E7080 in advanced radioiodine (RAI)-refractory differentiated thyroid cancer (DTC). *J Clin Oncol*, **29** (2011),
[6] Rosing H, Man WY, Doyle E, Bult A, Beijnen JH, Bianalytical liquid chromatographic method validation. A review of current practices and procedures, *J.Liq.Chromatogr.Relat.Technol.*, **23** (2000) 329-354.
[7] US FDA, Department of Health and Human Services, Guidance for Industry, Bioanalytical Method Validation, www.fda.gov/downloads/Drugs/GuidanceComplianceRegulatoryInformation/Guidances/ucm070107.pdf, (2001), Accessed at: 9-1-2012
[8] Peters FT, in A.Polettini (Editor), Application of LC-MS in toxicology, Pharmaceutical Press, London, 2006, p. 71.
[9] Snyder RL, Kirkland JJ, and Dolan JW, Introduction to Modern Liquid chromatography, John Wiley & Sons, Inc, Hoboken, New Jersey, 2010, p. 19.
[10] Viswanathan CT, Bansal S, Booth B, DeStefano AJ, Rose MJ, Sailstad J, Shah VP, Skelly JP, Swann PG, Weiner R, Quantitative bioanalytical methods validation and implementation: best practices for chromatographic and ligand binding assays, *Pharm.Res.*, **24** (2007) 1962-1973.
[11] Wang W, Zhou H, Lin H, Roy S, Shaler TA, Hill LR, Norton S, Kumar P, Anderle M, Becker CH, Quantification of proteins and metabolites by mass spectrometry without isotopic labeling or spiked standards, *Anal.Chem.*, **75** (2003) 4818-4826.

Chapter 4.2

Pharmacokinetics and excretion of ^{14}C-lenvatinib in patients with advanced solid tumours or lymphomas

Anne-Charlotte Dubbelman, Hilde Rosing, Alwin D.R. Huitema, Marja Mergui-Roelvink, Anubha Gupta, David Verbel, Rita Sellecchia, Jean Fan, Gary A. Thompson, Robert Shumaker, Jos H. Beijnen, Jan H.M. Schellens

Preliminary data

Abstract

Lenvatinib is an orally available multi-targeted tyrosine kinase inhibitor with anti-angiogenic and antitumour activity. To get more insight into the disposition of lenvatinib, a mass balance study was performed in patients with advanced solid tumours.

A single 24 mg (100 μCi) dose of ^{14}C-lenvatinib was administered to six patients as an oral solution, followed by collection of blood, plasma, urine and faeces for 7 to 10 days. The collected material was analyzed for total radioactivity, unchanged lenvatinib and selected metabolites. In the subsequent extension phase of the study, patients received a daily oral dose of 24 mg non-labelled lenvatinib in 28-day cycles, to assess the safety and to explore the antitumour effect of lenvatinib.

Peak plasma concentrations of lenvatinib were reached 1.6 h after administration and its terminal phase half-life was 34.5 h. Unchanged lenvatinib systemic exposure accounted for 60% of the total radioactivity in plasma. Ten days after the initial radioactive dose, the geometric mean (%CV) recovery of administered dose was 89% (10%), with 64% (11%) recovered in faeces and 25% (18%) in urine. Unchanged lenvatinib in urine and faeces accounted for 2.5% (68%) of the administered dose, indicating a major role of metabolism in the elimination of lenvatinib. Patients received a mean of 5.8 cycles of non-labelled lenvatinib-treatment. The safety profile of lenvatinib was acceptable with adverse events primarily consisting of gastrointestinal disorders. Of the six patients, best overall tumour response was a partial response in one patient and stable disease in three patients.

In conclusion, this mass balance study showed that lenvatinib is rapidly absorbed and extensively metabolized, with subsequent excretion in urine and, more predominantly, in faeces. In addition, lenvatinib showed acceptable safety and preliminary antitumour activity.

Introduction

Angiogenesis, the formation and proliferation of blood vessels, is essential for tumour progression and metastasis and is, therefore, an important target to arrest tumour growth. The onset of angiogenesis, the so-called "angiogenic switch", is a discrete step in tumour propagation and refers to an imbalance in pro-angiogenic and anti-angiogenic factors, in favour of the first [1]. Examples of pro-angiogenic factors are vascular endothelial growth factor (VEGF), fibroblast growth factor (FGF), platelet-derived growth factor (PDGF) and epidermal growth factor (EGF). Binding of these growth factors with their specific receptor tyrosine kinases on the surface of endothelial cells leads to activation of the kinases, causing a cascade of cellular signals and resulting in cellular responses such as proliferation and migration [2]. Over the last decade, several anticancer drugs, targeting various spectra of receptor tyrosine kinases, have been developed and approved. Multi-targeted tyrosine kinase inhibitors have shown notable clinical results and appear to be a very well tolerated class of drugs [3].

Lenvatinib (E7080) is an investigational orally active inhibitor of multiple receptor tyrosine kinases, including VEGF, FGF, PDGF and stem cell factor (SCF) receptors [4]. Apart from inhibiting angiogenesis by targeting endothelial cells [4-7], lenvatinib exerts a direct effect on tumour cells, by inhibiting their migration and invasion [8]. Promising antitumour effects of lenvatinib were observed in Phase I trials [9;10], leading to a number of disease-specific phase 2 and phase 3 trials with lenvatinib as a single agent or in combination with other anticancer agents.

To get more insight into the absorption, distribution, metabolism and excretion of lenvatinib in humans, a mass balance study was performed employing ^{14}C-radiolabelled lenvatinib. The primary objectives of this study were to determine the pharmacokinetics of lenvatinib and its excretion balance in patients with advanced tumours or lymphomas. To achieve this, a single dose of ^{14}C-lenvatinib was administered to patients, followed by collection of blood samples and excreta. The samples were analyzed for total radioactivity, unchanged lenvatinib and four lenvatinib metabolites (Figure 1), for which validated quantitative assays were available [11]. The secondary objectives of this study were to assess the safety of lenvatinib when given continuously as a single daily dose of 24 mg and to explore the antitumour activity of lenvatinib.

Methods

Study design

This was a Phase I, open-label, single centre (The Netherlands Cancer Institute, Amsterdam, the Netherlands) study, which enrolled six patients with advanced solid tumours or lymphomas. The study was conducted in accordance with the International Conference on Harmonisation Guidelines for Good Clinical Practice and the Declaration

of Helsinki. The protocol was approved by the Netherlands Cancer Institute Independent Ethics Committee.

The study comprised two phases: the study phase, designed to fulfil the primary objectives (determination of pharmacokinetics and excretion), and the extension phase, aimed to fulfil the secondary objectives (assessment of safety and efficacy). On day 1 of the study phase, each patient received a single administration of approximately 24 mg ^{14}C-labeled lenvatinib (approximately 100 μCi, 3.7 MBq) as an oral dosing solution. Blood, urine and faeces were collected during the subsequent 7 days, and, if necessary, collection of excreta continued on an out-patient basis until the radioactivity in urine and faeces samples was <1% of the administered radioactivity. In the extension phase, starting after collection of the last study sample, patients received a 24 mg oral dose of non-radiolabelled lenvatinib once daily in 28-day treatment cycles.

Patients

Patients aged 34 to 64 years with a histologically or cytologically confirmed advanced solid tumour or lymphoma, who were unsuitable or failed existing therapies, were enrolled in this study. Patients had an Eastern Cooperative Oncology Group (ECOG) performance status ≤ 2. Any previous treatment (including surgery and radiotherapy) was completed at least 4 weeks prior to study entry with any acute toxicity resolved. Patients were excluded if they had the following laboratory parameters: haemoglobin <9 g/dL, neutrophils <1.5 x 10^9/L, platelets <100 x 10^9/L, prothrombin time (PT) (or international normalized ratio [INR]) and partial prothrombin time (PTT) >1.5 x the upper limit of normal (ULN), serum bilirubin >1.5 x ULN, other liver parameters >3 x ULN and creatinine clearance <60 mL/min. Other exclusion criteria included brain or subdural metastases (unless completed therapy and stable signs and/or symptoms for at least 4 weeks prior to study start), meningeal carcinomatosis, marked baseline prolongation of QT/QTc interval, pregnancy and breast-feeding, proteinuria >1+ on bedside testing, history of gastrointestinal malabsorption, bleeding or thrombotic disorders or use of an anticoagulant, such as warfarin, with a therapeutic international normalized ratio, poorly controlled hypertension or hypertension at screening, previous lenvatinib therapy, and any significant disease, disorder or condition that, in the investigator's opinion, excluded the patient from the study.

Study medication

For the study phase, individual ^{14}C-lenvatinib dosing solutions were prepared by mixing non-labelled lenvatinib mesylate powder (chemical purity 98.2% Eisai Co. Ltd., Ibaraki, Japan) dissolved in 3 mM hydrochloric acid solution with a ^{14}C-lenvatinib solution (chemical and radiochemical purity ≥98.2%, GE Healthcare Life Sciences, Cardiff, United Kingdom) to a final concentration of 2 mg/mL lenvatinib as anhydrous free base with a radioactivity of around 8.3 μCi/mL. A small portion of the mixture was used to analyze the exact radioactive concentration. A volume of 12 mL containing 24 mg ^{14}C-lenvatinib (100

μCi) was orally administered to the patient from a syringe. The syringe was washed with water, which was also administered orally. The residual radioactivity in the syringe was measured after flushing it and used to calculate the actual administered dose.

In the extension phase, the daily dose of 24 mg lenvatinib was taken as 2 tablets of 10 mg and 1 tablet of 4 mg.

Total radioactivity analysis

Total radioactivity in (i) plasma (of venous blood collected pre-dose, and 15 and 30 min and 1, 2, 4, 6, 8, 12, 24, 48, 72, 96, 120, 144, and 168 h after ^{14}C-lenvatinib administration), (ii) whole blood (collected pre-dose, and 15 and 30 min and 1, 2, 4, 8, 24, 72 and 168 h after ^{14}C-lenvatinib administration), (iii) urine (collected pre-dose, over 6-h periods during the first 48 h after ^{14}C-lenvatinib administration and over 24-h periods thereafter) and (iv) faecal samples (collected per portion, pre-dose and post-dose until radioactivity was <1% of administered dose) was determined by liquid scintillation counting.

To this end, aliquots of whole blood (0.2 mL) and faecal homogenates (0.2 mL of homogenate consisting of faeces-water 1:3 w/v) were prepared as described elsewhere [12], using Solvable (Perkin Elmer), 30% hydrogen peroxide and 0.1 M EDTA or isopropanol, respectively. The resulting decolourized and dissolved blood and faeces samples were, in addition to non-processed plasma (0.2 mL) and urine (1 mL) aliquots, mixed with 10 mL liquid scintillation cocktail (Ultima Gold, Perkin Elmer, Waltham, MA, USA) and counted on a Tri-Carb 2800TR liquid scintillation counter (Perkin Elmer). The exact lower limit of quantification (LLOQ) was dependant on the radioactive concentration of the individual dosing solutions and varied therefore slightly between patients. In plasma and blood, the LLOQ was ~13 ng eq/mL, in urine ~2.5 ng eq/mL and in faeces ~50 ng eq/mL.

Quantitative bioanalysis

All samples that were analyzed for total radioactivity were additionally analyzed using validated liquid chromatography tandem mass spectrometry (LC-MS/MS) assays, described elsewhere [11]. Unchanged lenvatinib was quantified in all matrices and the lenvatinib metabolites M1, M2, M3 and M5 (of which reference standards were provided by Eisai Co. Ltd, Tsukuba, Japan) (Figure 1) were quantified in plasma, urine and faeces.

Briefly, plasma, urine and faeces samples were extracted with acetonitrile and separated on a 50 x 2.1 mm I.D. XTerra MS C18 column with gradient elution. Whole blood samples were extracted with diethyl ether and separated on a 150 x 2.1 mm I.D. Symmetry Shield RP8 column. Detection was performed in multiple reaction monitoring mode on a API3000 triple quadrupole mass spectrometer (AB Sciex, Foster City, CA, USA). The LLOQ of lenvatinib and its metabolites in plasma and of lenvatinib in whole blood was 0.25 ng/mL. In urine, the LLOQ of lenvatinib, M1, M2 and M3 was 1.0 ng/mL and the

LLOQ of M5 was 2.5 ng/mL. In faeces, the LLOQ of lenvatinib was 0.1 μg/mL and the LLOQ of M1, M2, M3 and M5 was 0.02 μg/mL.

Quality control samples were prepared and analysed together with the study samples and acceptance criteria for bioanalytical data during routine drug analysis, as described in the FDA guidelines [13], were applied.

Pharmacokinetic analysis

Individual plasma/blood concentration-time data were analyzed using non-compartmental analysis with WinNonlin™ Professional (version 5.1.1 and 5.2, Pharsight Corp, Mountain View, CA, USA). The pharmacokinetic parameters calculated for lenvatinib in plasma or blood included the following: maximum concentration (C_{max}), terminal phase half-life ($t_{½}$) area under the plasma/blood concentration time curve (AUC), renal clearance (CL_r), apparent oral clearance (CL/F) and apparent volume of distribution (V_z/F). Also the cumulative percentage of the ^{14}C-lenvatinib dose recovered in urine and/or faeces as total radioactivity, lenvatinib, M1, M2, M3 or M5 (Figure 1) was determined.

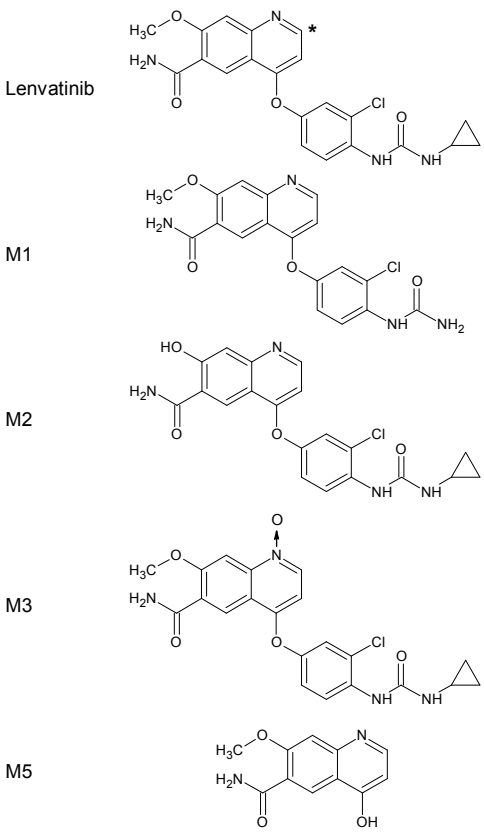

Figure 1: Chemical structure of ^{14}C-lenvatinib, with the asterisk indicating the position of the ^{14}C-label, and lenvatinib metabolites: products of decyclopropylation (M1), demethylation (M2), N-oxidation (M3) and *O*-dearylation (M5).

Safety and efficacy assessments

The safety/tolerability of lenvatinib was assessed throughout the study by evaluation of physical examinations, ECOG performance status, vital signs, clinical laboratory tests, electrocardiograms, concomitant medications, adverse events and serious adverse events. Adverse events were graded using CTCAE v3.0.

The efficacy of lenvatinib was evaluated by assessment of tumour response in accordance with Response Evaluation Criteria in Solid Tumors (RECIST). In patients evaluable according to RECIST, a best response was assigned by the investigator. Responses (complete response [CR] or partial response [PR]) and stable disease (SD) were confirmed according to RECIST.

Results

Patients

Six patients were enrolled (three male and three female), with a median age of 49 years (range 34-64), a mean weight of 95.7 kg (range 60 – 166), a mean height of 179.8 cm (range 168 – 210) and a mean body surface area of 2.17 m^2 (range 1.7 – 3.1).

Pharmacokinetics

Plasma and whole blood concentration curves of total radioactivity and lenvatinib over 168 h after administration of the ^{14}C-lenvatinib dose are presented in Figure 2. Also the plasma concentrations of M2 versus time are shown in Figure 2; the plasma concentrations of the other metabolites were below the lower limit of quantification (0.25 ng/mL). The mean lenvatinib C_{max} is approximately 88% of the C_{max} for total radioactivity (Figure 2, Table 1).

Table 1 provides a summary of the pharmacokinetic parameters. The peak concentration of total radioactivity and lenvatinib in plasma and whole blood was reached between 1.4 and 1.8 h after oral administration of the ^{14}C-lenvatinib solution. Based on $AUC_{0\text{-}24h}$, the blood concentrations of total radioactivity and lenvatinib were approximately 29% and 36%, respectively, lower than the plasma concentrations (Table 2). Based on $AUC_{0\text{-}\infty}$, unchanged lenvatinib accounted for 60% of the total radioactivity in plasma and 64% of the total radioactivity in blood.

Plasma concentrations of the metabolites M1, M2, M3 and M5 were generally below the lower limit of quantification of the assay. Only peak concentrations of M2 (n=6) and M5 (n=1) were quantifiable. All peak metabolite concentrations were over 700-fold lower than the peak plasma concentration of lenvatinib.

Based on plasma concentrations of unchanged lenvatinib, the terminal phase half-life of lenvatinib was 34.5 h, the apparent oral clearance was 6.7 L/h, the renal clearance was 0.042 L/h and the apparent volume of distribution was 336 L.

Table 1: Plasma and whole blood pharmacokinetic parameters for total radioactivity, lenvatinib and its metabolites M1, M2, M3 and M5 following a single oral dose of 24 mg (100 µCi) of ^{14}C-lenvatinib.

Parameter	TRA blood (n=6)	TRA plasma (n=6)	Lenvatinib blood (n=6)	Lenvatinib plasma (n=6)	M1 plasma (n=0)	M2 plasma (n=6)	M3 plasma (n=0)	M5 plasma (n=1)
C_{max} (ng/mL)	313.4 (39.1)	485.2 (37.1)	248.1 (45.9)	426.8 (46.6)	<LLOQ	0.6106 (23.9)	<LLOQ	0.300
t_{max} (h)	1.42 (0.95-2.12)	1.42 (0.95-2.12)	1.80 (0.95-4.02)	1.60 (0.95-2.12)	NC	1.42 (0.95-4.02)	NC	0.25
AUC_{0-24h} (µg.h/mL)[a]	2.97 (39.9)	4.20 (42.0)	1.89 (45.1)	2.93 (48.1)	NC	NC	NC	NC
AUC_{0-t} (µg.h/mL)[a]	3.54 (53.4)	5.22 (55.0)	2.21 (47.1)	3.44 (49.7)	NC	NC	NC	NC
$AUC_{0-\infty}$ (µg.h/mL)[a]	3.73[b] (60.4)	5.78 (48.2)	1.52[c] (59.0)	3.47 (50.0)	NC	NC	NC	NC
$t_{½}$ (h)	10.8[b] (32.6)	17.8 (39.4)	11.8[c] (3.95)	34.5 (25.1)	NC	NC	NC	NC
CL/F (L/h)	ND	ND	15.0[c] (65.8)	6.74 (49.5)	NC	NC	NC	NC
CL_r (L/h)	ND	ND	0.065 (114)	0.042 (140)	NC	NC	NC	NC
V_z/F (L)	ND	ND	255[c] (70.9)	336 (36.7)	NC	NC	NC	NC

Values are presented as geometric means (CV%), except for t_{max}, which is presented as geometric mean (range). TRA: total radioactivity; n: number of patients with quantifiable data; C_{max}: maximum blood/plasma concentration; t_{max}: time at which maximum blood/plasma concentration was reached; AUC_{0-24h}: area under the blood/plasma concentration-time curve from time zero to 24 h; AUC_{0-t}: area under the blood/plasma concentration-time profile from time zero to last observed quantifiable concentration; $AUC_{0-\infty}$: area under the blood/plasma concentration-time curve from time zero up to infinity; $t_{½}$: terminal exponential half-life; CL/F: oral clearance; CL_r: renal clearance; V_z/F: apparent terminal volume of distribution; LLOQ: lower limit of quantification; NC: not calculated (inadequate data to estimate parameter); ND: not determined. [a]µg eq.h/mL for total radioactivity. [b]n=4, [c]n=2 (for the other patients too few data points were above the limit of quantitation to estimate an terminal disposition rate constant, therefore these parameters could not be calculated)

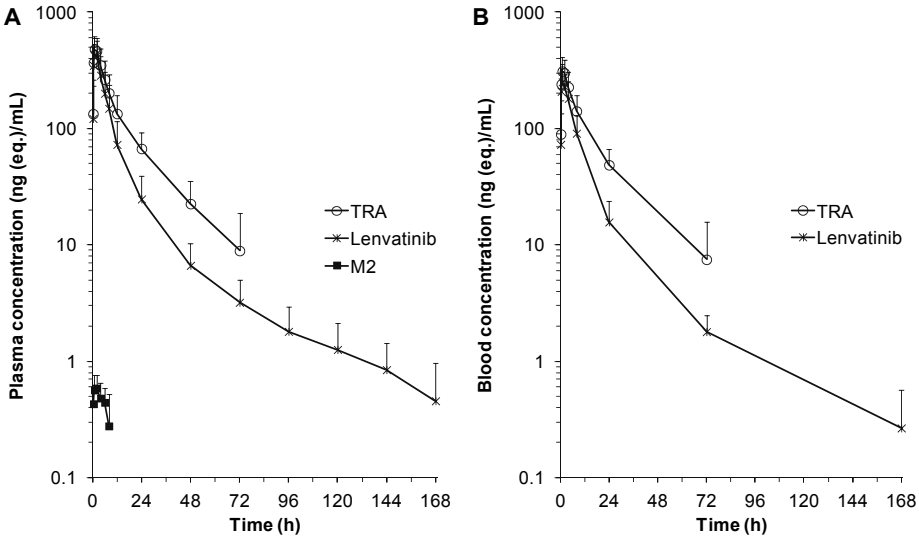

Figure 2: Mean (± standard deviation) concentration-time curves of total radioactivity (TRA), lenvatinib and M2 in plasma (A) and of TRA and lenvatinib in whole blood (B) following a single oral administration of 24 mg (100 µCi) ^{14}C-E7080.

Table 2: Blood and plasma exposure ratios of lenvatinib and total radioactivity following a single oral dose of 24 mg (100 µCi) of ^{14}C-lenvatinib (n=6).

	TRA	Lenvatinib	Blood	Plasma
$AUC_{0\text{-}24h\ blood}$ / $AUC_{0\text{-}24h\ plasma}$	0.71 (8.8)	0.64 (13.1)	NA	NA
$AUC_{lenvatinib}$ / $AUC_{total\ radioactivity}$[a]	NA	NA	0.64 (9.4)	0.60 (11.1)

Values are presented as geometric means (CV%). TRA: total radioactivity; NA: not applicable.
[a]AUC= $AUC_{0\text{-}24h}$ for blood and $AUC_{0\text{-}\infty}$ for plasma

Excretion balance

For all 6 patients, urine and faeces was collected as planned during the first 7 days after administration of ^{14}C-lenvatinib. The last urine and faecal samples that were collected in this period generally contained <1% of the administered radioactivity. For two patients the collection of faeces was continued for 1 and 3 additional days.

Figure 3A shows the mean cumulative urinary, faecal and total recovery of total radioactivity during the first 240 h after ^{14}C-lenvatinib administration. Figure 3B, C and D show the mean cumulative percentage recovery of dose as unchanged lenvatinib, M1, M2, M3, M5 and total radioactivity in urine, in faeces and in urine and faeces combined, respectively. The total recovery after 240 h was approximately 89% of the administered dose (Table 3), with approximately 64% in faeces and 25% in urine.

The recovery of unchanged lenvatinib accounted for approximately 2.5% of the administered dose and M2 for approximately 5%. The total recovery of lenvatinib, M1, M2, M3 and M5 combined comprised less than 8% of the administered dose.

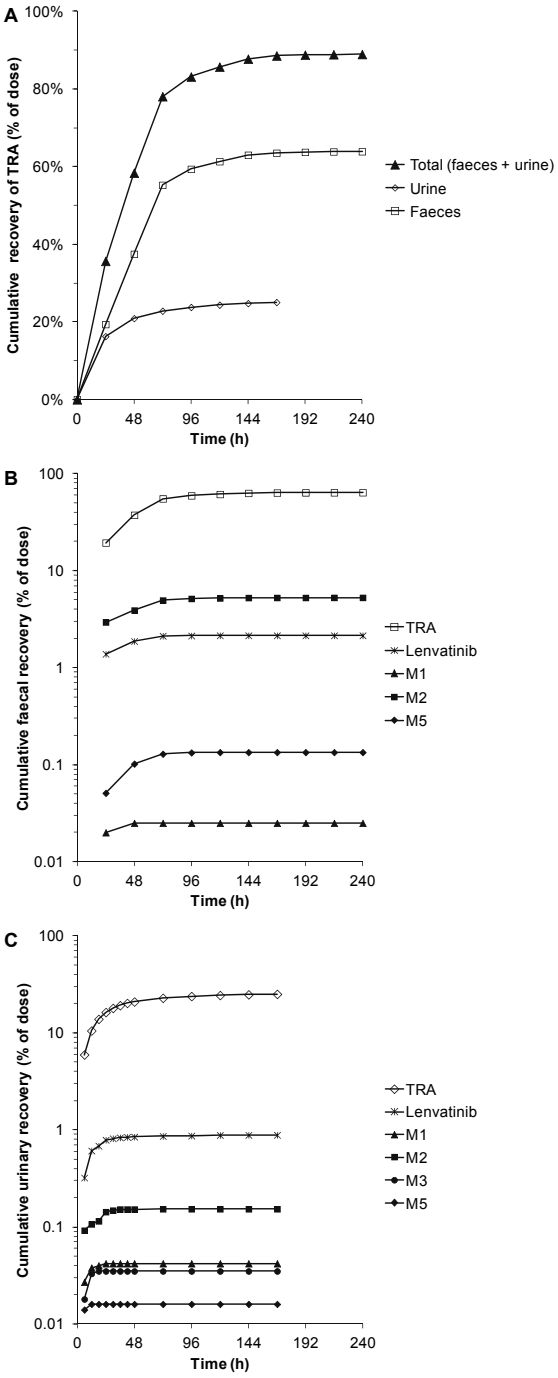

Figure 3: Mean cumulative percent of dose recovery of total radioactivity (TRA) in urine, faeces and in total (urine and faeces combined) (A), of TRA, lenvatinib, M1, M2, M3 and M5 in faeces (B) and of TRA, lenvatinib, M1, M2, M3 and M5 in urine (C), following a single oral administration of 24 mg (100 µCi) ^{14}C-lenvatinib.

Table 3: Percent dose recovery in urine, faeces and in total (urine and faeces combined), following a single oral administration of 24 mg (100 µCi) ^{14}C-lenvatinib (n=6).

	TRA	Lenvatinib	M1	M2	M3	M5
Urine	24.74 (17.76)	0.636 (95.58)	0.030 (119.2)	0.133 (60.38)	0.025 (114.5)	0.014 (195.9)
Faeces	63.56 (11.24)	1.864 (58.95)	0.025 (77.89)	4.755 (54.26)	NC	0.130 (30.77)
Total	88.55 (10.43)	2.522 (67.68)	0.056 (77.27)	4.901 (53.57)	0.025 (114.5)	0.146 (18.7)

Values are presented as geometric means (CV%) and percent dose recovery is at the end of the collection period, which is 168 h post-dose for urine and 240 h post-dose for faeces. TRA: total radioactivity; NC: not calculated, concentrations in all samples were <LLOQ

Safety and efficacy

The mean duration of lenvatinib treatment was 152.8 days (range 42 to 279 days). The mean number of cycles received was 5.83, with a range of 2 to 10. Dose reductions due to treatment emergent adverse events (TEAEs) were applied for five patients.

During the study phase, there were no serious adverse events or Grade 3 or above TEAEs. During the extension phase, five serious adverse events (other than death) were reported in two patients (33%). Grade 3 or above TEAEs were reported in 3 patients (50%). All 6 patients experienced at least one TEAE that was considered treatment-related. TEAEs considered probably related to the lenvatinib treatment were stomatitis in four patients (67%), diarrhea and dysphonia in three patients (33%), dry skin in two patients (33%), and constipation, glossodynia, nausea, oral pain, vomiting, fatigue, oral candidiasis, blood pressure increase, weight decrease, proteinuria and hypertension in one patient (17%).

Two deaths occurred in the serious adverse event follow-up period of the extension phase, a 30-day period post study drug administration. Both deaths were due to disease progression and considered unrelated to the study drug.

From start to the end of the study, no clinically important changes in mean haematology, biochemistry and urinalysis values were noticed and no clinically significant changes in mean vital signs and ECGs were observed.

The efficacy of lenvatinib treatment, in terms of best overall tumour response as assessed by the investigator, was partial response in one patient (17%) and stable disease in three patients (50%). Two patients (33%) had progressive disease.

Discussion

In this study, radiolabelled lenvatinib was used to investigate the pharmacokinetics and excretion of lenvatinib in humans. Secondary objectives were to assess the safety and to explore the antitumour effect of lenvatinib as a single daily dose of 24 mg.

The short time to peak plasma concentration (1.6 h) indicates rapid absorption of lenvatinib and is consistent with previous studies, wherein the maximum lenvatinib plasma concentrations were typically observed between 1 and 3 h post-dose [9;14]. Also the subsequent rapid decline and the final slower decline with an elimination half-life of 34.5 h is in line with previous studies [9]. Lenvatinib's rapid absorption, long terminal elimination half-life and large apparent volume of distribution (V_z/F=336 L), are similar to those of other tyrosine kinase inhibitors [3;15]. The low whole blood to plasma ratio of the $AUC_{0\text{-}24h}$ of total radioactivity (0.707) and lenvatinib (0.644), suggest that lenvatinib and lenvatinib-related products are less well distributed into red blood cells.

The half-life based on the plasma total radioactivity measurements was smaller than the half-life of lenvatinib in plasma. This can be explained by the difference in LLOQ, which was 13-14 ng eq/mL for total radioactivity measurements and 0.25 ng/mL for unchanged lenvatinib in plasma. While total radioactivity was quantifiable up to 24 – 96 h post-dose, unchanged lenvatinib could be measured up to 144 h – 168 h post-dose, allowing a more accurate determination of half-life. For a similar reason, the pharmacokinetic parameters of lenvatinib based on whole blood concentrations are likely less accurate than those obtained with plasma concentrations. Although the LLOQ of lenvatinib was the same in whole blood and plasma, the sampling for plasma was more frequent than for blood. This may partly explain the high oral and renal clearance and the low apparent terminal volume of distribution and half-life calculated based on blood concentrations as compared to the values obtained with plasma concentrations.

Metabolism is important in the elimination of lenvatinib. Unchanged lenvatinib comprised 60% of the exposure to total radioactivity in plasma, indicating the presence of other lenvatinib-related products. The lenvatinib metabolites formed by decyclopropylation (M1), demethylation (M2), N-oxidation (M3) and O-dearylation (M5), however, were only present in small quantities. Measurable plasma concentrations of these metabolites were only found for M2 and M5 and maximum concentrations were at least 700 times lower than the lenvatinib peak plasma concentration. Therefore, other lenvatinib metabolites are expected to be present in plasma. Efforts to identify and quantify these metabolites are ongoing.

The excretion of lenvatinib and its metabolites occurred mainly via the faecal route (Figure 4). lenvatinib metabolites other than the analyzed metabolites M1, M2, M3 and M5 are also expected in urine and faeces, since the recovery of lenvatinib, M1, M2, M3 and M5 in urine and faeces combined accounted for less than 8% of the administered dose. The identification of these metabolites is subject of further investigation.

Adverse events observed in this study that were considered probably treatment-related were mainly of gastrointestinal origin and were comparable with side effects observed for other tyrosine kinase inhibitors [3]. Although designed as a secondary objective, antitumour activity of lenvatinib may have been observed, since partial response was observed in one

and stable disease in three of the total six patients, as the best overall tumour response. The efficacy of lenvatinib is being further explored in Phase II and Phase III trials.

In conclusion, this study showed that lenvatinib is rapidly and well absorbed and extensively metabolized, with subsequent excretion in urine and, more predominantly, in faeces. In addition, lenvatinib showed acceptable safety and preliminary antitumour activity.

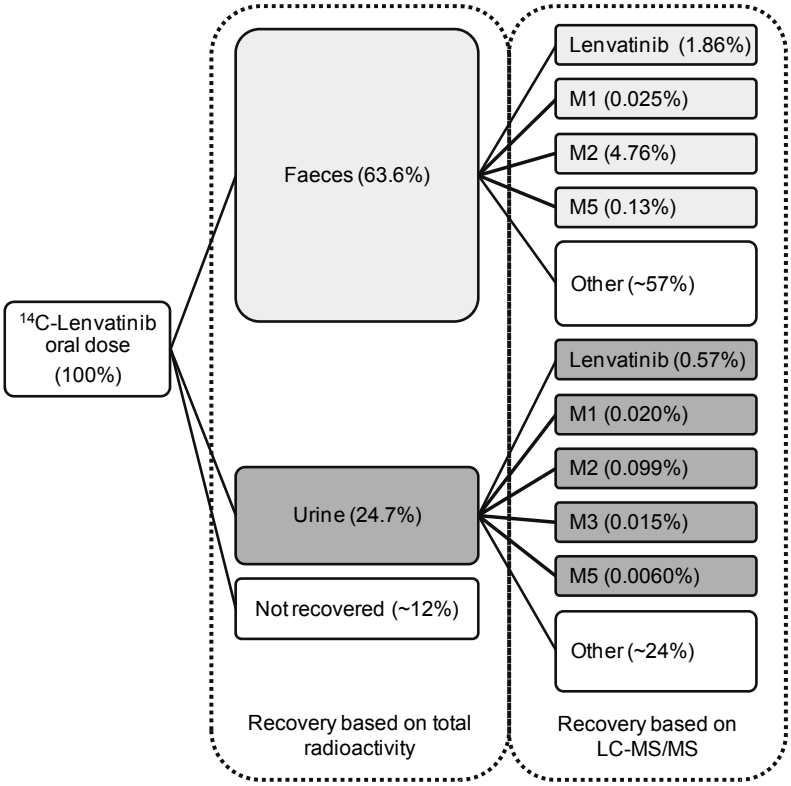

Figure 4: Overview of the average mass balance of ^{14}C-lenvatinib in 6 cancer patients following a single oral administration of 24 mg (100 µCi) ^{14}C-lenvatinib. Values are geometric means and percent dose recovery is at the end of the collection period, which is 168 h post-dose for urine and 240 h post-dose for faeces.

Acknowledgement

The authors aknowledge Abadi Gebretensae for his bioanalytical support and thank the patients that participated in this study.

References

[1] Bergers G, Benjamin LE, Tumorigenesis and the angiogenic switch, *Nat.Rev.Cancer*, **3** (2003) 401-410.

[2] Mazitschek R, Giannis A, Inhibitors of angiogenesis and cancer-related receptor tyrosine kinases, *Curr.Opin.Chem.Biol.*, **8** (2004) 432-441.

[3] Hartmann JT, Haap M, Kopp HG, Lipp HP, Tyrosine kinase inhibitors - a review on pharmacology, metabolism and side effects, *Curr.Drug Metab*, **10** (2009) 470-481.

[4] Matsui J, Yamamoto Y, Funahashi Y, Tsuruoka A, Watanabe T, Wakabayashi T, Uenaka T, Asada M, E7080, a novel inhibitor that targets multiple kinases, has potent antitumor activities against stem cell factor producing human small cell lung cancer H146, based on angiogenesis inhibition, *Int.J.Cancer*, **122** (2008) 664-671.

[5] Matsui J, Funahashi Y, Uenaka T, Watanabe T, Tsuruoka A, Asada M, Multi-kinase inhibitor E7080 suppresses lymph node and lung metastases of human mammary breast tumor MDA-MB-231 via inhibition of vascular endothelial growth factor-receptor (VEGF-R) 2 and VEGF-R3 kinase, *Clin.Cancer Res.*, **14** (2008) 5459-5465.

[6] Ikuta K, Yano S, Trung VT, Hanibuchi M, Goto H, Li Q, Wang W, Yamada T, Ogino H, Kakiuchi S, Uehara H, Sekido Y, Uenaka T, Nishioka Y, Sone S, E7080, a multi-tyrosine kinase inhibitor, suppresses the progression of malignant pleural mesothelioma with different proangiogenic cytokine production profiles, *Clin.Cancer Res.*, **15** (2009) 7229-7237.

[7] Bruheim S, Kristian A, Uenaka T, Suo Z, Tsuruoka A, Nesland JM, Fodstad O, Antitumour activity of oral E7080, a novel inhibitor of multiple tyrosine kinases, in human sarcoma xenografts, *Int.J Cancer*, **129** (2011) 742-750.

[8] Glen H, Mason S, Patel H, Macleod K, Brunton VG, E7080, a multi-targeted tyrosine kinase inhibitor suppresses tumor cell migration and invasion, *BMC.Cancer*, **11** (2011) 309.

[9] Yamada K, Yamamoto N, Yamada Y, Nokihara H, Fujiwara Y, Hirata T, Koizumi F, Nishio K, Koyama N, Tamura T, Phase I dose-escalation study and biomarker analysis of E7080 in patients with advanced solid tumors, *Clin.Cancer Res.*, **17** (2011) 2528-2537.

[10] Glen, H, Boss, DR, Morrison, R, Roelvink, M, Wanders, J, Mazur, A, Gupta, A, Das, A, Evans, TR, and Schellens, JH, A phase I study of E7080 in patients (pts) with advanced malignancies, *J Clin Oncol*, **26** (2008),

[11] Dubbelman AC, Rosing H, Thijssen B, Gebretensae A, Lucas L, Chen H, Shumaker R., Schellens JHM, Beijnen JH, Development and validation of LC-MS/MS assays for the quantification of E7080 aand metabolites in various human biological matrices, *J.Chromatogr.B Analyt.Technol.Biomed.Life Sci.*, (2012) (in press).

[12] Dubbelman AC, Rosing H, Jansen RS, Mergui-Roelvink M, Huitema AD, Koetz B, Lymboura M, Reyderman L, Lopez-Anaya A, Schellens JH, Beijnen JH, Mass Balance Study of 14C-eribulin in Patients with Advanced Solid Tumours, *Drug Metab Dispos.*, (2011).

[13] FDA, U.S. Department of Health and Human Services, Food and Drug Administration, Guidance for Industry, Bioanalytical Method Validation, http://www.fda.gov/downloads/Drugs/GuidanceComplianceRegulatoryInformation/Guidances/ucm070107.pdf, (2001), Accessed at: 14-10-2010

[14] Keizer RJ, Gupta A, Mac Gillavry MR, Jansen M, Wanders J, Beijnen JH, Schellens JH, Karlsson MO, Huitema AD, A model of hypertension and proteinuria in cancer patients treated with the anti-angiogenic drug E7080, *J.Pharmacokinet.Pharmacodyn.*, **37** (2010) 347-363.

[15] van Erp NP, Gelderblom H, Guchelaar HJ, Clinical pharmacokinetics of tyrosine kinase inhibitors, *Cancer Treat.Rev.*, **35** (2009) 692-706.

Chapter 5

Dovitinib

Chapter 5

Disposition and metabolism of ^{14}C-dovitinib (TKI258), an inhibitor of FGFR and VEGFR, after oral administration in patients with advanced solid tumours

Anne-Charlotte Dubbelman*, Alana Upthagrove*, Jos H. Beijnen, Serena Marchetti, Eugene Tan, Kimberly Krone, Suraj Anand, Jan H.M. Schellens

*These authors contributed equally

Preliminary data

Abstract

Purpose: This study investigated the metabolism and excretion of dovitinib (TKI258), a tyrosine kinase inhibitor that inhibits fibroblast, vascular endothelial, and platelet-derived growth factor receptors, in patients with advanced solid tumours.

Methods: Four patients (cohort 1) received a single 500-mg oral dose of ^{14}C-dovitinib, followed by collection of blood, urine, and faeces for ≤10 days. Radioactivity concentrations were measured by liquid scintillation counting and plasma concentrations of dovitinib by liquid chromatography–tandem mass spectrometry. Both techniques were applied for metabolite profiling and identification. A continuous-dosing extension phase (nonlabelled dovitinib 400 mg daily) was conducted with 3 patients from cohort 1 and 9 patients from cohort 2.

Results: The majority of radioactivity was recovered in faeces (52%–69%), as compared with urine (13%–21%). Only 6%–19% of the radioactivity was recovered in faeces as unchanged dovitinib, suggesting high oral absorption. ^{14}C-dovitinib was eliminated predominantly via oxidative metabolism, with prominent primary biotransformations including hydroxylation on the fluorobenzyl ring and *N*-oxidation and carbon oxidation on the methylpiperazine moiety. Dovitinib was the most prominent radioactive component in plasma. The high apparent volume of distribution (2,160 L) may indicate that dovitinib distributes extensively to tissues. Adverse events were predominantly mild to moderate and most common events included nausea, vomiting, constipation, diarrhea, and fatigue.

Conclusions: Dovitinib was well absorbed, extensively distributed, and eliminated mainly by oxidative metabolism, followed by excretion, predominantly in faeces. The adverse events were as expected for this class of drug.

Introduction

Receptor tyrosine kinases such as vascular endothelial growth factor receptor (VEGFR), fibroblast growth factor receptor (FGFR), and platelet-derived growth factor receptor play key roles in angiogenesis and tumour proliferation [1-3]. Therapies targeting VEGFR are useful, but resistance often occurs. Signaling through FGFRs may be a mechanism of tumour escape from other antiangiogenic therapies [4;5]. Therefore, inhibition of these growth factor receptor kinases could provide powerful and broad inhibition of angiogenesis and provide potent antitumour effects.

Dovitinib (TKI258) is a tyrosine kinase inhibitor with demonstrated in vitro activity against FGFRs, VEGFRs, and platelet-derived growth factor receptors. Following the demonstration of antitumour and antiangiogenic activity in preclinical models [6;7], clinical studies were undertaken and showed dovitinib to have antitumour activity in a number of cancer types [8-11]. In these and other studies, continuous daily dosing of dovitinib followed time-dependent pharmacokinetic (PK) characteristics at doses of 25–600 mg/day.

In this study, we used ^{14}C-dovitinib to characterize its metabolism and excretion pathways in patients with advanced cancer.

Methods

Trial design

This single-arm, open-label, nonrandomized, single-centre phase I study was conducted in patients ≥18 years with histologically confirmed solid tumours that were resistant or refractory to approved therapies or had no available appropriate therapies. Patients must have had World Health Organization (WHO) performance status ≤2 and had completed any previous treatments ≥4 weeks before study entry with resolution of acute toxicities. Patients were required to have the following laboratory values: absolute neutrophil count ≥1.5 × 10^9/L, platelets ≥75 × 10^9/L, haemoglobin ≥80 g/L, serum creatinine <1.5 × upper normal limit (ULN) or creatinine clearance >60 mL/min, bilirubin ≤1.5 ULN, and aspartate aminotransferase (AST) and alanine aminotransferase (ALT) ≤2.5 × ULN, except for patients with tumour involvement of the liver who needed AST and ALT ≤5 × ULN. Urinalysis must have been negative for proteinuria, or in the case of a positive dipstick reading, total urinary protein must have been ≤500 mg and measured creatinine clearance ≥50 mL/min/1.73 m^2 from a 24-hour urine collection. Exclusion criteria included clinically significant cardiac impairment or unstable ischemic heart disease within 6 months before study entry, centrally located or squamous cell carcinoma of the lung, uncontrolled infections, surgery involving intestinal anastomosis within 4 weeks before study entry, history of gastrointestinal malabsorption, and primary brain tumour or symptomatic leptomeningeal metastases.

Patients were enrolled in one of 2 cohorts. Patients in cohort 1 received a single oral dose of ^{14}C-dovitinib (500 mg, 50 μCi) in the middle of a 4-hour fasting period. Blood, urine, and faeces were collected during the subsequent 7–10 days. Following a 1-week washout period, patients in cohort 1 could participate in a continuous-dosing extension stage with nonlabelled dovitinib 400 mg administered daily in 28-day cycles until disease progression or unacceptable toxicity. Dose reductions and dose interruptions (≤21 days) were permitted for patients who were unable to tolerate the dosing schedule. Patients enrolled in cohort 2 were treated in the continuous-dosing extension stage as described above.

Study ethics

The study was conducted in accordance with International Committee on Harmonization guidelines and the Declaration of Helsinki. The study protocol and informed consent forms were approved by a properly constituted independent ethics committee, and written informed consent was obtained from each patient before study entry.

Radiolabelled study drug

^{14}C-dovitinib lactate salt was prepared by the isotope laboratory (Novartis Pharmaceuticals Corp., East Hanover, NJ). The site of radiolabel is shown in Figure 1. Chemical purity of >99% and radiochemical purity of 99.4% were confirmed by high-performance liquid chromatography (HPLC) analysis with ultraviolet and radiochemical detection, respectively.

Figure 1: Dovitinib and metabolites derived from the prominent biotransformation pathways are shown. Additional metabolites, including combinations of the modifications shown below, additional oxidations, and conjugations, were detected (not shown).

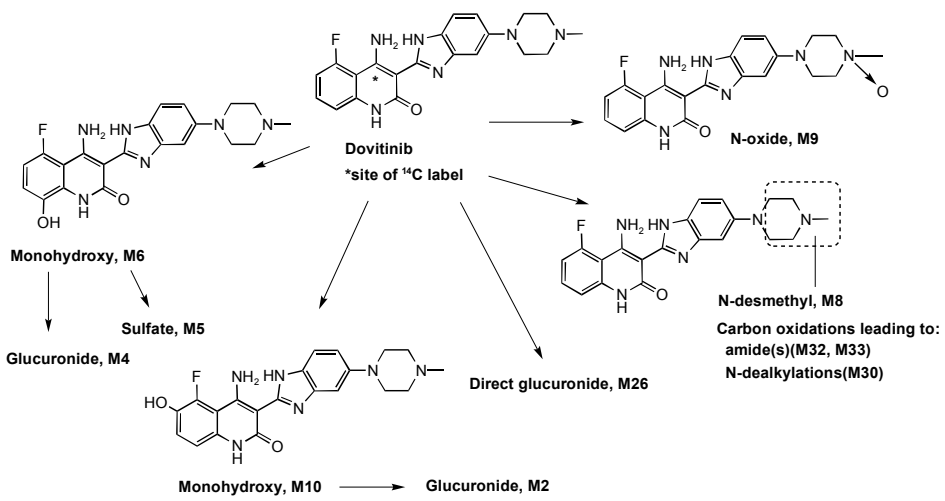

Sample collection

Blood and plasma samples were collected before dosing and at 1, 3, 5, 7, 9, 12, 24, 36, 48, 72, 96, 120, 144, and 168 h after ^{14}C-dovitinib administration. Urine and faeces samples were collected before dosing for each patient, and all excreted urine (over 6-h periods) and faeces (as individual bowel movements) were collected after dosing, ≤168 h or ≤240 hours if radioactivity recovery was <85%.

Dovitinib measurement in plasma

Plasma concentrations of dovitinib were measured by a validated liquid chromatography–tandem mass spectrometry assay. Samples were prepared by liquid–liquid extraction followed by evaporation of the extracts to dryness and analysis of the reconstituted samples. The lower limit of quantification was 1 ng/mL, using 100 μL of plasma.

Total radioactivity measurements

Total radioactivity concentrations in plasma, blood, faeces, and urine were determined by liquid scintillation counting using Ultima Gold LSC cocktail (PerkinElmer, Inc., Waltham, MA). Plasma and urine sample aliquots were combined directly with scintillation cocktail and counted, whereas blood aliquots were decolorized (1 mL of Solvable [PerkinElmer], 100 μL of 0.1 M ethylenediaminetetraacetic acid, 0.5 mL of 30% hydrogen peroxide) before counting. Fecal samples were homogenized with water and decolorized (1 mL of Solvable, 1 mL of 2-propanol, 0.4 mL of 30% hydrogen peroxide) before counting. Measured radioactivity was converted to a percent of dose recovery (urine and faeces) or concentration of dovitinib equivalents (blood and plasma).

Determination of PK parameters

PK parameters for dovitinib in plasma, and for total radioactivity in blood and plasma, were derived from blood or plasma concentration versus time data by established noncompartmental methods using WinNonlin Pro (version 5.2; Pharsight, St. Louis, MO).

Metabolite profile analysis and structural characterization

Sample preparation

Urine and fecal pools were prepared for each patient by combining equal percent by volume aliquots to include ≥90% of the total radioactivity. Pooled urine was adjusted to pH 8 and centrifuged, with the supernatants subsequently diluted and subjected to solid-phase extraction (Oasis HLB 20 cc/1g cartridges; Waters Associates, Milford, MA). Samples were eluted with methanol/1% formic acid, concentrated, and counted by liquid scintillation counting to determine recovery. Pooled fecal samples were diluted as necessary and extracted 3 times with a mixture of methanol:acetonitrile (1:1, v/v, 33% of total volume), formic acid 1%, and ammonium acetate 50 mM. Combined extracts were concentrated under nitrogen.

Two plasma pools were prepared for each patient. For the time to reach maximum concentration plasma pool, equal volumes of 3 consecutive samples with peak or near-peak concentrations of radioactivity were combined. For the area under the concentration–time curve (AUC) plasma pool, different volumes were combined, as previously described [12]. Each plasma pool was subjected to solid-phase extraction as described for urine above.

Separation and quantitative analysis of metabolites

Metabolites were separated with HPLC using an Acquity system (Waters Associates), a C18 column (150 × 4.6 mm, 4 μm; Echelon Biosciences Inc., Salt Lake City, UT), and a mobile-phase–gradient elution at a flow rate of 1 mL/min using aqueous ammonium acetate 5 mM and acetonitrile. The postcolumn flow was split by 1:20. One part was directed to a mass spectrometer for structure characterization (see below). The other 20 parts were collected into 96-Deepwell LumaPlates coated with solid scintillant (PerkinElmer). The plates were dried at 45°C with a stream of nitrogen and then counted for radioactivity in a TopCount scintillation counter (NXT; PerkinElmer). Radiochromatogram data were evaluated using Laura 4 software (version 4.0275; LabLogic, Sheffield, United Kingdom). The amounts of metabolites or parent drug in plasma or excreta were derived from the radiochromatograms by multiplying the relative peak areas by the radioactivity in the original sample.

Metabolite structure characterization

Mass spectra for metabolite structure characterization were acquired using either an LTQ-Orbitrap hybrid mass spectrometer with high resolution and accurate mass capabilities or an LTQ mass spectrometer (both Thermo Fisher Scientific Inc., Waltham, MA). Analyses were carried out using electrospray ionization in the positive ion mode. Metabolite structures were proposed based on their elemental compositions derived from the accurate mass data, their product ion mass spectra, and the comparison with available reference standards (available for dovitinib and M6). In addition, deuterium exchange experiments (performed by replacement of water with deuterated water in the HPLC mobile phase) were used to distinguish between carbon and nitrogen oxidations.

Safety assessments

Physical examinations were conducted and vital signs, WHO performance status, electrocardiogram, laboratory tests, and adverse events (AEs) were recorded throughout both portions of the study. AEs were captured as mild, moderate, or severe.

Results

Patient disposition and baseline demographics

Four patients (3 women, 1 man), with a mean age of 51 years (range, 44–60 years), mean weight of 67.6 kg (range, 45.5–78.0 kg), mean height of 171 cm (range, 169–175 cm), and mean body mass index of 23.0 kg/m^2 (range, 15.9–27.3 kg/m^2), were enrolled in cohort 1

and completed the planned analysis with radiolabelled dovitinib. The primary site of cancer was lung (n = 2), esophagus (n = 1), and other (n = 1; mix of poorly differentiated epithelial cells and mesenchymal components). Three of these patients continued in the extension phase involving daily dosing of nonlabelled dovitinib 400 mg.

An additional 9 patients (3 women, 6 men), with a mean age of 51 years (range, 24–66 years), mean weight of 90.0 kg (range, 71.0–105.0 kg), mean height of 180 cm (range, 168–194 cm), and mean body mass index of 27.8 kg/m^2 (range, 24.6–34.0 kg/m^2) enrolled in cohort 2 were also treated in this extension phase. The primary site of cancer was categorized as breast (n = 2), melanoma (n = 1), soft tissue sarcoma (n = 1), pleura (n = 1) and other (n = 4). In total, the 13 patients from cohorts 1 and 2 were all Caucasian, and all but one had a WHO performance status of 0 or 1.

PK of dovitinib and total radioactivity (cohort 1)

PK parameters were determined following administration of a single dose of ^{14}C-labelled oral dovitinib 500 mg. The PK parameters of blood and plasma radioactivity and plasma dovitinib are reported in Table 1, and the individual plasma concentration–time profiles of dovitinib for each patient are shown in Figures 2a and 2b. Peak plasma concentrations of dovitinib were reached approximately 4 h postdose. Dovitinib mean plasma exposure (AUC_{inf}) was 12,500 h·ng/mL, mean apparent clearance was 42.6 L/h, and mean apparent volume of distribution was 2,160 L. Unchanged dovitinib in plasma, as measured by AUC_{inf}, accounted for 7%–31% of the total radioactivity in plasma.

Table 1: Pharmacokinetic parameters for dovitinib in plasma and total radioactivity in blood and plasma[a]

	Plasma dovitinib[b]	Blood radioactivity	Plasma radioactivity
T_{max} (h)	4 (3–5)	7 (3–48)	6 (3–48)
C_{max} (ngEq/mL)	548 ± 142	834 ± 150	828 ± 276
$AUC_{0-24\ h}$ (h·ngEq/mL)	7,710 ± 1,730	13,600 ± 1,490	12,500 ± 1,320
AUC_{last} (h·ngEq/mL)	12,500 ± 3,330	48,800 ± 23,900	60,100 ± 28,600
AUC_{inf} (h·ngEq/mL)	12,500 ± 3,300	54,000 ± 28,300	70,500 ± 33,300
$t_{1/2}$ (h)	32.2 ± 12.0	44.9 ± 17.2	58.2 ± 7.66
CL/F (L/h)	42.6 ± 13.6		
V_z/F (L)	2,160 ± 1,560		

$AUC_{0-24\ h}$ area under the curve from time 0–24 h; AUC_{inf} AUC from time zero to infinity; AUC_{last} AUC from time zero to the last measurable concentration time sampling; CL/F clearance as a function of bioavailability; C_{max} maximum concentration; $t_{1/2}$, elimination half-life; T_{max} time to reach C_{max}; V_z/F apparent volume of distribution. [a]All values are means ± standard deviation except T_{max}, which is median (range). [b]C_{max} values are ng/mL, and AUC values are hr·ng/mL

Figure 2: After a single dose of ^{14}C-dovitinib 500 mg, concentrations of dovitinib were measured in plasma of patients in cohort 1 on a linear scale (a) and semilog scale (b) and the cumulative excretion of radioactivity in urine (c) and faeces (d)

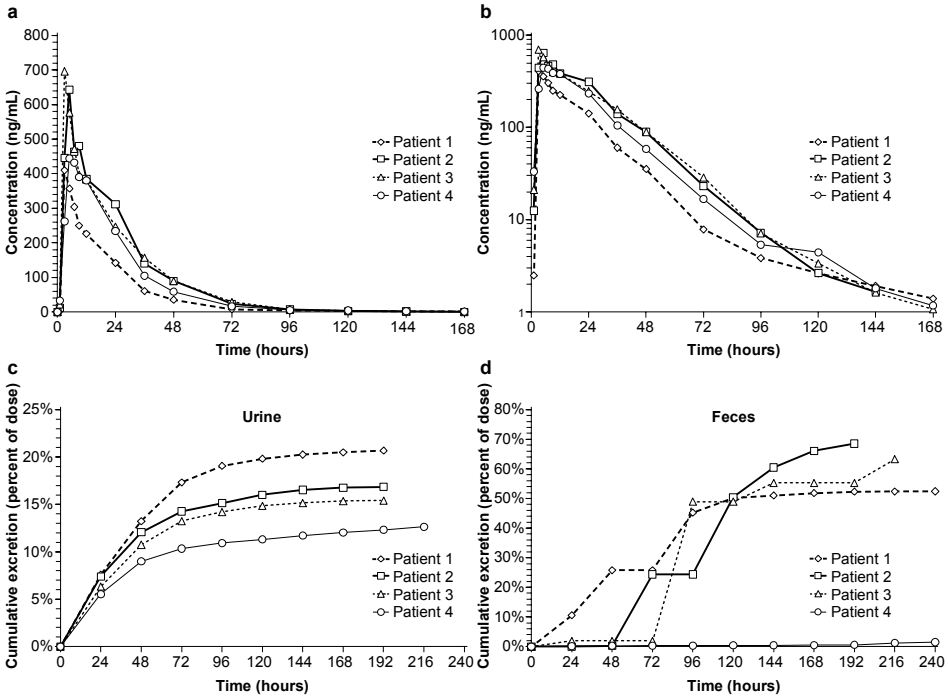

Excretion of radioactivity

The urinary and fecal excretion of radioactivity for each patient is shown in Figures 2c and 2d. The majority of the dose was excreted in faeces in 3 patients (mean recovery, 61.4% of total dose), whereas only 1.5% of the dose was recoveFred in faeces of the fourth patient. The mean recovery in urine among all 4 patients was 16.4% of the total dose. The overall excretion of radioactivity was 73%–85% of the dose for patients 1–3.

Dovitinib metabolism

A number of metabolites of dovitinib were identified in excreta or in plasma. The prominent primary biotransformations, summarized in Figure 1, included hydroxylation on the fluorobenzyl ring to form M6 and M10, *N*-oxidation on the piperazine ring to form M9, and *N*-demethylation on the piperazine ring to form M8. Direct glucuronidation of parent dovitinib occurred as well, and numerous additional metabolites, mostly resulting from combinations or further modifications of the prominent primary metabolites, were observed. HPLC retention times and mass spectral data used to characterize the prominent metabolites are summarized in Table 2. The exact structure of M6 was confirmed by comparison with a synthetic standard. The structures of M2, M4, M5, and M10 are

proposed, based on comparisons with mass spectra and relative retention times for previously reported metabolites (Novartis, data on file).

Table 2: LC-MS data for dovitinib and prominent metabolites

	Proposed biotransformation	RT (min)[a]	Molecular ion MH+ (m/z)[b]	Fragment ions (m/z)
Dovitinib		33.7	393.1834	362, 336, 308, 294
M4[c]	Glucuronide of M6	19.6	585.2104	409, 378, 352, 324
M2[c]	Glucuronide of M10	20.4	489.1351	409, 378, 352, 324
M26	Direct glucuronide	24.2	569.2155	393, 362, 336, 308
M5[c]	Sulfate of M6	24.9	425.1732	409, 378, 352, 324
M10[c]	Fluorobenzyl ring hydroxylation	25.7	409.1783	378, 352, 324, 310
M9	Piperazine *N*-oxide	27	409.1783	392, 377, 322, 309
M30	Piperazine *N*-dealkylation	29.2	367.1677	336, 310
M8	*N*-demethylation	29.7	379.1677	362, 336, 308, 294
M6[c]	Fluorobenzyl ring hydroxylation	30.9	409.1783	378, 352, 324, 310
M32	2 (+O, −2H) on piperazine	32.1	421.1419	393,336, 308, 294
M33	(+O, −2H) on piperazine	37.6	407.1626	336, 308, 294

LC/MS liquid chromatography–mass spectrometry; RT retention time. [a] Approximate high-performance liquid chromatography retention time. [b] Theoretical exact mass; measured masses were within 4 ppm of this value. [c] Exact structure of M6 proposed by comparison with a synthetic standard. Exact structures of M2, M4, M5, and M10 proposed based on comparison of mass spectra and relative retention times with previously reported metabolites.

Metabolite profiles in plasma

Unchanged dovitinib was the most prominent component in plasma (Table 3, Figures 3a and 3b). In early time point pools (3–7 h after dosing, chosen to reflect peak concentrations of dovitinib and total radioactivity), dovitinib accounted for 71%–87% of the radioactivity. The *N*-oxide M9 was the most prominent metabolite in the early time plasma pool, representing 4%–19% of the radioactivity. The *N*-desmethyl metabolite M8 and a direct glucuronide (M26) each accounted for ≤2% of the radioactivity. Additional metabolites, including glucuronides and sulfates of various oxidative metabolites, were detected in plasma, at levels too low to quantify by radioactivity. A second plasma pool, constructed to reflect the relative plasma AUCs of metabolites, was also prepared for each of the patients. Because of the low radioactivity of the AUC pools and the limited sample preparation recovery, the processed AUC plasma samples of patients 1, 2, and 4 did not have sufficient radioactivity to generate metabolite profiles. In patient 3, unchanged dovitinib and M9 were the only prominent components in the radiochromatogram (Figure 3b). Like the earlier time pooled samples, numerous additional metabolites consistent with those identified in the excreta were detected in the plasma.

Figure 3: Representative radiochromatograms for patient 3 of a plasma pool at approximately the time to reach maximum concentration (3, 5, and 7 h) (a), an AUC plasma pool (0–168 h) (b), pooled urine (0–90 h) (c), and pooled faeces (0–216 hours) (d), following a single oral 500-mg (50 μCi) dose of ^{14}C-dovitinib

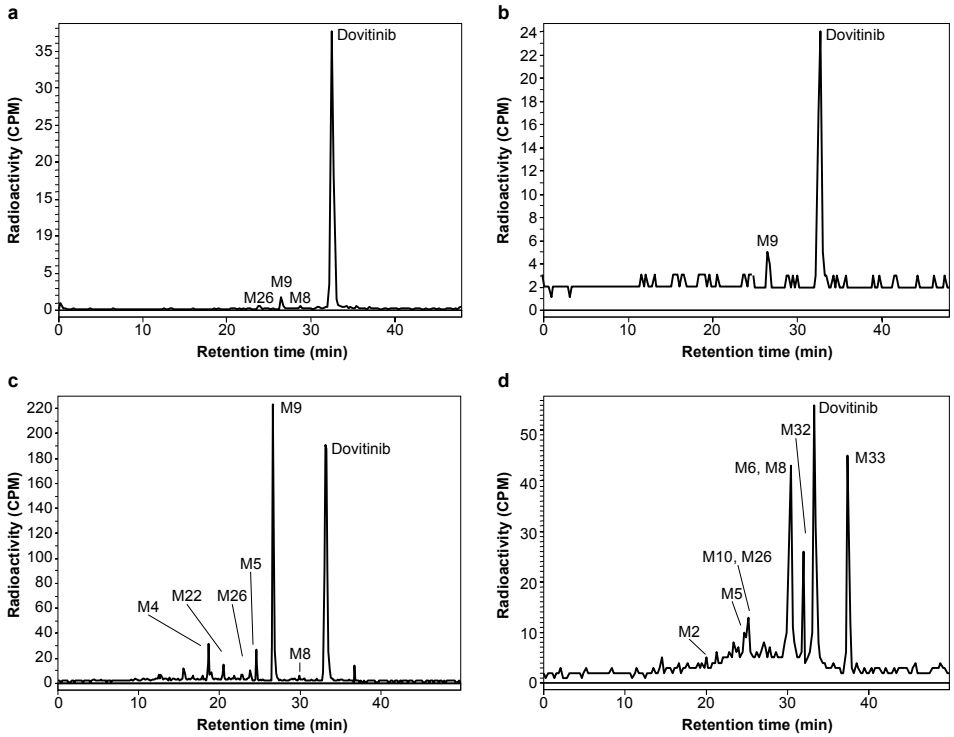

Metabolite profiles in urine and faeces

The radioactivity in urine and faeces was composed mainly of metabolites (Figures 3c and 3d). The most prominent metabolites in urine and faeces are summarized in Table 3. Unchanged dovitinib in urine accounted for only 0.6%–7% of the dose. M9 was the predominant metabolite in urine (4.5%–11% of the dose). Other metabolites including M4, M5, M6, M8, and additional secondary metabolites were detected at lower levels in urine. Unchanged dovitinib in faeces accounted for 6%–19% of the dose among the 3 patients with good faecal excretion (Table 3). M6 and M8 together were the most prominent metabolites found in faeces. Of note, although these metabolites were not resolved in the radiochromatogram, mass spectrometry results indicated that the majority of the peak was composed of M6. Other oxidative metabolites (M32 and M33) were prominent in the faeces, and additional secondary metabolites were detected at lower levels.

Table 3: Dovitinib and predominant metabolites in T_{max} plasma pools, urine, and faeces

	Plasma (ngEq/mL)				Urine (% of total dose)				Faeces[a] (% of total dose)		
Patient	1	2	3	4	1	2	3	4	1	2	3
Unchanged dovitinib	315	506	675	407	2.2	0.68	6.8	0.62	19	6.4	15
Metabolite M9	85.2	72.2	28.2	96.8	8.6	11	4.5	9.1	ND	ND	ND
Metabolite M8	7.41	≤9.63[b]	8.66	≤9.68[b]	0.39	0.04	0.08	0.10	≤8.2[c]	≤24[c]	≤13[c]
Metabolite M6	ND	ND	t	ND	0.39	0.07	0.06	0.03	≤8.2[c]	≤24[c]	≤13[c]
Metabolite M10	ND	ND	ND	ND	ND	ND	ND	ND	≤1.9[d]	≤5.0[d]	≤3.1[d]
Metabolite M26	11.1	4.82	13.1	ND	0.38	0.22	0.25	0.16	≤1.9[d]	≤5.0[d]	≤3.1[d]
Metabolite M30	ND	≤9.63[b]	ND	≤9.68[b]	ND	ND	ND	ND	ND	ND	ND
Metabolite M32	ND	ND	ND	ND	ND	ND	ND	ND	2.5	2.0	4.3
Metabolite M33	ND	ND	ND	ND	ND	ND	ND	ND	5.7	4.3	8.1
Total radioactivity recovered					20.7	16.9	15.4	12.6	52.4	68.5	63.3

ND not detected; t trace (detected by mass spectrometry but too low to quantify). [a] Metabolite profile of the faeces of patient 4 was not determined because of the limited (1.5%) recovery of radioactivity [b]Metabolites M8 and M30 were not resolved in the radiochromatogram; as such, the values represent an upper limit for each compound. [c]Metabolites M6 and M8 were not resolved in the radiochromatogram; as such, the values represent an upper limit for each compound. Of note, these metabolites were resolved with mass spectrometry detection, which indicated that M6 accounted for the majority of the peak. [d]Metabolites M10 and M26 were not resolved in the radiochromatogram; as such, the values represent an upper limit for each compound.

Safety

Most AEs were mild to moderate. Gastrointestinal disorders were the most frequent AEs, including nausea, vomiting, constipation, and diarrhea. Other common AEs included fatigue, rash, dyspnea, ALT/AST level increase. Biochemistry values that worsened during the course of the study included grade 3 AST/ALT level increases and/or grade 2 or grade 3 total bilirubin level increases in 5 of the 13 patients. No clinically significant newly occurring or worsening electrocardiogram abnormalities or relevant changes in vital signs occurred.

Two patients discontinued treatment because of AEs: one patient experienced moderate hypocalcemia, which was suspected to be related to treatment, and the second patient was reported to have severe general physical health deterioration, which was not suspected to be related to treatment. No patients died during treatment, although 2 patients died due to disease progression within 28 days after discontinuing treatment.

Discussion

This study aimed to describe the metabolism and excretion of ^{14}C-dovitinib in humans. The PK properties of ^{14}C-dovitinib were similar to those observed in previous studies using nonlabelled dovitinib [10]. Maximum plasma concentrations were reached

approximately 4 h after oral administration of the single 500-mg radiolabelled dose, and the mean elimination half-life was 32.2 h. The mean apparent oral clearance was moderate (42.6 L/h), and the mean apparent volume of distribution of ^{14}C-dovitinib was high (2,160 L), suggesting an extensive distribution outside of the plasma compartment.

Unchanged dovitinib represented 7%–31% of the total plasma radioactivity and was the most prominent drug-related component of radioactivity in plasma. A piperazine *N*-oxide (M9) was the most prominent metabolite in plasma. Additional oxidative metabolites, glucuronide and sulfate conjugates of these metabolites, and a direct glucuronide of dovitinib itself were detected in plasma.

The overall recovery of administered dose was good (73%–85%) for 3 of the 4 patients. In these patients, excretion of dovitinib and its metabolites was primarily via the faecal route: 52%–69% of the radioactive dose was recovered in faeces. However, only 1.5% of the radioactive dose was recovered from faeces of the fourth patient. This result was not likely due to an inherent difference in dovitinib disposition in this patient because urine excretion and plasma and blood levels were similar to those of the other patients. Instead, this was likely due to constipation and faecaloma, diagnosed in this patient 1 day before receiving dovitinib. Faeces collected 9–10 days after dosing contained more radioactivity than the faeces collected over the previous 8 days, suggesting that longer faeces collection in this patient may have resulted in higher recovery.

Unchanged dovitinib in faeces accounted for 6%–19% of the dose in the 3 patients with good recovery, suggesting that oral absorption was approximately ≥75% after adjustment for the overall recovery of the radioactive dose. The prominent primary biotransformations included hydroxylation on the fluorobenzyl ring, *N*-oxidation on the piperazine ring, and carbon oxidations on the methylpiperazine moiety. Direct glucuronidation of parent dovitinib was observed as well. Metabolites formed via carbon oxidations, including M6, M32, and M33, were recovered predominantly in the faeces. These metabolites may have been excreted to some extent as glucuronide and/or sulfate conjugates that were hydrolyzed in the gastrointestinal tract.

Excretion via the urinary route accounted for 13%–21% of the radioactive dose among all patients. Unchanged dovitinib excreted in urine was only 1%–7% of the dose, whereas the *N*-oxide M9 was the most prominent metabolite in the urine. Numerous other metabolites were excreted in the urine at much lower levels.

The AEs observed in this study were as expected for this class of drug [13] and comparable with the AEs reported in other clinical studies of dovitinib [10]. Additional preclinical and clinical studies are ongoing to elucidate the role of FGFR and VEGFR inhibition in cancer treatment.

In conclusion, this study showed that dovitinib was well absorbed, extensively distributed, and eliminated mainly by oxidative metabolism, followed by excretion in faeces, and to a lesser extent, in urine. AEs, mostly mild to moderate, were most frequently of gastrointestinal origin.

Acknowledgments

Supported by Novartis Pharmaceuticals Corporation. Financial support for medical editorial assistance was provided by Novartis Pharmaceuticals Corporation. We thank Peter J. Simon, PhD, and Leah Bernstein, PhD, ArticulateScience, for medical editorial assistance with this manuscript. In addition, AU and KK thank the bioanalytics group at Novartis for providing dovitinib plasma concentration data used in pharmacokinetic analysis.

Conflict of Interest

Alana Upthagrove, Eugene Tan, Kimberly Krone, and Suraj Anand are current or former employees of Novartis Pharmaceuticals Corporation.

References

[1] Dvorak HF, Rous-Whipple Award Lecture. How tumors make bad blood vessels and stroma, *Am.J.Pathol.*, **162** (2003) 1747-1757.
[2] Haugsten EM, Wiedlocha A, Olsnes S, Wesche J, Roles of fibroblast growth factor receptors in carcinogenesis, *Mol.Cancer Res.*, **8** (2010) 1439-1452.
[3] Turner N, Grose R, Fibroblast growth factor signalling: from development to cancer, *Nat.Rev.Cancer*, **10** (2010) 116-129.
[4] Fernando NT, Koch M, Rothrock C, Gollogly LK, D'Amore PA, Ryeom S, Yoon SS, Tumor escape from endogenous, extracellular matrix-associated angiogenesis inhibitors by up-regulation of multiple proangiogenic factors, *Clin.Cancer Res.*, **14** (2008) 1529-1539.
[5] Welti JC, Gourlaouen M, Powles T, Kudahetti SC, Wilson P, Berney DM, Reynolds AR, Fibroblast growth factor 2 regulates endothelial cell sensitivity to sunitinib, *Oncogene*, **30** (2011) 1183-1193.
[6] Lee SH, Lopes dM, Vora J, Harris A, Ye H, Nordahl L, Garrett E, Samara E, Aukerman SL, Gelb AB, Heise C, In vivo target modulation and biological activity of CHIR-258, a multitargeted growth factor receptor kinase inhibitor, in colon cancer models, *Clin.Cancer Res.*, **11** (2005) 3633-3641.
[7] Trudel S, Li ZH, Wei E, Wiesmann M, Chang H, Chen C, Reece D, Heise C, Stewart AK, CHIR-258, a novel, multitargeted tyrosine kinase inhibitor for the potential treatment of t(4;14) multiple myeloma, *Blood*, **105** (2005) 2941-2948.
[8] Andre, F, Bachelot, TD, Campone, M, Dalenc, F, Perez-Garcia, JM, Hurvitz, SA, Turnere, NS, Rugo, HS, Baselga, J, and Zhang, Y, A multicenter, open-label phase II trial of dovitinib, a fibroblast growth factor receptor 1 (FGFR1) inhibitor, in *FGFR1*-amplified and nonamplified metastatic breast cancer (BC), *J Clin Oncol*, **29** (2011),
[9] Angevin, E, Grünwald, V, Ravaud, A, Castellano, DE, Lin, C, Gschwend, JE, Harzstark, AL, Chang, J, Wang, Y, Shi, MM, and Escudier, BJ, A phase II study of dovitinib (TKI258) , an FGFR- and VEGFR-inhibitor, in patients with advanced or metastatic renal cell cancer (mRCC), *J Clin Oncol*, **29** (2011),

[10] Kim KB, Chesney J, Robinson D, Gardner H, Shi MM, Kirkwood JM, Phase I/II and Pharmacodynamic Study of Dovitinib (TKI258)-an Inhibitor of Fibroblast Growth Factor Receptors and VEGF Receptors-in Patients with Advanced Melanoma, *Clin.Cancer Res.*, (2011).
[11] Sarker D, Molife R, Evans TR, Hardie M, Marriott C, Butzberger-Zimmerli P, Morrison R, Fox JA, Heise C, Louie S, Aziz N, Garzon F, Michelson G, Judson IR, Jadayel D, Braendle E, de Bono JS, A phase I pharmacokinetic and pharmacodynamic study of TKI258, an oral, multitargeted receptor tyrosine kinase inhibitor in patients with advanced solid tumors, *Clin.Cancer Res.*, **14** (2008) 2075-2081.
[12] Hamilton RA, Garnett WR, Kline BJ, Determination of mean valproic acid serum level by assay of a single pooled sample, *Clin.Pharmacol.Ther.*, **29** (1981) 408-413.
[13] Hartmann JT, Haap M, Kopp HG, Lipp HP, Tyrosine kinase inhibitors - a review on pharmacology, metabolism and side effects, *Curr.Drug Metab*, **10** (2009) 470-481.

Chapter 6

Conclusions & Perspectives

Chapter 6

Conclusions & Perspectives

Conclusions & perspectives

The main theme of this thesis is the assessment of the disposition of anticancer drugs, by employing mass balance studies. We aimed to increase knowledge on the absorption, distribution, metabolism and excretion of selected anticancer drugs in humans, by providing bioanalytical support to mass balance studies of these drugs. In this chapter we discuss the main conclusions and put the results of the studies in a wider context whereby we suggest some approaches for future investigations.

Bioanalytical method development

We successfully developed LC-MS/MS assays for the quantification of bendamustine in plasma and urine and of eribulin (E7389) and lenvatinib (E7080) in plasma, whole blood, urine and faeces, to support mass balance studies with these investigational drugs. High sensitivity was important for the eribulin assays, since the recommended dose of eribulin is as low as 1.4 mg/m^2. With a lower limit of quantification of 0.2 ng/mL in plasma we succeeded to quantify eribulin up to a week after the administration of a single dose, making it possible to accurately determine its pharmacokinetic parameters. For lenvatinib as well as bendamustine it was challenging to quantify the unchanged compound as well as several of its metabolites. Since a stable isotope was not available for any of the analytes, alternative structural analogues had to be used as an internal standard for the quantification. An additional problem for bendamustine was its quick chemical degradation in aqueous environment, limiting the stability of bendamustine in urine. By dilution of urine samples in control human plasma, the stability was extended, making storage and sample handling of bendamustine feasible. The assays for both lenvatinib and bendamustine and their metabolites proved their value in the mass balance studies of these compounds, although it appeared that the selected lenvatinib metabolites were, if at all, only present in very low concentrations. This last point stresses the importance of a well-considered choice of metabolites to be included in the quantitative assay, as each additional analyte increases the complexity of the assay development and validation. Recent developments, such as high-resolution mass spectrometry and the application of mass defect filters and other data mining techniques, facilitate the detection of unknown metabolites even without a radiolabel. These techniques could be applied to an explorative analysis of metabolites in a few samples collected in the earliest clinical studies. In future drug investigations, such an analysis could be beneficial to determine a strategy for quantification of metabolites in following pharmacokinetic studies, including a mass balance study.

Mass balance studies

The mass balance study of bendamustine showed that this compound is extensively metabolised, and that the bendamustine-related products are predominantly excreted in urine as compared to faeces. The pharmacologically relevant plasma half-life of bendamustine was short and the renal excretion of unchanged bendamustine was very low.

In combination with the dosing schedule of two consecutive days in 28-day cycles, these findings suggest that patients with renal impairment are not likely to have a substantially higher exposure to bendamustine. Based on the variety of metabolic pathways, also hepatic impairment is not suspected to have a considerable effect on the exposure to bendamustine. Formal studies to the effect of renal or hepatic impairment on bendamustine exposure would however be required to confirm this. The plasma levels of two known active bendamustine metabolites, γ-hydroxybendamustine and *N*-desmethylbendamustine, were almost one and two orders of magnitude lower than bendamustine, respectively. Therefore, they are expected to have a minimal contribution to the antitumor effect and toxicity of bendamustine. In urine, we detected 25 bendamustine-related compounds. Most metabolic conversions of bendamustine occurred at the metchlorethamine moiety and were previously reported for rats. The occurrence of some less common metabolic conversions, such as conjugation of bendamustine with creatinine or with uric acid, was explained by their formation in the urine bladder. Currently, bendamustine is used for the treatment of chronic lymphocytic leukaemia and indolent B-cell non-Hodgkin's lymphoma. Additionally, it is extensively investigated as mono-therapy or as part of a combination therapy in other types of cancer.

Eribulin was, in contrast to the other investigated compounds, primarily excreted unchanged. The major part of the dose was recovered in faeces, and metabolite profiling in plasma, urine and faeces samples revealed only very minor metabolites. This was an important finding, since it suggests that the safety and efficacy of eribulin will hardly be influenced by the formation of metabolites. The results of this mass balance study were used for the registration of eribulin, which made it possible to prescribe this drug to patients with metastatic breast cancer. Additional studies will have to prove the potential efficacy of eribulin against other types of cancer.

Lenvatinib showed a rapid absorption and extensive metabolism, with subsequent excretion in urine and, more predominantly, in faeces. Unchanged lenvatinib was the most abundant lenvatinib-related compound in plasma. We are currently investigating the metabolism of lenvatinib, whereby we also directly compare the metabolites formed in human with those formed in preclinical test species. Thereby we can determine whether these test species are representative for humans in their metabolism of lenvatinib and therefore suitable to test the toxicity. At the moment, lenvatinib is investigated in clinical Phase II and Phase III trials against various types of cancer.

The fourth anticancer drug that was investigated in a mass balance study was dovitinib. Dovitinib and its metabolites were primarily excreted in faeces and oxidative metabolism was the main elimination route. A major metabolite was detected in plasma and identified as a piperazine *N*-oxide of dovitinib. Further research will be necessary to determine the pharmacological activity of this metabolite. Apart from the mass balance, also the safety profile and the preliminary efficacy of dovitinib were evaluated in an additional cohort of

patients. Most common adverse effects were gastrointestinal in nature and an unconfirmed partial response was achieved in one patient. The efficacy of dovitinib against metastatic renal cell carcinoma is currently tested in a Phase III trial and several Phase II trials investigate the efficacy of dovitinib against other types of cancer.

Value and limitations of mass balance studies

This thesis demonstrates that mass balance studies are a wealthy source of pharmacokinetic information. However, to limit the number of patients that is exposed to the radioactivity and the burden involved in a mass balance study, the number of patients in this type of studies is small; only four to six patients were included in the studies described in this thesis. Due to high inter-patient variability in drug absorption, metabolism and excretion, the patients that participated in the study may not be representative for all patients. Nevertheless, even this small group of patients can provide a clear picture of the drug disposition and form a basis for further investigations.

These investigations could for example focus on the metabolites that are identified in a mass balance study. These metabolites may possess pharmacological activity and could contribute either to the anticancer activity or the toxicity of the drug. Therefore, the assessment of the activity of metabolites would be a logical follow-up study of mass balance studies. Another follow-up investigation could identify the enzymes that are involved in the metabolism of the drug. Identification of these enzymes may help to explain differences in dose-response relationships, since enzyme activity is not a constant factor but may be increased or reduced due to for example genetic polymorphism, varying disease states or concomitantly applied drugs. Anticancer drugs often have a narrow therapeutic window. Thus a fast metabolism of the drug, compared with the populations' average, may result in under-exposure and consequently a reduced anticancer effect. In contrast, slow metabolism compared with the populations' average may result in sustained high exposure and severe toxicity. A clear example of this are the severe and potentially lethal adverse events following standard-dose capecitabine treatment of patients with a polymorphism-related deficiency of dihydropyrimidine dehydrogenase (DPD), a crucial enzyme in the (detoxifying) metabolism of capecitabine [1].

Despite the rich information they provide, mass balance studies also have their drawbacks. The use of radioactivity impacts the environment with radioactive waste and is, although small, an additional risk for the patient, the nursing staff and the laboratory personnel that handles the samples. Another major drawback of these studies is the burden that patients experience because of the collection of excreta, but even more because of the required hospitalisation period (which was at least 8 days in the presented studies). Because many anticancer drugs have a mutagenic effect, mass balance studies hereof are only performed in advanced cancer patients who might benefit from the treatment with the drug. However, these patients are often in the last stages of their lives and prefer to spend these at home instead of in a hospital.

There are some developments that counteract these disadvantages. A few mass balance studies have been performed with a radioactivity of around three orders of magnitude lower than was used in the studies described in this thesis. However, the technique to quantify these low amounts of radioactivity, accelerator mass spectrometry, is both very complex and expensive, properties that thus far hampered a wide-spread use. Recently, an interesting alternative has been proposed to perform mass balance studies of fluorine-containing compounds. Instead of using a radiolabel and determining the radioactivity, this method employed quantitative ^{19}F-NMR techniques to quantify both parent compound and all (fluorine-containing) metabolites in biological matrices [2].

The inclusion of healthy volunteers instead of advanced cancer patients in mass balance studies was possible for some targeted and non-mutagenic anticancer drugs, which have known a huge development over the last decade. For drugs that can, because of aforementioned reasons, only be tested in cancer patients, it would be valuable to investigate the necessity of a long hospitalisation. The presented studies showed that the bulk of the radioactivity was often excreted within three days after administration. A short hospitalisation period with continued collection of excreta on an outpatient basis could be considered for future mass balance studies.

Future perspectives

Future mass balance studies may benefit from the technological advances in the bioanalysis and from intensified use of computational methods. Developments in the bioanalytical field are mainly focussed on higher sensitivity and higher speed. High sensitivity is advantageous in the quantification of highly potent anticancer agents, such as eribulin, that are administered in a very low dose. Advances leading to a higher speed include the use of ultra performance liquid chromatography (UPLC) combined with small inner diameter chromatographic columns to achieve the same selectivity as with conventional high performance liquid chromatography (HPLC) within a shorter analytical runtime. Sample analysis, however, is usually not the rate-limiting step in a mass balance study. In our experience, one of the most time-consuming steps in the mass balance study was the analysis of the metabolite profiling data and the metabolite detection and identification. Data that was collected within a few hours run-time sometimes took weeks to be analysed, indicating that this part of the process is open to an increase in efficiency. A promising development in the detection of metabolites is the use of the aforementioned mass defect filters. These facilitate metabolite detection by filtering high-resolution mass data for metabolites with similar mass defects as the parent drug. Also use of knowledge-based and *in silico* prediction of metabolites may considerably reduce the amount of time required to detect and identify metabolites. Metabolite identification using mass spectrometry sometimes remains inconclusive, notwithstanding the use of high-resolution mass data and multiple fragmentation steps. For example, the exact location of a hydroxylation may not always be derived from the mass spectral data and NMR analysis may be required. Current practice in such cases is usually to isolate and purify the metabolite and subject it to static

NMR. In future, the use of hyphenated LC-NMR or even LC-MS-NMR could make it possible to eliminate the time-consuming isolation and purification steps and to acquire both mass spectrometric and NMR data for unambiguous structural elucidation in a single chromatographic run.

Conclusion

We successfully developed and validated quantitative bioanalytical assays for selected anticancer drugs in various human matrices and applied these assays in mass balance studies. Additionally, we used the collected samples to elucidate the drug's metabolites and identify the major metabolic pathways. The obtained results provided a better understanding of the pharmacokinetics of bendamustine, eribulin, lenvatinib and dovitinib.

References

[1] Deenen MJ, Tol J, Burylo AM, Doodeman VD, de Boer A, Vincent A, Guchelaar HJ, Smits PH, Beijnen JH, Punt CJ, Schellens JH, Cats A, Relationship between single nucleotide polymorphisms and haplotypes in DPYD and toxicity and efficacy of capecitabine in advanced colorectal cancer, *Clin.Cancer Res.*, **17** (2011) 3455-3468.

[2] Mutlib AE, Espina RR, Atherton J, Wang J, Talaat R, Scatina J, Chandrasekaran A, Alternate Strategies to Obtain Mass Balance without the Use of Radiolabeled Compounds: Application of Quantitative Fluorine (19F) Nuclear Magnetic Resonance (NMR) Spectroscopy in Metabolism Studies, *Chem.Res.Toxicol.*, (2012).

Summary

Cancer has affected people's lives throughout recorded history. In spite of the advances in cancer treatment that have been made over the centuries, and especially in the last decades, it is one of the most common causes of death worldwide. One of the assets in the treatment of cancer is the use of drugs. Anticancer drug development has brought us valuable products. However, before a drug is admitted to the market and available for patients, it has to survive a lengthy path of pre-clinical and clinical studies to demonstrate its efficacy and its safety. Critical information required to understand the clinical behaviour of a drug is its disposition: the absorption, distribution, metabolism and excretion. This thesis focuses on the ultimate clinical study in which these drug characteristics can be determined, which is the mass balance study. After an introductory review outlining the bioanalytical aspects of mass balance studies, it describes the results of these studies for the anticancer agents bendamustine, eribulin, lenvatinib and dovitinib, and thereby contributes to the development of these drugs.

In a typical mass balance study in oncology, a drug is mixed with a radiolabelled isotope and administered to a small group of patients. After administration, blood samples and excreta (e.g. urine and faeces) are collected and analysed for total radioactivity (unchanged drug and metabolites), unchanged drug and (unknown) metabolites. The gathered data is used to determine the pharmacokinetic parameters of the drug and to identify metabolites and major biotransfomation pathways. This is important, because biotransormations may result in the formation of active or toxic metabolites. The bioanalytical support of mass balance studies brings about some typical challenges. **Chapter 1** reviews these challenges and provides practical solutions and suggestions for the quantification in complex biological matrices: sample storage and pooling procedures, quantification of a drug with its radiolabelled isotope and the presentation of the results of a mass balance study.

The anticancer drug investigated in **Chapter 2** is the alkylating agent bendamustine. Bendamustine is a relatively old drug, being first synthesised in 1963 in Germany. Recently, the interest in this drug has revived and it has been approved by de United States Food and Drug Administration (FDA) and the European Medicines Agency (EMA) for the treatment of chronic lymphocytic leukaemia, indolent B-cell non-Hodgkin's lymphoma and multiple myeloma under certain conditions. Although the excretion and metabolism of bendamustine had been investigated in rats, the available information on the elimination of bendamustine in humans was limited. A clinical mass balance study with bendamustine was, therefore, very desired. In preparation of a mass balance study, we developed quantitative methods for bendamustine and three of its metabolites in human plasma and urine, which are described in **Chapter 2.1**. The limited stability of bendamustine in urine complicated the method development and validation. We showed that dilution of urine with plasma resulted in an improved stability of the drug. The diluted urine samples could

be prepared and analysed identically to the plasma samples, and plasma calibration standards could be used for the quantification.

The analytical methods of Chapter 2.1 are suitable to support pharmacokinetic studies with bendamustine, as demonstrated in **Chapter 2.2**. Herein, we describe the mass balance study of bendamustine. Six patients with relapsed or refractory malignancies were enrolled in this study and received a dose of 120 mg/m^2, 80-95 μCi ^{14}C-bendamustine. Up to three weeks later about half of this radioactivity was recovered in urine and about a quarter in faeces. The pharmacologically relevant half-life of bendamustine was short (0.65 h) and less than 5% of the administered dose was recovered in urine as unchanged bendamustine and two known active metabolites, suggesting a limited impact of renal impairment on the exposure of bendamustine.

The large difference between total radioactivity (49%) and unchanged bendamustine plus analysed metabolites (9.0%) recovered in urine rationalised additional investigation of urine for bendamustine metabolites. In **Chapter 2.3**, we report the detection and tentative identification of 25 bendamustine-related compounds in patient urine samples. Important biotransformation routes were hydrolysis, oxidation and conjugation with, among others, cysteine. These metabolic reactions are similar to those previously identified in rats.

In **Chapter 3** we focus on eribulin, a synthetic analogue of a marine sponge product that exerts its anticancer activity by inhibiting microtubule dynamics and thereby blocking cellular division. In 2010 and 2011, the FDA and EMA, respectively, granted approval for eribulin as a third-line treatment for patients with metastatic breast cancer. To investigate the distribution, metabolism and excretion of this compound, we developed LC-MS/MS methods for the quantification of eribulin in human plasma, urine, whole blood and faeces. The high potency of eribulin results in the use of low doses and the necessity of highly sensitive methods, which are reported in **Chapter 3.1**.

The practical applicability of these methods is demonstrated in **Chapter 3.2**, which provides the results of a mass balance study wherein the disposition of ^{14}C-eribulin was investigated in six patients with advanced solid tumours. The pharmacokinetic parameters of unchanged eribulin and total radioactivity were very similar, suggesting that the contribution of metabolism to the elimination of eribulin is minimal. This was confirmed by the metabolite profile, which revealed only minor eribulin metabolites in plasma, urine and faeces. The majority of the eribulin dose was excreted unchanged in faeces. The results of this mass balance study support the recommendation to use eribulin at a lower dose in patients with reduced liver function (it is recommended to reduce the standard dose of 1.4 mg/m^2 to 1.1 mg/m^2 in patients with mild hepatic impairment and 0.7 mg/m^2 in patients with moderate hepatic impairment [1]). They also help to explain that modulation of the activity of metabolizing CYP enzymes by co-medication has no effect on the exposure to eribulin.

The routes of elimination of eribulin are in high contrast with those of lenvatinib, the tyrosine kinase inhibitor that is the subject of **Chapter 4**. Lenvatinib is an investigational oral drug that inhibits multiple receptor tyrosine kinases, causing an inhibition of the formation and proliferation of blood vessels, which are required for tumour growth. Also for this compound we developed a set of accurate and precise bioanalytical assays for quantification in plasma, urine, whole blood and faeces. In addition, four metabolites of lenvatinib were included in the assays. The method development and validation are described in **Chapter 4.1**.

The mass balance study of lenvatinib, described in **Chapter 4.2**, showed that lenvatinib is extensively metabolised. Seven to ten days after administration of ^{14}C-lenvatinib to six patients with advanced cancer, the mean recovery of the dose in urine and faeces was 89%, while only 2.5% of the dose was recovered as unchanged lenvatinib. The metabolites that were included in the bioanalytical assays described in Chapter 4.1 turned out to be minor, indicating the presence of additional lenvatinib metabolites. The structural identity, pharmaceutical or toxicological activity and the contribution of these metabolites to the total exposure to lenvatinib-related products are subjects for future research.

In **Chapter 5**, another tyrosine kinase inhibitor is investigated: the oral drug dovitinib, which is built up of a benzimidazole, quinoline and piperazine moiety. This compound inhibits multiple tyrosine kinase receptors leading to inhibited angiogenesis and tumour proliferation. Currently, dovitinib is tested in Phase II and Phase III trials against various types of cancer. To obtain a better knowledge of the pharmacokinetics of dovitinib, we performed a mass balance study with ^{14}C-dovitinib in four patients with advanced solid tumours. In addition, the safety and preliminary efficacy of dovitinib were evaluated in a second cohort of 9 patients. Plasma concentrations of dovitinib showed that the compound is rapidly absorbed. Unchanged dovitinib was the most prominent dovitinib-related compound in plasma, followed by M9, a product of N-oxidation at the piperazine ring. Dovitinib was mainly eliminated via oxidative metabolism followed by excretion in faeces, wherein 52-69% of the radioactivity was recovered, as opposed to 13-21% in urine. Various other metabolites were identified, including products of hydroxylation, demethylation and glucuronidation. The adverse events were predominantly of gastrointestinal origin and were as expected for this type of drug.

In conclusion, we developed quantitative bioanalytical methods for selected anticancer drugs and successfully applied these in mass balance studies, to extensively investigate their pharmacokinetics. This thesis demonstrates the value of mass balance studies and provides a better understanding of the disposition of bendamustine, eribulin, lenvatinib and dovitinib. With this information we hope to optimize the therapeutic use of these agents in patients with cancer.

References

[1] Devriese, L, Witteveen, P, Voest, E, Overkleeft, EN, Langenberg, M, Beijnen, JH, Reyderman, L, Wanders, J, Mould, DR, Gupta, A, Hussein, Z, and Schellens, JHM, Eribulin dosing in patients with advanced solid tumors and hepatic impairment, *J Clin Oncol 29: 2011 (suppl abstr 2544)*, (2011).

Samenvatting

Door de geschiedenis heen heeft kanker het leven van mensen beïnvloed. Ondanks de vorderingen in de behandeling van kanker die gedurende de eeuwen, en met name in de laatste decennia, zijn gemaakt, is het op de dag van vandaag wereldwijd een van de meest voorkomende doodsoorzaken. Een van de mogelijkheden in de behandeling van kanker is het gebruik van medicijnen. De ontwikkeling van antikankermiddelen heeft waardevolle producten opgeleverd. Echter, voordat een middel wordt toegelaten op de markt en beschikbaar is voor patiënten moet het een lange weg van pre-klinisch en klinisch onderzoek doorlopen om de effectiviteit en veiligheid aan te tonen. Uiterst belangrijke informatie die nodig is om het gedrag van een middel in de kliniek te begrijpen is de dispositie: de absorptie, distributie, het metabolisme en de excretie. Dit proefschrift richt zich op de ultieme klinische studie waarin deze karakteristieken van een middel bepaald kunnen worden: de massabalansstudie. Na een inleidend overzicht over de bioanalytische aspecten van massabalansstudies beschrijft het proefschrift de resultaten van deze studies voor de antikankermiddelen bendamustine, eribuline, lenvatinib en dovitinib en draagt daarbij bij aan de ontwikkeling van deze middelen.

Bij een massabalansstudie in de oncologie wordt een geneesmiddel gemengd met een radioactieve isotoop en toegediend aan een kleine groep patiënten. Na de toediening worden bloedmonsters en excreta (bijvoorbeeld urine en faeces) verzameld. Vervolgens wordt hierin de totale radioactiviteit (onveranderde middel plus metabolieten), het onveranderde middel en de (onbekende) metabolieten gemeten. De verzamelde gegevens worden gebruikt om de farmacokinetische parameters van het middel te bepalen en om de metabolieten en de belangrijkste biotransformatie routes te identificeren. Dit is belangrijk omdat biotransformaties kunnen resulteren in de vorming van actieve of toxische metabolieten. De bioanalytische ondersteuning van massabalansstudies brengt nogal bijzondere uitdagingen met zich mee. **Hoofdstuk 1** bespreekt deze uitdagingen en biedt praktische oplossingen en suggesties voor de kwantificering in complex biologisch materiaal: procedures voor opslag en samenvoegen van monsters, kwantificering van geneesmiddelen met hun radioactief gelabelde isotoop en de presentatie van resultaten.

Het antikankermiddel dat onderzocht wordt in **Hoofdstuk 2** is de alkylerende stof bendamustine. Bendamustine is een relatief oud geneesmiddel, dat voor het eerst in 1963 in Duitsland gesynthetiseerd is. De laatste tijd is er een hernieuwde interesse in dit middel en onlangs is het goedgekeurd door de FDA en de EMA voor de behandeling van bepaalde vormen van chronische lymfatische leukemie, indolente non-Hodgkin lymfomen en multiple myelomen. Hoewel de excretie en het metabolisme van bendamustine in ratten is onderzocht, was de beschikbare informatie over de eliminatie van bendamustine bij mensen beperkt. Een klinische massabalansstudie zou hier verandering in kunnen brengen. Ter voorbereiding op een massabalansstudie hebben we kwantitatieve methoden ontwikkeld voor bendamustine en drie metabolieten van bendamustine in humaan plasma

en urine (**Hoofdstuk 2.1**). De beperkte houdbaarheid van bendamustine in urine was een moeilijkheid bij de methodeontwikkeling en -validatie. We toonden aan dat verdunnen van urine met plasma in een afname van de chemische degradatie resulteerde. Dit had als bijkomend voordeel dat de verdunde urinemonsters op identieke wijze als plasmamonsters konden worden opgewerkt en geanalyseerd, gebruik makend van calibratiestandaarden in plasma.

De analytische methoden van Hoofdstuk 2.1 zijn geschikt voor de ondersteuning van farmacokinetische studies, zoals wordt aangetoond in **Hoofdstuk 2.2**. In dit hoofdstuk beschrijven we de massabalansstudie van bendamustine. Zes patiënten met een recidiverende of refractaire maligniteit werden geïncludeerd in deze studie en ontvingen een dosis van 120 mg/m^2, 80-95 μCi ^{14}C-bendamustine. Binnen maximaal drie weken was ongeveer de helft van deze radioactiviteit teruggevonden in urine en ongeveer een kwart in feces. De farmacologisch relevante halfwaardetijd van bendamustine was kort (0.65 uur) en minder dan 5% van de toegediende dosis was teruggevonden in urine als onveranderde bendamustine en twee bekende actieve metabolieten. Dit resultaat suggereert een beperkte invloed van een nierinsufficiëntie op de blootstelling aan bendamustine.

Het grote verschil tussen de totale radioactiviteit (49%) en de onveranderde bendamustine en bekende metabolieten (9%) dat in urine werd teruggevonden was een reden voor vervolgonderzoek naar bendamustinemetabolieten in urine. In **Hoofdstuk 2.3** rapporteren we de detectie en identificatie van 25 bendamustine-gerelateerde stoffen in urinemonsters van patiënten. Belangrijke biotransformatieroutes waren hydrolyse, oxidatie en conjugatie, onder andere met cysteine. Deze metabole reacties zijn vergelijkbaar met reacties die eerder werden gevonden in ratten.

In **Hoofdstuk 3** richten we ons op eribuline, een synthetisch analoog van een product van een zeespons, dat antikankeractiviteit uitoefent door het remmen van de dynamiek van microtubuline eiwitten, waardoor de celdeling geblokkeerd wordt. In 2010 heeft de FDA en in 2011 de EMA toestemming verleend om eribuline te gebruiken bij de derdelijns behandeling van gemetastaseerde borstkanker. Om de distributie, het metabolisme en de excretie van dit middel te onderzoeken hebben we LC-MS/MS methoden ontwikkeld voor de kwantificering van eribuline in humaan plasma, urine, volbloed en feces. De hoge potentie van eribuline heeft als gevolg dat patiënten met een lage dosis behandeld worden, waardoor zeer gevoelige methoden nodig zijn. Deze methoden zijn gerapporteerd in **Hoofdstuk 3.1**.

De praktische toepassing van deze methoden wordt beschreven in **Hoofdstuk 3.2**, waarin de resultaten worden gerapporteerd van een massabalansstudie met ^{14}C-eribuline bij patiënten met vergevorderde solide tumoren. De farmacokinetische parameters van onveranderde eribuline en van de totale radioactiviteit waren vergelijkbaar, wat suggereert dat de bijdrage van metabolisme aan de eliminatie van eribuline minimaal is. Dit werd bevestigd door het metabolietprofiel, dat slechts kleine hoeveelheden van

eribulinemetabolieten liet zien in plasma, urine en feces. Het grootste deel van de eribulinedosis werd onveranderd uitgescheiden in feces. De resultaten van deze massabalansstudie ondersteunen de aanbeveling om eribuline in een lagere dosis toe te dienen aan patiënten met verminderde leverfunctie (de aanbevolen dosis voor patiënten met mild en matig leverlijden is respectievelijk 1.1 mg/m^2 en 0.7 mg/m^2 op dag 1 en 8 van 21-daagse cycli, terwijl de standaard dosis 1.4 mg/m^2 is [1]). Tevens verklaren de resultaten dat het beïnvloeden van de activiteit van CYP-enzymen door comedicatie geen effect heeft op de blootstelling aan eribuline.

De eliminatieroutes van eribuline staan in groot contrast met die van lenvatinib, de tyrosine kinase remmer die beschreven is in **Hoofdstuk 4**. Lenvatinib is een experimenteel oraal toegediend middel dat tyrosine kinases van meerdere receptoren remt. Daarmee remt het de vorming en groei van bloedvaten, die nodig zijn voor de groei van een tumor. Ook voor dit middel ontwikkelden we een set accurate en precieze bioanalytische methoden voor kwantificering in plasma, urine, volbloed en feces. Bovendien werden vier metabolieten van lenvatinib geïncludeerd in de methoden. De methodeontwikkeling en -validatie zijn beschreven in **Hoofdstuk 4.1**.

De massabalansstudie van lenvatinib, beschreven in **Hoofdstuk 4.2**, liet zien dat lenvatinib uitgebreid gemetaboliseerd wordt. Zeven tot tien dagen na toediening van ^{14}C-lenvatinib aan zes patiënten met vergevorderde kanker was gemiddeld 89% van de dosis teruggevonden in urine en feces, waarbij slechts 2.5% was teruggevonden als onveranderde lenvatinib. De bijdrage van de metabolieten die geïncludeerd waren in de bioanalytische methoden van Hoofdstuk 4.1 bleek gering te zijn, wat duidde op de aanwezigheid van additionele lenvatinibmetabolieten. De structuur, farmaceutische of toxische activiteit en de bijdrage van deze metabolieten aan de totale blootstelling aan lenvatinib-gerelateerde producten zijn onderwerpen voor vervolgonderzoek.

In **Hoofdstuk 5** is een andere tyrosine kinase remmer onderzocht: het oraal beschikbare middel dovitinib, wat is opgebouwd uit een benzimidazool-, chinoline- en een piperazine-eenheid. Dit middel remt meerdere tyrosine kinase receptoren wat leidt tot remming van angiogenese en tumorgroei. Momenteel wordt dovitinib getest in Fase II en Fase III studies tegen verscheidene vormen van kanker. Om een beter inzicht te krijgen in de farmacokinetiek van dovitinib hebben we een massabalansstudie uitgevoerd met ^{14}C-dovitinib in vier patiënten met vergevorderde solide tumoren. Bovendien werd de veiligheid en preliminaire effectiviteit van dovitinib geëvalueerd in een tweede cohort van 9 patiënten. Plasma concentraties van dovitinib lieten een snelle absorptie van het middel zien. Onveranderde dovitinib was het meest voorkomende dovitinib-gerelateerde product in plasma, gevolgd door M9; een metaboliet gevormd door een *N*-oxidatie aan de piperazine ring. De eliminatie van dovitinib verliep voornamelijk via oxidatief metabolisme gevolgd door uitscheiding in feces, waarin 52-69% van de radioactiviteit werd teruggevonden, tegenover 13-21% in urine. Verscheidene andere metabolieten werden

geïdentificeerd, zoals producten van hydroxylering, demethylering en glucuronidering. De ongewenste effecten waren voornamelijk van gastro-intestinale aard, zoals verwacht voor dit type middel.

Concluderend hebben we bioanalytische methoden opgezet voor een aantal antikankermiddelen. Deze methoden zijn vervolgens met succes toegepast in massabalansstudies, om uitgebreid de farmacokinetiek van de betreffende middelen te onderzoeken. Dit proefschrift toont de waarde aan van massabalansstudies en geeft een beter inzicht in de dispositie van bendamustine, eribuline, lenvatinib en dovitinib. Met deze informatie hopen we het therapeutisch gebruik van deze middelen in patiënten met kanker te optimaliseren.

Referenties

[1] Devriese, L, Witteveen, P, Voest, E, Overkleeft, EN, Langenberg, M, Beijnen, JH, Reyderman, L, Wanders, J, Mould, DR, Gupta, A, Hussein, Z, and Schellens, JHM, Eribulin dosing in patients with advanced solid tumors and hepatic impairment, *J Clin Oncol 29: 2011 (suppl abstr 2544)*, (2011).

Dankwoord

Promoveren doe je niet alleen; en dat dat cliché klopt heb ik de afgelopen jaren wel geleerd. Van alle mensen die een bijdrage hebben geleverd aan de totstandkoming van dit proefschrift wil ik er een aantal in het bijzonder bedanken.

Allereerst wil ik mijn dank uiten aan de patiënten die hebben deelgenomen aan de in dit proefschrift beschreven studies. Het meedoen aan een massabalansstudie zou voor een gezonde vrijwilliger al bezwaarlijk zijn, maar voor iemand die ziek is en een beperkte levensverwachting heeft is dit helemaal een opgave. Ik bewonder de moed van de twintig patiënten waarvan ik gedurende een week of langer monsters heb mogen verzamelen. Ik ben hen en ook hun familie die hen daarin ondersteunde enorm dankbaar. Zonder hun medewerking was dit onderzoek niet mogelijk geweest.

Daarnaast wil ik mijn promotoren Jan Schellens en Jos Beijnen en mijn co-promotor Hilde Rosing bedanken. Jan, je gedrevenheid en enthousiasme voor het onderzoek is motiverend. Na elk gesprek met jou begon ik weer met nieuwe energie. Jos, ook jouw steun was erg inspirerend, en ik waardeer je snelle en kritische commentaar op mijn manuscripten. Hilde, jij was mijn eerste aanspreekpunt en daar heb ik dan ook vaak gebruik van gemaakt. Met je praktische insteek weet jij problemen altijd terug te brengen tot kleinigheidjes en ik zie je als een goed voorbeeld.

Ook anderen hebben bijgedragen aan het onderzoek in dit proefschrift. In de kliniek wil ik de (kinetiek)verpleegkundigen bedanken voor het verzamelen van monsters in de late uren en in het weekend. Ook de verpleegkundig specialisten, in het bijzonder Marianne en Annemarie, bedankt voor jullie hulp met het geregel en de logistiek rondom de studies. Jolanda en Marja, jullie stonden altijd klaar met goede raad en samen met Brenda delen jullie een enthousiasme waardoor ik altijd vrolijk jullie kamer verlaat. David, van jou heb ik het “kinetieken” geleerd en jij bent ingesprongen toen ik er niet was, dankjewel voor de fijne samenwerking.

Op het radionucliden centrum (RNC), waar ik heel wat donkere (in de kelder) uurtjes heb doorgebracht heeft Dick me de fijne kneepjes van radioactiviteit meten uitgelegd, Dick, dankjewel hiervoor. Henny en Theo, jullie zorgden er voor dat een bezoekje aan het RNC nooit saai was en hielpen me enorm met alle wensen en verzoeken die ik had. Desiree, jij hebt de rol van Henny met succes overgenomen en ik wens je het allerbeste met het vervolg daarvan. Alwin, bedankt voor je hulp bij de radioactieve bereidingen en Ly, super hoe je mij wegwijs hebt gemaakt door het NKI-AvL en het Slotervaart ziekenhuis en dat je zo vroeg op wilde staan om voor mij radioactieve bereidingen te maken!

Ook op het bioanalyse lab zijn er velen die bijgedragen hebben aan de studies in dit proefschrift. In eerste instantie Abadi en Luc, jullie hebben mij de beginselen van werken op een GLP-gecertificeerd lab aangeleerd met veel geduld en nog meer plezier. Ik nodig

jullie graag een keer uit voor een balletvoorstelling. Bas en Matthijs, jullie hebben enorm veel gedaan voor de bioanalyse van E7080, E7389 en bendamustine en jullie weten (de humor op) het lab naar een hoger niveau te tillen. Michel, je was er altijd om problemen met de massaspectrometers op te lossen en daarnaast konden we mooi onze ervaringen met auto's delen. Roel, dankjewel voor je hulp als ik een acuut probleem had met mijn computer en Denise, ik vond het leuk om met je samen te werken en hoop dat je toch nog een keer die reis naar Brazilië kan maken.

I would like to thank the co-authors of the manuscripts in this thesis for the pleasant cooperation during the mass balance studies and manuscript preparation.

Natuurlijk is ook een prettige werkomgeving "of paramount importance" voor een geslaagd onderzoek. Gelukkig is die in "de keet" wel aanwezig. Nynke, onze theemomentjes waren altijd een fijne onderbreking van het werk. Ik vind het superleuk dat je mijn paranimf wil zijn. Anita, met je chocoladelekkernijen en goede verhalen was je een goede aanwinst voor onze kamer. Succes met je onderzoek! En Thomas, onze beroemde specialist op het gebied van (verwaarloosde) tropische ziekten, je was er vaker niet dan wel, maar dankjewel voor de rust die je op onze kamer bracht. Bas, sinds je de keet achter je hebt gelaten mis ik je (beetje slechte) grappen. Robert, we waren een ontzettend goed "metabolite profiling" team. Ik heb veel van je geleerd en vind het fijn dat ook jij mijn paranimf wil zijn.

Jelte, Rik: mooi hoe jullie ervoor zorgen dat er altijd wel wat te lachen maar ook serieus te discussiëren valt. Bojana, bedankt voor de gezellige lunchwandelingen. Ook andere (ex-) collega-oio's uit de keet en van het NKI, ik wil jullie bedanken voor de goede sfeer op het werk en de oio-uitjes en -borrels. Een fijnere werkplek kan ik me nauwelijks voorstellen.

Lieve oma, ik heb dit proefschrift aan opa opgedragen omdat hij een belangrijke aanleiding voor mij is geweest om onderzoek naar kanker te willen doen. In gedachten is hij bij ons. Opapa, ook aan jou heb ik dit werk opgedragen; mijn wetenschappelijke aanleg heb ik ongetwijfeld van jou gekregen en daar ben ik dankbaar voor. Lieve omama, dankjewel voor je luisterend oor en het feestje dat je er van maakt wanneer we op bezoek komen.

Peter en Marloes, Peter en Jacqueline, leuk dat jullie altijd zoveel interesse hebben in mijn onderzoek. Ook dank ik alle andere familieleden voor jullie interesse.

Papa, mama, Stephanie-Elise, bij jullie kan ik altijd mijn verhalen kwijt en ook al komen ze niet altijd even helder over, ik vind het fijn dat jullie me altijd steunen. Tot slot, Wouter, met goede tips en een stevige knuffel weet jij me altijd op te vrolijken als ik in een dip zit. Ik heb het gevoel dat ik altijd op jou kan terugvallen en dat zou ik niet graag willen missen. Dankjewel voor alle steun die je me gegeven hebt.

Anne-Charlotte

Curriculum Vitae

Anne-Charlotte Dubbelman was born on December 15, 1984 in Leiden. From 1996 she attended the Dr. Mollercollege in Kaatsheuvel and later Waalwijk, where she gained her Gymnasium diploma (cum laude) in 2002. In the same year she started the study Chemical Engineering at the Eindhoven University of Technology, whereby she finished her first year with an award for the best propaedeutic results of her study. In 2005 she obtained her bachelor's degree (cum laude). She continued her education with the master Medical Engineering; a study of the Eindhoven University of Technology in cooperation with the University of Maastricht. During an internship she investigated the analysis of polymorphisms related to the graft-versus-host disease at the Laboratoire de Biochimie et Biologie Moléculaire of the Centre Hospitalier Universitaire in Nancy, France, under the supervision of Prof. J.L. Guéant and Dr F. Namour. Her graduation project, entitled "Proteomic profiling of cerebrospinal fluid to detect potential biomarkers for multiple sclerosis", was executed at the department of clinical chemistry at the University Hospital Maastricht, whereby she was supervised by Prof. Marja van Dieijen-Visser and Dr Judith Bons in Maatricht and by Prof. Huib Vader in Eindhoven. In 2007 she obtained her master's degree (cum laude) and the following year she started the investigations described in this thesis. This research was performed at the Netherlands Cancer Institute – Antoni van Leeuwenhoek Hospital and the Slotervaart Hospital in Amsterdam, the Netherlands and was supervised by Prof. Jan H.M. Schellens, Prof. Jos H. Beijnen and Dr Hilde Rosing.

Curriculum Vitae

Anne-Charlotte Dubbelman is geboren op 15 december 1984 in Leiden. Vanaf 1996 was zij leerling aan het Dr. Mollercollege te Kaatsheuvel en later Waalwijk, waar zij in 2002 haar gymnasium diploma (cum laude) behaalde. In hetzelfde jaar begon ze met de studie Scheikundige Technologie aan de Technische Universiteit Eindhoven, waar ze het eerste jaar afsloot met een civi-aanmoedigingsprijs voor de beste propedeuseresultaten van de opleiding. In 2005 ontving zij haar bachelordiploma (cum laude). Ze vervolgde haar studie met de master Medical Engineering; een opleiding van de Technische Universiteit Eindhoven in samenwerking met de Universiteit Maastricht. Tijdens een stage onderzocht ze analysemethoden van polymorfismen gerelateerd met graft-versus-host disease op het Laboratoire de Biochimie et Biologie Moléculaire van het Centre Hospitalier Universitaire in Nancy, Frankrijk, onder begeleiding van prof. dr. J.L. Guéant en dr. F. Namour. Haar afstudeeronderzoek, getiteld "Proteomic profiling of cerebrospinal fluid to detect potential biomarkers for multiple sclerosis" voerde zij uit op de afdeling klinische chemie in het Academisch ziekenhuis Maastricht, waarbij ze begeleid werd door prof. dr. Marja van Dieijen-Visser en dr. Judith Bons in Maastricht en door prof. dr. ir. Huib Vader in Eindhoven. In 2007 studeerde zij (cum laude) af om het daaropvolgende jaar te starten met het onderzoek dat beschreven wordt in dit proefschrift. Dit onderzoek werd uitgevoerd op het Nederlands Kanker Instituut - Antoni van Leeuwenhoek Ziekenhuis en het Slotervaartziekenhuis te Amsterdam, onder begeleiding van prof. dr. Jan H.M. Schellens, prof. dr. Jos H. Beijnen en dr. Hilde Rosing.

List of publications

Articles related to this thesis

Dubbelman AC, Rosing H, Thijssen B, Lucas L, Copalu W, Wanders J, Schellens JH, Beijnen JH, Validation of high-performance liquid chromatography-tandem mass spectrometry assays for the quantification of eribulin (E7389) in various biological matrices, *J.Chromatogr.B Analyt.Technol.Biomed.Life Sci.*, **879** (2011) 1149-1155.

Dubbelman AC, Rosing H, Schellens JH, Beijnen JH, Bioanalytical aspects of clinical mass balance studies in oncology, *Bioanalysis*, **3** (2011) 2637-2655.

Dubbelman AC, Rosing H, Jansen RS, Mergui-Roelvink M, Huitema AD, Koetz B, Lymboura M, Reyderman L, Lopez-Anaya A, Schellens JH, Beijnen JH, Mass balance study of [14C]eribulin in patients with advanced solid tumors, *Drug Metab Dispos.*, **40** (2012) 313-321.

Dubbelman AC, Rosing H, Thijssen B, Gebretensae A, Lucas L, Chen H, Shumaker R, Schellens JH, Beijnen JH, Development and validation of LC-MS/MS assays for the quantification of E7080 and metabolites in various human biological matrices, *J.Chromatogr.B Analyt.Technol.Biomed.Life Sci.*, **887-888** (2012) 25-34.

Dubbelman AC, Tibben M, Rosing H, Gebretensae A, Nan L, Gorman SH, Robertson P, Jr., Schellens JH, Beijnen JH, Development and validation of LC-MS/MS assays for the quantification of bendamustine and its metabolites in human plasma and urine, *J.Chromatogr.B Analyt.Technol.Biomed.Life Sci.*, **893-894** (2012) 92-100.

Dubbelman AC, Jansen RS, Rosing H, Darwish M, Hellriegel E, Roberson, Jr. P, Schellens JHM, Beijnen JH, Metabolite profiling of bendamustine in urine of cancer patients after administration of ^{14}C-bendamustine, *Drug Metabolism and Disposition* (2012) April 4, epub ahead of print.

Dubbelman AC, Rosing H, Darwish M, D'Andrea D, Bond M, Hellriegel E, Roberson, Jr. P, Schellens JHM, Beijnen JH, Pharmacokinetics and excretion of ^{14}C-bendamustine in patients with relapsed or refractory malignancy, submitted for publication

Articles not related to this thesis

Pulinx B, Dubbelman AC, Bons JAP, van Dieijen-Visser MP, Hupperts RMM, Wodzig WKWH, Proteomic profiling of cerebrospinal fluid to detect potential biomarkers for multiple sclerosis, *Ned Tijdschr Klin Chem Labgeneesk* **33** (2008) 196-8.

Abstracts

Dubbelman AC, Rosing H, Darwish M, D'Andrea D, Bond M, Hellriegel ET, Beijnen JH, Schellens JHM, An Open-Label Phase I Pharmacokinetic Study of ^{14}C-Bendamustine in Patients with Relapsed or Refractory Malignancy. Poster at Annual meeting of the American Society of Hematology (ASH), 10-13 December 2011, San Diego, CA, USA

Dubbelman AC, Mergui-Roelvink M, Koetz B, Lymboura M, Reyderman L, Lopez-Anaya A, Rosing H, Marchetti S, Beijnen JH, Schellens JHM. Metabolism and excretion of ^{14}C-eribulin in patients with advanced solid tumors. Poster at Annual meeting of the American Association for Cancer Research (AACR), 2-6 April 2011, Orlando, FL, USA

Dubbelman AC, Rosing H, Mergui-Roelvink M, Gupta A, Verbel D, Sellecchia R, Fan J, Thompson GA, Shumaker R, Huitema ADR, Beijnen JH, Schellens JHM, A mass balance study of ^{14}C-lenvatinib (E7080) in patients with advanced solid tumours or lymphomas. Poster at the scientific spring meeting of the dutch society for clinical pharmacology and biopharmacy (NVKFB), 30 March 2012, Utrecht, the Netherlands